1995

The distribution and transport of suspended sediment in the southern North Sea

Moffat, Timothy Julian

THE DISTRIBUTION AND TRANSPORT OF SUSPENDED SEDIMENT IN THE SOUTHERN NORTH SEA

by

TIMOTHY JULIAN MOFFAT

A thesis submitted to the University of Plymouth
in partial fulfilment for the degree of

DOCTOR OF PHILOSOPHY

Institute of Marine Studies

In collaboration with

Plymouth Marine Laboratory
and
Proudman Oceanographic Laboratory

June 1995

THE DISTRIBUTION AND TRANSPORT OF SUSPENDED SEDIMENT IN THE SOUTHERN NORTH SEA

TIMOTHY JULIAN MOFFAT

ABSTRACT

Observational studies have been undertaken in the southern North Sea with the aims of describing the seasonal cycle of suspended sediments in three dimensions, and comparing the results with other measured physical and biological parameters in order to investigate some of the processes that control the distribution and transport of suspended sediments in shelf seas.

A systematic investigation of the horizontal and vertical suspended sediment distributions, and the inorganic and organic components, over a period of fifteen months, has described major features, including a high turbidity region off the East Anglian coast, low turbidity regions in the northern and central parts of the southern North Sea, and the seasonal development of a plume emanating from the East Anglian coast, and high organic matter contents along the coasts of the Southern and German Bights.

Comparison with coincident measurements of salinity, temperature, river discharge, chlorophyll and phytoplankton productivity indicated that the suspended sediment distributions were strongly influenced by water mass interactions, haline and thermal stratification and primary production. The distribution of water masses accounted for the basic division between the turbid coastal waters and the relatively clear offshore waters of Atlantic origin. Density differences tended to trap sediment in coastal waters, and were also responsible for localised suspended matter minima at periods of high river discharge. Primary production was 2-3 times greater in the eastern half of the southern North Sea than the western half, and consequently suspended sediment distributions in the English coastal waters were dominated by an inorganic component and in continental European coastal waters by an organic component.

Fluxes of suspended sediment were calculated within the plume. The total annual flux was estimated to be 6.6 Mt a^{-1} ± 50%. This flux was compared with sediment budgets for the coast of eastern England. Only one of the budgets provided enough material to supply the plume. Errors in the flux and budget calculations suggested that more data were required before the results could be accepted unequivocally.

These results provide important qualitative and quantitative information on North Sea suspended sediment distributions and transport. The data can be used for validating mathematical models of suspended sediment transport and for improving interpretation methods of remote sensing imagery. They provide a valuable baseline study for future research programmes such as the Land Ocean Interaction Study (LOIS).

LIST OF CONTENTS

LIST OF CONTENTS CONT'D

LIST OF FIGURES

LIST OF FIGURES CONT'D

LIST OF FIGURES CONT'D

LIST OF FIGURES CONT'D

LIST OF FIGURES CONT'D

LIST OF FIGURES CONT'D

LIST OF TABLES

LIST OF TABLES CONT'D

ACKNOWLEDGMENT

I am extremely grateful to Professor K.R. Dyer, as Director of Studies, in providing support, advice and motivation for the duration of the North Sea Project and in the preparation of the thesis.

In addition, there are many individuals to whom I would like to express my gratitude:

Dr. R.K Lowry of the British Oceanographic Data Centre for coordinating the establishment of the North Sea Database, and providing invaluable support and advice in accessing the database and plotting of data.

Mr. M.J. Howarth of the Proudman Oceanographic Laboratory for his astute project management, and his colleagues Dr. J.E. Jones and Dr. R. Proctor for providing additional data and plotting services.

Drs. J. Aiken, I.R. Joint, R.M. Warwick and NERC Computer Services of the Plymouth Marine Laboratory for permission to use their respective laboratory and computer facilities.

J. Atherton, K. Black, M. Evans, G. Glegg, S Jones, J. McCabe, D. Mills, D. Plummer, A. Pomroy, D. Purdie, D. Sturley, C. Symon and others for generously volunteering to assist in the acquisition of the data during the North Sea survey cruises.

Mr. K. Robertson, Mr. R. Powell and colleagues of Research Vessel Services; the Masters and crew of the R.R.S. Challenger and the ship's agents, Escombe Lambert of Great Yarmouth, for providing invaluable technical and logistical support for the entire North Sea Project.

Dr. A. Turner and other co-workers and students within the North Sea Project community.

A.M. Moffat for her support and encouragement.

AUTHOR'S DECLARATION

At no time during the registration for the degree of Doctor of Philosophy has the author been registered for any other University award.

This study was financed with the aid of funding of a Special Topic Award (GST/02/332) and Research Assistantship from the Natural Environment Research Council, and carried out in collaboration with the Plymouth Marine Laboratory and the Proudman Oceanographic Laboratory.

A programme of advanced study was undertaken, which included supervised micro and mainframe computer instruction, a course on database management, and practical instruction and experience of oceanographic survey techniques.

Relevant scientific seminars and conferences were regularly attended at which work was often presented; and several papers prepared for publication.

Publications

Dyer, K.R. and Moffat, T.J. (1992). Suspended Sediment Distributions in the North Sea. *Inst. Marine Studies Rep.*, University of Plymouth. 42 pp.

Howarth, M.J., Dyer, K.R., Joint, A.R., Hydes, D.J., Purdie, D.A., Edmunds, H., Jones, J.E., Lowry, R.K., Moffat, T.J., Pomroy, A.J. and Proctor, R. (1993). Seasonal cycles and their spatial variability. *Phil. Trans. R. Soc. Lond.* A **343**, 383-403.

Howarth, M.J., Dyer, K.R., Joint, A.R., Hydes, D.J., Purdie, D.A., Edmunds, H., Jones, J.E., Lowry, R.K., Moffat, T.J., Pomroy, A.J. and Proctor, R. (1994). Seasonal cycles and their spatial variability. In: *Understanding the North Sea System.* Charnock, H., Dyer, K.R., Huthnance, J.M., Liss, P.S., Simpson, J.H. and Tett, P.B. (eds.). Chapman and Hall, London for the Roy. Soc., pp. 5-25.

Presentations and Conferences Attended

UK Oceanography '88, University of East Anglia, 1988.

Moffat, T.J. *Suspended sediment distributions*. Presentation at North Sea Project Modelling Workshop, Gregynog (Wales), September, 1989

North Sea Project Users' Club for general purpose model, Gregynog (Wales), November 1989.

Moffat, T.J. *Seasonal cycle of suspended sediments*. Presentation at North Sea Project Seasonal Cycle Workshop, Proudman Oceanographic Laboratory, Bidston, February 1990.

North Sea Project Process Studies Workshop, Proudman Oceanographic Laboratory, Bidston, May 1990

Moffat, T.J. and Dyer, K.R. *Suspended sediment in the North Sea*. Conference paper given at U.K. Oceanography '90, Polytechnic South West (Plymouth), 1990.

Moffat, T.J. and Dyer, K.R. *Suspended sediment transport in the North Sea*. Conference paper given at U.K. Oceanography '92, University of Liverpool, 1992.

North Sea Project Discussion Meeting. Royal Society, London, November, 1992.

Signed .. 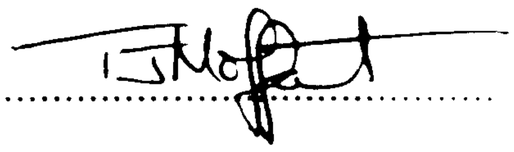

Date ..30th June 1995

CHAPTER 1

INTRODUCTION

1.1: The Study of Suspended Sediments in Shelf Seas

Natural products of weathering and erosion, materials of biological origin, and man-made materials are held in suspension in water as solids or as dissolved materials. Suspended sediment, suspended matter, suspended solids and suspended material are all common terms that are used to describe the total solids held in suspension in water. As with other authors [*e.g.* Sackett, 1978; McCave, 1979] these terms are considered synonymous.

Suspended sediments have many important roles, influences and impacts on the aquatic and marine environments. They are a significant factor in controlling the geochemistry of the oceans [Turekian, 1977; Balistrieri *et al.*, 1981]. As well as fluxes of particles and elements from the surface of the ocean to the deep sea, suspended particles are being transported from coastal areas to the open sea, thereby providing a transport mechanism for elements and other substances as part of the chemical mass balance between rivers and oceans [Mackenzie and Garrels, 1966; Bewers and Yeats, 1977; Burton, 1976; Turekian, 1977]. Suspended sediments are also important carriers for pollutants [Odum *et al.*, 1969; Turekian, 1977; Duinker, 1980; Eisma, 1981a]. Heavy metals, nutrients and organic contaminants are easily adsorbed on to particles and therefore can be transported in suspension. In this way, suspended sediments play an important role in the dispersal of pollutants through estuaries and the nearshore seas towards the open oceans. Suspended sediments will also influence water quality in terms of, for example, controlling the amount of sunlight that penetrates the water column and is available for photosynthesis.

The evaluation and understanding of these impacts and influences presents a challenge. Baseline information is required on the distribution and concentration of suspended sediments in shelf seas, on the underlying mechanisms and processes of suspended sediment transport and deposition, and on the physical factors that affect the distribution and transport of suspended sediments. Some of the early research into shelf sea suspended sediments has been reviewed by McCave [1972]. He found that there were two distinct features that were common to many of the measured suspended sediment distributions. The most pronounced feature was the general exponential decrease in concentrations in a seaward direction. The causes for this were firstly, that the sources of the sediment were situated along the coast and secondly that there may be advective transport shorewards as a result of, for example, density differences between the nearshore and offshore water masses that established a form of quasi-estuarine circulation. Both these factors tended to reinforce the concentration gradient. The second significant feature was the existence of plumes of higher concentration extending across the

shelf sea. Such plumes were commonly associated with major deltas (*e.g.* the Mississippi, Orinoco and Irrawaddy) or at the convergence of coastal currents, resulting in a current across the shelf (*e.g.* the North Sea). These plumes were major pathways for the transport of suspended sediment from nearshore areas to the outer shelf.

The broad distribution of suspended sediments in shelf seas characterized above will be complicated by physical and biological factors that affect the distributions and transport of suspended sediments on both spatial and temporal scales. For example, fluctuations in meterological conditions (*e.g.* wind stress, precipitation and solar radiation) will control the concentration and distribution of suspended sediments by influencing the supply of sediment from coastal erosion and from riverine inputs, and may also contribute to the short term transformation of the prevailing current circulation resulting in modified transport paths of suspended sediment. The consequences of these factors manifest themselves in the seasonal cycle which is the fundamental and predominant shelf sea process.

The relationships between suspended sediment distributions and transport, and the seasonal cycle are poorly understood, chiefly because field observations are generally too limited and patchy in both time and space to be able to define in any rational detail the seasonal cycle. Therefore, the primary aim and motivation for the research was to build on the basic understanding of the processes that control the distribution and transport of suspended sediments by investigating one shelf sea site in an intensive and systematic way. The framework for the research was provided by the North Sea Project [§1.2].

1.2: The NERC North Sea Project

Concern over the water quality status and environmental impact of pollutants in the North Sea has been voiced for a very long time now, culminating in a variable array of publications of scientific data and analyses on the status of the North Sea [*e.g.* Goldberg, 1973; Hey and Peet, 1986; Parker and Tett, 1987; Peet, 1987; Newman and Agg, 1988; Salomons *et al.*, 1988; Lancelot *et al.*, 1990]; by quasi-scientific discussion groups comprising both the scientific and industrial communities [*e.g.* North Sea Forum, 1987; Marine Forum, 1990]; and by environmental pressure groups [*e.g.* Greenpeace, 1987]. In very recent years, public awareness has also been heightened by media coverage [*e.g.* Daily Telegraph, 1988; Sunday Times, 1988] of, for example, the seal virus outbreak in the spring of 1988 and the reports of the deleterious effects of the blooms of toxic algae off the coasts of Scandinavia.

At the Second International Conference on the Protection of the North Sea, a report by the Scientific and Technical Working Group [1987] on such matters as the sources, distribution and effects of pollutants, and another report by the Oceanography Sub-Group [1987] on the current scientific understanding of the North Sea, resulted in an agreement between participating ministers to not only reduce the discharges of persistent and toxic substances into the North Sea, but also *inter alia*, to

improve and provide more consistent and dependable data as a basis for future managerial decision-making and to test the effectiveness of measures taken already [Ministerial Declaration, 1987]. The response of the scientific community in the U.K. was the initiation of the five year long *North Sea Project*, a multi-disciplinary and a multi-institutional scientific programme of research, sponsored by the Natural Environment Research Council. This project followed on from previous collaborative projects, such as the *Zirkulation und Schadstoffumsatz in der Nordsee* (ZISCH) project managed by Hamburg University [Sündermann and Degens, 1989].

The ultimate goal of the North Sea Project together with three intermediate and parallel objectives are given in Table 1.1. The framework and schedule of the present study is related primarily to the third intermediate objective, the Survey Programme. The aim of the Survey Programme was to define a seasonal cycle in the southern North Sea for various physical, chemical, biological and sedimentological parameters, which could then be used as a database for testing and forcing mathematical models. The details of the individual experiments together with the overall objectives of the Survey Programme are given by Howarth [1987]. The Survey Programme was also complemented by the second intermediate objective, the Process Studies, which targeted in detail specific phenomena such as sediment resuspension, sand wave transport, estuarine plumes and phytoplankton blooms.

Table 1.1: North Sea Project Aims.

WATER QUALITY MODEL:	Ultimate goal: the effective management of the North Sea by utilising computer-based models that are able to predict the impact of potentially conflicting activities under different scenarios
3-D TRANSPORT MODEL:	To develop a transport model for any passive constituent, incorporating improved representations of the hydrodynamics and dispersion
PROCESS STUDIES:	To identify and quantify non-conservative processes which determine the cycle and fate of individual constituents
SURVEY PROGRAMME:	To define a complete seasonal cycle as a database for all the observational studies needed to formulate, drive and test the models

Within the context of the Survey Programme the aims of the research were to measure the concentrations of suspended sediment, and the organic and inorganic components, in three dimensions in the southern North Sea during the prescribed observational period [detailed in §2.1]. The suspended sediment data were to be incorporated, along with all the other measurements, into the North Sea Database held at the British Oceanographic Data Centre (BODC) so that they could provide three-dimensional information on suspended sediment concentrations to the wider North Sea Project scientific community as background for the process studies; as input data for mathematical models simulating suspended sediment transport for different river flows, meteorological and tidal conditions; and as sea truth for the calibration of remote-sensing images in terms of suspended sediment concentration.

1.3: Study Site - The North Sea

The North Sea is a shallow and semi-enclosed shelf sea bordered by the British Isles to the west, by the European Continent to the south-east and by the Scandinavian Peninsula to the north-east [Figure 1.1]. It has two openings to the North Atlantic Ocean between Shetland and Norway and through the Straits of Dover, and an opening to the Baltic Sea through the Skagerrak. The total surface area of the North Sea depends on the geographical boundaries employed, and therefore estimates range from 525,000 km^2 [Zijlstra, 1988] to 575,000 km^2 [Eisma, 1987a; Reid *et al.*, 1988] and 722,000 km^2 [North Sea Forum, 1987], the latter including the Channel (86,000 km^2) and the Skagerrak (36,000 km^2). Accordingly, the total water volume varies from 43,000 km^3 to 54,000 km^3 and 55,000 km^3 respectively.

BATHYMETRY

The general shape of the North Sea basin is determined by the predominant north-west to south-east direction of the geological fault structures that reflect older structural trends formed in pre-Permian times (*e.g.* Hercynian faulting). These had important influences on subsequent sedimentation and subsequent folding and faulting in the Permian and younger sediments [Pegrum *et al.*, 1975]. The bathymetry of the present sea floor [general bathymetry is given in Figure 1.1] reflects both the underlying geological structure of a much more recent age, *viz.* the latter part of the Pleistocene epoch (*e.g.* the Saalian and Weichselian glaciations), and also recent (*e.g.* Holocene and present day) sedimentary processes [*q.v.* BOTTOM SEDIMENTS].

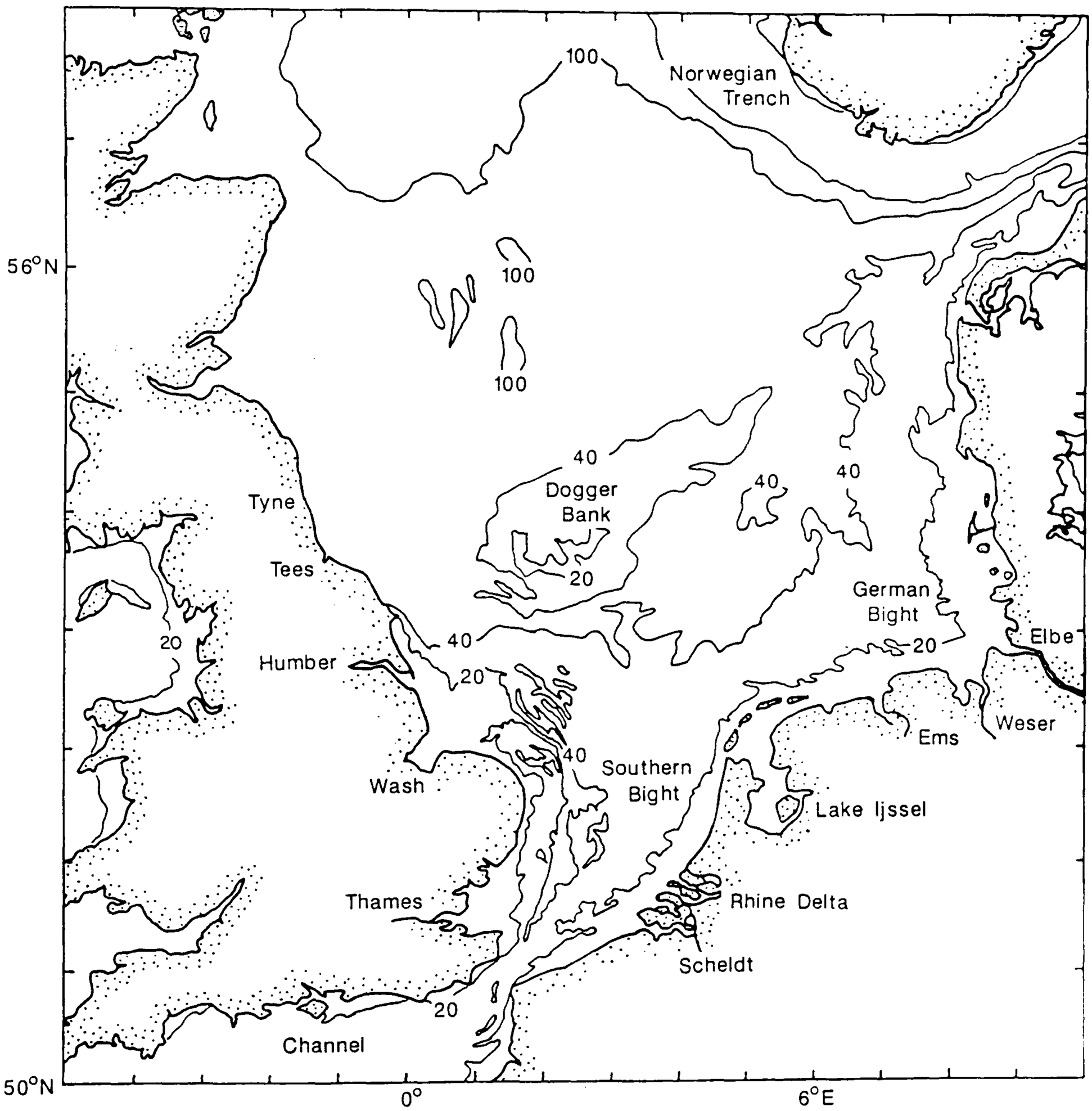

Figure 1.1: Geographic boundaries and bathymetry of the North Sea.

The bathymetry of the North Sea is generally less that 200m and includes two prominent features: the Norwegian Channel and the Dogger Bank. The Norwegian Channel is the largest single feature on the north-west European continental shelf [Caston, 1979] and was formed together with the Skagerrak by glacier excavation in the Upper Pleistocene. Here the greatest water depths are reached: water depths in excess of 225m in the Norwegian Channel, and a maximum depth of 700m in the Skagerrak. The Dogger Bank is the largest positive topographic feature in the North Sea and stands more than 20m higher than the surrounding sea-floor. The bank was formed from large quantities of sand and gravel brought down by glaciers from Scandinavia and Scotland either during the Saalian [Eisma, 1987a] or Weichselian [Caston,1979] glaciations, which overlie earlier Elsterian (Middle Pleistocene) fluvioglacial deposits [McCave *et al.*, 1977]. Elsewhere, the shallowest water depths are found in either coastal areas or associated with other sand bank systems, especially in the southern North Sea (*e.g.* south of 56°N) such as the water depths of between 30 and 50m in the German Bight, and depths less than 30m off the Norfolk coast (*e.g.* the Norfolk, Lincolnshire and Indefatigable Banks).

HYDROGRAPHY

Atlantic water of high salinity enters the North Sea between Shetland and Norway, and through the Straits of Dover. Lower salinity water enters the North Sea as coastal run-off from the British coast, the Low countries, Germany and Denmark as well as the outflow from the Baltic Sea through the Skagerrak. Several classifications of these water masses and their inter-mixing have been conceived according to their origins or properties. Laevastu [1963] identified three primary and five secondary water types [Table 1.2]. The secondary water masses arise from the mixing of the primary water types with the continental lower salinity water. Lee [1980] has modified Laevastu's classification into six basic water types [Table 1.2] using temperature, salinity, and nutrients and trace metal concentration data. The delimitation of these water mass classifications is somewhat arbitrary however, and so in 1983 a study group of the International Council for the Exploration of the Sea (ICES) adopted a more rigorous classification in terms of a set of nine rigid geographical boxes [Figure 1.2] taking into account hydrographic and biological conditions [Oceanography Sub-Group, 1977; Reid *et al.*, 1988; *cf.* Table 1.2].

Although the North Sea is mostly shallow enough so that water masses are considered to extend from the sea surface to the sea bed (except in the much deeper Norwegian Channel and the Skagerrak), there are nonetheless strong seasonal differences in the vertical structure of the water column. Dietrich [1950] subdivided the North Sea into hydrographical regions based upon the extent

Table 1.2: Classifications of water masses in the North Sea.

Laevastu [1963]	Lee [1980]	ICES areas (1983)
1. North Atlantic	1. North Atlantic	1, 2, 3', 6, 7' & 7"
2. Channel	2. Channel	7" & 4
3. Skagerrak	3. Skagerrak	6 & 5
i. Scottish Coastal	4. Scottish Coastal	2, 7' & 3'
ii. English Coastal	5. English Coastal	3"
iii. Continental Coastal	6. Continental Coastal	4 & 5
iv. Northern North Sea	admixture of 1 & 2	
v. Southern North Sea	admixture of 1,2,5 & 6	

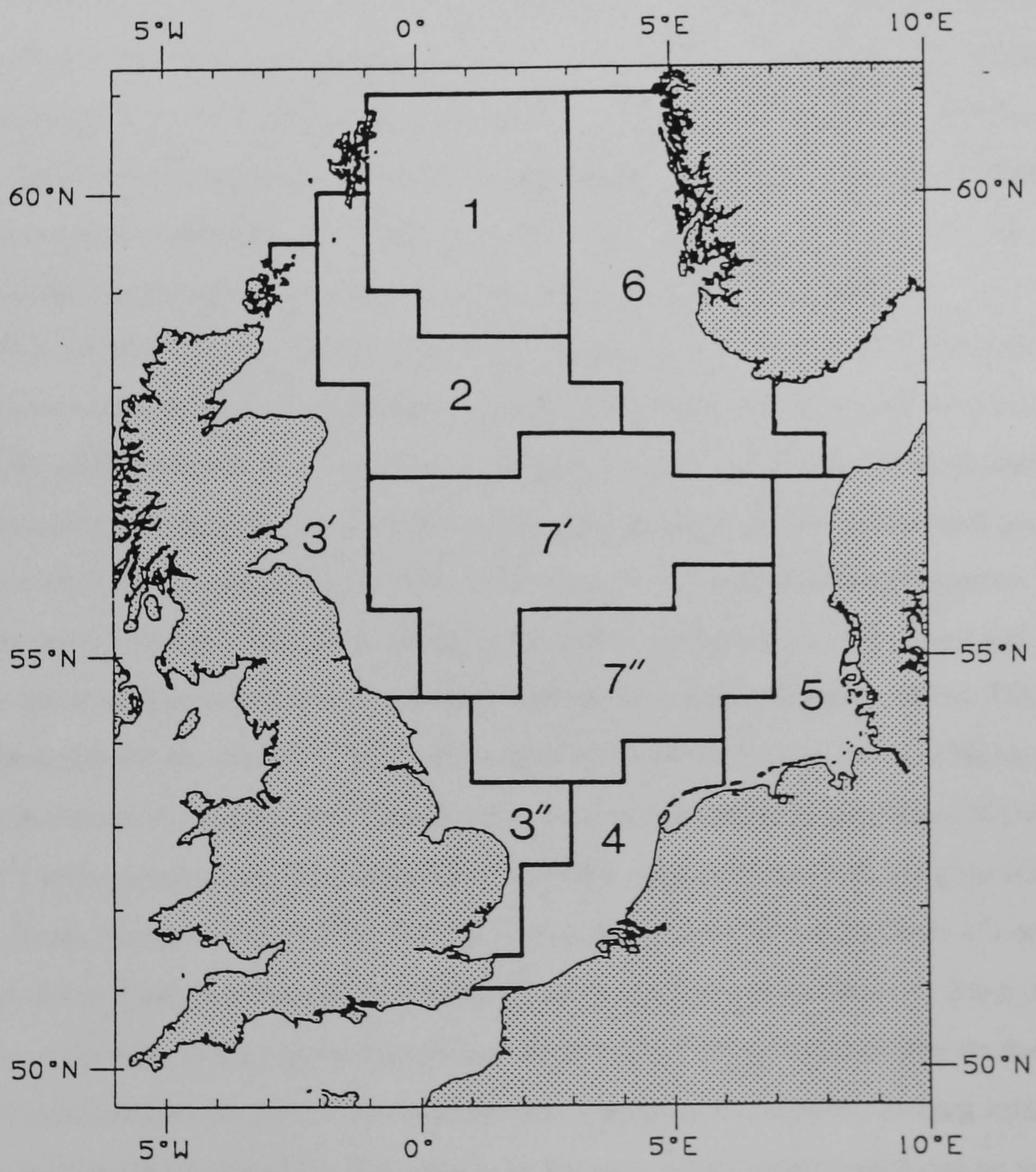

Figure 1.2: Subdivisions of the North Sea used by the ICES study group.

to which stratification of the water column takes place either seasonally or throughout the year. During the winter, much of the North Sea is well-mixed whereas between spring and autumn some areas remain well-mixed and others become stratified. For example, ICES areas 3" and 4 remain thermally mixed; areas 3' and 5 form minor stratification; and all other areas develop a strong thermocline by June which breaks down in November [Reid *et al.*, 1988].

Another feature of the North Sea water mass regime is the occurrence of fronts at the boundaries of the different regimes, such as the Flamborough Head Front which is taken as the boundary between the Scottish Coastal and English Coastal water masses [Lee, 1980]. Some of these fronts may be characterized by sharp gradients in temperature and/or salinity [Pingree and Griffiths, 1978; James, 1983] and can be observed at the surface by clear infrared satellite images which indicate thermal differences across the front [Holligan *et al.*, 1989].

The currents and tidal motions of the North Sea have been reviewed by Hill [1973], Huntley [1980] and Lee [1980]. Comparable current patterns have been deduced from surface salinity charts [*e.g.* Böhnecke, 1922], from drift bottle and card experiments [Lee and Ramster, 1968; summarized by Lee, 1970], from current meter measurements [Ramster, 1977; summarized by Howarth, 1983], from mathematical modelling [*e.g.* Maier-Reimer, 1977; Davies, 1983a; 1987], and from the distribution and modelling of Caesium 137 [*e.g.* Kautsky, 1973; Prandle, 1984].

The residual surface current system of the North Sea [Figure 1.3] exhibits a general anticlockwise circulation produced as Atlantic water, forced into the North Sea from the north and south by the predominantly westerly winds, propagates around the North Sea in an anticlockwise direction past the coasts of Scotland, England, Belgium, Holland, Germany, Denmark and Norway. Local gyres and other secondary circulations are superimposed upon this general pattern. These are induced by bottom topography (*e.g.* the Dogger Bank), the configuration of the coast and, in coastal waters, by density differences between nearshore and offshore waters [Eisma, 1987b]. Tidal currents are strongest close to the coasts, in the shallow parts of the North Sea, in straits or bights where the tidal flow is constricted or impeded. The strongest tidal currents occur in the Straits of Dover (more than 1m s^{-1}), in the Southern Bight, especially off the East Anglian Coast, and along the coasts of the southern North Sea [Howarth, 1990]. The weakest tidal currents (less than 20cm s^{-1}) occur in the central and eastern North Sea towards the Skagerrak and in the Norwegian Channel, due to the energy dissipation of the tides as they travel around the North Sea and where water depths are the deepest.

The residual current circulation described above is likely to encounter marked variations, not least by variations in wind forcing. The effects of different wind forcing conditions on the residual currents have been indicated in a report by an ICES Working Group on permanent moored current meter stations [Hill and Dickson, 1978]. This suggests that the residual current system of the

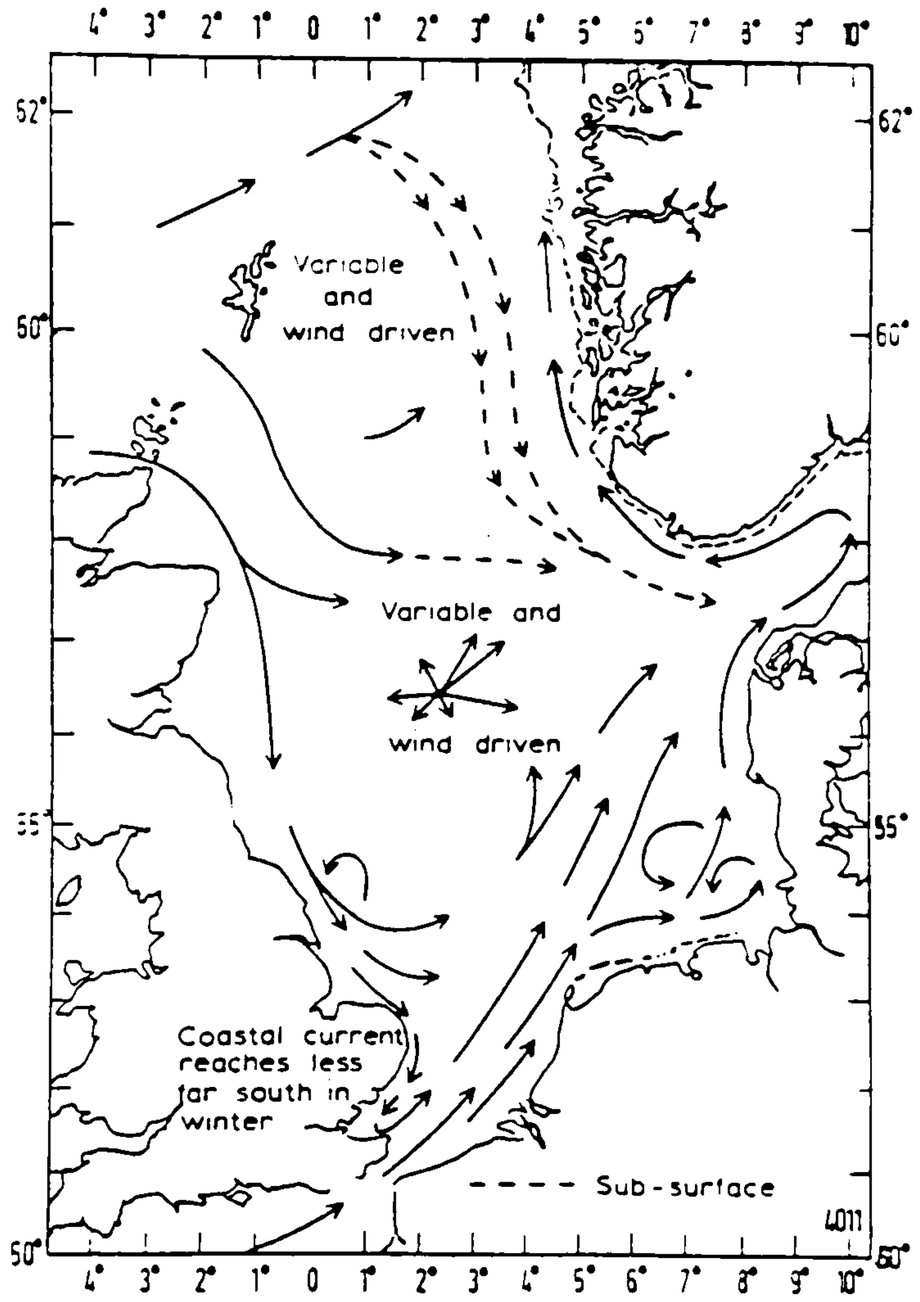

Figure 1.3: General surface current system of the North Sea [after Hill and Dickson, 1978].

North Sea is completely reversed so that the main flow is southwesterly and out of the Straits of Dover. The importance of wind induced residual currents noted in the ICES report is supported by mathematical models [*e.g.* Backhaus and Maier-Reimer, 1983; Davies, 1983b; §6.1].

BOTTOM SEDIMENTS

Most of the sea floor of the North Sea is covered by Holocene sediments of a few metres in thickness. These sediments are subdivided by Veenstra [1971] into a mud fraction (< 50 μm grain size), a sand fraction (50 μm to 2 mm) and a gravel fraction (> 2mm) [Figure 1.4]. The majority of the sea floor is dominated by sandy sediments and these deposits and their associated bedforms (*e.g.* sand waves and elongated sand ridges or banks) have been the subject of considerable investigation especially in the southern North Sea, such as the sand waves fields and ridges off the Belgian-Dutch coasts [*e.g.* McCave, 1971; Terwindt, 1971; Veenstra, 1971] and together with the foregoing, the sand ridges and associated waves off East Anglia and the Outer Thames Estuary [*e.g.* Houbolt, 1968; Caston, 1972; Caston, 1979; Eisma *et al.*, 1979; Kenyon *et al.*, 1981; Stride *et al.*, 1982]. Mud deposits are considered in SUSPENDED SEDIMENTS.

Figure 1.4: The bottom sediment distribution of the North Sea [after Veenstra, 1971].

One aspect of the distribution of bedforms is that they have developed in response to sediment transporting processes [Caston, 1979]. Sand transport processes and patterns have been evaluated and summarised by Stride [1973] and Johnson *et al.* [1982]. Figure 1.5 shows the net sand transport directions around the British Isles as deduced from several lines of evidence including sand wave asymmetry, sand bank polarity and tidal current data [Johnson *et al.*, 1982]. For the southern North Sea, there is a zone of bed-load parting in the Southern Bight which determines that sand moves on one side, either northwestwards along the English Coast, with some being transported into the Wash, or north-northeastwards along the Belgian-Dutch Coasts towards the German Bight, and on the other side, southwestwards into the Thames Estuary or towards the Straits of Dover. At the Straits of Dover there is a bed-load convergence where sand from the North Sea meets sand transported along the Eastern Channel. Further aspects of sand transport in the North Sea are considered in SUSPENDED SEDIMENTS in relation to suspended sediment transport.

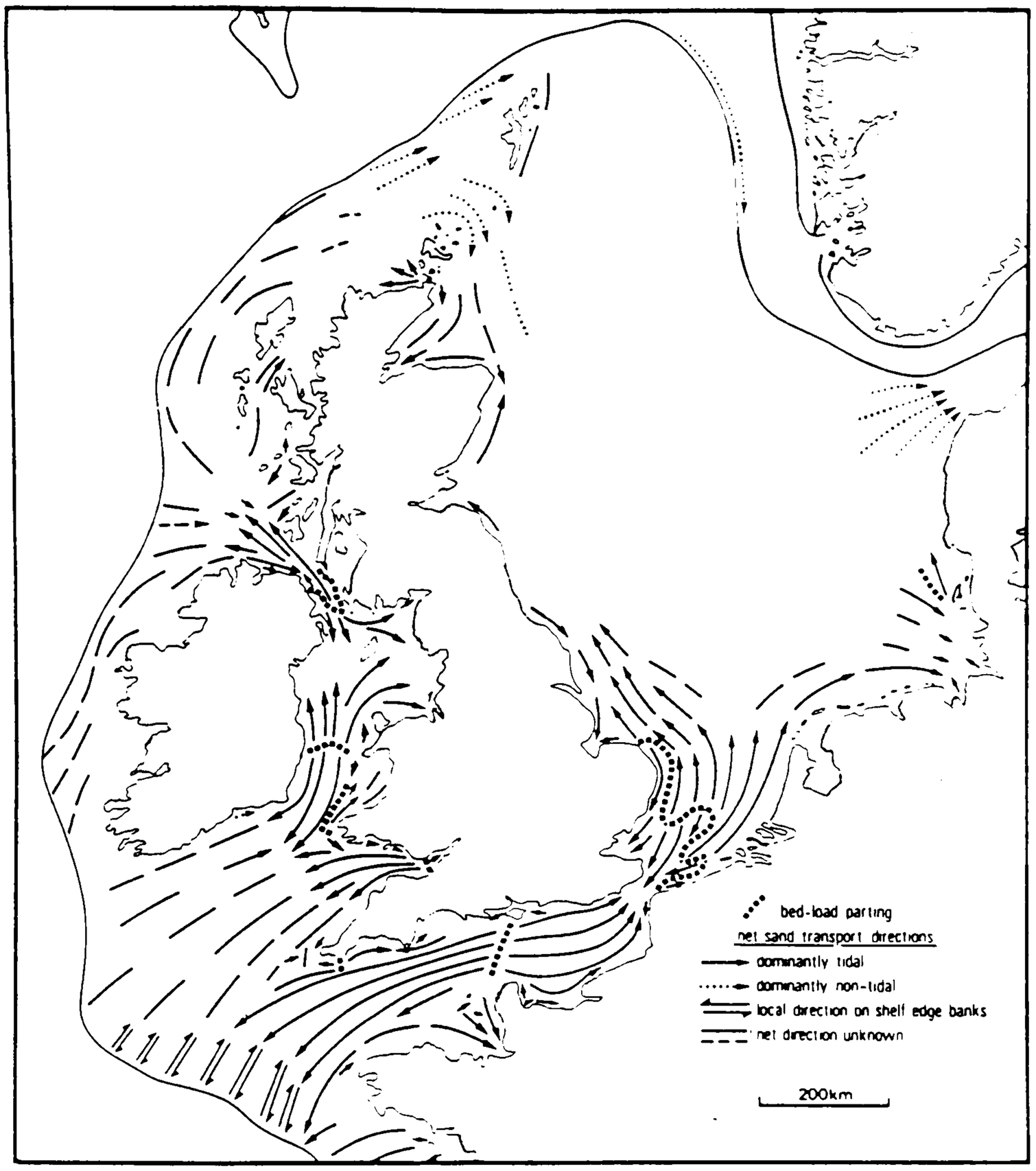

Figure 1.5: Net sand transport directions on the continental shelf around the British Isles [after Johnson *et al.*, 1982].

SUSPENDED SEDIMENTS

Previous research on suspended sediments in the North Sea has centred on three broad aspects. Firstly, budgetary studies [*e.g.* McCave, 1973; Eisma, 1981b; 1981c; 1990; Eisma and Kalf, 1987a] have attempted to describe the origins and dispersion of suspended sediment by estimating the budget of supply, deposition, and outflow to the Atlantic Ocean. Such studies are of practical value since they can be used, for example, to estimate the fate of pollutants associated the suspended sediment, but there are considerable uncertainties in the estimated figures not least because of the variable interpretations of the available data. Secondly, turbidity studies [*e.g.* Joseph, 1953; 1955; Postma, 1961; Otto, 1966; 1967; Lee and Folkard, 1969; Visser, 1970] have employed primarily optical techniques and form part of the overall investigations into the properties and discrimination of water masses in the North Sea, and the inter-relationships therein. Thirdly, regional studies, which include the collection of data on suspended sediment concentrations, organic content, particle size and mineralogy, have been made mostly in the Southern Bight [summarized by Eisma and Kalf, 1979], and also in the German Bight

[*e.g.* Irion *et al.*, 1987], the Skagerrak [*e.g.* van Weering *et al.*, 1987] and for the whole of the North Sea [*e.g.* Eisma and Kalf, 1987a; 1987b; Hölemann and Wirth, 1988; Nolting and Eisma, 1988; Wirth and Seifert, 1988].

Suspended sediment is supplied to the North Sea from a variety of sources and these are listed in Table 1.3 together with estimates of their relative quantities. The major supply comes from the North Atlantic and the Channel, despite the low concentrations involved (0.01-0.2 mg l^{-1} and *ca.* 3 mg l^{-1} respectively) but owing to the large inflows of water from these two sources (*ca.* 51,000 km^3 a^{-1} and 4900 km^3 a^{-1} respectively) [Eisma, 1987b]. Other significant sources include rivers and seafloor erosion, although in the case of the latter the figure is more uncertain than most due to the paucity of precise data [Eisma, 1981b]. Smaller yet substantial quantities are supplied from cliff erosion, particularly along the coasts of East Anglia and the Holderness Peninsula. These two areas are the dominant British sources of suspended sediment and supply more than the Thames and Humber rivers combined [McCave, 1973; 1987].

Table 1.3: Suspended Sediment Budget of the North Sea [from Eisma, 1990].

Supply	**Mt a^{-1}**
North Atlantic Ocean	10.4
Channel	17
Baltic	0.5
Rivers	4.8
Seafloor Erosion	9-13.5 (+?)
Coastal Erosion	2.2
Atmosphere	1.6
Primary Production	1
	46.5-64.0 (+?)

Outflow + Deposition	**Mt a^{-1}**
Outflow	11.4 + < 3
Deposition	
Estuaries	1.8
Waddensea + The Wash	5
Outer Silver Pit	1-4 (?)
Elbe Rinne	?
Oyster Grounds	2 (+?)
German Bight	3-7.5
Kattegat	8
Skagerrak + Norwegian Channel	17 (+?)
Dumped on Land	2.7
	51.9-62.4 (+?)

The transport of suspended sediment supplied from the sources shown in Table 1.3 principally follows the general residual circulation of the North Sea, resulting in a general suspended sediment distribution shown in Figure 1.6. Concentrations tend to decrease markedly from the Southern Bight to the north and towards the Skagerrak and Norwegian Channel. The 2 mg l^{-1} suspended sediment contour line [Figure 1.6a] largely coincides with the frontal transition zone described by Pingree and Griffiths [1978] and this separates the water in the Southern Bight and English, Dutch, German and Danish coasts from the main body of North Sea water [Eisma and Kalf, 1987a]. The highest concentrations of suspended sediment (> 10 mg l^{-1}) occur below this transition zone along the coasts of the Southern Bight and in the German Bight. Even higher concentrations (> 50 mg l^{-1}) occur in isolated areas, such as the high turbidity zones off the East Anglian and Belgian-Dutch coasts, and also in the German Bight southeast of Helgoland. Generally, concentrations measured close to the bottom are similar to those at the surface (*i.e.* < 10 mg l^{-1}), except in coastal waters where they are higher, such as the 130 mg l^{-1} measured in the German Bight southeast of Helgoland [Eisma and Kalf, 1987a].

The budget of suspended sediment is approximately balanced by an outflow (*ca.* 20% of the total supply) along the Norwegian coast into the Norwegian Sea between Shetland and Norway, and (Recent) deposition within the North Sea itself, within marginal estuaries and tidal flats and by dumping on land [Figure 1.6b]. Of the total amount of suspended sediment that is deposited in the North Sea, most (*ca.* 35-45%) is deposited in the Skagerrak and Norwegian Channel, and the Kattegat (*ca.* 15-20%). The remainder is deposited in other areas including the German Bight [Irion *et al.*, 1987]; the tidal flats of the Waddensea [Postma, 1981]; and the tidal flats of the Wash, and off the Belgian-Dutch and East Anglian coasts [McCave, 1981]. There are also other larger mud (or sandy mud) deposits in the North Sea outside the areas mentioned above which are relict features and have early Holocene origins [Figure 1.6b]. These deposits are reworked and tend to be associated with overlying water of low suspended sediment concentrations; hence the lack of Recent deposition in the northern and central North Sea and most of the southern North Sea, except for perhaps parts of the Elbe Rinne and the Outer Silver Pit [Eisma, 1981b; Eisma and Kalf, 1987a].

The concentration and composition of suspended sediment is influenced by seasonal and short term variations in water movements. During periods of storms and generally in winter, concentrations are several times higher than those during the summer and periods of calm conditions because suspended sediment is eroded or resuspended from the seafloor in the shallower parts of the North Sea. Johnson *et al.* [1982] recognize that sand transport rates and directions not only vary with the tidal cycles but also with non-tidal currents, such as wind-induced currents, that change the direction of net water transport. Likewise, Dickson and Reid [1983] have examined the effects of variations in the wind

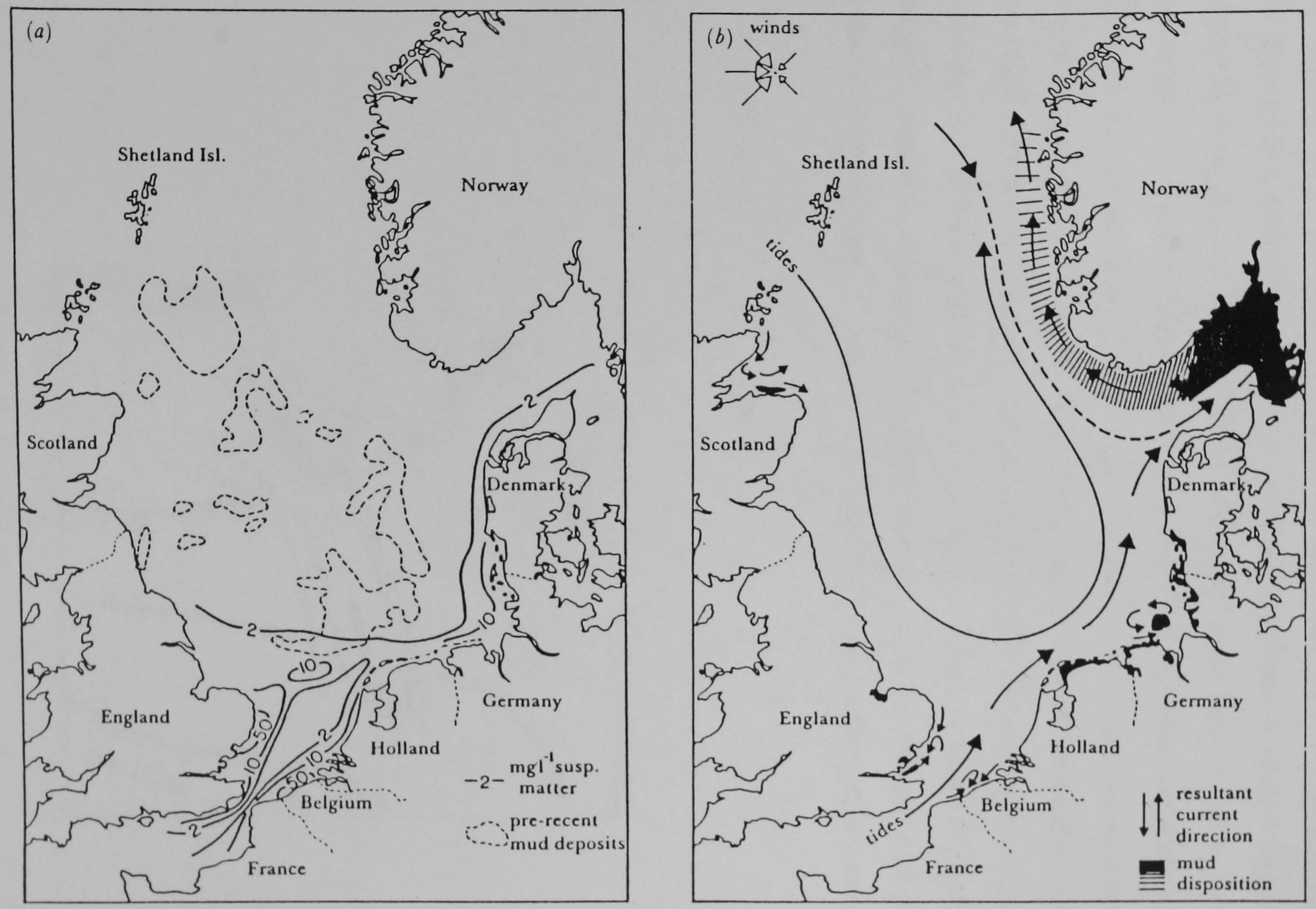

Figure 1.6: (a) General distribution of suspended sediment in the North Sea (in mg l^{-1}) and (b) resultant transport directions, location of recent mud deposits (in black) and older mud deposits [from Eisma, 1987b].

fetch and swell on water column turbidity in the Southern Bight in relation to development of the spring phytoplankton bloom. Lee and Folkard [1969] have also described an instance when increased turbidity levels in the Southern Bight were brought about during a period of northwesterly and northeasterly winds. Changes in water movement of this kind have been simulated in mathematical models [HYDROGRAPHY].

Another feature of sediment transport in the North Sea is that the net sand transport direction at any given point may deviate from the net suspended sediment (*i.e.* mud) transport direction at the same point by as much as 180° [Johnson *et al.*, 1982] as demonstrated in Figure 1.7. As observed by several turbidity studies [*e.g.* Joseph, 1957; Lee and Folkard, 1969] and others [*e.g.* McCave, 1972; §1.1], there is a zone of high turbidity off the East Anglian coast with an associated plume that is transporting suspended sediment northeastwards across the top of the Southern Bight towards the German Bight. The suspended sediment transport path is approximately at right angles to the peak tidal flow. Johnson *et al.* [1982] conclude that this apparent divergence is related to the different transport modes of the sand and mud fractions: the sand is transported by the stronger of the peak ebb or flood tidal flow and the suspended sediment by the weak net (residual) transport of water.

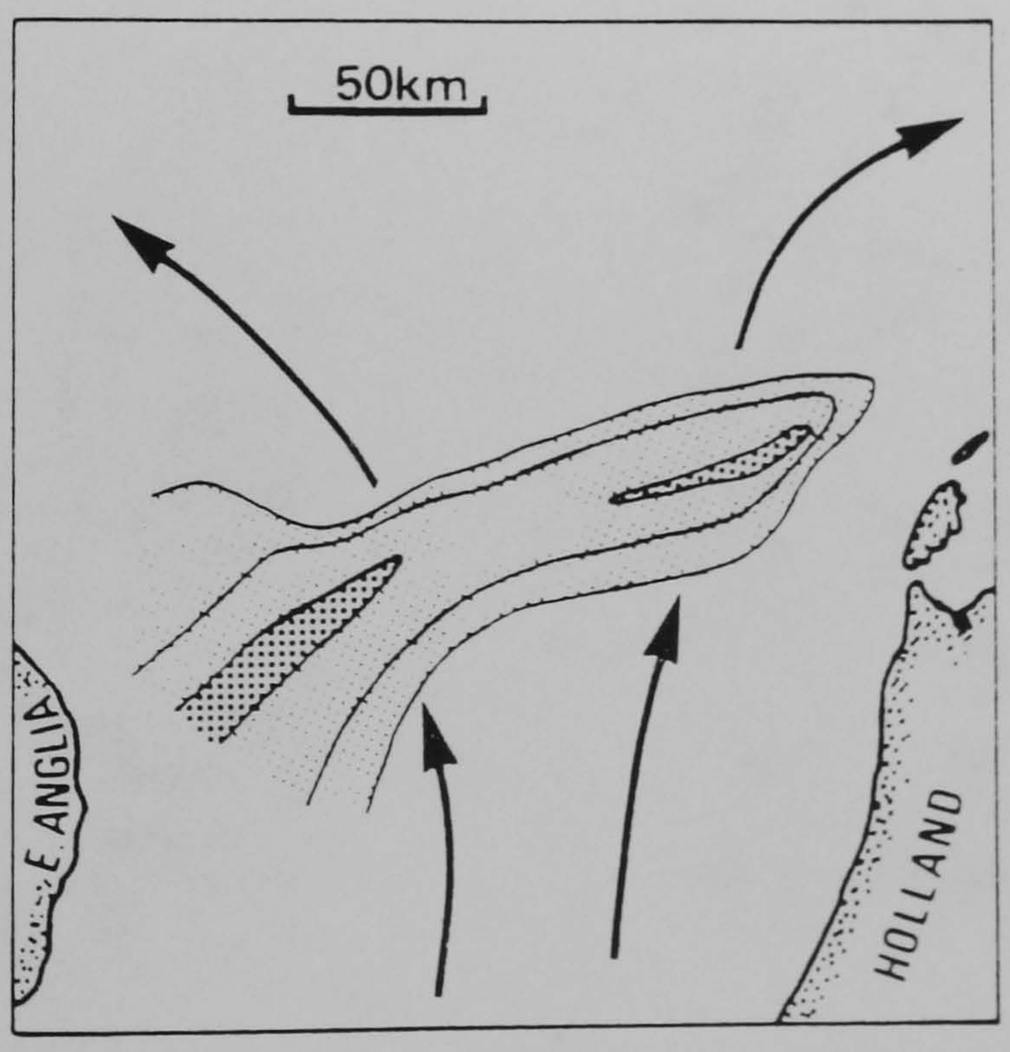

Figure 1.7: Plume of suspended sediment off East Anglia in relation to the peak tidal flow that transports the sand fraction [from Stride *et al.*, 1982].

Primary production produces living organic and non-living organic particles or detritus which may include inorganic components such as opal (*e.g.* diatom frustules) and carbonate (*e.g.* coccoliths). During the spring to autumn months, such organic matter temporarily forms part of the suspended sediment in the North Sea, sometimes in large quantities, particularly as *Phaeocystis* sp. along the margins and nutrient enriched waters of the Belgian-Dutch coasts and in the German Bight [Lancelot, 1990]. In winter there is very little primary production in the North Sea, and almost all of the organic matter produced during the year is mineralized, except for a few percent (< 10%) which remains in suspension as aggregates with mineral particles [Eisma and Kalf, 1987a].

The distribution and variability of organic matter concentrations in the North Sea are still uncertain not least because most field measurements have tended to be undertaken in winter [Eisma and Kalf, 1979]. Nonetheless, Eisma and Kalf [1987b] have reported that for January 1980 the highest concentrations of organic matter were observed in the continental coastal water in the southern North Sea and off Scotland (> 1 mg l^{-1}) [Figure 1.8a]. Concentrations were also generally high along the eastern side of the southern North Sea, decreasing towards the Skagerrak and the Norwegian Channel.

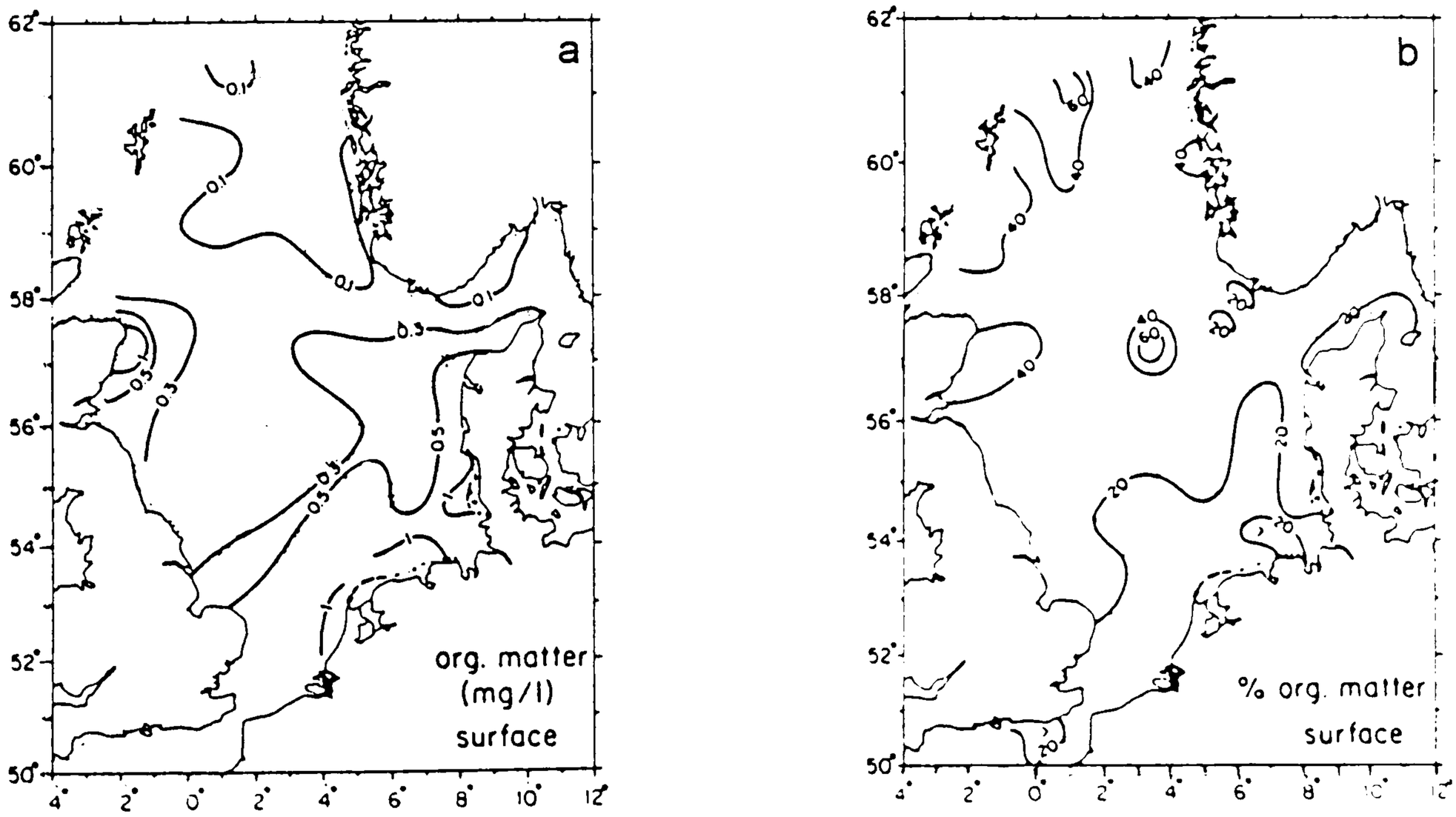

Figure 1.8: Distributions of (a) suspended organic matter (mg l^{-1}) and (b) organic content (%) in the surface waters of the North Sea for January 1980 [from Eisma and Kalf, 1987b].

The organic content (in % of the total suspended matter dry weight) exhibited a reverse trend: lowest in the eastern part of the southern North Sea (< 20%) and increasing towards the north (to > 60%) [Figure 1.8b]. Measurements of organic matter made in an earlier but less extensive cruise in June 1979 showed much higher and variable organic contents because of the presence of organic matter from localized primary production.

As with organic matter, data on particle size distributions for the North Sea (typically measured by using Coulter Counters) are also limited because sampling is typically carried out during the winter in order to avoid an admixture of living plankton which complicates the interpretation of the counts since the amount and the size distribution of the living plankton and the dead fraction (the inorganic fraction plus the organic detritus) vary to a large extent independently [Eisma and Kalf, 1979]. Winter data exists for the Southern Bight [Eisma and Kalf, 1979] and for the whole of the North Sea [Eisma and Kalf, 1987b]. These studies indicated that more than 90% of all the samples analyzed consisted of a number of admixtures of two main types of particle size distribution: one (Type A) with a peak at 30 to 100 μm, which dominates in the deeper water of the North Sea, north of the Dogger Bank and in the Skagerrak, and one (Type B) with a peak around 10 μm (5-15 μm), which is bell-shaped and dominates in the shallower coastal waters of, for example, the Southern and German Bights [Figure 1.9]. Both types were also found in measurements made in the summer but were strongly influenced by living plankton which produced additional peaks at sizes generally smaller than 20 μm (mostly at 2-5 μm).

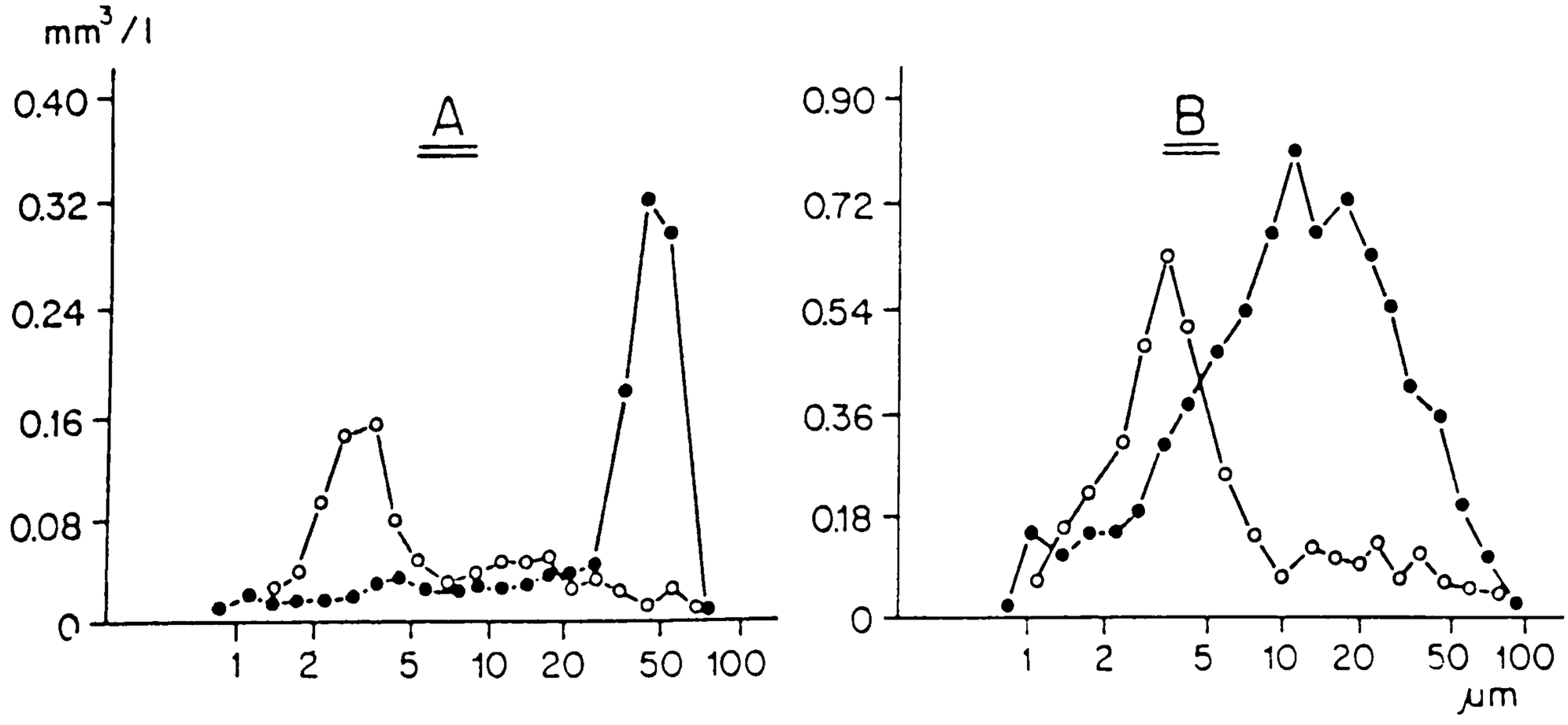

Figure 1.9: North Sea Type A and B particle size distributions [after Eisma and Kalf, 1987b].

DATA ACQUISITION AND PROCESSING

The following chapter describes the sampling strategy and techniques employed to collect the suspended sediment data for the Survey Programme; and the subsequent processing and quality control of the data.

2.1: North Sea Measurements

SAMPLING STRATEGY

For an adequate representation and resolution of the seasonal cycle, the Survey Programme was conducted for a period of 15 months, during which time 15 cruises, each lasting 12 days and repeated monthly, followed the same survey track. The duration of 15 months was adopted so that the seasonal cycle measurements would overlap by three months, and August (1988) was chosen as a starting date because this was expected to be a relatively quiescent period, thus allowing the autumnal overturn to be measured twice [Howarth, 1987]. The repeat period of about 30 days for each survey was linked to the spring/neap tidal cycle with the aim of visiting each position on the survey track at approximately the same stage in the cycle.

The survey track is shown in Figure 2.1 and is approximately 3700 km long. The track is constrained by the length of time available (*i.e.* 12 days) and is therefore restricted to only the southern North Sea. However, this still allows for the coverage of some of the more important features of the North Sea, such as the different density regimes either side of the Flamborough Head frontal transition zone; and the measurement of the longshore and offshore gradients near the mouths of all the major estuaries in the southern North Sea. Since the survey track represents a compromise between spatial coverage and spatial resolution, there are some weaknesses, albeit largely inevitable, in the survey design. For example, the survey track does not keep close to the Belgian-Dutch-German-Danish coastlines owing to operational constraints. This does result in some important loss of resolution in terms of suspended sediment concentrations and other parameters for these nearshore regions.

Continuous surface measurements and vertical profile measurements at a possible 120 stations were made along the survey track. The approximate positions of the North Sea survey stations are indicated in Figure 2.2. The stations in the well-mixed region of the southern North Sea (*i.e.* to the south of the Flamborough Head Front) are about 75 km apart and about 20-30 km apart in the frontal and stratified regions [Howarth, 1987].

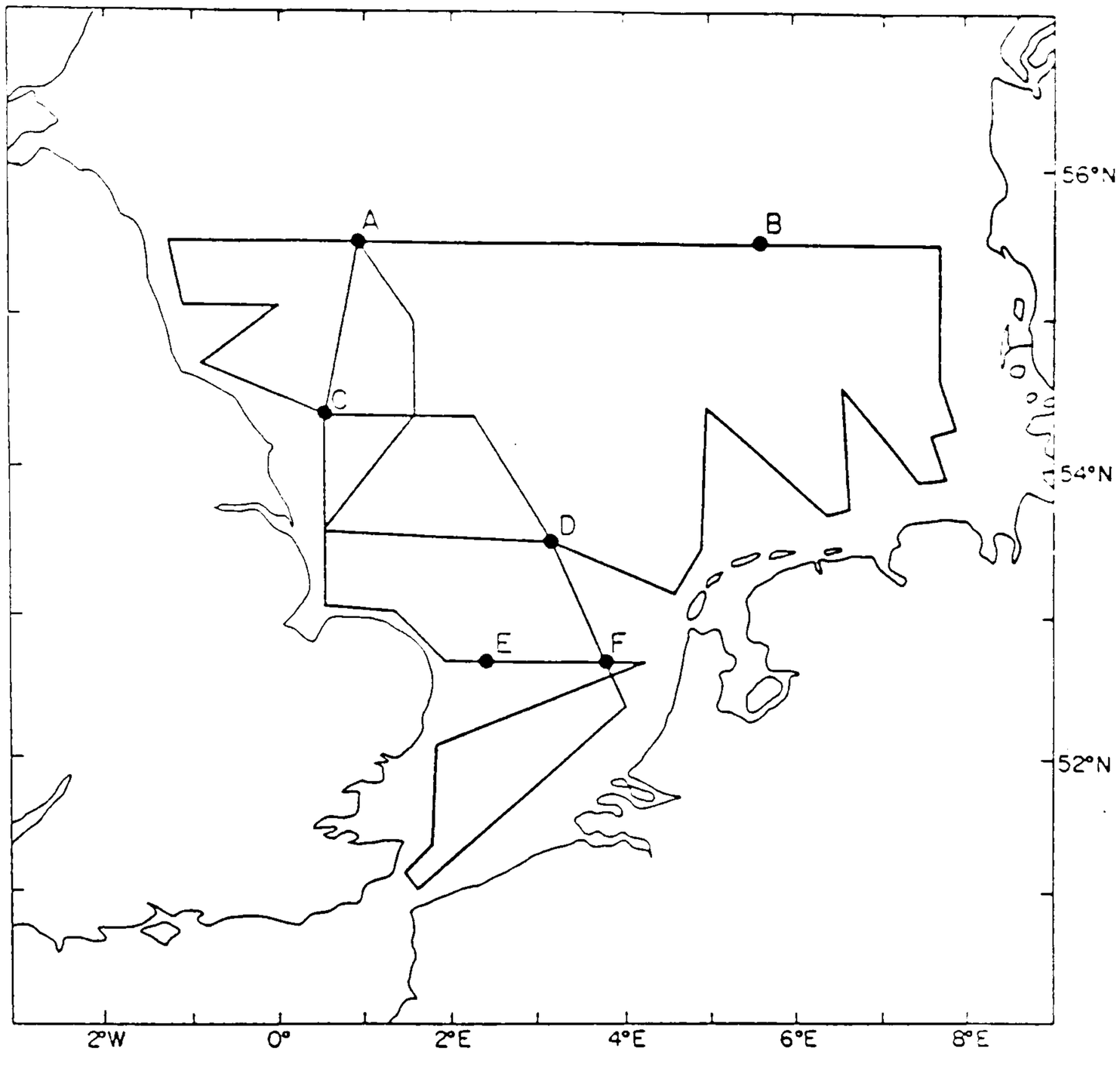

Figure 2.1: North Sea Survey Track.

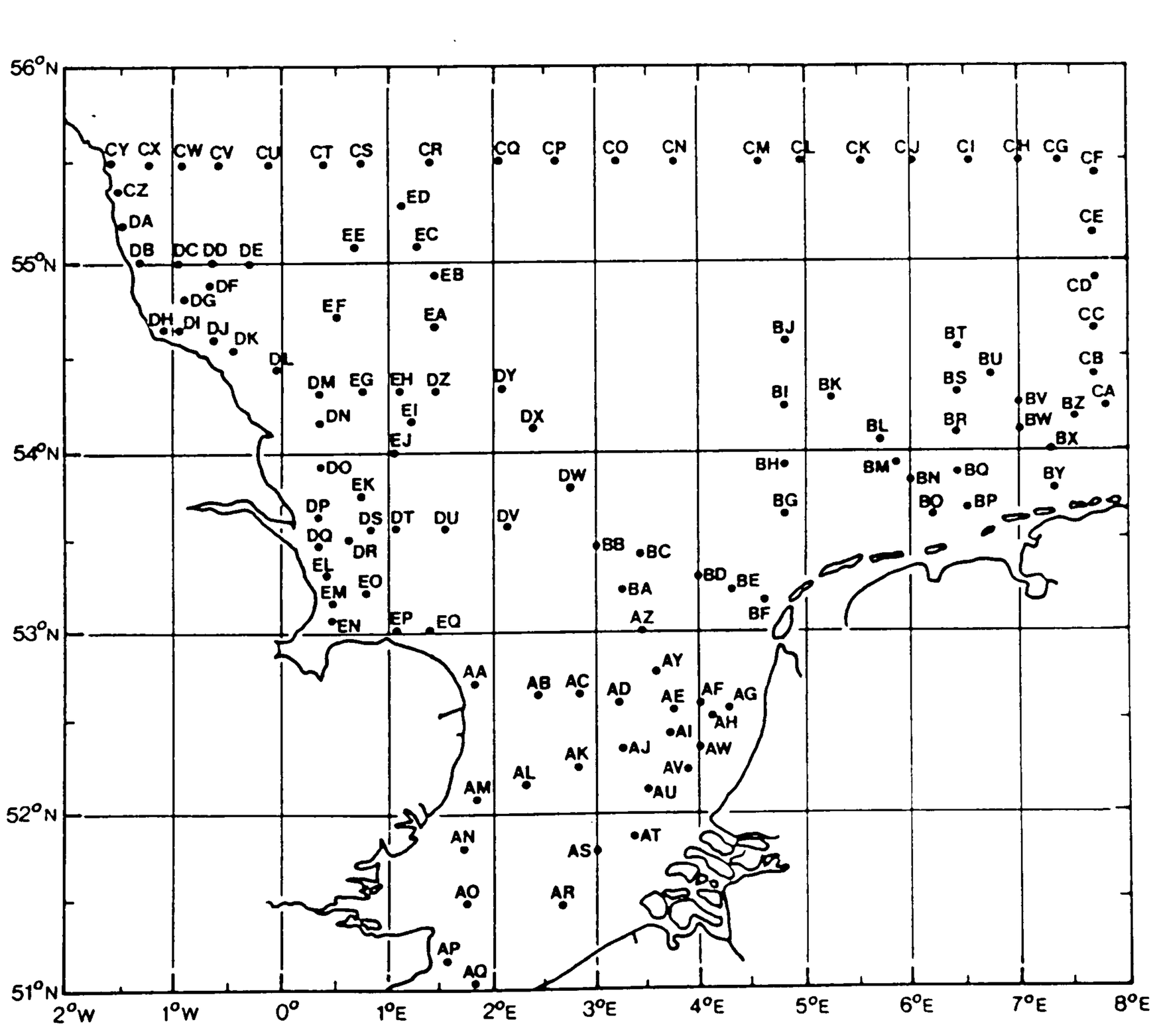

Figure 2.2: North Sea Survey Station Positions.

Table 2.1: North Sea Survey Cruise Information

Cruise ID	Cruise Dates	No. of Stations
	Shakedown Cruise	
CH28	29 April - 15 May 1988	164
	Survey Programme	
CH33	4 - 16 August 1988	110
CH35	3 - 15 September 1988	104
CH37	2 - 14 October 1988	72
CH39	1 - 14 November 1988	106
CH41	1 - 13 December 1988	61
CH43	30 December - 12 January 1988/1989	103
CH45	28 January - 10 February 1989	99
CH47	27 February - 12 March 1989	120
CH49	29 March - 10 April 1989	75
CH51	27 April - 9 May 1989	106
CH53	26 May - 7 June 1989	110
CH55	24 June - 7 July 1989	118
CH57	24 July - 6 August 1989	99
CH59	23 August - 4 September 1989	111
CH61	21 September - 3 October 1989	114
	Repeat Surveys	
CH66a	20 - 31 May 1990	82
CH72a	20 September - 2 October 1990	80

All the surveys were carried out on the NERC ship, *R.R.S. Challenger* and Table 2.1 gives details of the survey cruise dates and identification codes, together with the number of survey stations as given in Figure 2.2 that were sampled at least once on each survey. The table also includes 3 additional cruises outside the 15 cruises of the Survey Programme proper: firstly, a shakedown cruise (CH28) and secondly, 2 repeat surveys (CH66a and CH72a). These cruises extended the data set by allowing for comparison, 3 consecutive months of May (*e.g.* CH28, CH51 and CH66a) and 3 consecutive months of September (*e.g.* CH35, CH61 and CH72a).

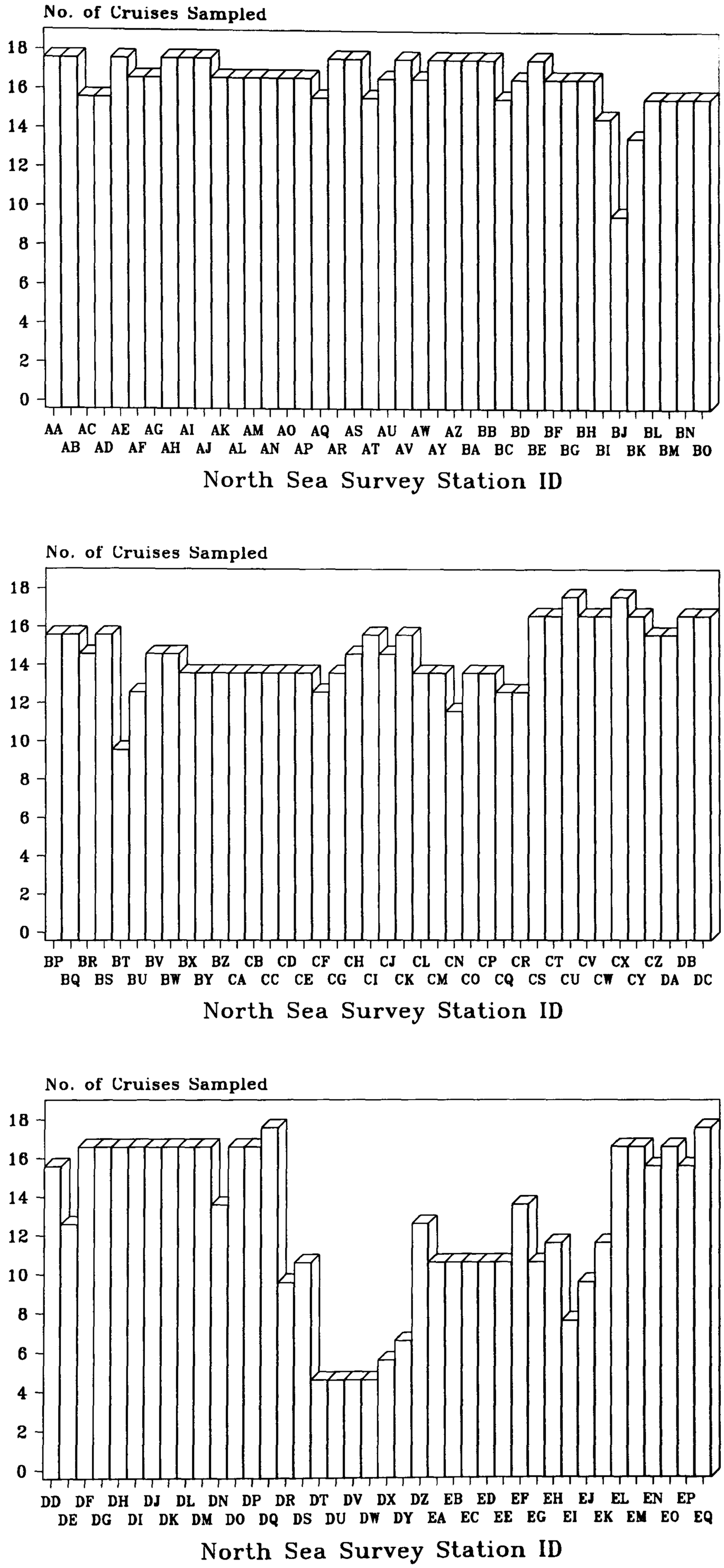

Figure 2.3: Bar charts showing the frequency of sampling at each Survey Station.

Some of the cruises fared better than others in terms of the number of stations sampled [*cf.* Table 2.1 and Figure 2.3]: the low station counts of particularly CH37 and CH41 were attributable to time lost through extremely bad weather, whereas for CH66a and CH72a, time was lost because of equipment failure. Furthermore, as regards the frequency of sampling of each station, Figure 2.3 reveals that stations DT to DY were sampled infrequently (*e.g.* only on 5 of the 18 cruises). These stations formed part of two sides of a triangle that was omitted when survey time was short, so that the spatial coverage at the boundaries of the survey area was not seriously affected [Howarth, 1987]. Inevitably this has resulted in a considerable loss of spatial and temporal resolution in an area close to the frontal transition zone.

BEAM TRANSMISSION

The measurement of suspended sediment concentrations in three dimensions was achieved by using *Sea Tech* 25 cm path-length beam transmissometers. The use of highly collimated beam transmissometers for this purpose has been previously demonstrated by Tyler *et al.* [1974] and Bartz *et al.* [1978] and the use of optical measurements as indicators of suspended sediment concentration is a well accepted practice [Biscaye and Eittreim, 1974; Carder *et al.*, 1974; Kullenberg, 1974; Pak, 1974; Pak and Zaneveld, 1978; Peterson, 1978; Pak *et al.*, 1980; Phillips and Scholz, 1982; Spinrad, 1986a; 1986b; Moody *et al.*, 1987; Qin *et al.*, 1988].

Continuous horizontal (surface) profiles of beam transmission were made along the survey track with a shipboard sampling system, incorporating transmissometers held in water jackets mounted on deck and installed within the flow of the ship's non-toxic (sea water) supply. Figure 2.4 shows diagrammatically the main elements of the shipboard transmissometer system. Two transmissometers were used for the simple reasons that two water jackets were constructed, one by Polytechnic South West (PSW) and one by NERC's Research Vessel Services (RVS); and either one of the transmissometers could be used as a spare for the others. Header tanks were also used to try and reduce the aeration effects caused by air bubbles in the non-toxic water supply entering the water jackets and affecting the signal of the transmissometers [*q.v.* §2.2]. The flow meters were normally set at a water flow of *ca.* 20-25 l min^{-1}, except during bad weather when the flow was reduced to approximately 10 l min^{-1}, again to try and minimize aeration effects. At a nominal ship's survey cruising speed of 10 knots (18.5 km h^{-1}) and a shipboard computer logging interval of 30 seconds for the deck-mounted transmissometers, a horizontal resolution of *ca.* 150 m was achieved.

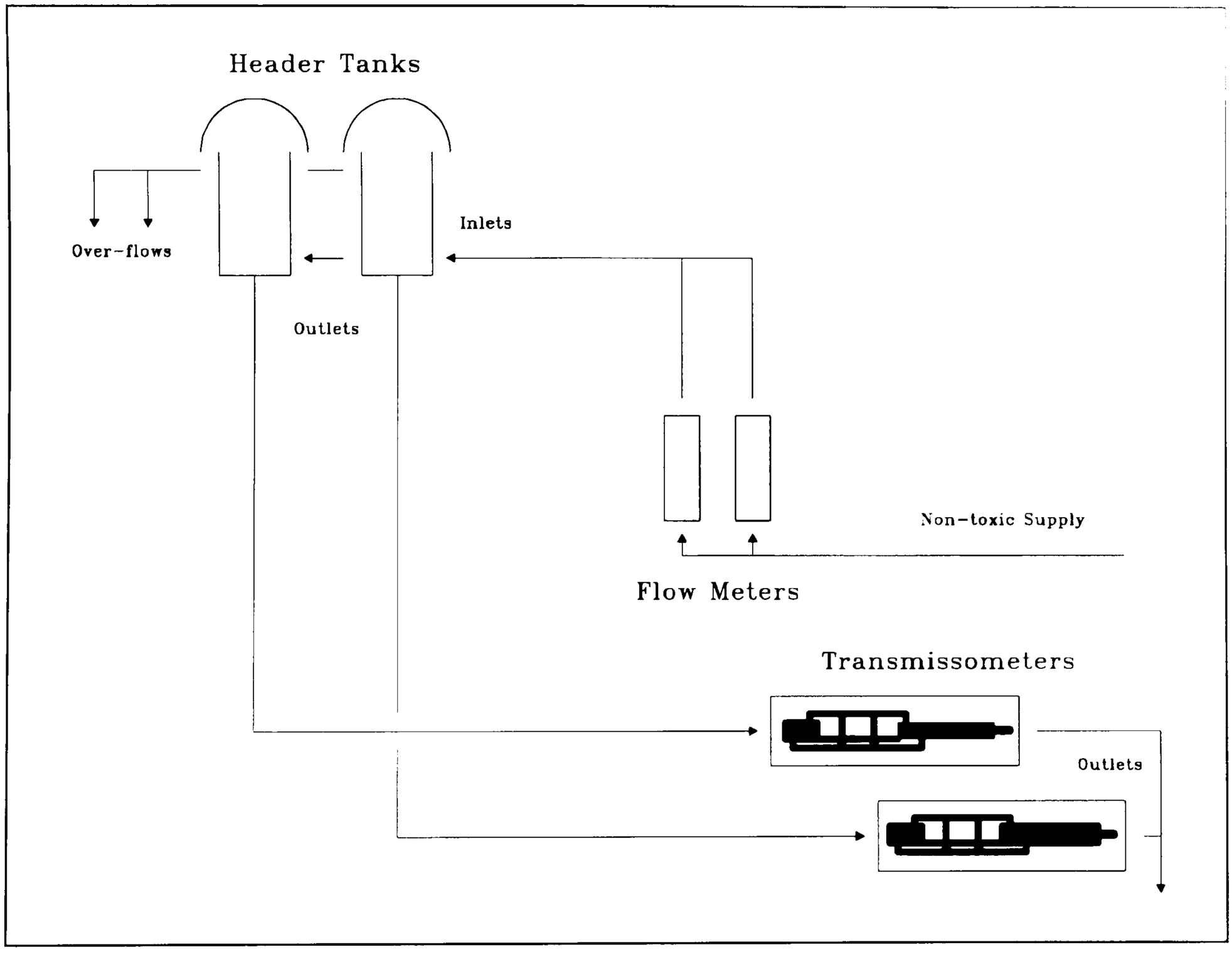

Figure 2.4: Principal components of the shipboard transmissometer system.

Vertical profiles of beam transmission were made by means of a transmissometer mounted horizontally on to the support frame of a *Neil Brown* CTD instrument which was deployed at each survey station and provided both a down-cast profile and an up-cast profile. The transmissometer was mounted as low down on the frame as possible so that the profiles of beam transmission would extend close to the sea bed: generally *ca.* 1-2 m off the sea bed during calm conditions, and > 2 m during rough seas. The CTD-mounted transmissometer was logged at 1 second intervals by the shipboard computer.

As part of the routine of each survey, all the transmissometers were maintained and cleaned on a daily basis, weather and other factors permitting: the windows of each transmissometer were cleaned using non-abrasive tissues with a solution of mild washing-up liquid and water, and then rinsed with distilled water. After drying the windows, the output voltage in air (the Air Reading) and the zero voltage output with the light path blocked, of each transmissometer were taken so that air calibration corrections could be applied [§2.2]. In addition, both water jackets were hosed down and cleaned to remove any sediment that might have settled inside.

SUSPENDED SEDIMENTS

In order to calibrate the data from the transmissometers in terms of suspended sediment concentration, water samples were taken by means of standard 10 l Go-Flo (**G**eneral **O**ceanics, **Flo**rida) water bottles supported on a single frame, 12 bottle rosette sampler, attached on top of the CTD support frame and above the CTD sensor and transmissometer. The distance between the base level of the water bottles and the transmissometer was about 1 m. At predetermined survey stations water samples were routinely taken from 3 depths: one at the surface, one at the bottom and one from the middle. The middle sample was generally taken at mid-depth, but sometimes at an interesting feature in the water column observed on the visual display of the BBC microcomputer CTD monitoring system (*e.g.* a nepheloid layer at the base of the thermocline). A total of 4,672 water samples were taken for suspended sediment analysis during the 18 survey cruises.

On completion of a CTD survey station, sub-samples from the water bottles were taken for use by other experiments (*e.g.* salinity calibration, nutrients, chlorophyll and trace gases), with the water remaining (*ca.* 6 l) available for the suspended sediments experiment. The residue water from each bottle in turn was discharged into a clean 10 l plastic bucket. Measured volumes of each water sample (between 0.5 and 6 l) were filtered for suspended sediments by using a vacuum filtration system situated within a laminar flow cabinet, as depicted in Figure 2.5. For cruises CH28 and CH33 to CH39, all samples were filtered through pre-weighed 47 mm diameter Whatman Type WCN (cellulose nitrate) membrane filters of pore size 0.45 μm. For cruises CH41 to CH72a, samples were filtered through pre-ashed and pre-weighed 47 mm

diameter Whatman GF/C (glass-fibre) filters with a nominal pore size of 1.2 μm. The reasons for the change in the type of filter used are discussed in §2.2. Once the samples were filtered, the filters were rinsed with distilled water to remove salt and suction continued to remove all traces of water. The filters were then placed in plastic petri-dishes, air dried in a laminar flow cabinet and then frozen.

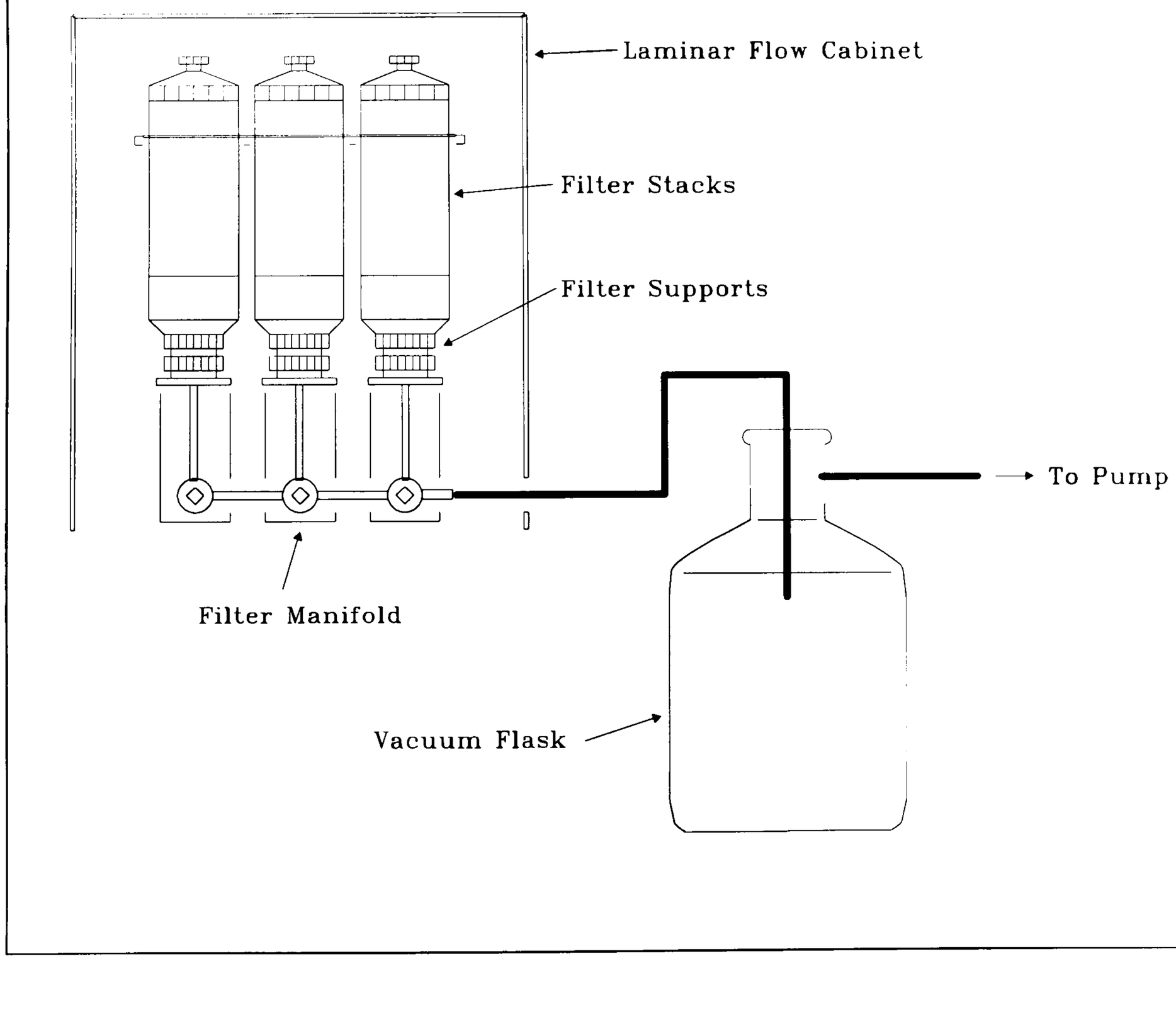

Figure 2.5: Vacuum filtration system.

OTHER MEASUREMENTS

In addition to the beam transmission and suspended sediments measurements, numerous other variables were measured during the course of the Survey Programme. A summary of the variables measured is given in Table 2.2. These data were included into the North Sea Database for use by the other participants of the Project. Further data were also obtained from other sources (*e.g.* the UK Water Authorities and the Meteorological Office).

Table 2.2: Other North Sea measurements.

Underway Measurements
Surface: Conductivity (Salinity), Temperature, Fluorescence (Chlorophyll), Dissolved Oxygen Current Profiles (Shipboard acoustic doppler current profiler (ADCP)), Irradiance, Air/Sea Fluxes
Water Column Measurements
Conductivity (Salinity), Temperature, Pressure (Depth), Fluorescence (Chlorophyll), Nutrients, Dissolved Oxygen, Trace Metals and Biogenic Trace Gases
Seabed Measurements
Benthic Fluxes (Coring)
Mooring Measurements
Temperature (Thermistor Chains), Currents (Seabed ADCP and Current Meter Strings), Fluorescence
Ancillary Data
UK River Discharge Data (1988-1989), Meteorological Data (Met. Office Model only) and Modelled Current Residual Data (POL)

2.2: Data Processing and Quality Control

BEAM ATTENUATION

All the initial processing and flagging (*e.g.* assigning a quality control tag) of the transmissometer data were undertaken by BODC to a specification prescribed by the author. Table 2.3 gives a summary of the basic procedures that were used for both the CTD-mounted and deck-mounted transmissometers.

Table 2.3: Data reduction of the transmissometer data to beam attenuation.

<table>
<tr><th colspan="2">Processing of the CTD and Surface Transmissometer Data</th></tr>
<tr><td colspan="2">Raw data cycles (in volts DC) air corrected using:

$V = (A/B) \,.\, (X-Z)$

where V is the corrected voltage output, A is the air calibration value at time of manufacture, B is the shipboard air calibration reading, X is the uncorrected data cycle and Z is shipboard zero offset</td></tr>
<tr><th>CTD Transmissometer</th><th>Surface Transmissometers</th></tr>
<tr><td>Air corrected data cycles converted to % Transmission (%T) using:

$\%\ Transmission = 20 \,.\, V$

Errant values flagged S suspect if outside prescribed range of
1 %T (≈saturated) to 91.3 %T (=clean water)</td><td rowspan="3">Air corrected data cycles de-spiked using:

(a) A First Difference Criterion (FDC) of 0.6 volts DC

(b) Box-car Averaging (using 12 data cycles, average of the 12, and a full overlap of 11)

Data cycles flagged S suspect if any of the 12 cycles deviate by more than FDC from the average</td></tr>
<tr><td>Delimitation of down-cast using the Iris CTD screening program</td></tr>
<tr><td>%T data de-spiked and errant data flagged S suspect</td></tr>
<tr><td>Determination of down-cast %T range spanned by each CTD Go-Flo water bottle</td><td>Conversion of data cycles to %T</td></tr>
<tr><td colspan="2">Conversion of %T to Beam Attenuation Coefficient c (m^{-1}) using:

$c = -4 \,.\, ln\ (\%T/100)$</td></tr>
</table>

The only correction applied to the raw data cycles was the air calibration correction which corrected for the loss in intensity of the light source (LED) of the transmissometer during its operation. During the Survey Programme, a total of 4 different transmissometers were used and each showed an approximate decrease in intensity of between 0.5 and 0.7% 1000 hr^{-1} of operation. The frequently measured air readings allowed for the compensation of this change.

An additional error in the beam transmission measurement cited in the scientific literature is that due to the inclusion of forward scattered light which has the effect of over-estimating the measured transmission [*e.g.* Jerlov, 1976; Bartz *et al.*, 1978; Sea Tech, 1988]. The magnitude of the error varies with, for example, the particle or suspended sediment concentration, and the type, index of refraction and size distribution of the particles. For example, Sea Tech [1988] have shown that for beam transmissions of < 1%T the measurement error caused by forward scattering can be as large as 40-50% in waters containing resuspended sediments or suspended sediment of terrigenous origins. In absolute terms however, these errors are small, and the beam transmission measurements were not corrected for forward scattering.

The essential differences in the processing of both sources of data relate to the nature of the de-spiking procedure. Individual CTD profiles were examined visually using the IRIS graphics workstation and BODC screening system [described in BODC, 1989]. The start and end of the down-cast profile was delimited since it was this profile that would be included in the database and also be used to draw the appropriate calibration beam attenuation values. The CTD transmissometer data were then checked and flagged manually. The decisions concerning the flagging of suspect data were taken by BODC but these were overseen for the first few cruises. Once the data had been checked, the up-cast pressure range spanned by each water bottle was determined and this range was used to extract a coincident range of % transmission values from the down-cast. Owing to the very large number of data cycles (typically 43,000 cycles transmissometer^{-1} cruise^{-1}) the surface transmissometer data were de-spiked and flagged automatically by a first difference computer program developed by BODC. The flagging of errant data as suspect did not result in their removal from the dataset but merely that they were ignored by computer applications software (*e.g.* plotting routines).

A particularly acute problem with the surface transmissometer output was the generation of signal noise caused by the presence of air bubbles in the non-toxic water supply. During CH28 pulses of air bubbles were observed passing through the PSW transmissometer water jacket (which was constructed of clear Perspex) as the survey ship pitched and rolled during periods of heavy seas. The bubbles were being drawn in through the non-toxic water intake located approximately 2 m below the water line just astern of the starboard bow of the ship. Optical studies of micro-bubble fields in the North Sea [*e.g.* Ling and Pao, 1988; Su *et al.*, 1988] have reported bubble diameters of between 20 to 400 μm under a wide range of wind speeds and water depths. The larger bubbles (*e.g.* > 100 μm) are produced by breaking waves, and together with the bubbles generated by the pitching motions of the ship's hull, these will contribute substantially to the attenuation of the transmissometer light beam as they enter the water jacket. An example of this aeration effect is given in Figure 2.6. The air bubbles have the effect of generating irregular fluctuations in the signal output by some 1-3 volts DC (≈ 20-60 %T) from a base-level output of about 4 volts DC (≈ 80 %T). The interluding quiescent periods

represent CTD survey stations when the ship is stopped and positioned so that the starboard side is protected from the full force of the wind for easier deployment of the CTD. As a result, the non-toxic intake is protected from the main direction of wave attack, and also the generation of bubbles is greatly reduced due to the less violent pitching of the ship's bow. Following CH28 and in conjunction with reducing the surface transmissometer flow rates during heavy seas, header tanks were incorporated into the system to try and alleviate the problem by allowing time for the air bubbles to rise out of the sea water at the top of the header tank. Some improvement was achieved in the signal-noise ratios in all cases of rough seas except for the more extreme cases (*e.g.* > wind force 7-8). For the purposes of data processing, the sections of noisy data due to heavy seas were flagged suspect: firstly by using the FDC procedure and secondly by a visual inspection of the data cycle record. Approximately 10% of the surface transmissometer data were removed in this way.

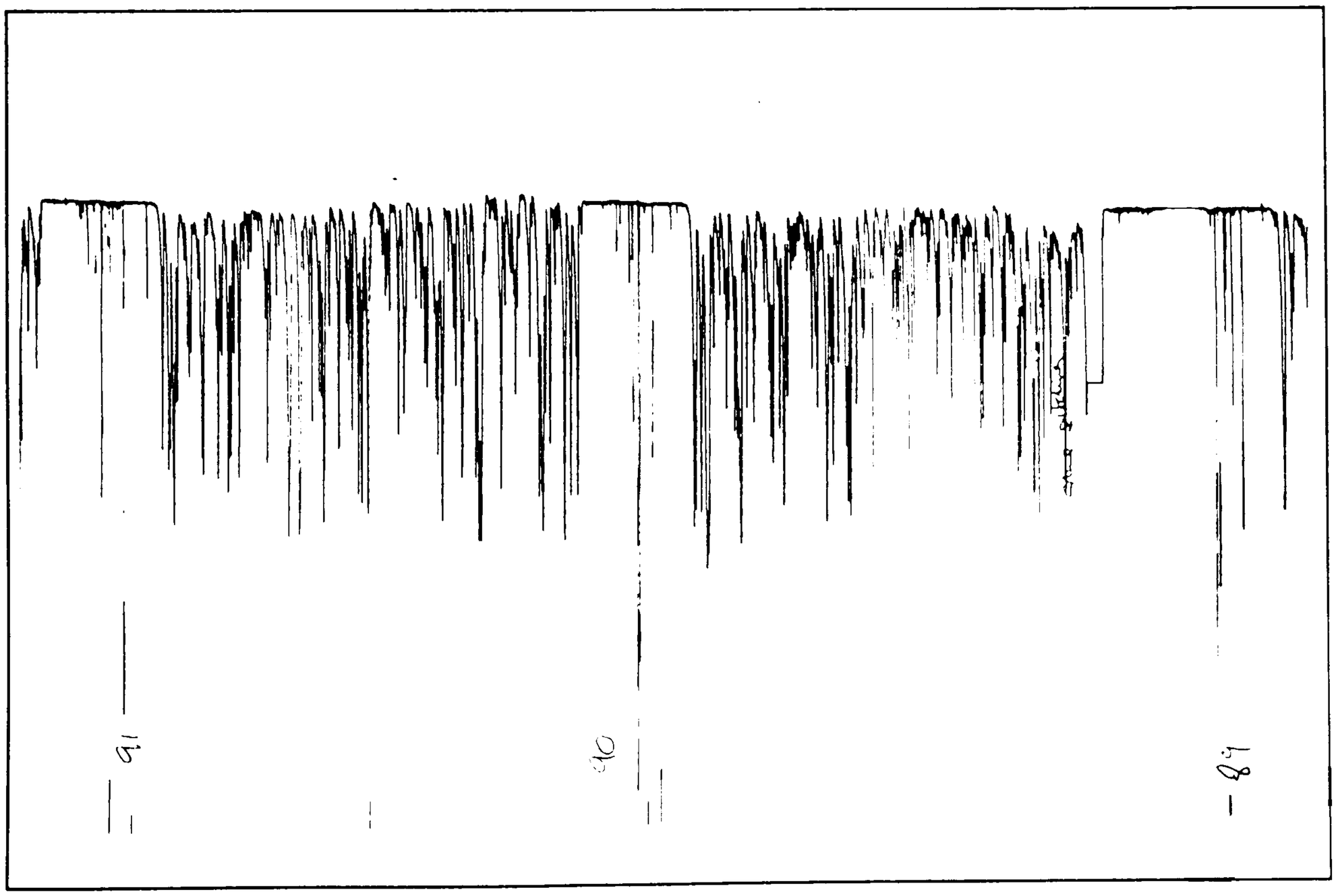

Figure 2.6: Extract of a plot of PSW surface transmissometer signal output (volts DC) from CH28 illustrating the aeration effect caused by bubbles in the non-toxic supply for a wind force 6.

The final processing procedure involved the conversion of the beam transmission measurement into beam attenuation. The beam attenuation coefficient c (m^{-1}) of a suspension is a standard optical parameter, defined by Baker and Lavelle [1984] as *a measure of the energy removed from a fixed-length light beam by both scattering and absorption* so that:

$$c = a + b$$

where a is the absorption coefficient (m^{-1}) and b is the volume scattering coefficient (m^{-1}). The light lost from a well-collimated and monochromatic beam of light can be written as:

$$T_z = e^{-cz}$$

where T_z is the % light transmitted over a distance z. The beam attenuation coefficient c can be computed accordingly by:

$$c = -ln(T)/z$$

where z is the pathlength of the transmissometer.

The beam attenuation coefficient can also be subdivided into 3 principal components: c_w, that due to water; c_p, that due to suspended sediment; and c_y, that due to dissolved organic substances (yellow matter); so that:

$$c = c_w + c_p + c_y$$

Because the Sea Tech transmissometer employs a light source with an operational wavelength of 670 nm (*i.e.* the red part of the spectrum) and yellow matter absorbs strongly in the blue part of the spectrum, the attenuation due to yellow matter is negligible [Jerlov, 1976; Sea Tech, 1988]. Therefore in this respect, attenuation is due to the suspended sediment and water only. For the purposes of the North Sea Database and the incorporation of the attenuation data therein, the term *Optical Attenuance*, *i.e.* $(c_w + c_p)_{670\ nm}$, was adopted.

SUSPENDED SEDIMENTS

All the processing and quality control of the water sample filter data were undertaken at Plymouth, and Table 2.4 gives a summary of the basic procedures and gravimetric methods that were employed to derive the total, inorganic and organic suspended sediments concentrations.

Table 2.4: Data reduction by gravimetry of the water sample filters to suspended sediment and component concentrations.

Processing of the Suspended Sediments Sample Data
Cruises CH28-CH39
WCN Filters air dried and stored in desiccator Weighed to 5 decimal places (*e.g.* 0.00001 g)
Total suspended sediment concentration (mg l^{-1}) derived by: $((PoW - BC_{PoW}) - PrW)$ / sample volume (l) where PrW is the filter pre-weight (mg), PoW is the filter post-weight after filtration (mg) and BC_{PoW} is the post-weight correction factor (mg)
Cruises CH41-CH72a
GF/C Filters oven dried at 100°C ± 5°C for 6 hours and cooled in desiccator to micro-balance temperature Weighed to 5 decimal places (*e.g.* 0.00001 g)
Total suspended sediment concentration (mg l^{-1}) derived by: $((PoW - BC_{PoW}) - PrW)$ / sample volume (l)
GF/C Filters ashed at 450°C ± 5°C for 8 hours in muffle furnace and cooled in desiccator to micro-balance temperature Re-weighed to 5 decimal places
Inorganic sediment concentration (mg l^{-1}) derived by: $((AsW - BC_{AsW}) - PrW)$ / sample volume (l) where AsW is the filter ash-weight (mg) and BC_{AsW} is the filter ash-weight correction factor (mg)
Organic sediment concentration (mg l^{-1}) derived by: Total suspended sediment - Inorganic suspended sediment

As part of the overall data quality control policy, and for every cruise except CH28, a single filter was taken from a batch of filters and set aside as a balance control. This was weighed about every tenth filter to monitor possible fluctuations in laboratory environmental conditions (*e.g.* temperature and humidity) and balance drift. The resulting balance control statistics are given in Table 2.5. The general improvement in the precision (s statistics) and the

accuracy (α statistics) of the measurements would seem to reflect firstly, the change from using WCN type filters to GF/C filters (*e.g.* CH39 $\rightarrow$ CH41) and secondly, the servicing of the first, mechanical balance, and the change from the latter to a second, electronic balance.

Table 2.5: Balance control filter statistics (in mg) for CH33 to CH72.

Cruise	Mean $\bar{x}$	Standard Deviation s	Standard Error α $(s/\sqrt{n})$
CH33	86.917	0.103	0.013
CH35	84.253	0.213	0.026
CH37	83.794	0.314	0.043
CH39	83.820	0.299	0.044
CH41	88.297	0.102	0.013
CH43	88.420	0.129	0.022
CH45 †	89.329	0.074	0.014
CH47	89.278	0.081	0.020
CH49	87.261	0.058	0.010
CH51	88.382	0.060	0.011
CH53	87.536	0.062	0.013
CH55	87.472	0.066	0.012
CH57 ††	89.982	0.029	0.006
CH59	90.152	0.031	0.008
CH61	90.887	0.047	0.009
CH66a	93.183	0.029	0.005
CH72a	93.262	0.023	0.009

† *Sartorius* 2474 Semi-micro Balance serviced under maintenance contract
†† Change to *Sartorius* R 200D Electronic Semi-micro Balance

An additional problem associated with the use of filters is the loss of some of the filter fabric during the filtration process itself. In order to gauge and correct for this loss a number of filters were set aside for use as blank correction (BC) filters. Generally a BC filter was used every tenth filter by placing it beneath a regular one so that both filters would undergo the same procedure. After filtration and rinsing, the BC filters were stored separately and then processed in exactly the same way as the regular ones. The resulting BC filter weights were used to derive the correction factors BC_{PoW} (post-weight) and BC_{AsW} (ash-weight) and these and other descriptive statistics are listed in Table 2.6.

Table 2.6: Weight correction factors and statistics (in mg) derived from the blank filters.

Cruise	Post-weight Correction			Ash-weight Correction		
	Mean $\bar{x}$ (BC_{PoW})	Standard Deviation s	Standard Error α	Mean $\bar{x}$ (BC_{AsW})	Standard Deviation s	Standard Error α
CH28	-0.529	0.912	0.186			
CH33	-0.855	0.599	0.115			
CH35	-1.213	0.663	0.133			
CH37	-0.121	0.552	0.130			
CH39	-0.189	1.134	0.222			
CH41	0.637	0.709	0.183	0.459	0.614	0.159
CH43	0.393	0.436	0.106	-0.138	0.302	0.073
CH45	0.074	0.194	0.039	-0.310	0.190	0.038
CH47	0.182	0.374	0.070	0.030	0.272	0.051
CH49	2.200	0.885	0.256	1.469	0.762	0.220
CH51	0.836	0.650	0.145	0.104	0.511	0.114
CH53	1.575	1.444	0.340	0.686	1.142	0.269
CH55	0.631	0.592	0.121	-0.397	0.560	0.114
CH57	0.659	0.546	0.141	0.213	0.523	0.135
CH59	1.542	0.602	0.116	1.027	0.511	0.100
CH61	0.262	0.226	0.052	-0.129	0.187	0.043
CH66a	0.223	0.230	0.066	-0.195	0.159	0.046
CH72a	0.548	0.564	0.156	-0.064	0.284	0.080

There is a striking contrast between the post-weight correction factors of the WCN and GF/C filters: all negative values in the case of the former and all positive in the case of the latter. The reasons for this phenomenon are uncertain but they may be concerned with different filter performances relating to a number of factors such as the loss of filter material (*e.g.* fibres) or leachable materials within the filters (*e.g.* wetting agents), and retention of dissolved organic substances and/or sea water salts. In the case of the WCN filters, the loss in weight of *ca.* 2% for filters typically weighing between 80 and 90 mg was anticipated, and is entirely consistent with the manufacturer's specification [Whatman, 1988] and other published data [*e.g.* Banse *et al.*, 1963; Eaton *et al.*, 1969]. This is a significant loss in gravimetric analyses when the suspended sediment concentrations are low (*e.g.* only a few mg l^{-1}) and the use of blank filters, therefore, is of paramount importance to correct for this. In the case of the GF/C filters the weight gain of up to 3% (*e.g.* CH49) was not anticipated. Reasons for this gain may be related

to the retention of dissolved organic substances by the filters [Cranston and Buckley, 1972; Abdel-Moati, 1990]. Cranston and Buckley [1972] found that for a 0.1l humic acid solution with a concentration of 10 mg l^{-1}, a glass fibre filter could retain on average about 5% of the dissolved humic acid. Such a possibility is also corroborated by the fact that on combustion in a muffle furnace all the *BC* filters lost weight as indicated by the smaller ash-weight corrections listed in Table 2.6. A further possibility to consider is the retention by the filter of sea water salts due to deficient or ineffectual rinsing with distilled water. This can largely be discounted because during the gravimetric analyses, all filters that displayed anomalously high weights (a subjective decision based on the difference between a visual estimate of the anticipated increase in filter weight and the actual measured one, and also on the hue of the material retained by the filter) were registered as being suspect due to possible salt retention. Suspicions were then later confirmed following the ashing process when un-rinsed or poorly rinsed filters displayed dendritic salt patterns [as coined by Peterson, 1978], and accordingly these filters were discounted from any further analysis.

As evident from Table 2.6, there are no ash-weight correction statistics for CH28 to CH39. This is owing to the extreme difficulties experienced in determining the organic/inorganic composition of the suspended sediment by adopting broadly similar procedures of other researchers [*e.g.* Manheim *et al.*, 1970; Eisma and Kalf, 1987b] and ashing the WCN filters in porcelain crucibles at 500°C for 8 hours. Once the filter and the organic component had been vaporized, the residue remaining in the crucible (*i.e.* the inorganic component) typically amounted to only a few mg in weight, corresponding to the generally low suspended sediment concentrations measured during the early cruises. Taking into consideration the difficulties in handling such small amounts and the errors listed in Tables 2.5 and 2.6, it was not possible to measure the organic/inorganic components with any degree of confidence or precision using the WCN type of filters. A concerted decision was made therefore, to switch from a membrane filter to a glass fibre depth filter.

The original decision to use WCN membrane filters was based firstly, on the common use of membrane filters apparent in the scientific literature [*e.g.* Manheim *et al.*, 1970; papers in Gibbs, 1974; Eisma and Kalf, 1979; 1987b]; secondly, on the use of 0.4 or 0.45 μm pore size filters as the operational distinction between dissolved and particulate forms [*e.g.* Burton, 1976; Danielsson, 1982], thereby eliminating glass fibre filters which normally only have nominal pore sizes of either 1.2 μm (*e.g.* Whatman Grade GF/C's) or 0.7 μm (*e.g.* Whatman Grade GF/F's); and thirdly, by considering the pros and cons (*e.g.* filter weight stability, sediment loading, flow rates and expense) associated with using cellulose ester type (*e.g.* Whatman, Millipore and Sartorius) membrane filters and nucleation-track (Nuclepore) membranes [*q.v.* Gibbs, 1974; McCave, 1979; Brock, 1983]. Due to problems with the WCN filters mentioned above, and also additional difficulties with filter weight variability related to static charges (*N.B.* no alpha-

emitting sources were used) and the uptake of hygroscopic moisture, which can largely explain the relatively large variations in the balance control filters for CH33 to CH39 in Table 2.5. Whatman GF/C filters were chosen as the only viable and affordable alternative since they are generally more robust than membranes and also remain intact during ashing so that they are ideal from an ease-of-use point of view for the determination of the components of the suspended sediment.

Since GF/C filters have a larger pore size than the membrane filters, a scheme of replicate sampling and filtering was employed to compare the repeatability and reproducibility of the results amongst identical and different types of filters.

Firstly, on five of the survey cruises sub-samples taken from the same sea water samples were filtered through batches of 10 GF/C filters. All the filters were subsequently processed in exactly the same way to derive the suspended sediment concentration and the organic/inorganic components. The variability (given by the standard deviation, s, the standard error, α and the coefficient of variation, cv) in the measured concentrations for the three components at different concentration ranges is shown in Table 2.7. At the lower concentration ranges (< 1 mg l^{-1} and 1-2 mg l^{-1}), the measured concentrations of all three components varied by about 20-45%. For the remaining ranges, the measured concentrations varied by about 10-15%.

Secondly, sub-samples taken from the same sea water sample were filtered through one GF/C, one replicate GF/C and one GF/F filter, and an example of the results of such a comparison is shown in Figure 2.7. There are good correlations for all the replicate filter data sets ($R^2 \geq 0.86$) with an average standard error, $\alpha = 0.03$ mg l^{-1} and standard deviation, $s = 0.19$ mg l^{-1} when comparing all 3 replicate filters. Similar results were attained for the inorganic ($R^2 \geq 0.84$, $\alpha = 0.04$, $s = 0.18$) and organic ($R^2 \geq 0.68$, $\alpha = 0.02$, $s = 0.08$) fractions.

Thirdly, samples filtered through GF/C filters during CH33 and CH43 were compared with samples that were collected at the same time with different water bottles and filtered through 0.4 μm Nuclepore filters using different equipment [*q.v.* Turner, 1991]. The results for CH33 are shown in Figure 2.8 and again, both data sets are well correlated ($R^2 = 0.84$) with an average standard error, $\alpha = 0.1$ mg l^{-1} and standard deviation, $s = 0.69$ mg l^{-1}.

The replicate sampling and analyses suggest that GF/C filters do provide a good and comparable representation of actual suspended sediment concentrations despite their relatively larger pore size, reflecting in part, the fact that they are likely to retain and remove suspended sediment far smaller than the stated pore size, as previously demonstrated by Sheldon and Sutcliffe [1969] and Sheldon [1972]. For the purposes of the North Sea Database and the incorporation of the water bottle suspended sediment data therein, the terms *Total Suspended Matter*, *Inorganic Suspended Matter*, and *Organic Suspended Matter* were adopted.

Table 2.7: Analysis of replicate filtered samples showing the variability in the measured suspended sediment concentrations.

TSM range (mg l^{-1})	**Standard Deviation** *s*	**Standard Error** α	**Coeffic. of Variation** *cv* (%)
< 1	0.39	0.27	30.46
1-2	0.32	0.23	18.42
2-5	0.60	0.42	15.82
5-10	1.16	0.82	15.13
10-15	1.37	0.97	12.33
15-20	1.48	1.05	8.26
20-30	3.04	2.15	12.14
> 30	6.71	4.75	11.71
Inorganic Component (mg l^{-1})			
< 1	0.26	0.18	44.45
1-2	0.47	0.33	27.89
2-5	0.60	0.42	17.12
5-10	1.05	0.74	15.15
10-15	1.29	0.91	10.98
15-20	1.52	1.01	9.64
20-30	3.60	2.59	11.69
> 30	7.87	5.56	14.03
Organic Component (mg l^{-1})			
> 1	0.22	0.16	30.41
1-2	0.34	0.24	19.09
2-5	0.41	0.29	13.29
> 5	1.36	0.96	16.12

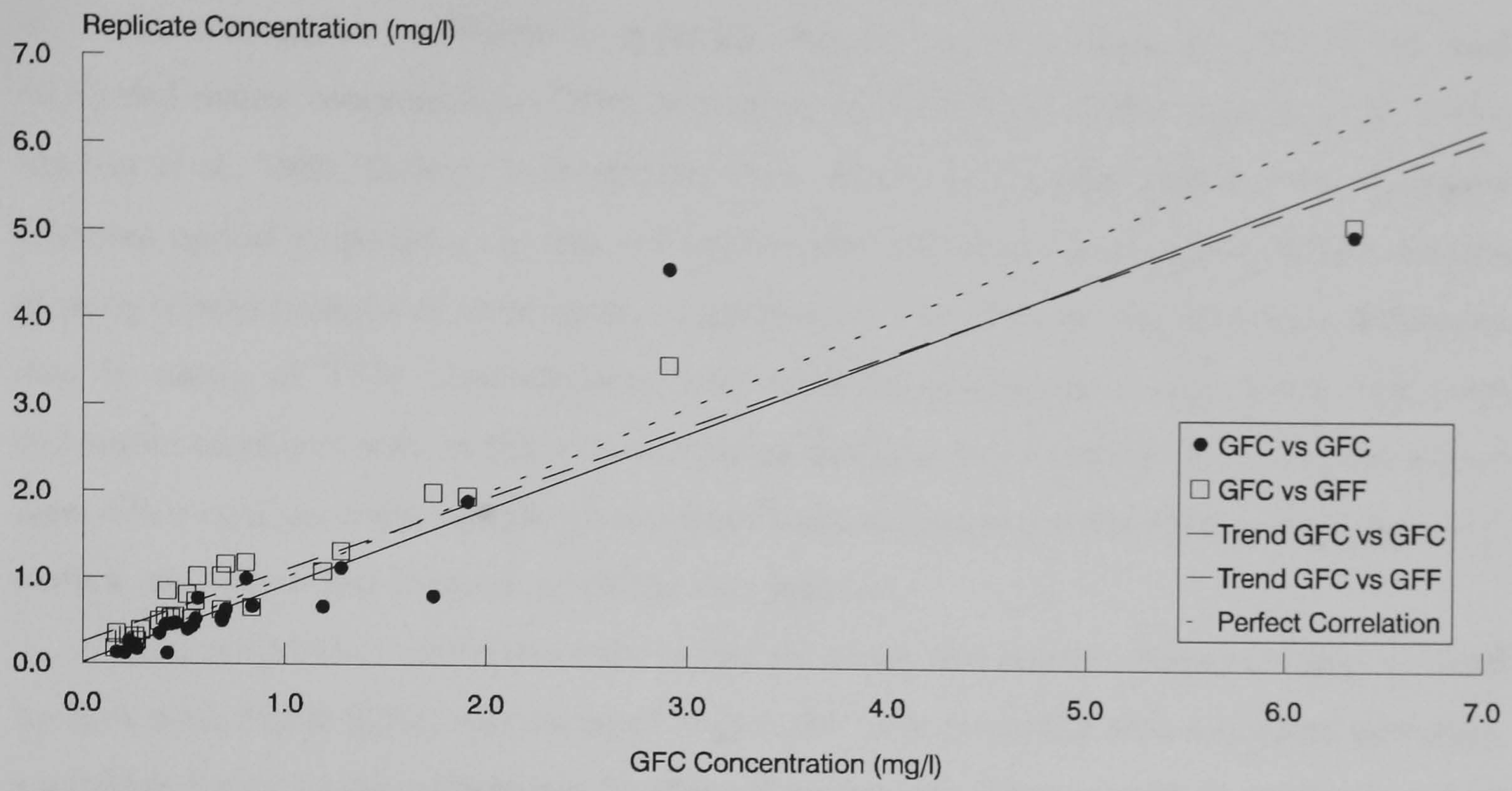

Figure 2.7: A scatter and trend plot showing the comparison of the total suspended sediment concentrations derived from GF/C filters with those derived from two replicate filters (GF/C and GF/F) for CH59.

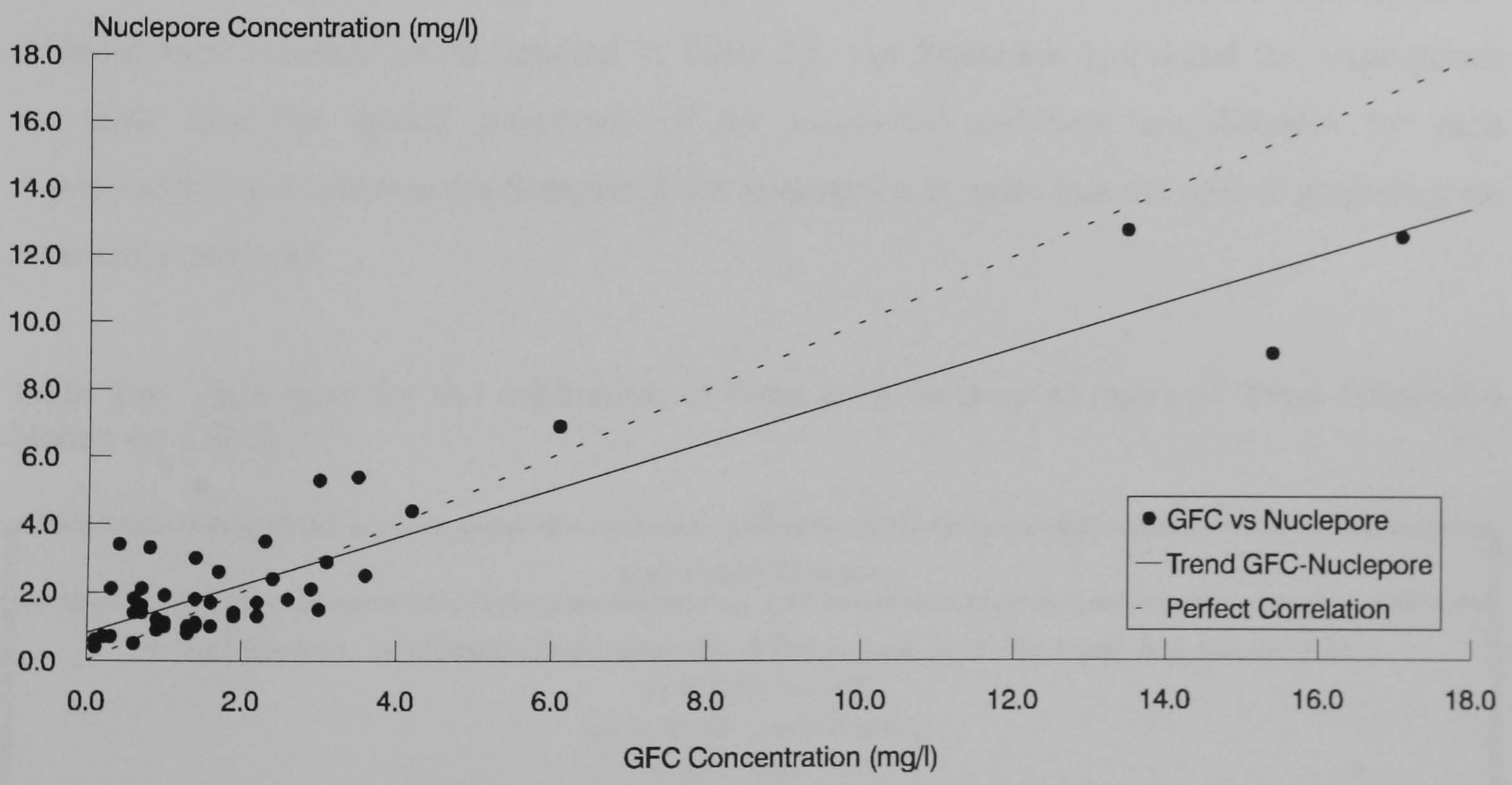

Figure 2.8: A scatter and trend plot showing the comparison of the total suspended sediment concentrations derived from GF/C filters with those derived from Nuclepore filters for CH33.

CALIBRATION

The beam attenuation coefficient is typically observed to be a linear function of the total suspended matter concentration (TSM) [Peterson, 1978; McCave, 1983; Spinrad *et al.*, 1983; Gardner *et al.*, 1985; Bishop, 1986; Moody *et al.*, 1987], that is providing that the suspended sediment optical properties (*e.g.* size, refractive index and shape distributions) within the area of study remain constant or are mutually compensating. The calibration of the optical attenuance data in terms of TSM concentrations was achieved employing simple linear regression techniques combined with an initial investigation into how best to utilize the optical attenuance data: either on a geographical/quasi-water mass basis, and/or on a water column layer basis (*e.g.* surface, mid-depth and bottom), or all the data together.

For the CTD-mounted transmissometer the down-cast optical attenuance range spanned by each water bottle [§2.2] was averaged to give the value (typically with a standard deviation, $s < 0.05\ m^{-1}$) used in the calibrations. For the surface transmissometers, optical attenuance values were extracted from a time interval of 1 min either side of the time of firing of the surface water bottle. These values (n=5) were then averaged and compared directly with the TSM concentrations derived from the surface water bottles to calibrate the surface transmissometers. Of the 4,672 water samples that were taken and filtered during the survey cruises, a total of 4,164 (89%) were available for inclusion in the calibration process (*i.e.* once filters that were damaged or poorly rinsed were discounted).

For survey cruise CH33, 4 different calibration scenarios were examined based upon the different various subdivisions detailed in Table 2.8. For Scenarios 1, 2 and 4 the assumptions are made that the optical properties of the suspended sediment are different for each region/subdivision whereas for Scenario 3 the assumption is made that the optical properties are essentially constant.

Table 2.8: Scenarios for the calibration of Optical Attenuance in terms of Total Suspended Matter for CH33.

Calibration Scenarios
1. Geographical subdivision based upon the ICES subregions of the North Sea [Figure 1.2]: (i) **ICES3**: area 3" (ii) **ICES45**: areas 4 and 5 (iii) **ICES7**: area 7" (+7')
2. Geographical and water column subdivision: as above, suffixed by **-s** (surface), **-m** (mid-depth) and **-b** (bottom)
3. No subdivision: **All** the data, irrespective of 1 or 2
4. All the data: water column subdivision into **Surface**, **Mid-depth** and **Bottom** samples

Table 2.9: Regression parameters for Optical Attenuance (m^{-1}) versus Total Suspended Matter (mg l^{-1}) for the CTD-mounted transmissometer during CH33, using different calibration scenarios.

Scenario	No. of Samples *n*	Coeffic. of Determination R^2	Intercept *a* (± 95% C.I.)	Regression Coeffic. *b* (± 95% C.I.)	Standard Deviation *s*	TSM Range (mg l^{-1})
ICES3	120	0.96	0.67 ± 0.044	0.24 ± 0.009	0.209	0.3 - 21.6
ICES45	122	0.28	0.67 ± 0.123	0.33 ± 0.093	0.276	0.4 - 4.1
ICES7	46	0.30	0.50 ± 0.089	0.29 ± 0.128	0.124	0.3 - 1.6
ICES3-s	41	0.94	0.69 ± 0.070	0.24 ± 0.018	0.183	0.3 - 18.1
ICES3-m	40	0.97	0.68 ± 0.078	0.24 ± 0.013	0.210	0.3 - 20.4
ICES3-b	39	0.94	0.65 ± 0.091	0.25 ± 0.020	0.241	0.4 - 21.6
ICES45-s	42	0.12	0.87 ± 0.226	0.22 ± 0.169	0.348	0.4 - 4.1
ICES45-m	41	0.42	0.55 ± 0.172	0.36 ± 0.134	0.200	0.6 - 2.4
ICES45-b	39	0.56	0.40 ± 0.209	0.54 ± 0.155	0.214	0.6 - 2.4
ICES7-s	15	0.32	0.50 ± 0.192	0.41 ± 0.318	0.118	0.3 - 0.9
ICES7-m	17	0.20	0.48 ± 0.193	0.31 ± 0.295	0.140	0.4 - 1.3
ICES7-b	14	0.64	0.44 ± 0.111	0.31 ± 0.134	0.233	0.3 - 1.6
All	288	0.91	0.71 ± 0.034	0.24 ± 0.008	0.644	0.3 - 21.6
Surface	98	0.78	0.75 ± 0.067	0.24 ± 0.026	0.275	0.3 - 18.1
Mid-depth	98	0.97	0.67 ± 0.046	0.23 ± 0.008	0.206	0.3 - 20.0
Bottom	92	0.85	0.69 ± 0.067	0.25 ± 0.022	0.278	0.3 - 1.3

The results of the linear regression analyses for the CTD-mounted transmissometer are given in Table 2.9. For those scenarios that include all or some of the data from the ICES3 subregion, there are well correlated linear relationships between optical attenuance and total suspended matter concentration, whereas for those that do not (*e.g.* ICES45 and ICES7), there are poor linear relationships, as illustrated by the examples in Figure 2.9. This is due to the disparity in the range of TSM values used in the analyses: large in the case of the former so that the regressions are well constrained by the higher concentrations associated with the Humber Plume and the Wash [Figure 2.9a]; and small in the case of the latter so that these data are not readily amenable to regression analysis [Figure 2.9b and Figure 2.9c]. The small TSM range for the ICES45 subregion is attributed to the limited spatial coverage of the survey track [§2.1] which skirts the nearshore areas of high suspended sediment concentrations, such as those off

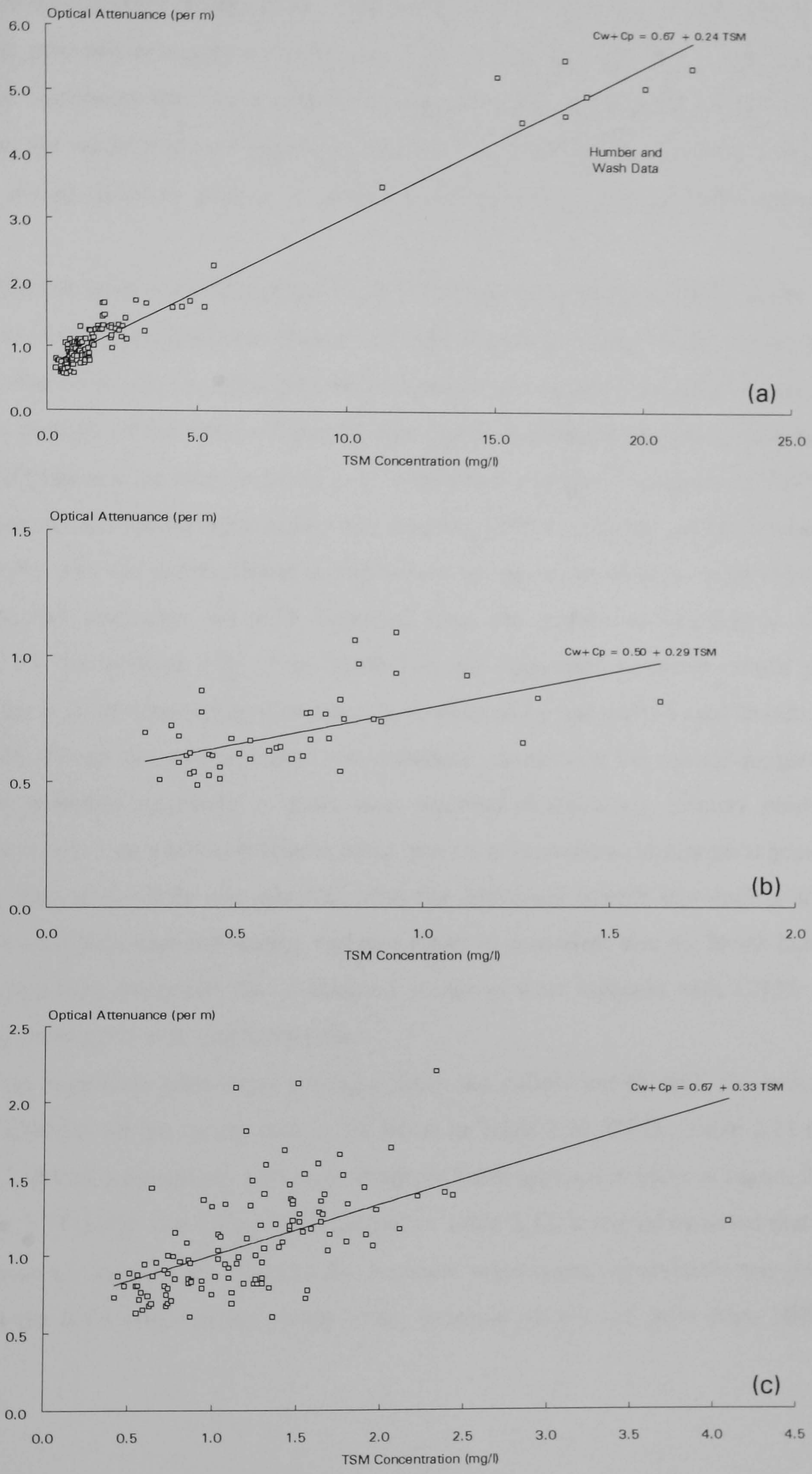

Figure 2.9: Linear regression plots of Optical Attenuance versus Total Suspended Matter for the (a) ICES3, (b) ICES7 and (c) ICES45 subregions for CH33.

the Belgian-Dutch coast [Eisma *et al.*, 1982]. The small TSM range for the ICES7 subregion reflects the generally low concentrations (*e.g.* < 2 mg l^{-1}) in the northern part of the survey area. Given the likelihood that the small TSM ranges would be measured in these subregions throughout the whole Survey Programme, and that the problems associated with the regression analyses would therefore persist, a calibration scheme based on the ICES subregions was rejected.

Another feature of the data in Table 2.9 is the apparent consistency in the regression coefficients of the *All* subdivision (Scenario 3) and the water column subdivisions (Scenario 4), implying that there are no significant differences in the optical properties of the suspended sediments throughout the water column for that cruise. Additional regression analyses had also shown that there was no relationship (*e.g.* $R^2 \approx 0$) between optical attenuance or TSM and water depth. These results can be explained by two interrelated factors: firstly, within a substantial part of the survey area the water column is well-mixed owing to the shallow water depth [§1.3] so that suspended sediments are well dispersed from the surface to the bottom waters; and secondly, for the southern half of the North Sea, the suspended sediment optical property of particle size is fairly constant as it is typically dominated by one type of size distribution [§1.3: Figure 1.9]. Given the second factor, the dominant changes in the optical properties of the suspended sediment are likely to result from seasonal changes (*e.g.* primary production and storm activity), *i.e.* on a cruise-to-cruise basis. For these reasons, a calibration scheme based on using the data as a whole was adopted, with the additional benefit that such a scheme was computationally less time consuming and also easier to assimilate into the North Sea Database. The investigations using different calibration scenarios were repeated with CH35, CH37 and CH39 and these gave very similar results.

The regression parameters resulting from the calibration of each transmissometer in terms of TSM for all the survey cruises are listed in Table 2.10 (CTD), Table 2.11 (PSW) and Table 2.12 (RVS), interspaced with some example linear regression plots in Figure 2.10 (CTD) and Figure 2.11 (PSW and RVS). With respect to Table 2.12, it should be noted that the phrase *Transmissometer unavailable* refers to the 3 cruises when a transmissometer was not available for use in the RVS water jacket owing to the pressure of demand from other NERC-funded projects.

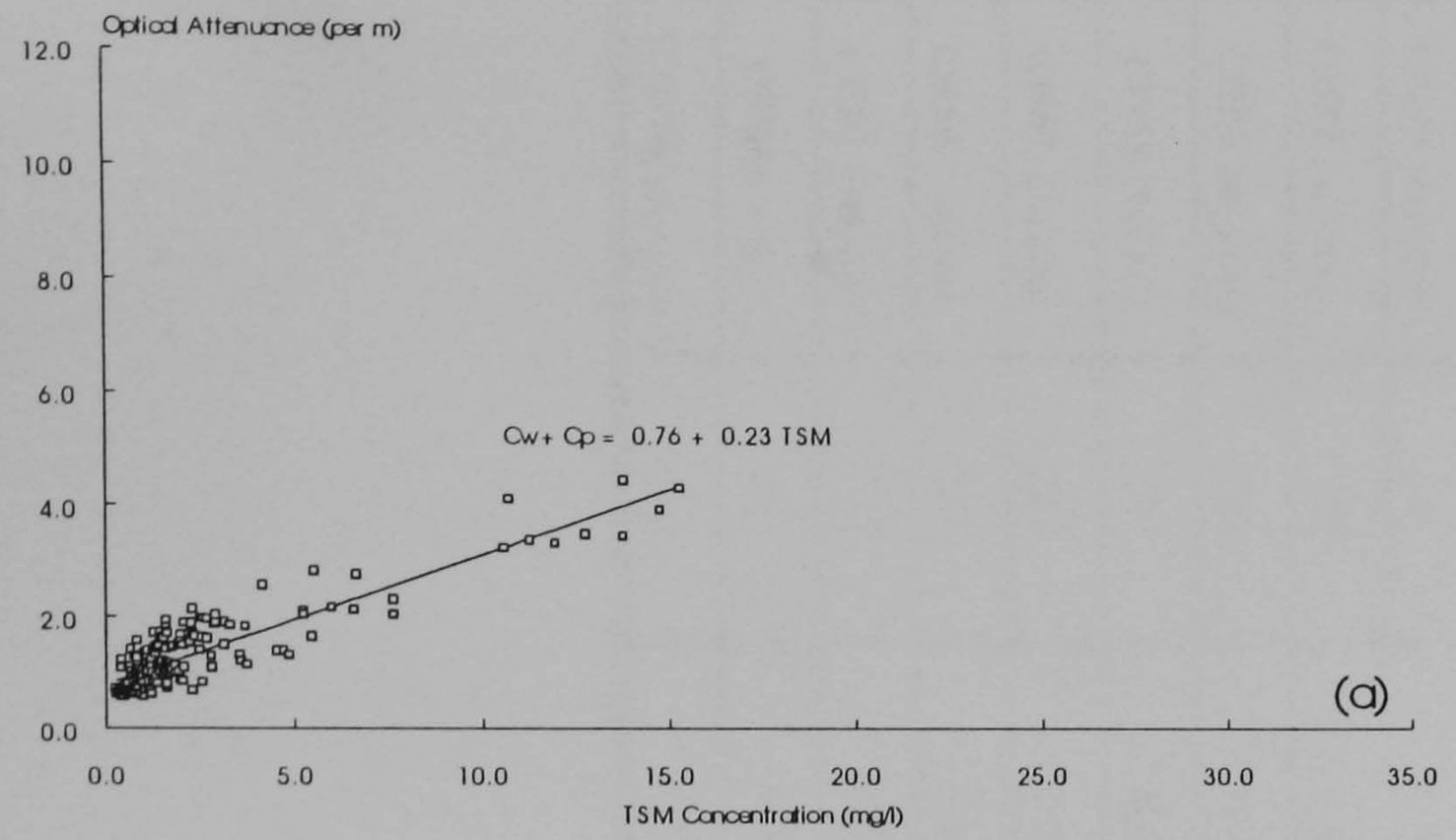

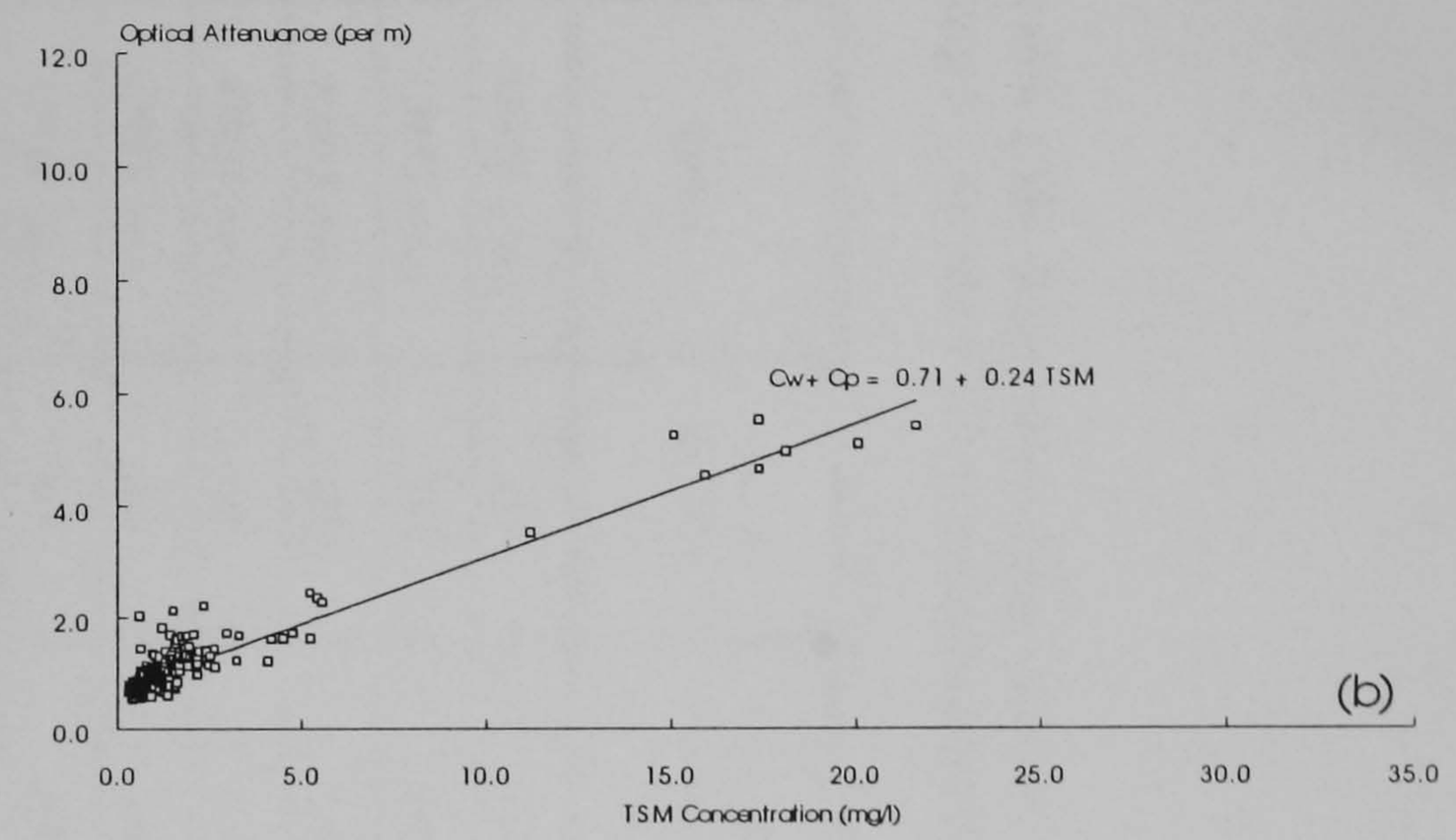

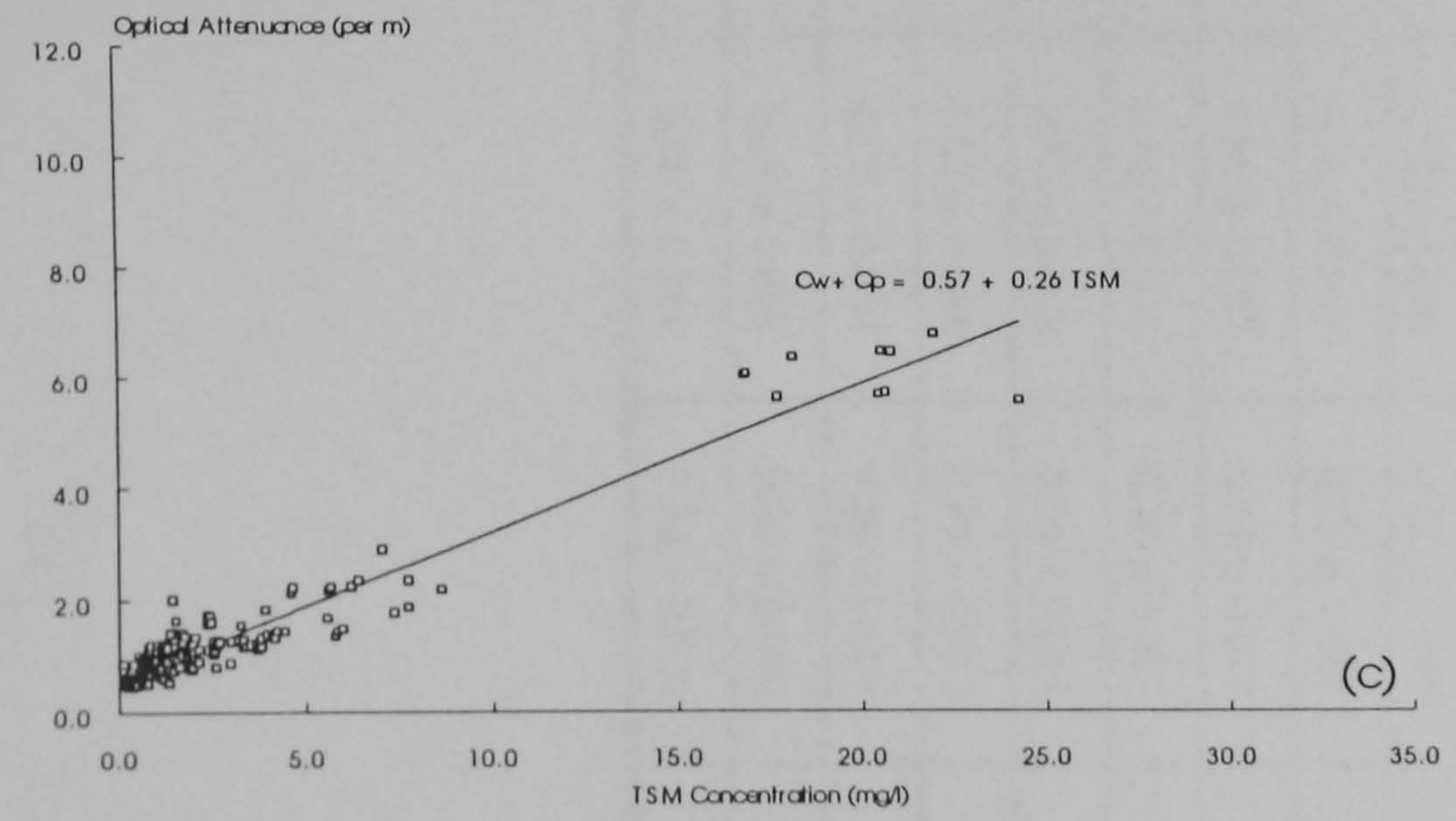

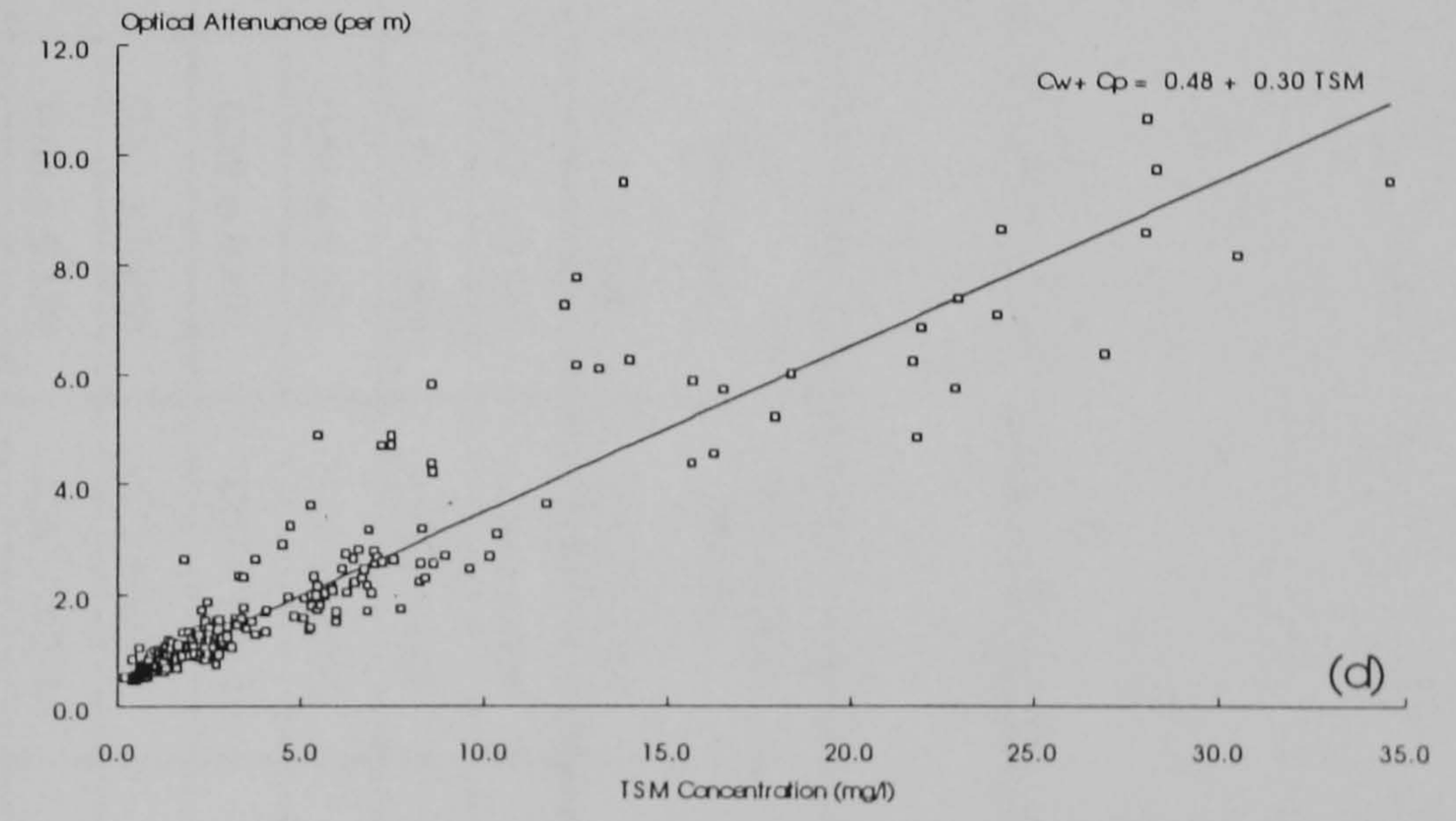

Figure 2.10: Linear Regression plots of Optical Attenuance versus Total Suspended Matter for the CTD-mounted transmissometer for 4 cruises at different seasons: (a) Spring (CH51), (b) Summer (CH33), (c) Autumn (CH61) and (d) Winter (CH43).

Table 2.10: Regression parameters for Optical Attenuance (m^{-1}) versus Total Suspended Matter ($mg\ l^{-1}$) for the CTD-mounted transmissometer.

Cruise	No. of Samples *n*	Coeffic. of Determination R^2	Intercept *a* (± 95% C.I.)	Regression Coeffic. *b* (± 95% C.I.)	Standard Deviation *s*
CH28 (May)	145	0.95	0.48 ± 0.118	0.29 ± 0.011	0.644
CH33 (Aug)	288	0.91	0.71 ± 0.034	0.24 ± 0.008	0.258
CH35 (Sep)	223	0.97	0.58 ± 0.043	0.29 ± 0.007	0.311
CH37 (Oct)	160	0.94	0.39 ± 0.107	0.27 ± 0.010	0.592
CH39 (Nov)	264	0.90	0.86 ± 0.066	0.20 ± 0.008	0.476
CH41 (Dec)	178	0.82	0.65 ± 0.129	0.20 ± 0.014	0.656
CH43 (Jan)	300	0.87	0.48 ± 0.094	0.30 ± 0.013	0.676
CH45 (Jan-Feb)	250	0.86	0.62 ± 0.098	0.26 ± 0.013	0.655
CH47 (Feb-Mar)	297	0.93	0.49 ± 0.077	0.28 ± 0.009	0.570
CH49 (Mar-Apr)	185	0.93	0.69 ± 0.089	0.23 ± 0.009	0.528
CH51 (Apr-May)	177	0.80	0.78 ± 0.063	0.23 ± 0.017	0.334
CH53 (May-Jun)	184	0.77	0.56 ± 0.057	0.34 ± 0.028	0.247
CH55 (Jun-Jul)	255	0.87	0.58 ± 0.026	0.26 ± 0.012	0.160
CH57 (Jul-Aug)	224	0.66	0.55 ± 0.058	0.24 ± 0.022	0.306
CH59 (Aug-Sep)	261	0.85	0.62 ± 0.048	0.24 ± 0.012	0.339
CH61 (Sep-Oct)	319	0.93	0.57 ± 0.033	0.26 ± 0.008	0.262
CH66a (May)	92	0.55	0.63 ± 0.080	0.24 ± 0.044	0.198
CH72a (Sep-Oct)	112	0.82	0.54 ± 0.188	0.30 ± 0.026	0.833

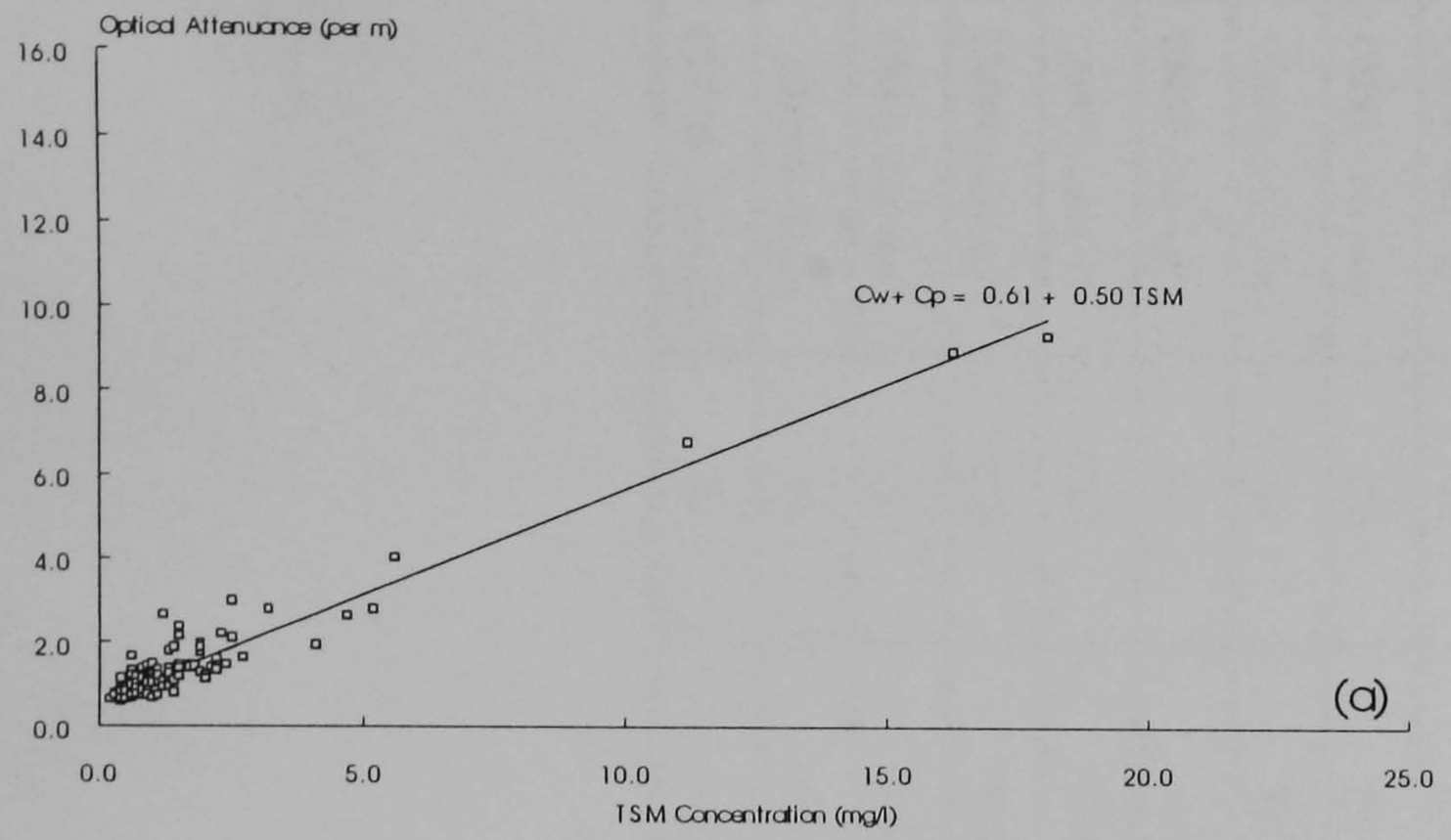

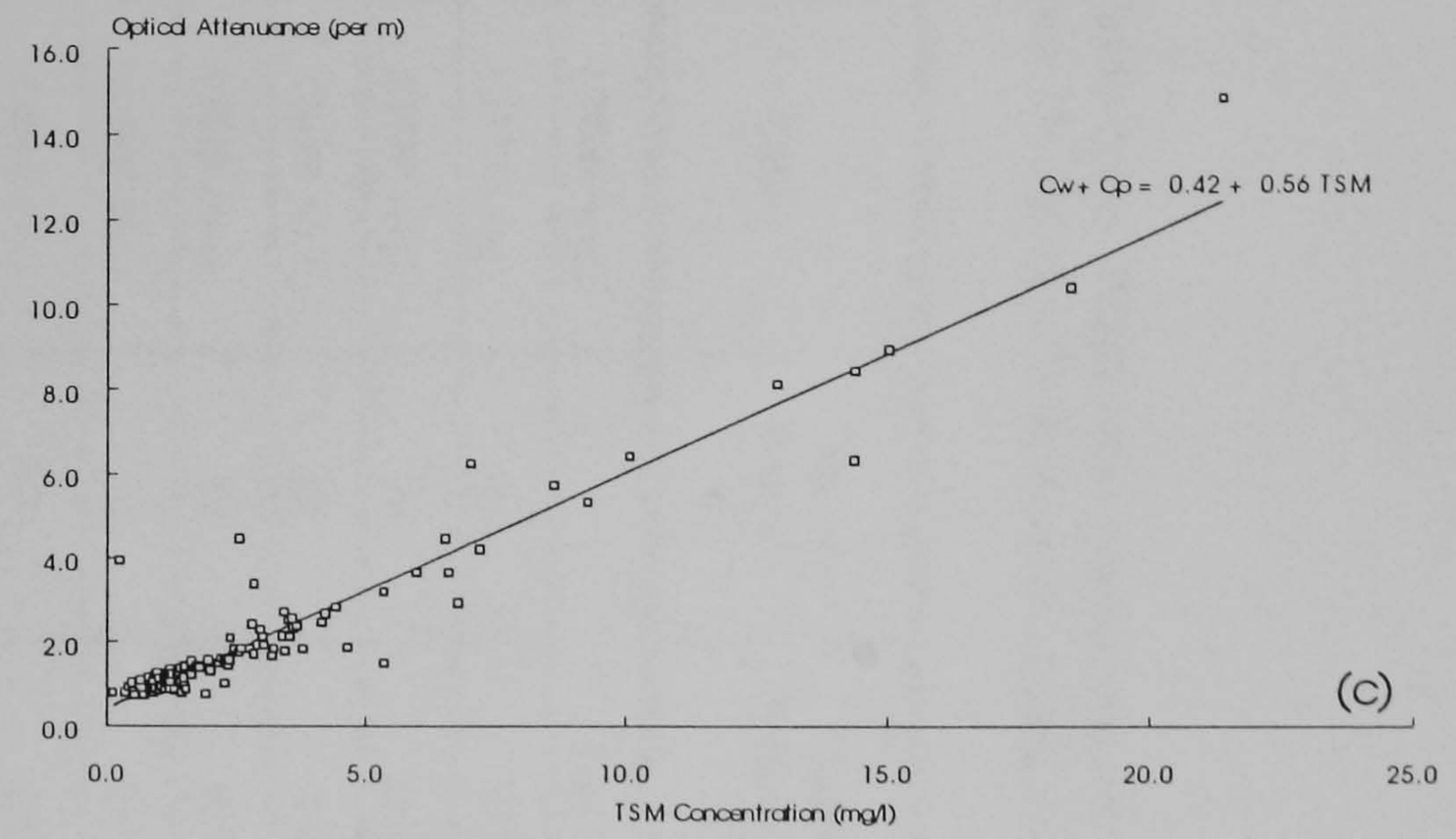

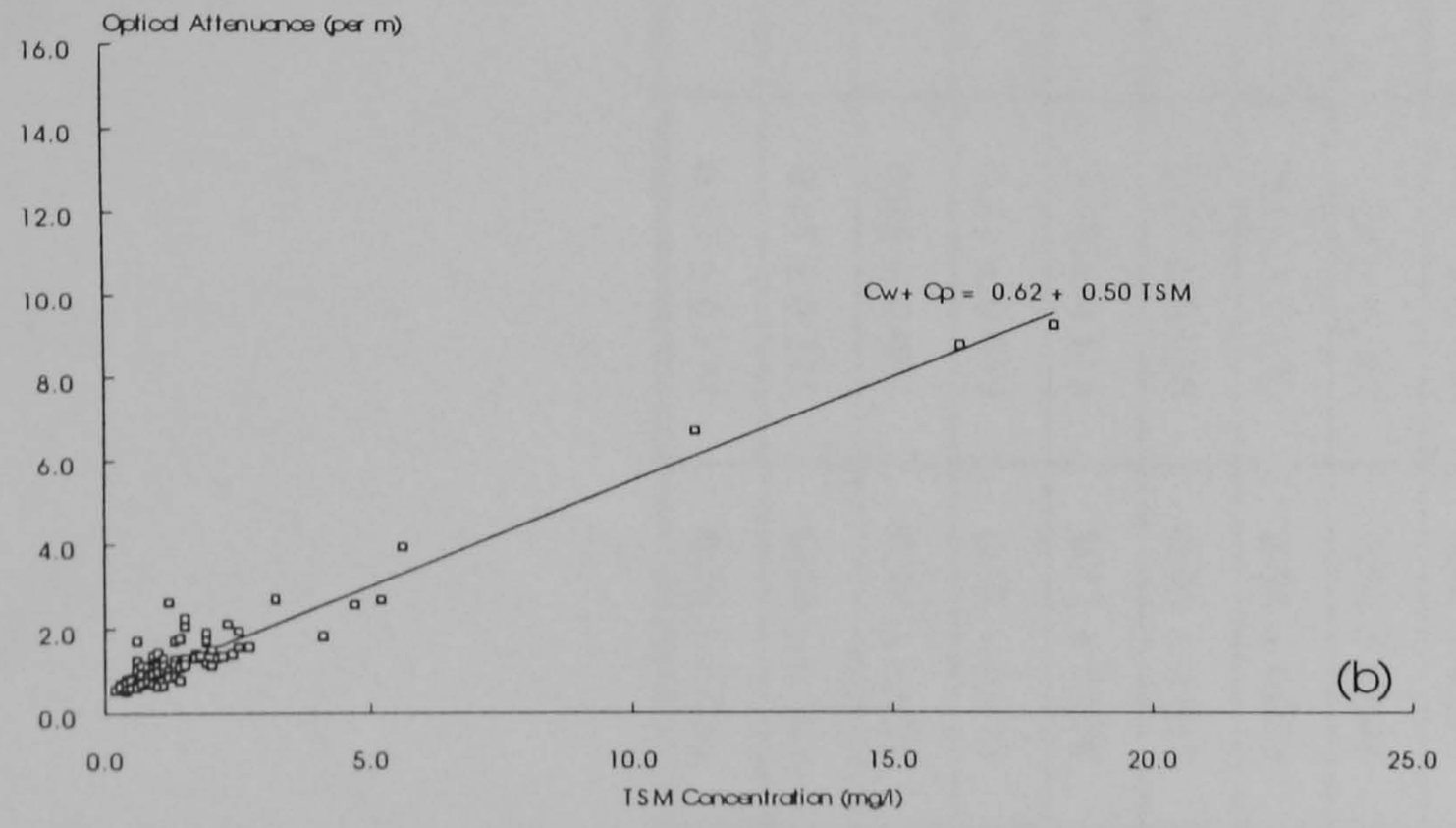

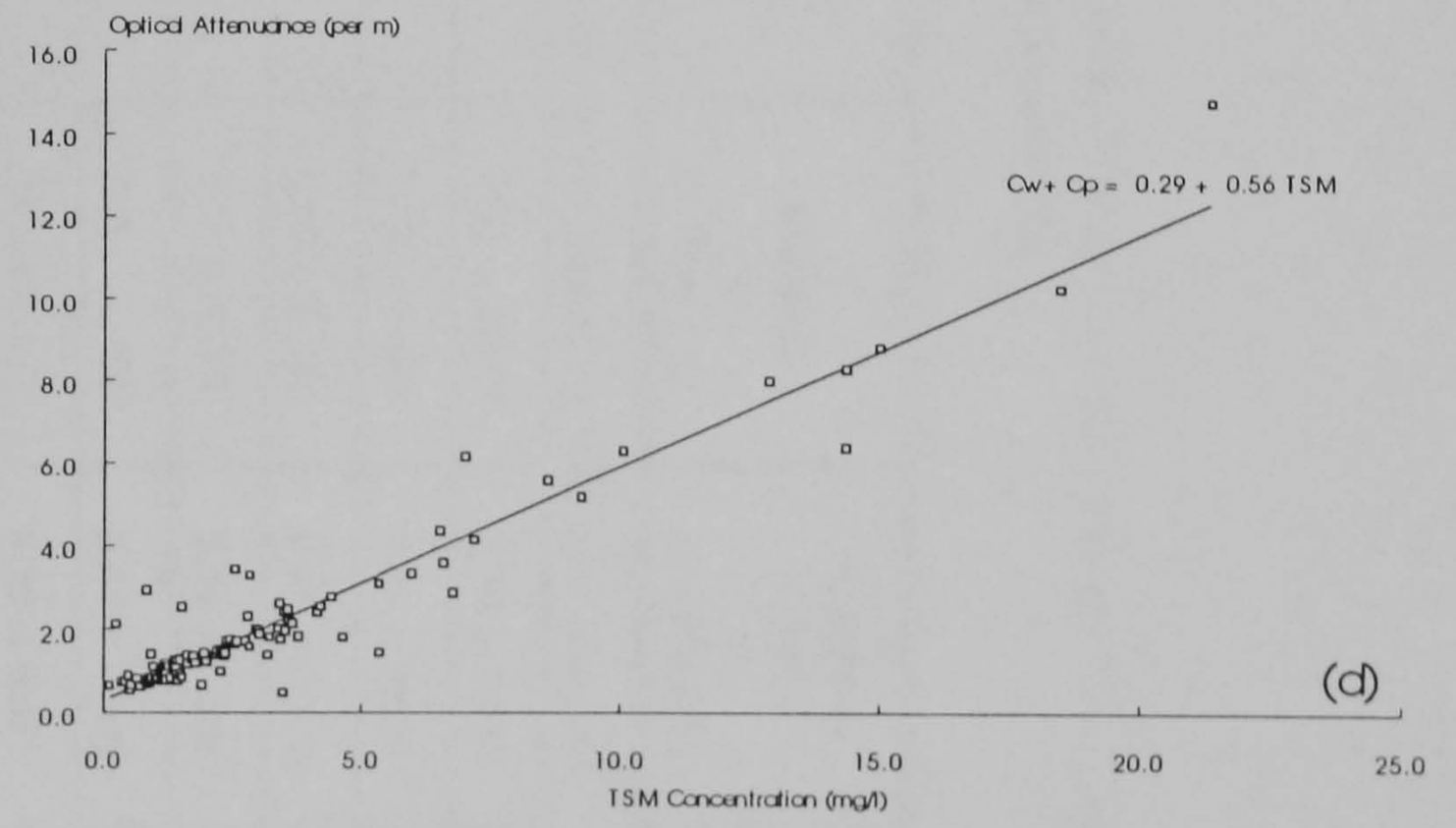

Figure 2.11: Linear Regression plots of Optical Attenuance versus Total Suspended Matter for the deck-mounted transmissometer for 2 cruises/seasons: Summer (CH33): (a) RVS and (b) PSW; and Winter (CH45): (c) RVS and (d) PSW.

Table 2.11: Regression parameters for Optical Attenuance (m^{-1}) versus Total Suspended Matter ($mg\ l^{-1}$) for the PSW deck-mounted transmissometer.

Cruise	No. of Samples *n*	Coeffic. of Determination R^2	Intercept *a* (± 95% C.I.)	Regression Coeffic. *b* (± 95% C.I.)	Standard Deviation *s*
CH28 (May)	Transmissometer not logged by shipboard computer				
CH33 (Aug)	99	0.94	0.62 ± 0.079	0.50 ± 0.025	0.353
CH35 (Sep)	96	0.89	0.50 ± 0.103	0.44 ± 0.031	0.433
CH37 (Oct)	68	0.94	0.22 ± 0.142	0.45 ± 0.028	0.413
CH39 (Nov)	83	0.75	1.09 ± 0.257	0.54 ± 0.068	0.770
CH41 (Dec)	74	0.86	0.51 ± 0.308	0.43 ± 0.040	1.020
CH43 (Jan)	106	0.82	0.42 ± 0.227	0.50 ± 0.045	0.969
CH45 (Jan-Feb)	114	0.92	0.29 ± 0.151	0.56 ± 0.032	0.622
CH47 (Feb-Mar)	133	0.92	0.46 ± 0.116	0.50 ± 0.025	0.510
CH49 (Mar-Apr)	89	0.94	0.73 ± 0.168	0.46 ± 0.023	0.695
CH51 (Apr-May)	65	0.87	1.25 ± 0.169	0.50 ± 0.048	0.552
CH53 (May-Jun)	60	0.76	0.56 ± 0.130	0.54 ± 0.079	0.318
CH55 (Jun-Jul)	85	0.87	0.51 ± 0.066	0.45 ± 0.037	0.220
CH57 (Jul-Aug)	90	0.76	0.39 ± 0.116	0.43 ± 0.050	0.368
CH59 (Aug-Sep)	158	0.80	0.51 ± 0.059	0.45 ± 0.035	0.269
CH61 (Sep-Oct)	132	0.94	0.45 ± 0.084	0.48 ± 0.021	0.432
CH66a (May)	28	0.68	0.45 ± 0.225	0.60 ± 0.162	0.261
CH72a (Sep-Oct)	37	0.92	0.87 ± 0.276	0.52 ± 0.051	0.648

Table 2.12: Regression parameters for Optical Attenuance (m^{-1}) versus Total Suspended Matter ($mg\ l^{-1}$) for the RVS deck-mounted transmissometer.

Cruise	No. of Samples *n*	Coeffic. of Determination R^2	Intercept *a* (± 95% C.I.)	Regression Coeffic. *b* (± 95% C.I.)	Standard Deviation *s*
CH28 (May)	38	0.88	0.42 ± 0.142	0.34 ± 0.041	0.335
CH33 (Aug)	103	0.93	0.61 ± 0.082	0.50 ± 0.027	0.353
CH35 (Sep)	98	0.82	0.65 ± 0.139	0.45 ± 0.043	0.592
CH37 (Oct)	57	0.91	0.22 ± 0.188	0.49 ± 0.041	0.505
CH39 (Nov)	Transmissometer unavailable				
CH41 (Dec)					
CH43 (Jan)					
CH45 (Jan-Feb)	113	0.91	0.42 ± 0.160	0.56 ± 0.033	0.655
CH47 (Feb-Mar)	133	0.93	0.51 ± 0.111	0.50 ± 0.024	0.486
CH49 (Mar-Apr)	89	0.95	0.71 ± 0.156	0.46 ± 0.022	0.645
CH51 (Apr-May)	Transmissometer faulty				
CH53 (May-Jun)	54	0.75	0.90 ± 0.136	0.50 ± 0.078	0.320
CH55 (Jun-Jul)	85	0.88	0.50 ± 0.064	0.45 ± 0.036	0.214
CH57 (Jul-Aug)	86	0.77	0.36 ± 0.118	0.45 ± 0.052	0.371
CH59 (Aug-Sep)	172	0.81	0.57 ± 0.053	0.45 ± 0.033	0.258
CH61 (Sep-Oct)	121	0.95	0.41 ± 0.084	0.52 ± 0.021	0.415
CH66a (May)	28	0.37	0.78 ± 0.307	0.44 ± 0.220	0.355
CH72a (Sep-Oct)	Water jacket damaged				

The regression coefficients or gradients (b) of the calibration lines pertaining to each transmissometer are reasonably uniform and consistent between individual survey cruises, with average regression coefficients of 0.26 ± 0.008, 0.49 ± 0.012 and 0.47 ± 0.014 for the CTD-mounted, PSW and RVS transmissometers respectively. However, there is a noticeable difference of about a factor of 2 between the regression coefficients of the CTD-mounted and the deck-mounted transmissometers. An example of the optical attenuance recorded by each transmissometer at concurrent times is given in Figure 2.12. As the suspended sediment concentration increases, indicated by the increase in the optical attenuance of the CTD-mounted

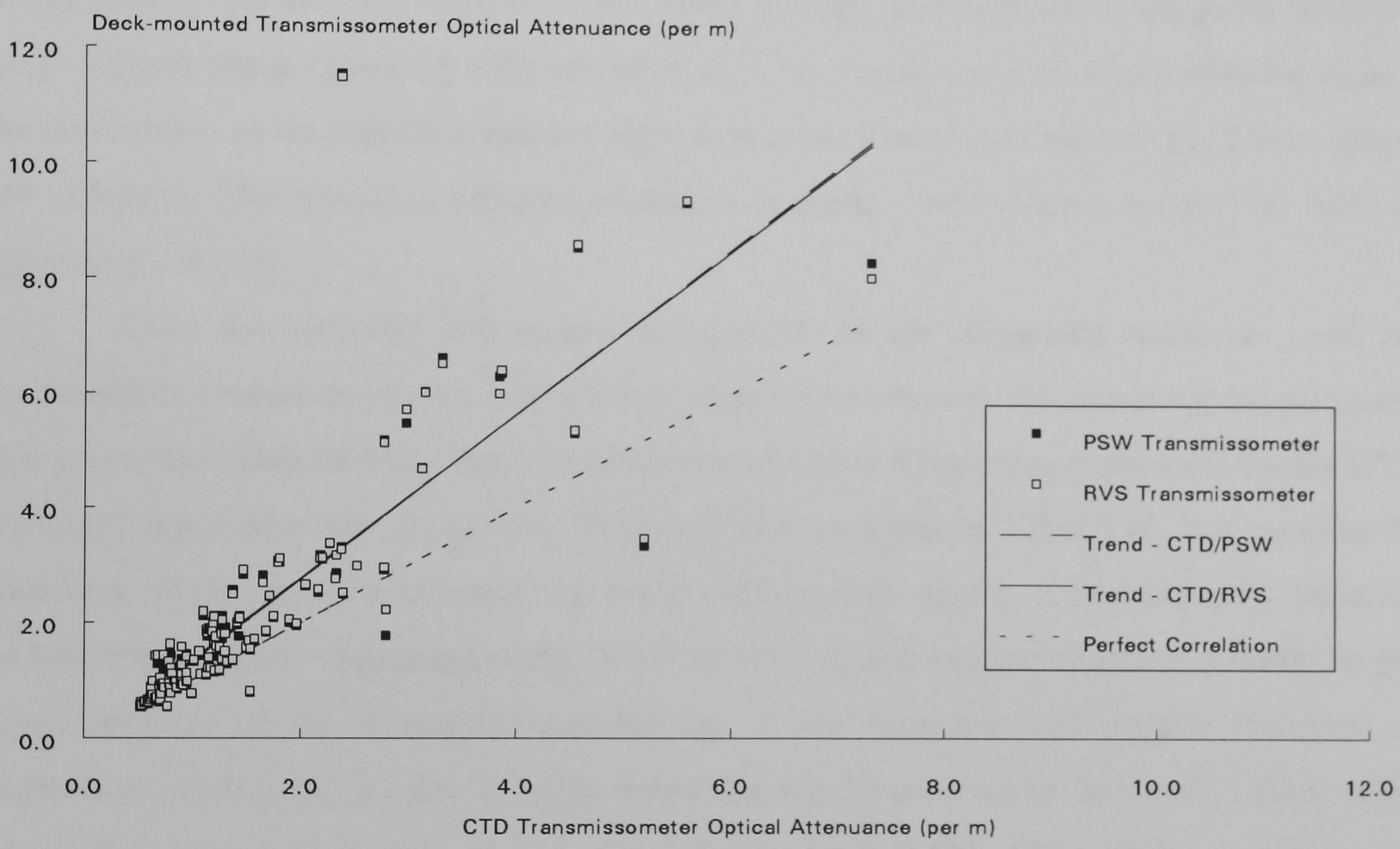

Figure 2.12: A scatter and trend plot showing the comparison between the Optical Attenuance (m^{-1}) recorded by the deck-mounted (PSW and RVS) and CTD-mounted transmissometers at concurrent time instants during CH33.

transmissometer, the divergence between the output from the CTD-mounted and deck-mounted transmissometers increases, as indicated by the trend line. The reasons for this divergence seem to be related to the tendency for those fractions of the suspended sediment that settle out of the water to get trapped in the water jackets since the water outlets were at the top of the water jackets, above the level of the inlets. For those regions of the survey area where the turbidity of the water is great (*e.g.* off the English Coast), the trapping phenomenon is particularly critical, resulting in anomalously high optical attenuance values and a larger disparity with the CTD-mounted transmissometer which is free of any confinement. An additional factor may also involve possible changes in the particle characteristics of the suspended sediment caused by the

shipboard water pump that extracts and distributes the non-toxic water supply. Although there are no data to confirm this, the pump may be breaking up the suspended sediment into smaller particles before they enter the water jackets. Baker and Lavelle [1984] have demonstrated that the gradients of light attenuation and particle mass concentration regressions vary with the size distributions of the particles: suspensions with small mean particle sizes attenuate light much more efficiently (*i.e.* have larger regression gradients) than suspensions with large mean particle sizes.

A further interesting result of the regression analyses are the intercept parameters (*i.e.* $c_{w\ (670nm)}$) which for nearly all the survey cruises, are greater than the values 0.3641 m^{-1} (91.3 %T) derived for pure distilled water [Sea Tech, 1988] and 0.4308 m^{-1} expected for pure sea water [Smith and Baker, 1981]. It seems likely that these discrepancies are partly related to measurement errors caused by colloidal material. This material will be responsible for some of the attenuation of the transmissometers' light beams but it may pass through the filters, despite the enhanced filter retention efficiencies due to clogging, and therefore be omitted from the gravimetric results.

Since the inorganic and organic components of the suspended sediments were also measured, an evaluation of their respective contributions to the optical attenuance measurements was attempted using multiple linear regression techniques. Regression parameters for the CTD-mounted transmissometer for cruises CH41 to CH72a are given in Table 2.13. It is apparent that variations in the optical attenuance are explained to a high degree of correlation by variations in both the inorganic suspended matter (ISM) and the organic suspended matter (OSM). To gain some measure of the respective contributions of the inorganic and organic fractions, the regression coefficients b_1 and b_2 were tested for significance using Student's t from which appropriate probability values p were derived [see Table 2.13]. Although the p data are not conclusive, there is some evidence to suggest that for all the cruises, the optical attenuance is strongly associated with variations in the ISM concentration but not with the OSM concentration during those cruises carried out in during the autumn/winter months (*e.g.* CH41 and CH72a). Such a result is consistent with the reality that the organic fraction of the suspended sediments increases during the spring and summer months as the result of primary production, and then subsequently decreases during the autumn and winter months as much of the organic matter is re-mineralized.

Table 2.13: Multiple regression parameters for Optical Attenuance (m^{-1}) versus Inorganic and Organic Suspended Matter (in mg l^{-1}) for the CTD-mounted transmissometer

Cruise	*n*	R^2	**Intercept** *a*	*Inorganic* **Regression Coeffic.** b_1	*p* (b_1=0)	*Organic* **Regression Coeffic.** b_2	*p* (b_2=0)	**St. Dev.** *s*
CH41	167	0.84	0.72 ± 0.167	0.23 ± 0.037	<0.001	-0.04 ± 0.345	0.830	0.620
CH43	280	0.89	0.39 ± 0.116	0.29 ± 0.043	<0.001	0.43 ± 0.298	0.004	0.463
CH45	243	0.88	0.26 ± 0.130	0.24 ± 0.034	<0.001	0.97 ± 0.319	<0.001	0.485
CH47	295	0.93	0.52 ± 0.102	0.26 ± 0.026	<0.001	0.31 ± 0.279	0.028	0.504
CH49	163	0.94	0.66 ± 0.100	0.22 ± 0.030	<0.001	0.23 ± 0.172	0.010	0.479
CH51	177	0.85	0.58 ± 0.077	0.18 ± 0.021	<0.001	0.61 ± 0.101	<0.001	0.290
CH53	157	0.79	0.42 ± 0.086	0.31 ± 0.034	<0.001	0.56 ± 0.105	<0.001	0.237
CH55	226	0.85	0.55 ± 0.047	0.24 ± 0.016	<0.001	0.30 ± 0.062	<0.001	0.166
CH57	201	0.74	0.56 ± 0.081	0.30 ± 0.026	<0.001	0.16 ± 0.074	<0.001	0.331
CH59	226	0.86	0.62 ± 0.084	0.23 ± 0.021	<0.001	0.24 ± 0.138	0.001	0.316
CH61	303	0.93	0.43 ± 0.065	0.22 ± 0.019	<0.001	0.66 ± 0.156	<0.001	0.257
CH66a	92	0.63	0.54 ± 0.087	0.16 ± 0.056	<0.001	0.54 ± 0.144	<0.001	0.182
CH72a	111	0.82	0.56 ± 0.226	0.31 ± 0.080	<0.001	0.24 ± 0.208	0.246	0.840

PREDICTIONS

As the concluding part of the data processing and the calibration of the optical attenuance data, the calibration equations were incorporated into the North Sea Database from which predictions of TSM could be derived. Some quality control flagging of the predicted or calibrated data was also carried out: firstly, much of the very clear water data gave negative TSM concentrations owing to the high intercepts of the regression curves and these were flagged *Q* for indeterminate values; and secondly, those predicted values that lay outside the maximum measured TSM concentration used in the calibrations were flagged *U* for outside the range of calibration since it was possible that these predicted or extrapolated values were underestimates, if saturation of the transmissometer light beam had occurred.

Since different calibrations were computed for each of the survey cruises, it is inevitable that the same optical attenuance values will predict different TSM concentrations. Clearly, this will have some bearing in relation to any comparisons between the suspended sediment concentrations for different survey cruises. Therefore, TSM concentrations were predicted using the calibration equations for each of the transmissometers to derive a mean concentration and a standard deviation for a range of optical attenuances. Figure 2.13 shows the mean predicted concentration plus or minus the standard deviation for optical attenuances ranging from 0.4 m^{-1} to 18 m^{-1}. The graphs indicate that the dispersion of the predicted TSM concentrations increases with increasing optical attenuance values. However, at concentrations of less than 10 mg l^{-1}, variations are relatively small.

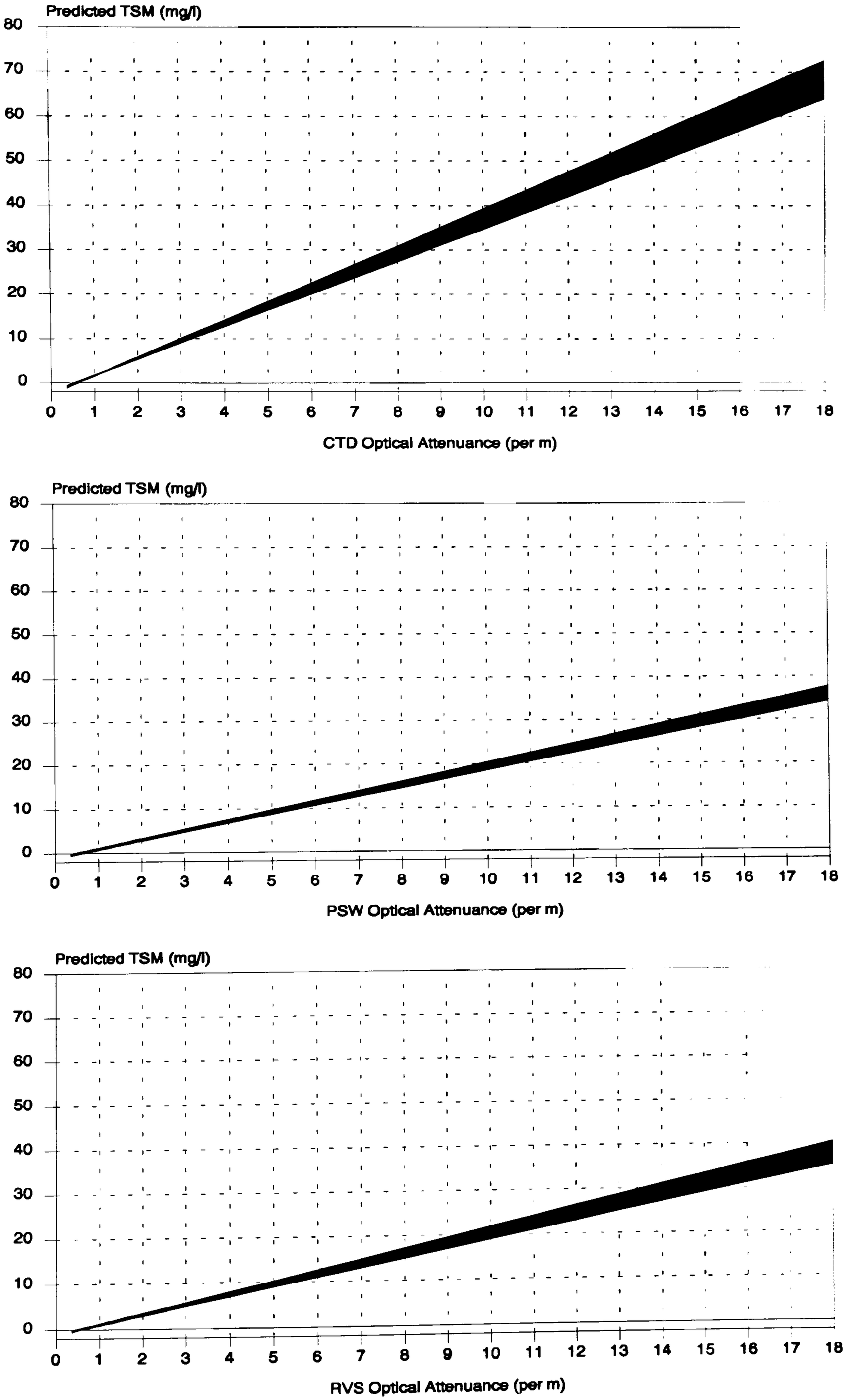

Figure 2.13: Plots of Optical Attenuance versus Predicted Total Suspended Matter using all the cruise calibration equations for each transmissometer to show the variability (standard deviation) in the predicted concentrations.

2.3: Tidal Biases in the Data

An analysis of the suspended sediment data was undertaken to investigate the presence of systematic biases in these data resulting from similarities (or differences) in the tidal states at which individual survey stations were sampled during each survey cruise (*e.g.* one survey station always sampled at slack water). The presence of tidal biases will have some bearing in relation to any comparisons between the suspended sediment concentrations for different survey cruises.

A sample of survey stations was selected and the start times of the CTD casts at each of these stations and for every cruise were converted into "tidal state" times by reference to the nearest predicted High Water (HW) for the reference port of Lowestoft. Figure 2.14 shows the tidal state times for six survey stations plotted with the corresponding depth-averaged TSM concentrations.

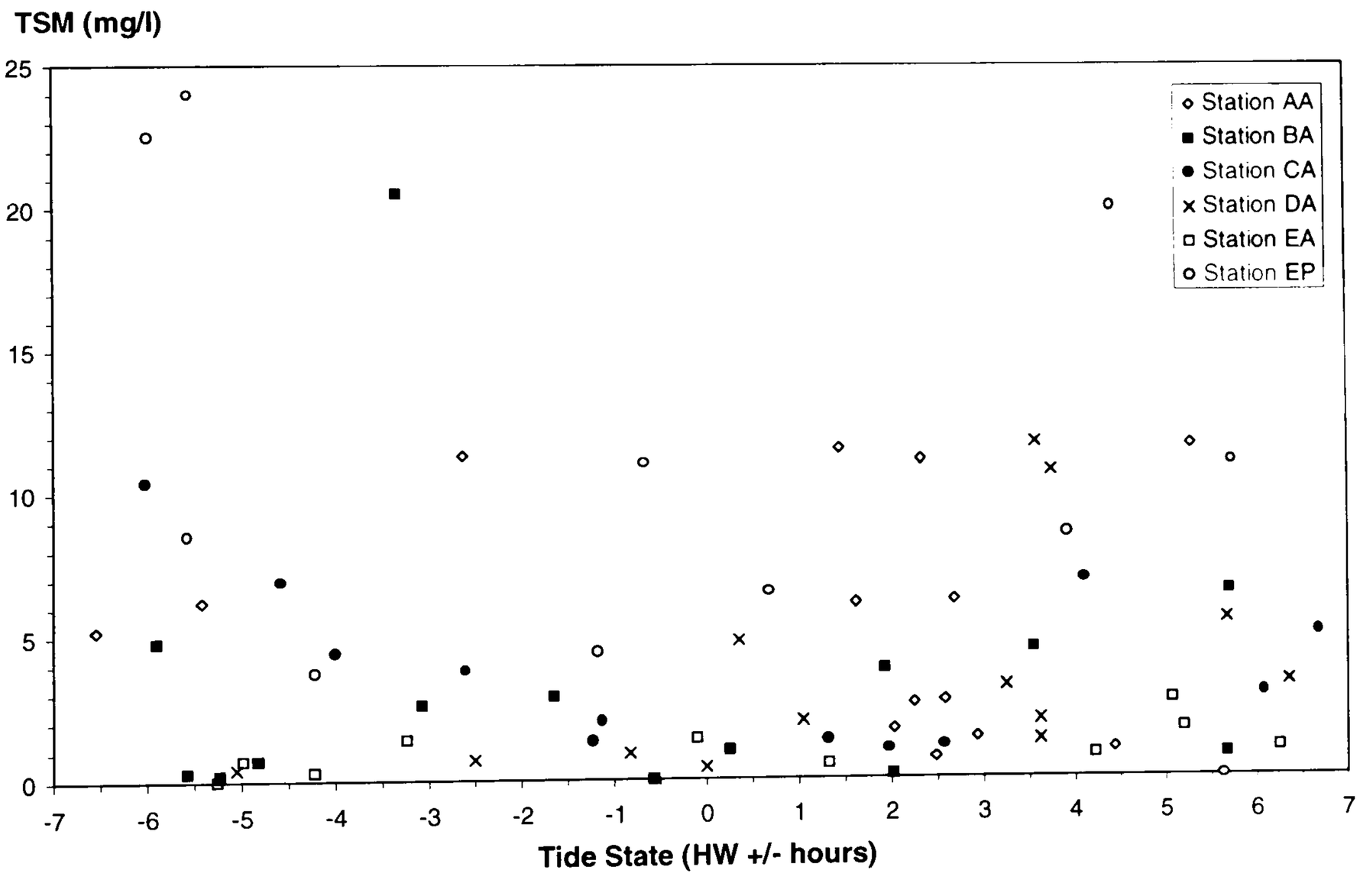

Figure 2.14: A scatter plot showing the relationship between the time at which a station was sampled (expressed as the tidal state with respect to the High Water predicted for Lowestoft) and the measured TSM concentration (in mg l^{-1}).

The scatter plot shows two general patterns. Firstly, there are no apparent systematic biases in the tidal states at which individual stations were sampled. For example, Station EA was sampled at or near slack water (*e.g.* HW-5, HW and HW+6) and at or near maximum rate (*e.g.* HW-3 and HW+1). Secondly, there is no correlation between the sediment concentration and tidal state: higher TSM concentrations are not specifically associated with maximum rates, or

lower concentrations with slack water. Although HW at Lowestoft may not correspond to either HW or slack water at the sampled stations, the plot still indicates that other factors may be influencing the sediment concentrations, such as primary production, fluvial supply and wind effects [see §5].

Given the results of the analysis, it was not possible to develop a scheme to correct for any tidal biases in the data. However, in order to minimize the effects of any biases, the survey cruises and stations were grouped into three seasons that were characteristic of winter (including autumn), spring and summer conditions (based on the cruise-by-cruise spatial distributions of TSM and OSM). The suspended sediment data for identical stations and water depths within each season were averaged. These data were used to derive seasonally averaged distribution plots of suspended sediment concentration.

2.4: Summary

The chapter has described the data acquisition, processing and quality control procedures undertaken during the research. The next two chapters present the main results of the suspended sediment surveys in the form of contour plots for individual cruises and some seasonally averaged plots, produced using the computer package UNIRAS. Because of the difficulties encountered in the acquisition, processing and calibration of the optical attenuance data from the deck-mounted transmissometers, and the doubts as regards the quality of these data, plots of surface TSM are based largely on the calibrated optical attenuance derived from the CTD-mounted transmissometer. All plots relating to the inorganic and organic suspended sediment components utilize only the observed data.

TOTAL SUSPENDED MATTER DISTRIBUTIONS

The following chapter presents the main results of the research by describing firstly, the horizontal distributions of TSM for the 15 consecutive months/cruises of the Survey Programme using the CTD data and also some of the underway data, and secondly, the vertical distributions of TSM along a number of sections for some of the survey cruises. The surface, bottom and depth-averaged distributions (with the organic contents) for each cruise have also been presented by Dyer and Moffat [1992].

3.1: Horizontal Distributions - CTD Data

The monthly distributions of TSM in the surface waters (*i.e.* within 2 m of the sea surface) of the southern North Sea for the period of August, 1988 to October, 1989 are presented in Figure 3.1 (*N.B.* the limits of each coloured region represent the extent of the survey track for each cruise). Generally, the highest concentrations (*e.g.* > 5 mg l^{-1}) tended to occur in the western coastal waters of the Southern Bight and periodically off the Continental European coastline and in the German Bight [*e.g.* Figures 3.1f and 3.1j]. As mentioned previously [§2.1 and §2.2], the limited spatial coverage near the Continental European coastline means that some of the high concentrations that occur in, for example, the eastern coastal waters of the Southern Bight [Eisma and Kalf, 1979; Visser *et al.*, 1991] are not shown. By comparison, the lowest concentrations (*e.g.* < 2 mg l^{-1}) tended to occur outside the coastal waters, particularly in the northern and central parts of the southern North Sea. Because of these basic differences between the coastal waters and the open sea, there was a gradient of TSM away from the coasts with concentrations typically decreasing towards the north and north-west to < 1 mg l^{-1}.

Accordingly, and for the purposes of more detailed considerations, the southern North Sea can be subdivided into 3 broad turbidity regions:

- The region of relatively high turbidity and TSM concentration off the East Anglian and Lincolnshire coasts,
- The region of relatively low turbidity and TSM concentration located primarily to the north but sometimes also to the east of the high turbidity zone, and
- The coastal waters of the eastern Southern Bight and the German Bight.

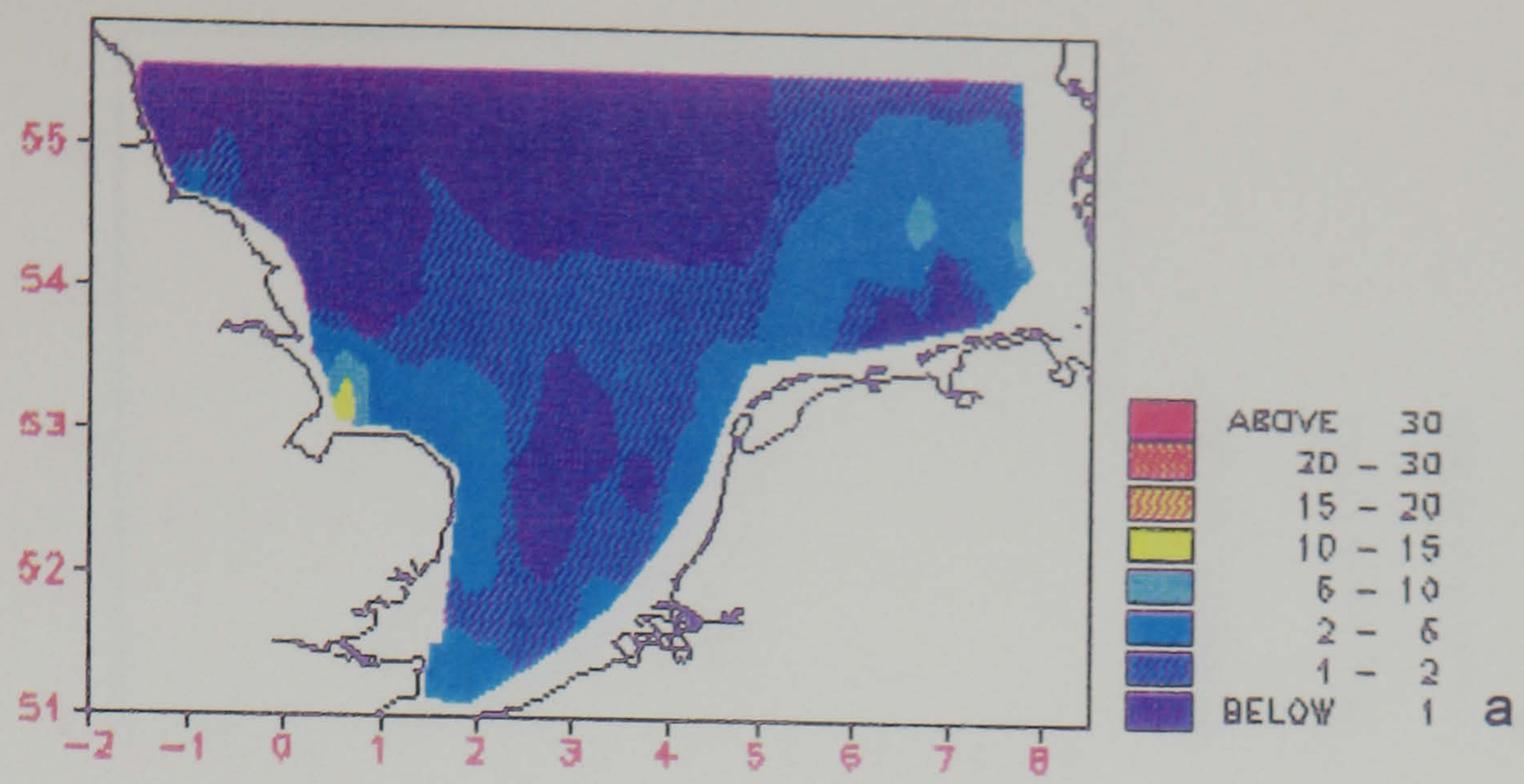

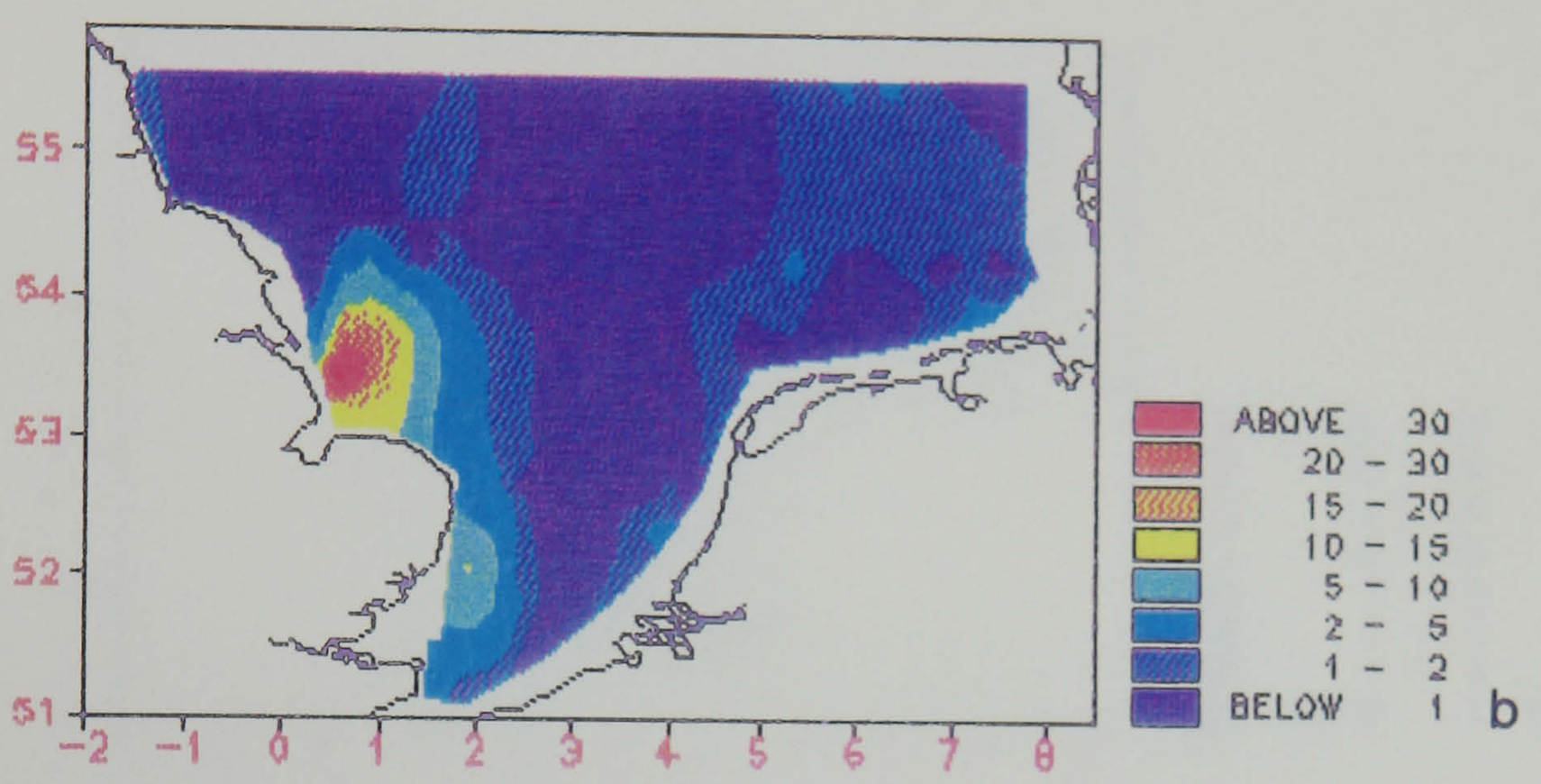

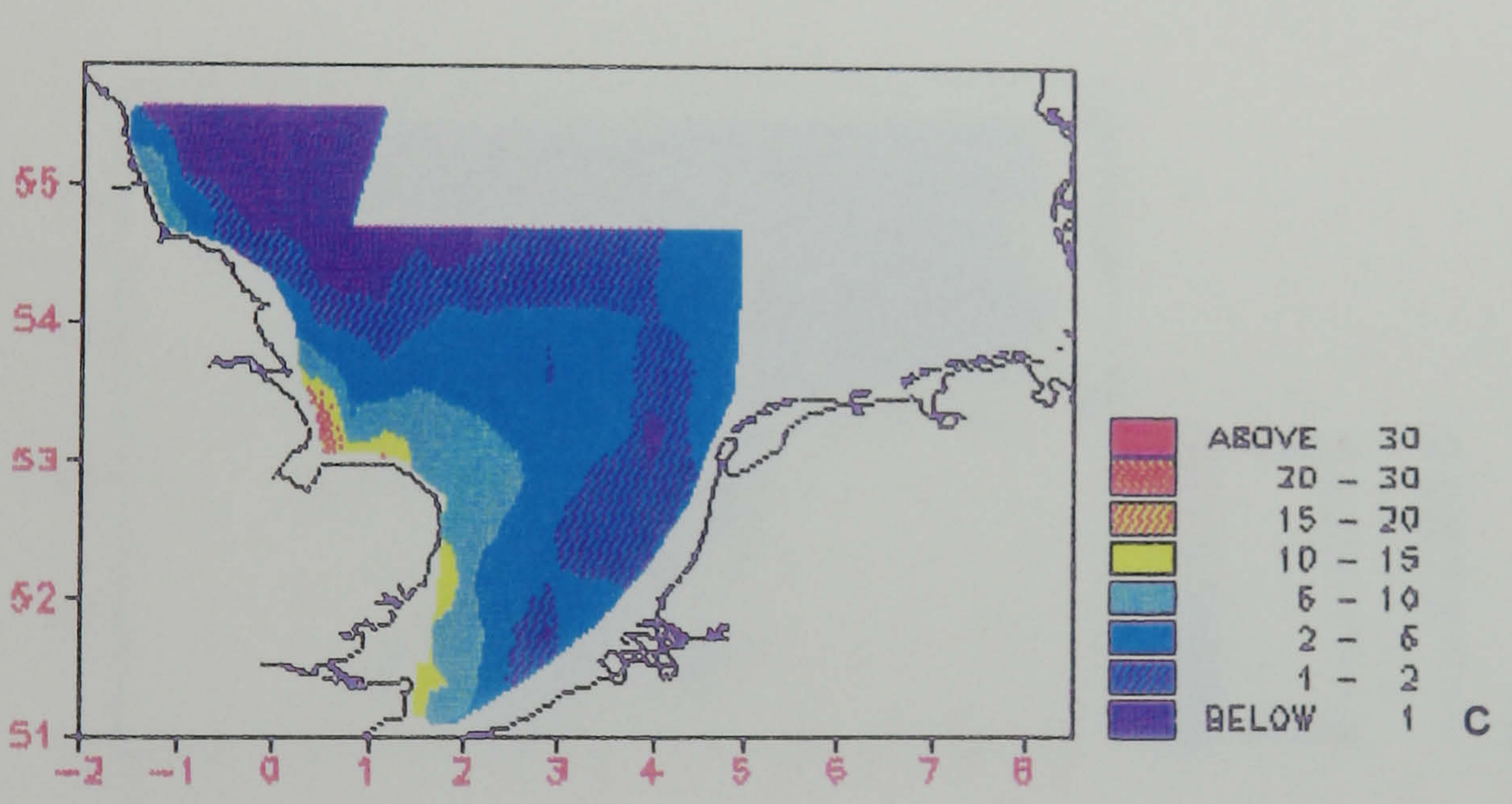

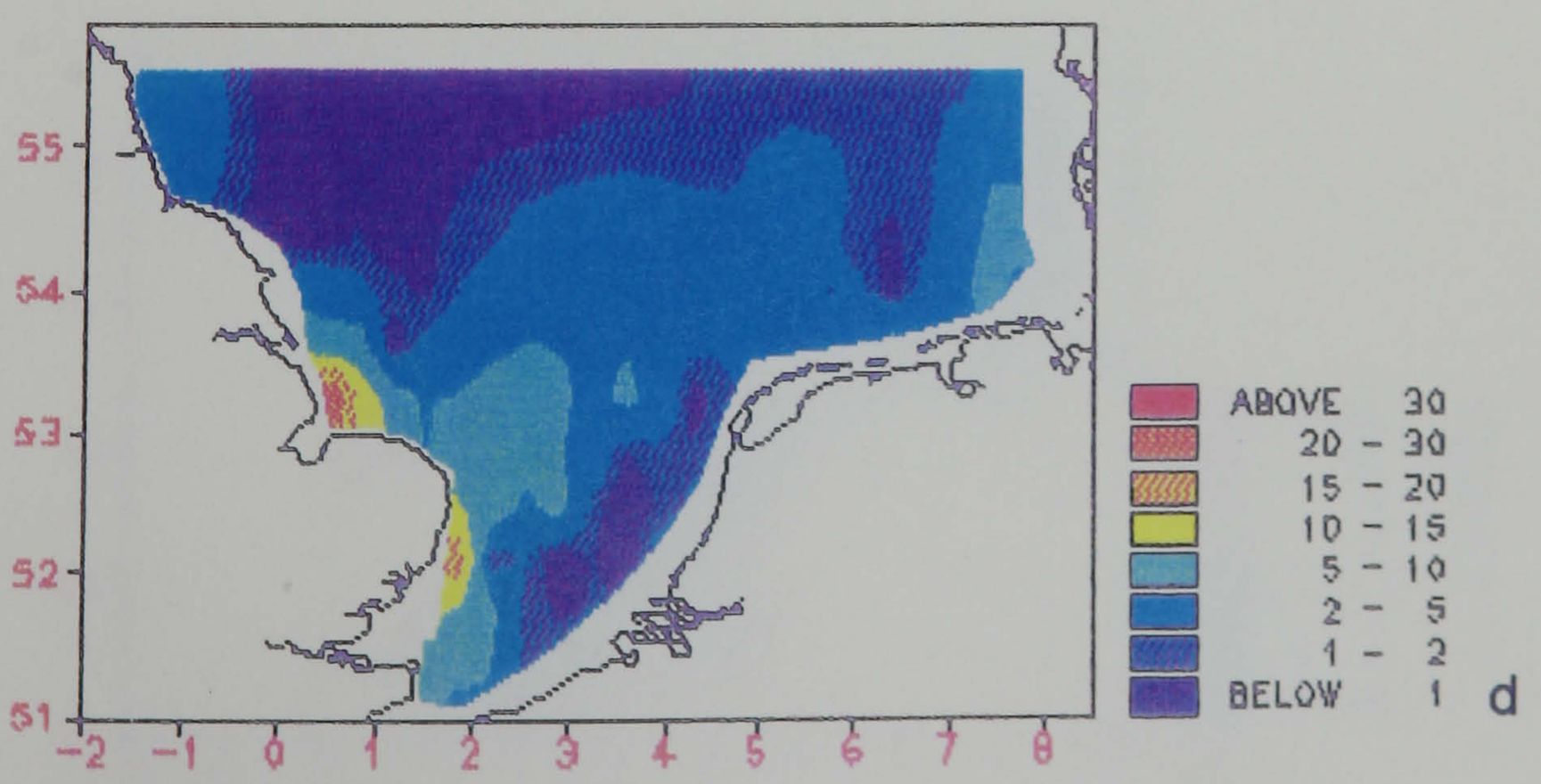

Figure 3.1: Distribution of TSM (mg l^{-1}) in the surface waters of the southern North Sea for (a) August 1988, (b) September 1988, (c) October 1988 and (d) November 1988.

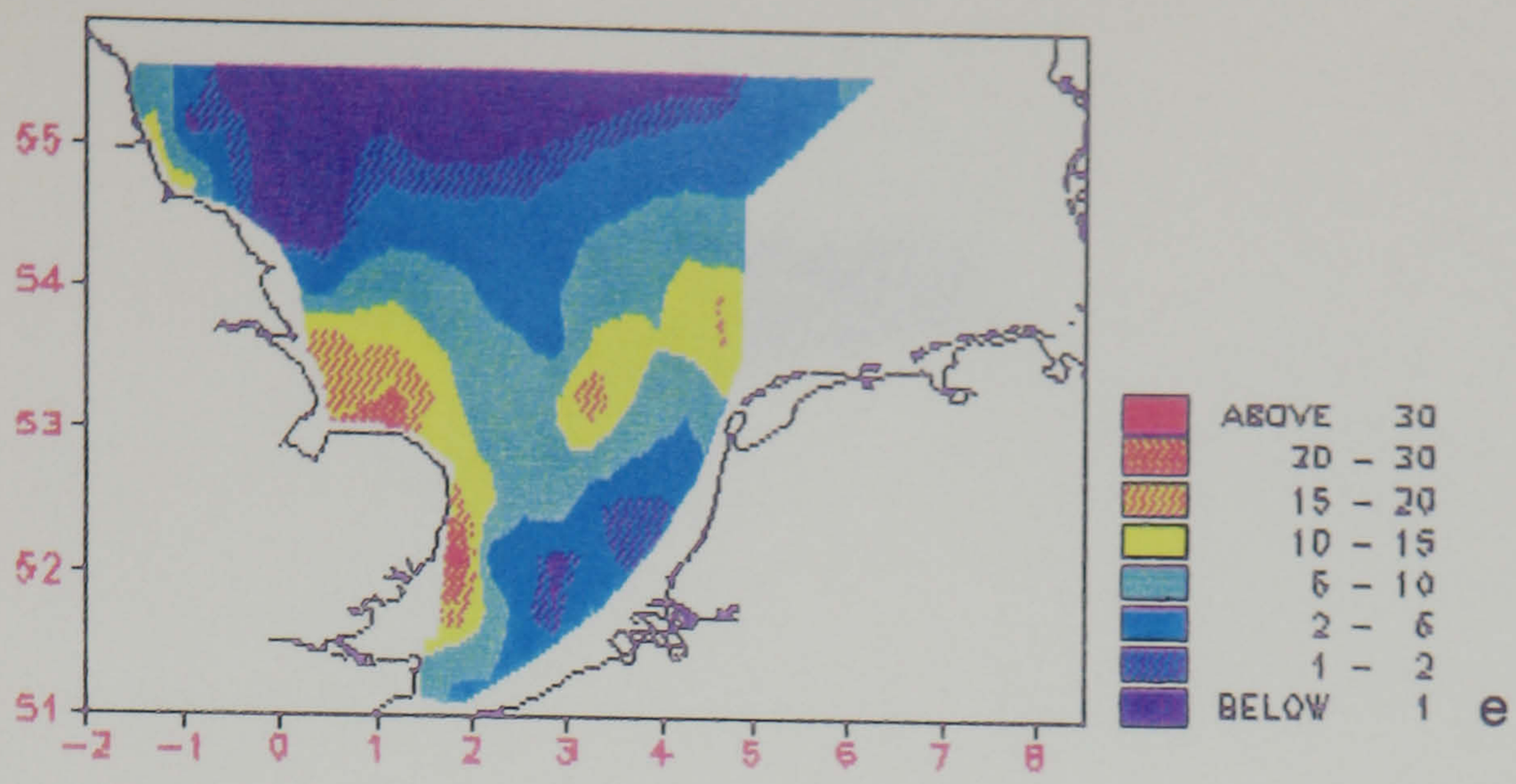

Figure 3.1 (cont/d): Distribution of TSM (mg l^{-1}) in the surface waters of the southern North Sea for (e) December 1988, (f) January 1989, (g) February 1989 and (h) March 1989.

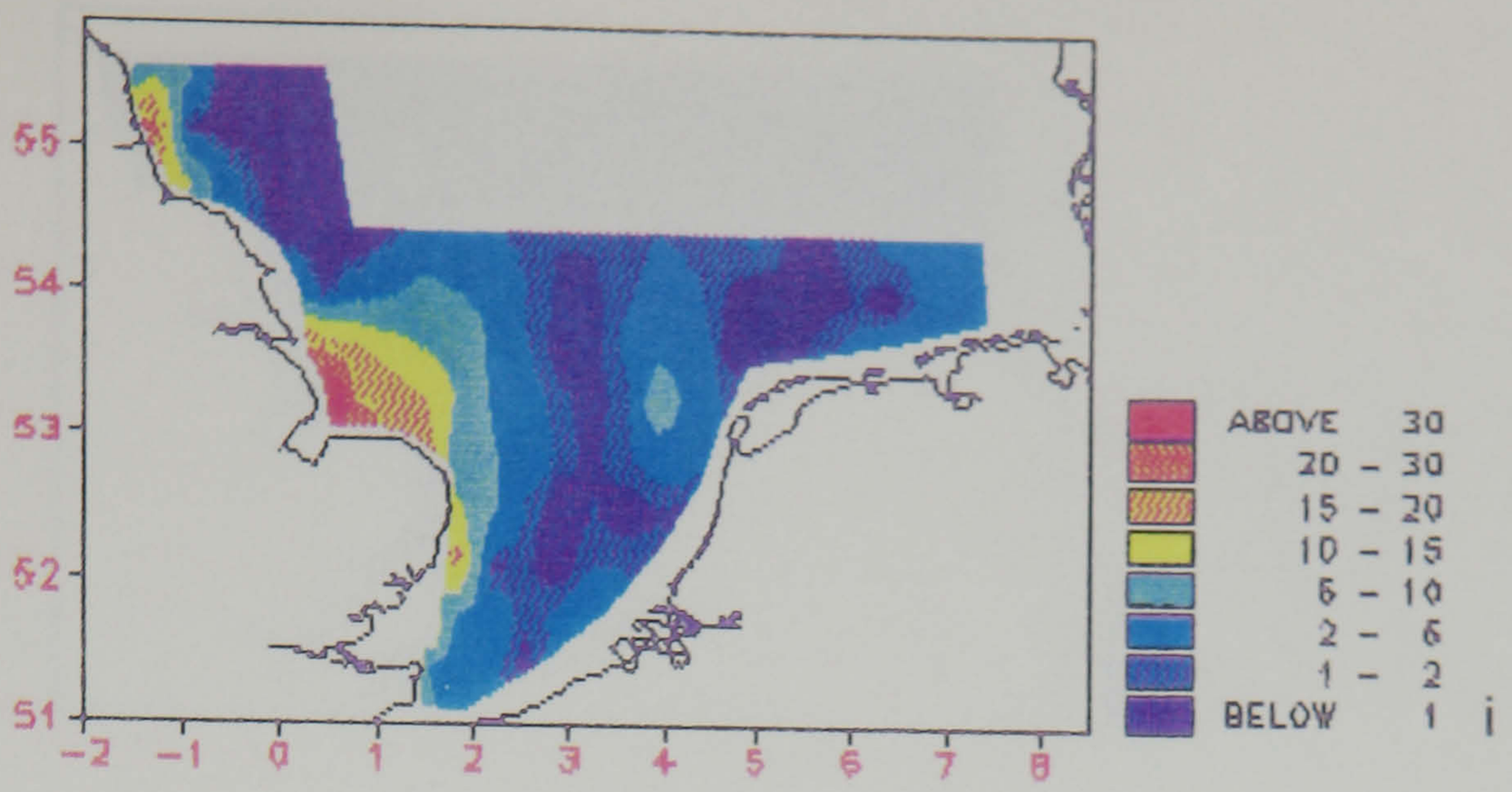

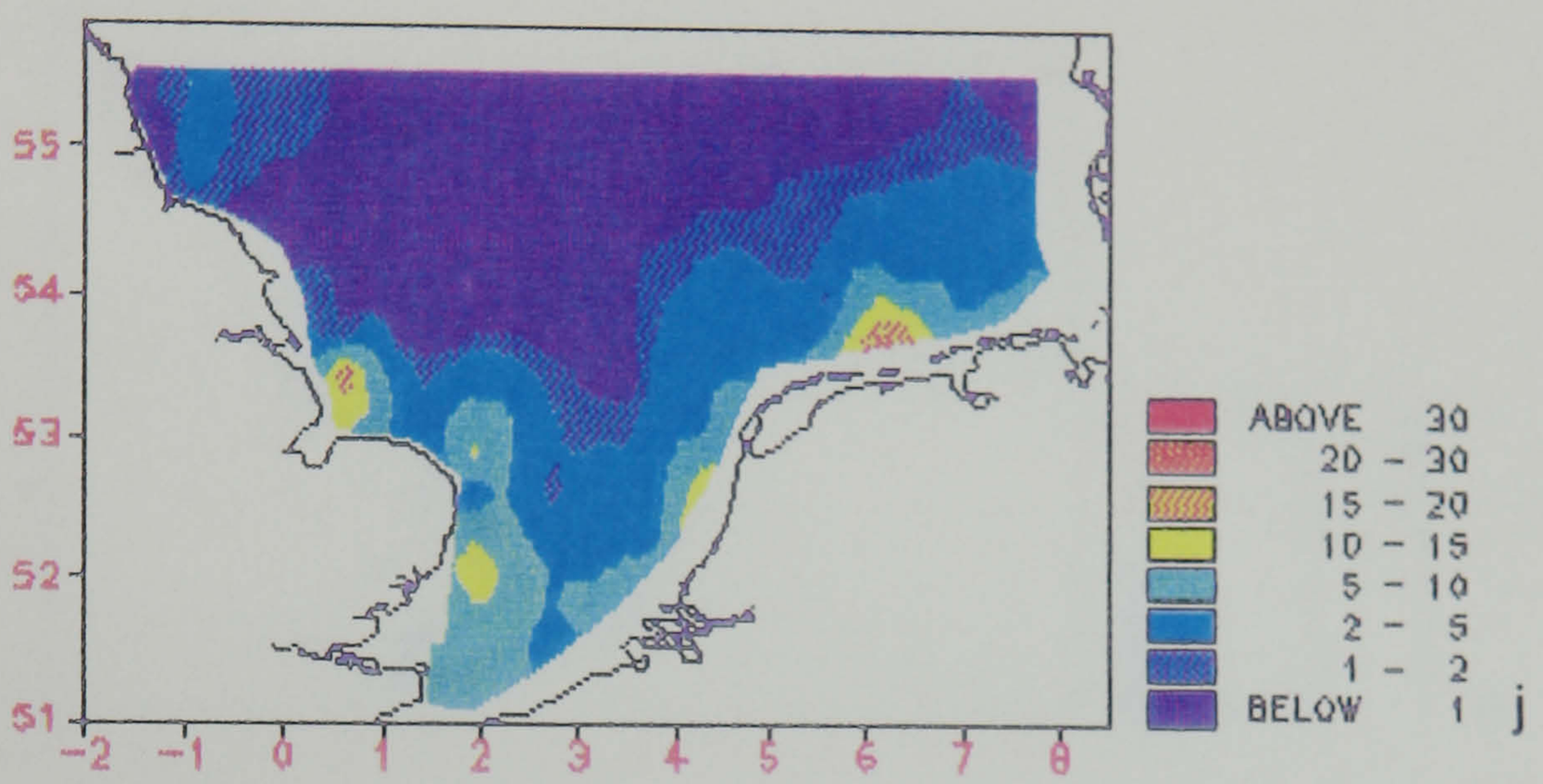

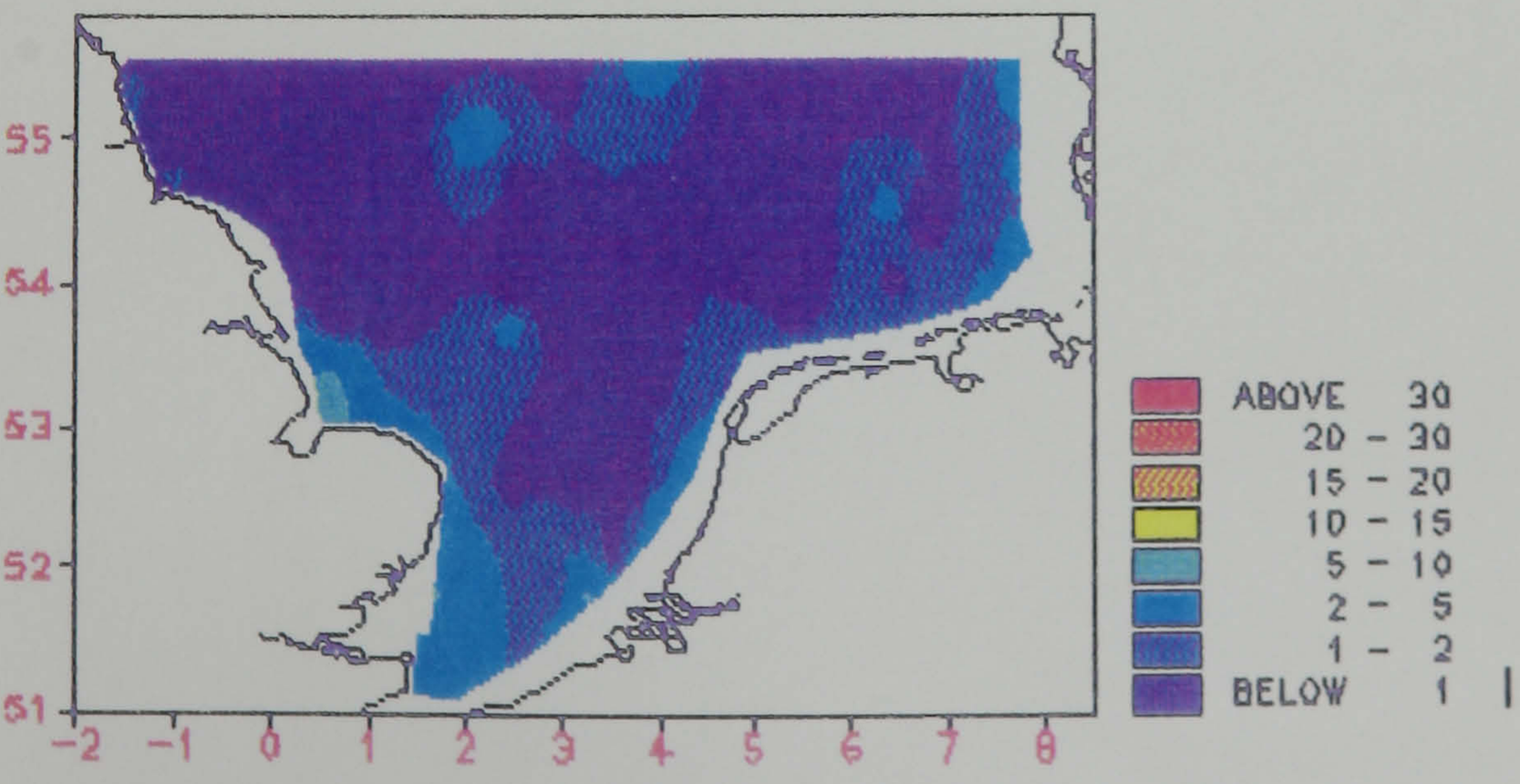

Figure 3.1 (cont/d): Distribution of TSM (mg l^{-1}) in the surface waters of the southern North Sea for (i) April 1989, (j) April-May 1989, (k) May-June 1989 and (l) June-July 1989.

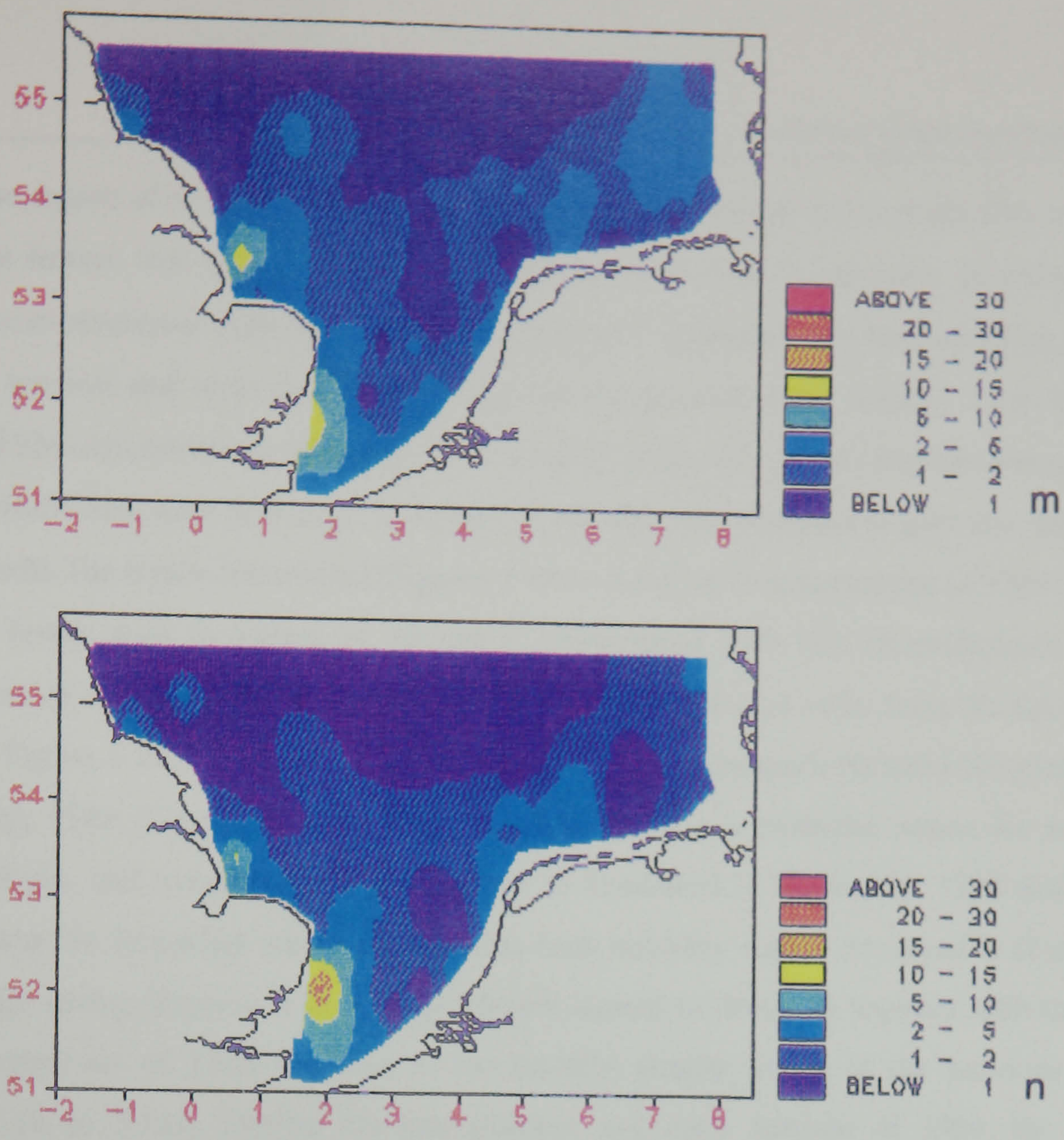

Figure 3.1 (cont/d): Distribution of TSM (mg l^{-1}) in the surface waters of the southern North Sea for (m) July-August 1989, (n) August-September 1989 and (o) September-October 1989.

The region of relatively high turbidity off the East Anglian and Lincolnshire coasts was a persistent feature that was conspicuous throughout the Survey Programme. Its existence and permanence is associated with the indigenous sources of suspended sediment resulting primarily from cliff erosion and river discharge [§1.3]. During August, 1988 [Figure 3.1a] the region sustained TSM concentrations in excess of *ca.* 2 mg l^{-1} when most concentrations throughout the southern North Sea were low (*e.g.* < 2 mg l^{-1}). As the year progressed into the autumn and winter months, the region intensified [Figures 3.1b to 3.1e] and concentrations of TSM increased to typical levels well in excess of 10 mg l^{-1}. Associated with this intensification was the development of a plume which extended to the north-east and east away from the East Anglian coast [*e.g.* Figure 3.1d]. The plume attained its maximum prominence between November, 1988 and January, 1989 [Figures 3.1d to 3.1f]. In these months, it extended across the top of the Southern Bight, and towards the German Bight as illustrated in November, 1988 and January, 1989. During the following winter months, the high turbidity region remained well developed until the late spring [Figures 3.1e to 3.1j] when it started to diminish together with the plume, and concentrations of TSM declined to the broadly similar levels of the previous summer [Figures 3.1k to 3.1m]. During the late summer and early autumn of 1989, the cycle of intensification started to be re-established [Figures 3.1n to 3.1o].

The region of relatively high turbidity was flanked to the north and sometimes to the east by a region of relatively low turbidity that had typical TSM concentrations of no more than 1-2 mg l^{-1}. The low TSM concentrations sustained by this region are associated with the inflow of low turbidity waters from the North Atlantic Ocean [§1.3]. During August and September, 1988, this region extended from the north to the south of the southern North Sea, flanking the higher turbidity region to the east [Figures 3.1a and 3.1b]. During the late autumn and early winter, as the high turbidity region intensified and the plume developed, the low turbidity region was bisected into a northern and a southern section [Figure 3.1c onwards]. It was not until the late spring and early summer of 1989 that these sections were permanently reconnected, as the plume diminished in prominence [Figure 3.1k]. Localized areas of relatively higher concentrations were also observed in the Dogger Bank region (*ca.* 54.75°N, 2.5°E), particularly during March, 1989 [Figure 3.1h], and between June and August, 1989 [Figures 3.1l and 3.1m].

The transition or boundary between the northern section of the low turbidity region, and the high turbidity region and the plume to the south, was generally delimited by the 2 mg l^{-1} contour line (*i.e.* the margin between the 1-2 and 2-5 mg l^{-1} contour intervals). The general position of this boundary, off the Yorkshire coast at Flamborough Head (0.08°W, 54.13°N) up to a longitude of about 2°E, largely coincided with the frontal transition zone observed in satellite imagery and predicted by mathematical models [Pingree and Griffiths, 1978; Holligan *et al.*, 1989]. Further to the east, however, the position of the boundary was more variable and indeterminate, owing primarily to the sparse number of survey stations [*q.v.* Figure 2.2] and also

the infrequency of sampling described in §2.1. Consequently, although there was substantial evidence for the development of a plume across the top of the Southern Bight, it was not possible to precisely delineate its northern boundary. Figure 3.1f is more representative of the true horizontal extent of the plume since during the corresponding cruise (CH43) stations DW to DY which help best to delineate the northern boundary were sampled, whereas during the preceding two cruises these stations were not sampled. Further facets of the northern boundary of plume are described in §3.2.

With respect to the spatially poorly-sampled third turbidity region of the coastal waters of the eastern Southern Bight, and the German Bight, typical concentrations of TSM tended to fluctuate between 1 and 5 mg l^{-1} for much of the seasonal cycle. The higher concentrations generally concurred with the intensification and development of the high turbidity region off the East Anglian coast during the winter months [Figures 3.1d to 3.1h]. Localized areas of intensification to concentrations in excess of 10 mg l^{-1} were particularly evident in the German Bight in November, 1988 [Figure 3.1d], and in January and February, 1989 [Figures 3.1f and 3.1g]. The most poignant event in this turbidity region was the widespread increase in TSM concentrations during April-May, 1989 [Figure 3.1j].

The monthly distributions of TSM in the bottom waters (*i.e.* nominally within 2-4 m of the sea floor) of the southern North Sea for the period of August, 1988 to October, 1989 are presented in Figure 3.2. The general TSM distributions, trends and features of the 3 main turbidity regions observed in the surface waters are repeated, in particular the cycle of intensification and the development of the plume off the East Anglian coast. Concentrations of TSM, however, tended to be marginally higher at the bottom than at the surface, most noticeably during the winter months of 1988-1989 [*e.g.* Figures 3.2d to 3.2f], during April-May, 1989 [Figure 3.2j] and during June-July, 1989 [Figure 3.2l]. An exception to this general rule were the regions of relatively higher concentrations in the surface waters bordering the Dogger Bank during March, 1989 [*cf.* Figures 3.1h and 3.2h].

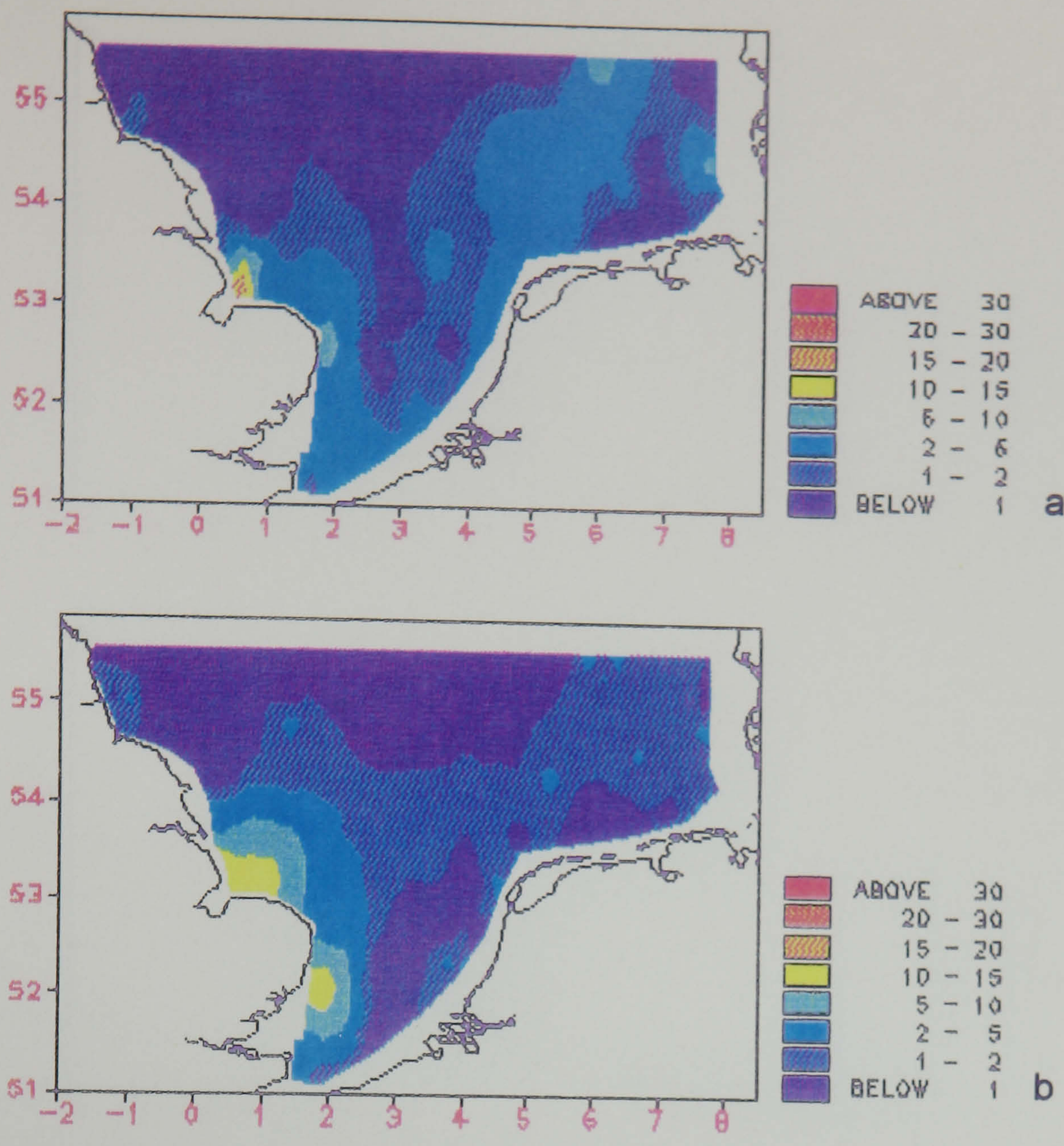

Figure 3.2: Distribution of TSM (mg l^{-1}) in the bottom waters of the southern North Sea for (a) August 1988, (b) September 1988, (c) October 1988 and (d) November 1988.

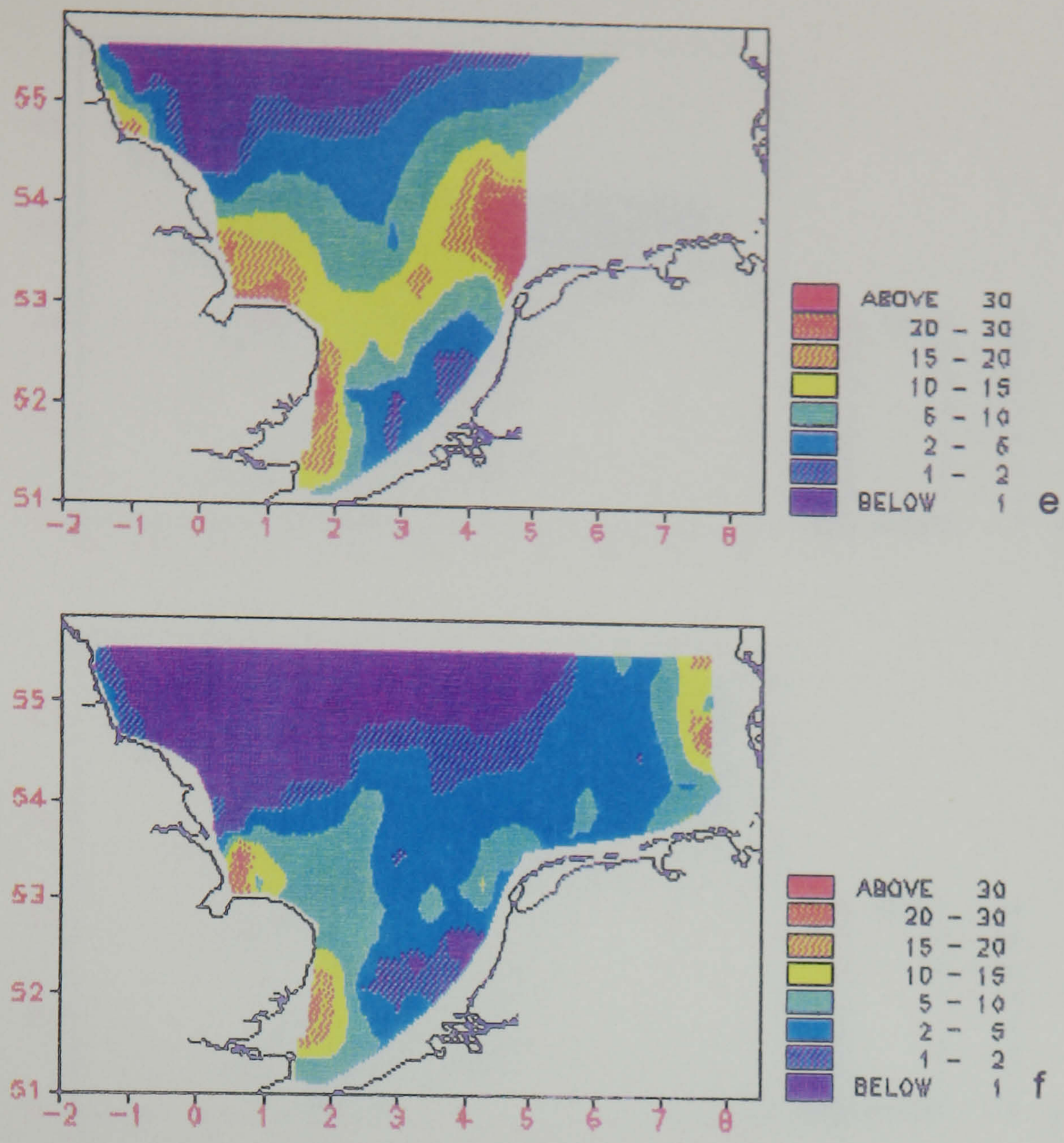

Figure 3.2 (cont/d): Distribution of TSM (mg l^{-1}) in the bottom waters of the southern North Sea for (e) December 1988, (f) January 1989, (g) February 1989 and (h) March 1989.

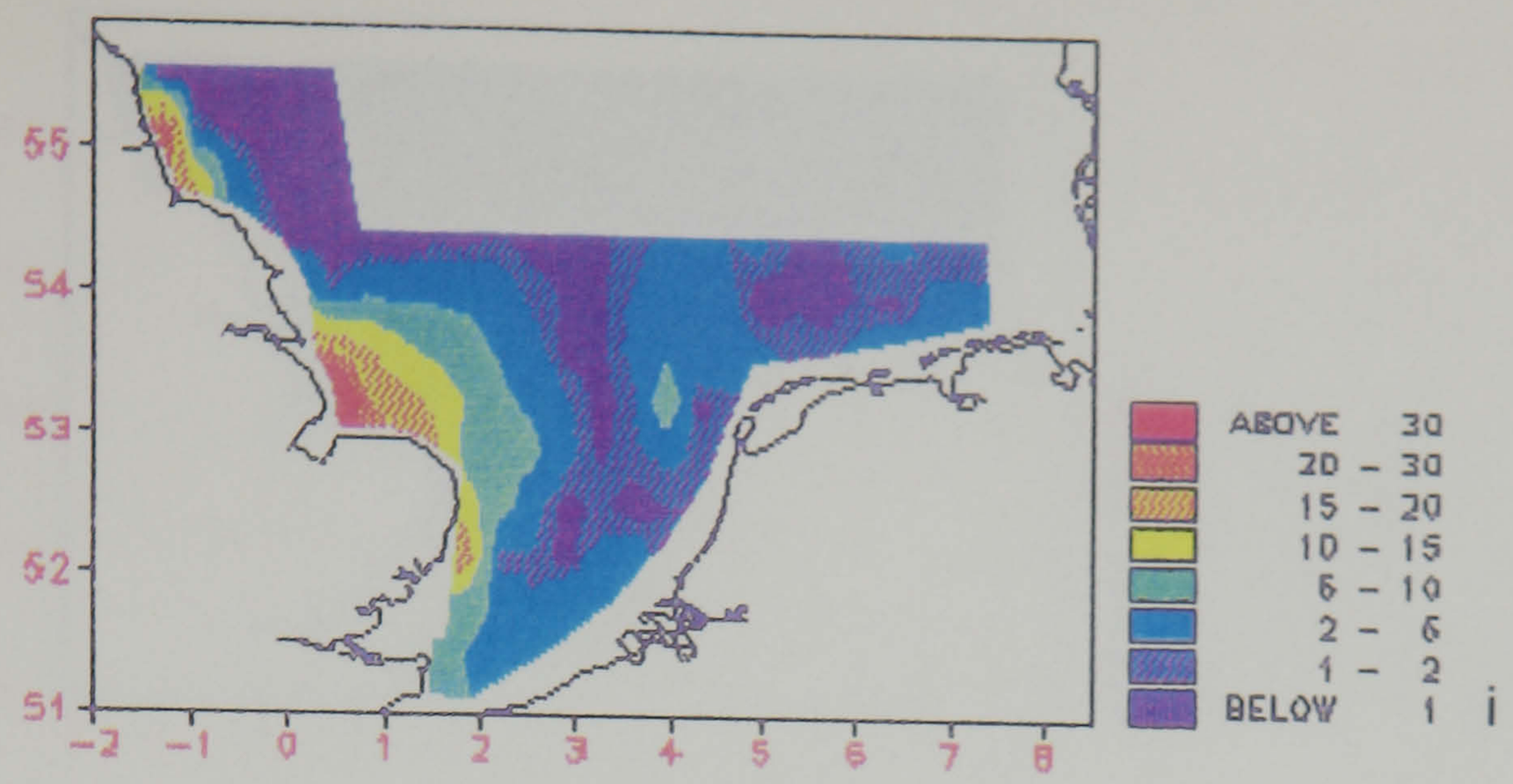

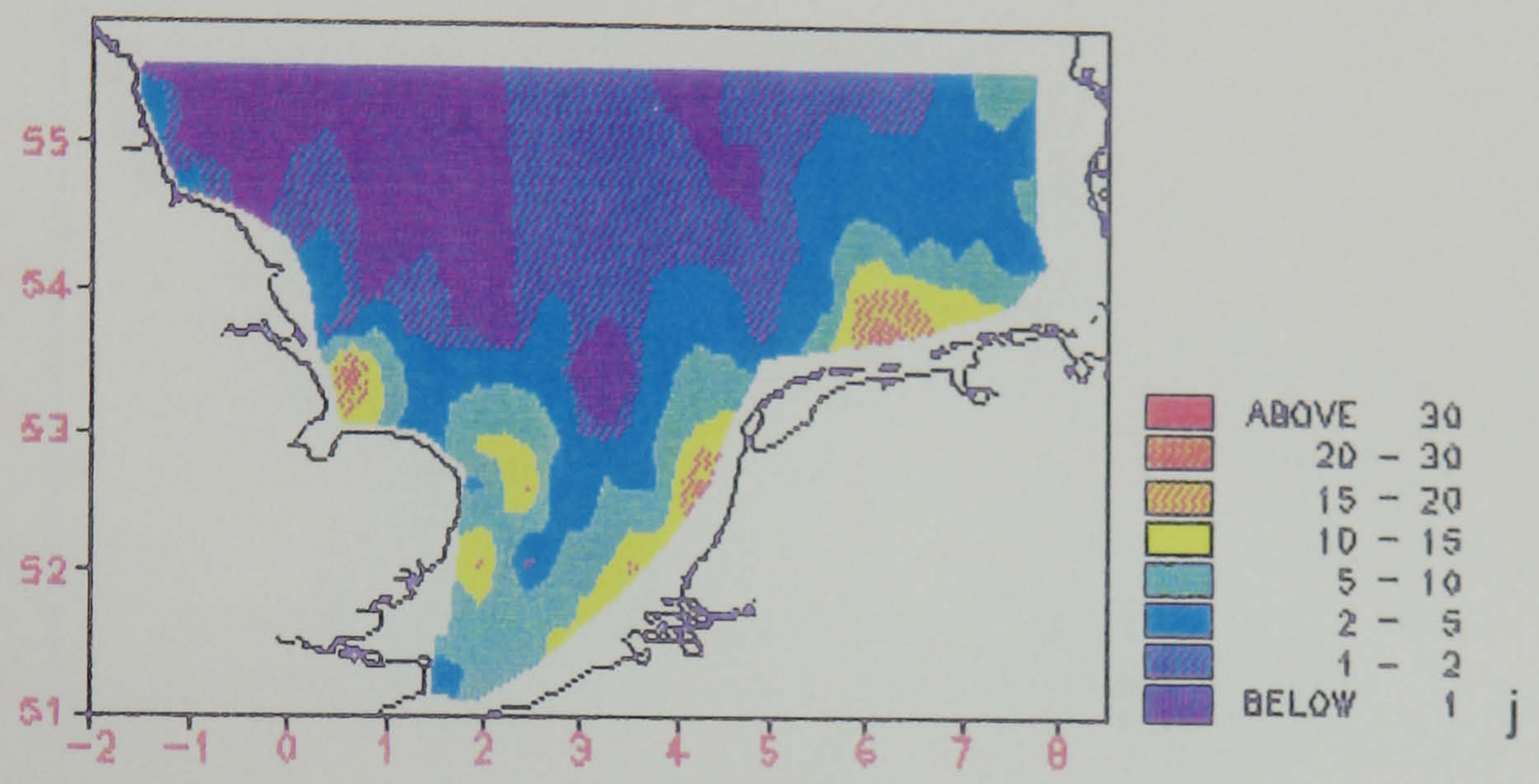

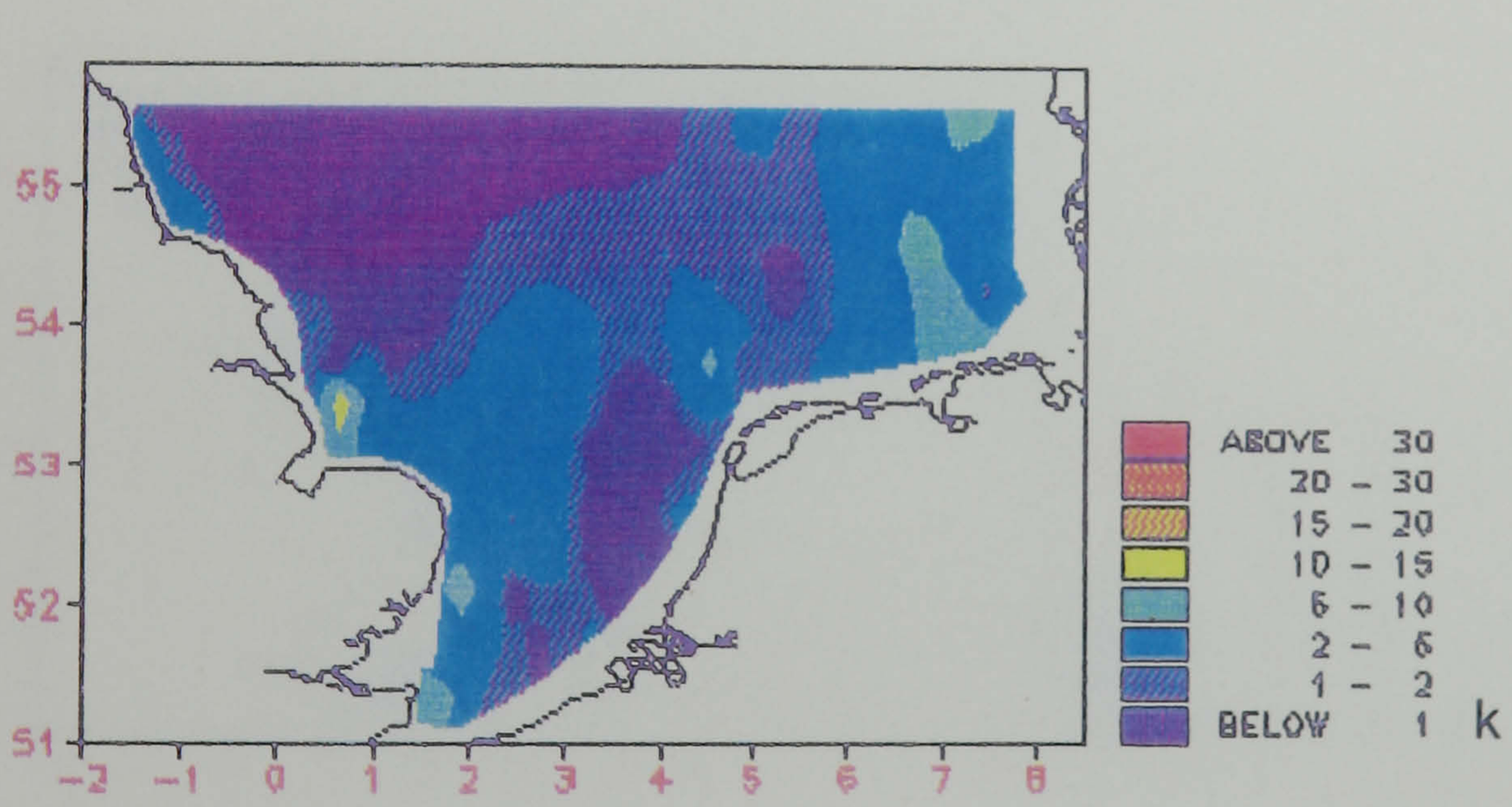

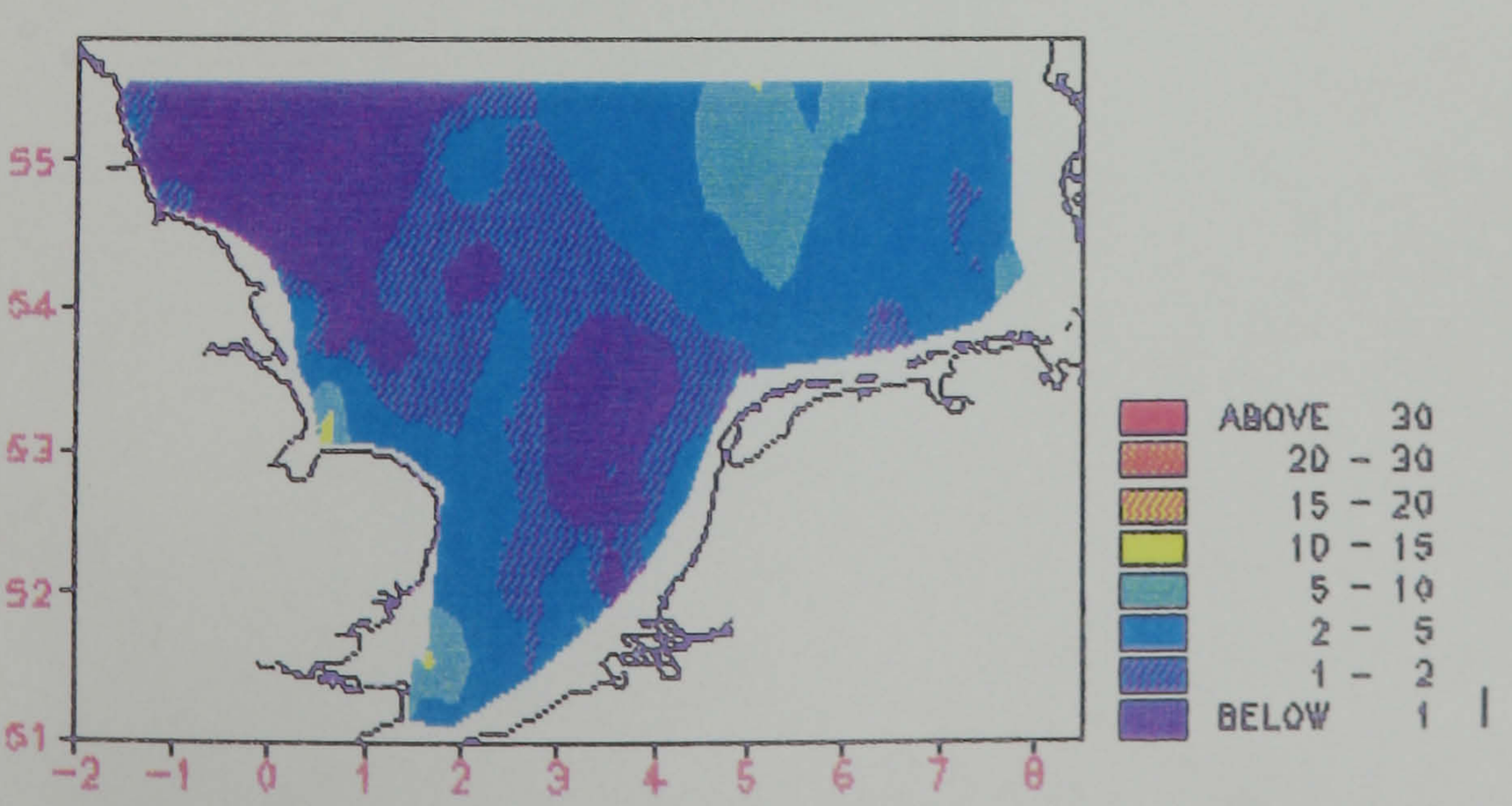

Figure 3.2 (cont/d): Distribution of TSM (mg l^{-1}) in the bottom waters of the southern North Sea for (i) April 1989, (j) April-May 1989, (k) May-June 1989 and (l) June-July 1989.

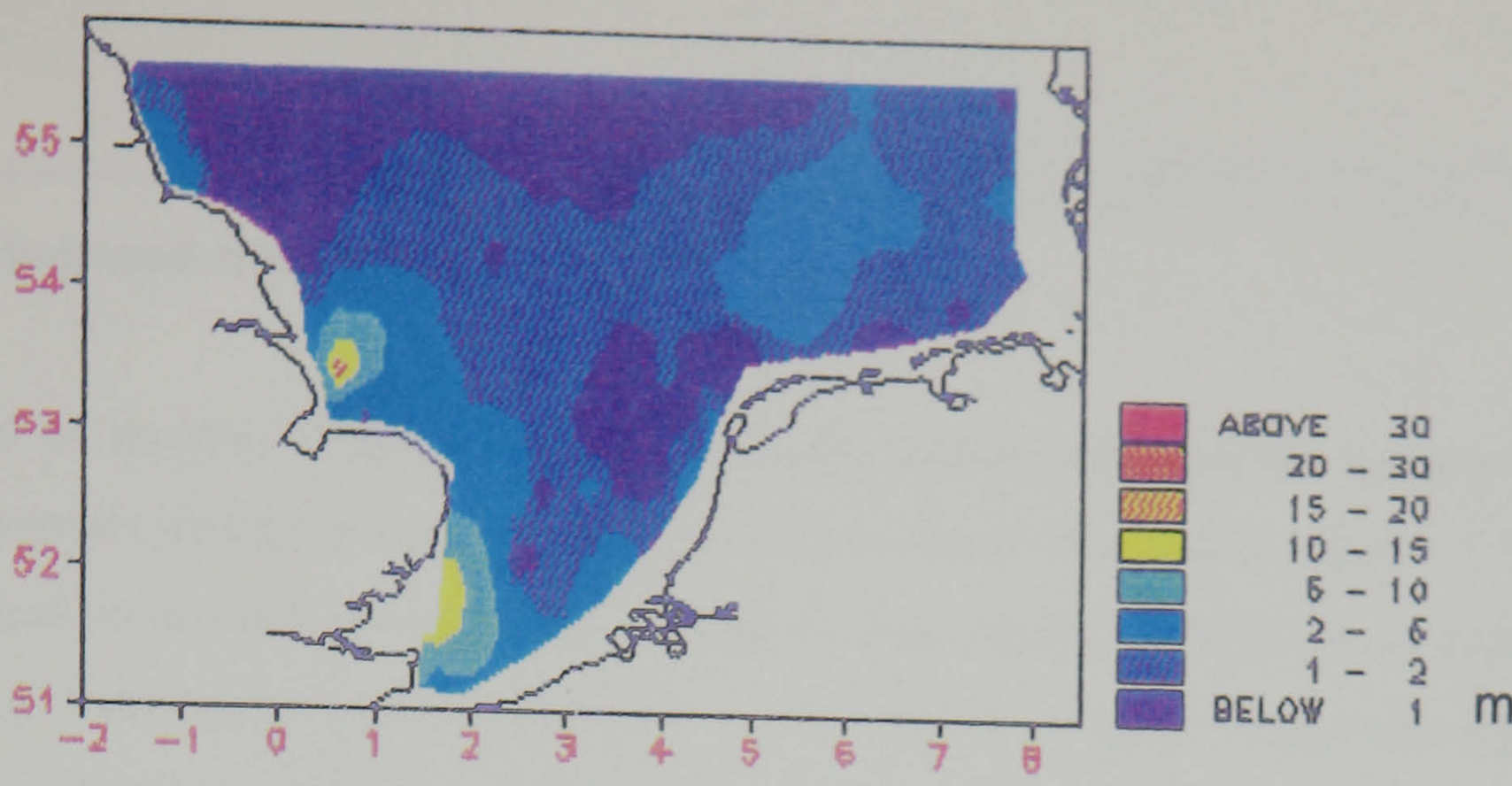

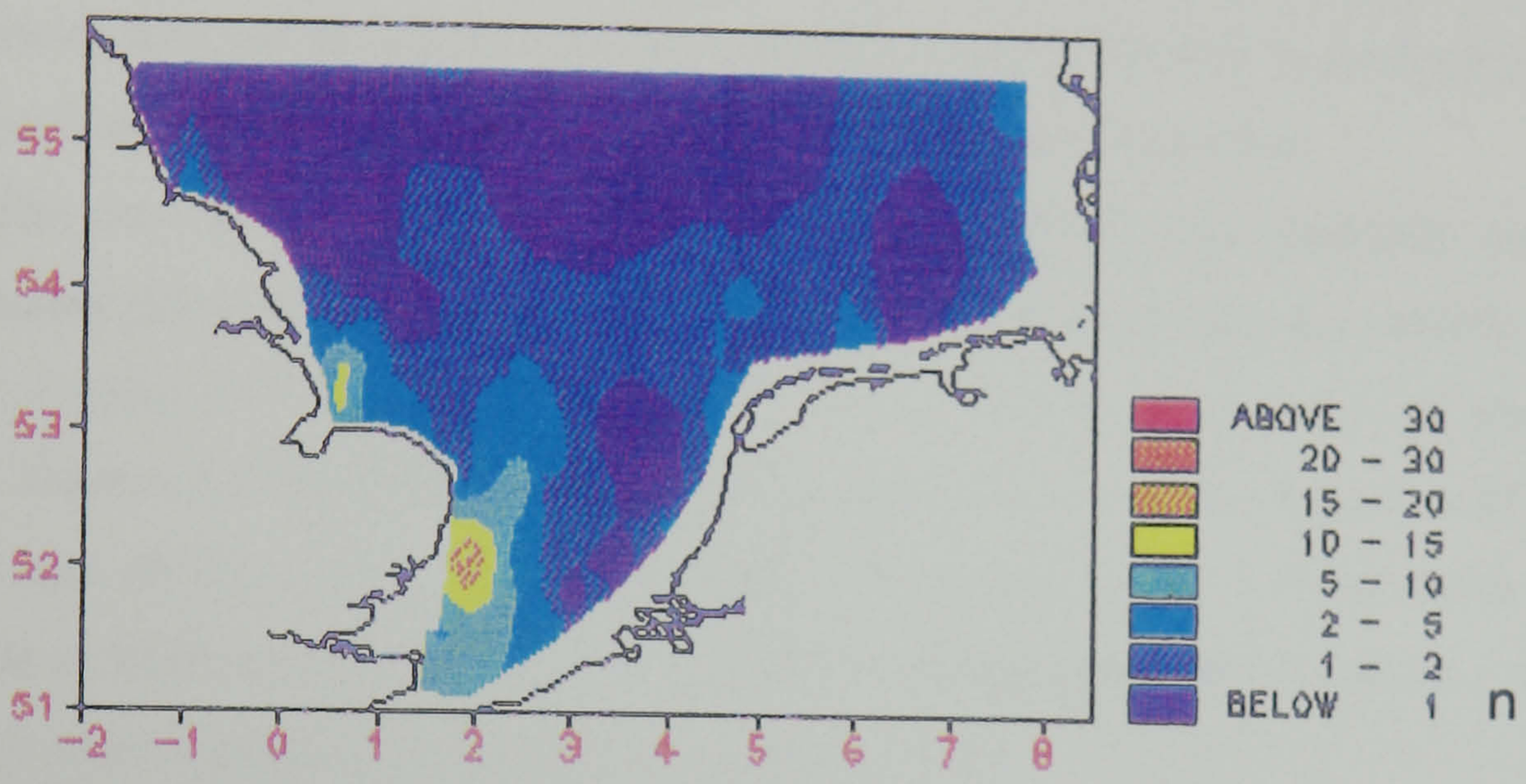

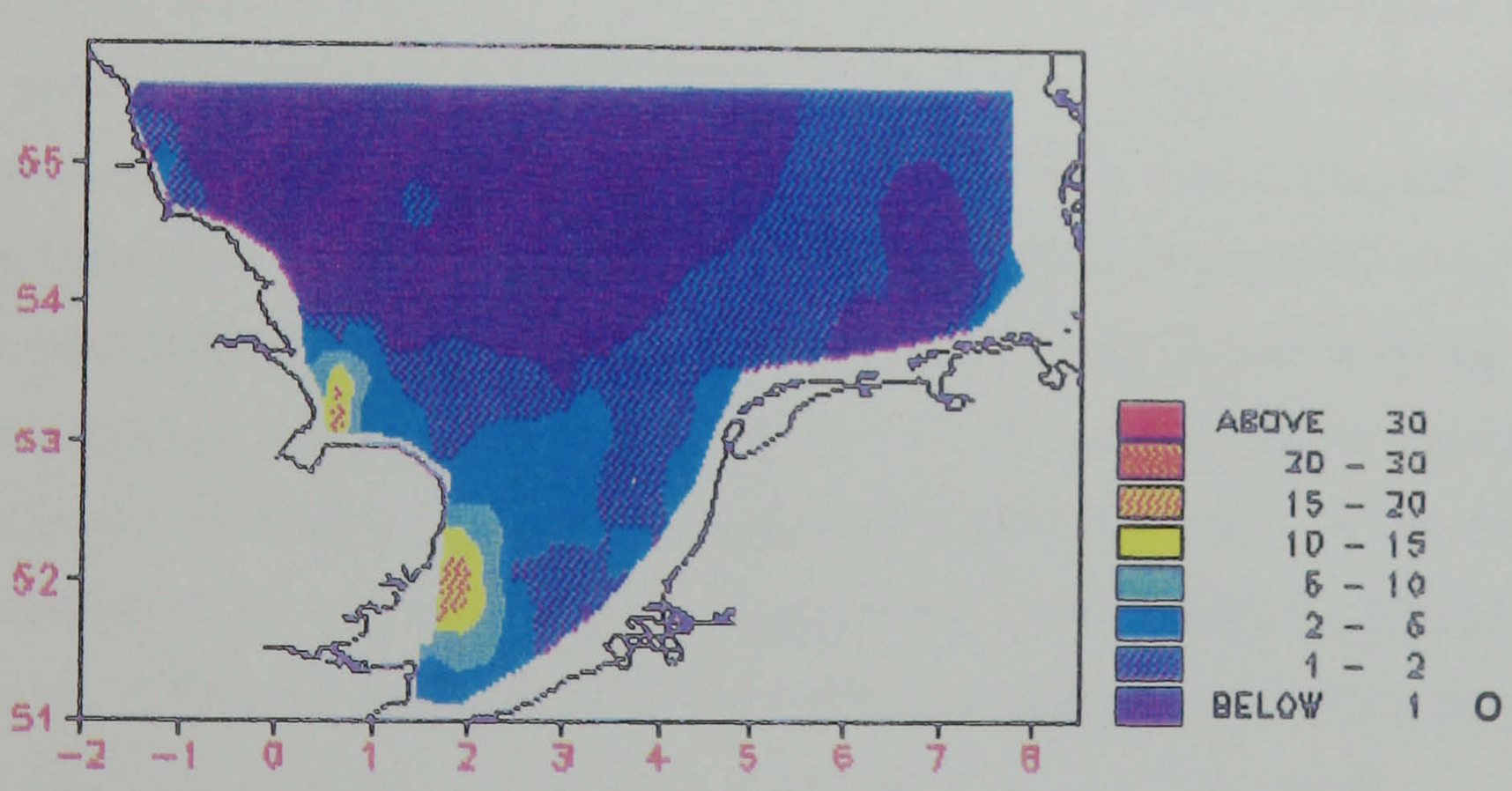

Figure 3.2 (cont/d): Distribution of TSM (mg l^{-1}) in the bottom waters of the southern North Sea for (m) July-August 1989, (n) August-September 1989 and (o) September-October 1989.

3.2: Horizontal Distributions - Underway Data

A number of monthly distributions of TSM in the surface waters of the southern North Sea derived from the underway surface transmissometer data are presented in Figure 3.3. The amount of data used in the plots is only 5% of the total surface transmissometer data available for each cruise (*e.g.* 1 data point every 10 minutes. or *ca.* 3 km) but this still represents approximately a 20-fold increase in the density of data points over the corresponding CTD plots. Consequently, the underway data can be used to test the accuracy of the CTD data in producing appropriate distributions and should also provide any detail that may have been lost.

The distributions of TSM derived from the underway data faithfully reproduce the corresponding distributions derived from the CTD data; in particular, the months of January, 1989 [*cf.* Figures 3.1f and 3.3c], April-May, 1989 [*cf.* Figures 3.1j and 3.3e] and June-July, 1989 [*cf.* Figures 3.1l and 3.3f]. The extent and magnitude of specific features such as the high turbidity zone off East Anglia and the associated plume, and the low turbidity zone to the north are similar in both sets of plots. There are, however, some significant differences in detail and omissions, most notably in August and November, 1988.

During August [Figures 3.1a and 3.3a] there were 2 patches of higher TSM in the northern part of the underway plot which are not apparent in the CTD plot. Similar features were also observed in the CTD plot of March, 1989 [Figure 3.1h] in almost identical locations but not in the corresponding underway plot [Figure 3.3d] owing to the breakdown of the PSW deck-mounted transmissometer. This part of the North Sea is well known as being an area of *Coccolithophore sp.* blooms [Holligan *et al.*, 1989] and this may explain the existence of these features. During November [Figures 3.1d and 3.3b], there was quite an extensive area of relatively higher TSM concentrations in the Dogger Bank region apparent in the underway plot but not in the CTD plot. It is likely that this area was produced by localized resuspension of sediment due to the shallower water depths associated with the Dogger Bank.

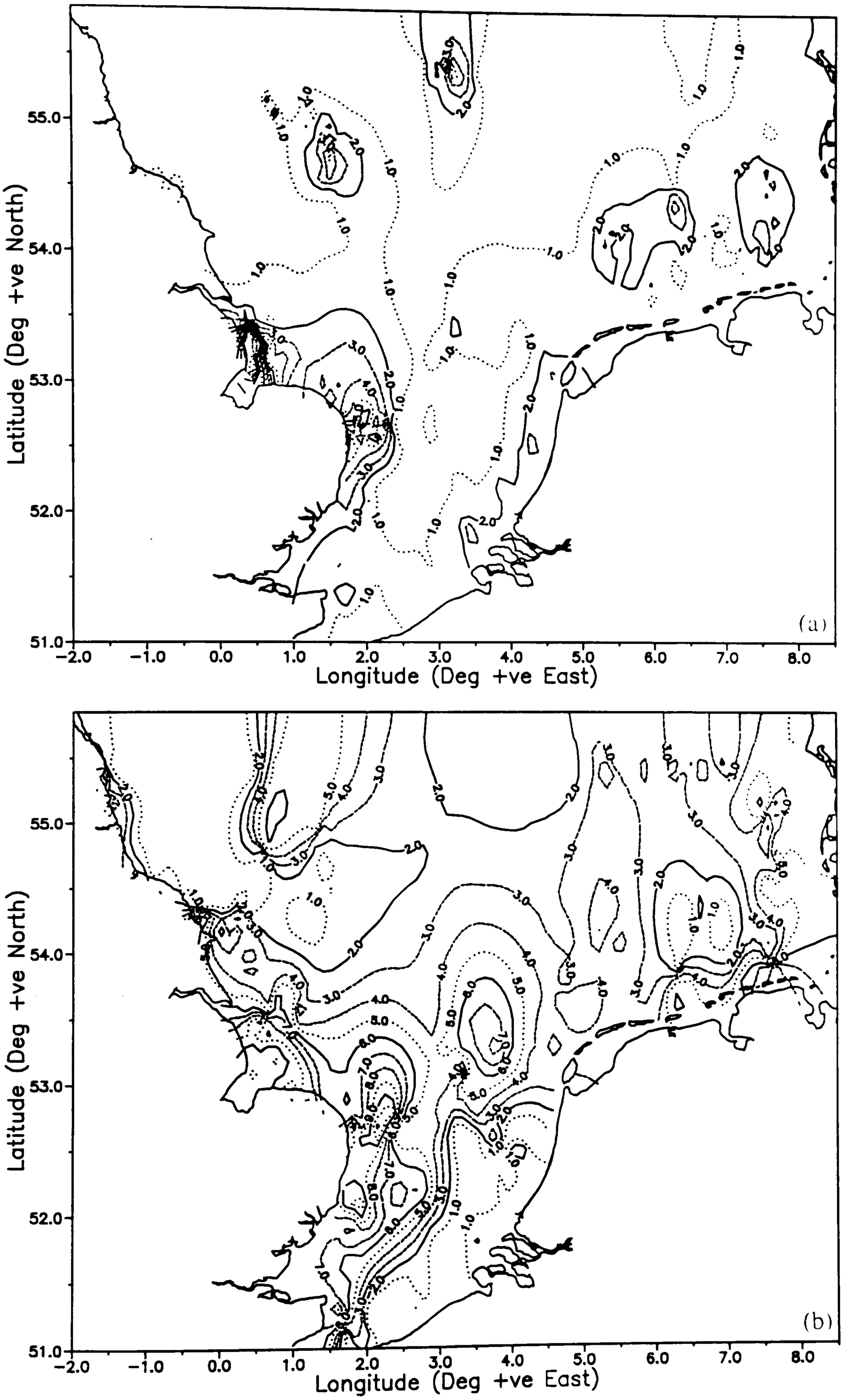

Figure 3.3: Distribution of TSM (mg l^{-1}) in the surface waters of the southern North Sea for (a) August, 1988 and (b) November, 1988. (Derived from surface transmissometer data only).

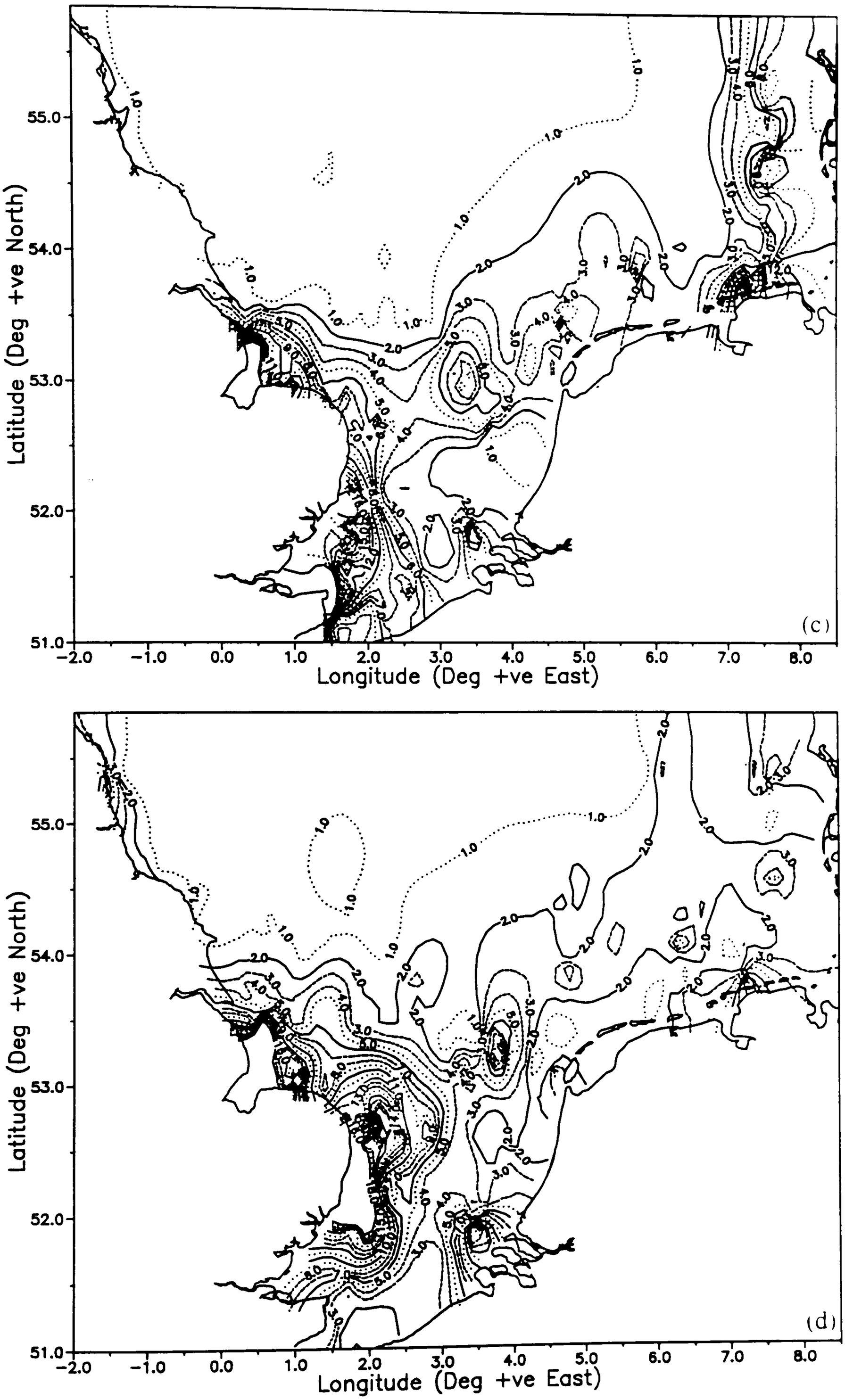

Figure 3.3 (cont/d): Distribution of TSM (mg l^{-1}) in the surface waters of the southern North Sea for (c) January, 1989 and (d) March, 1989. (Derived from surface transmissometer data only).

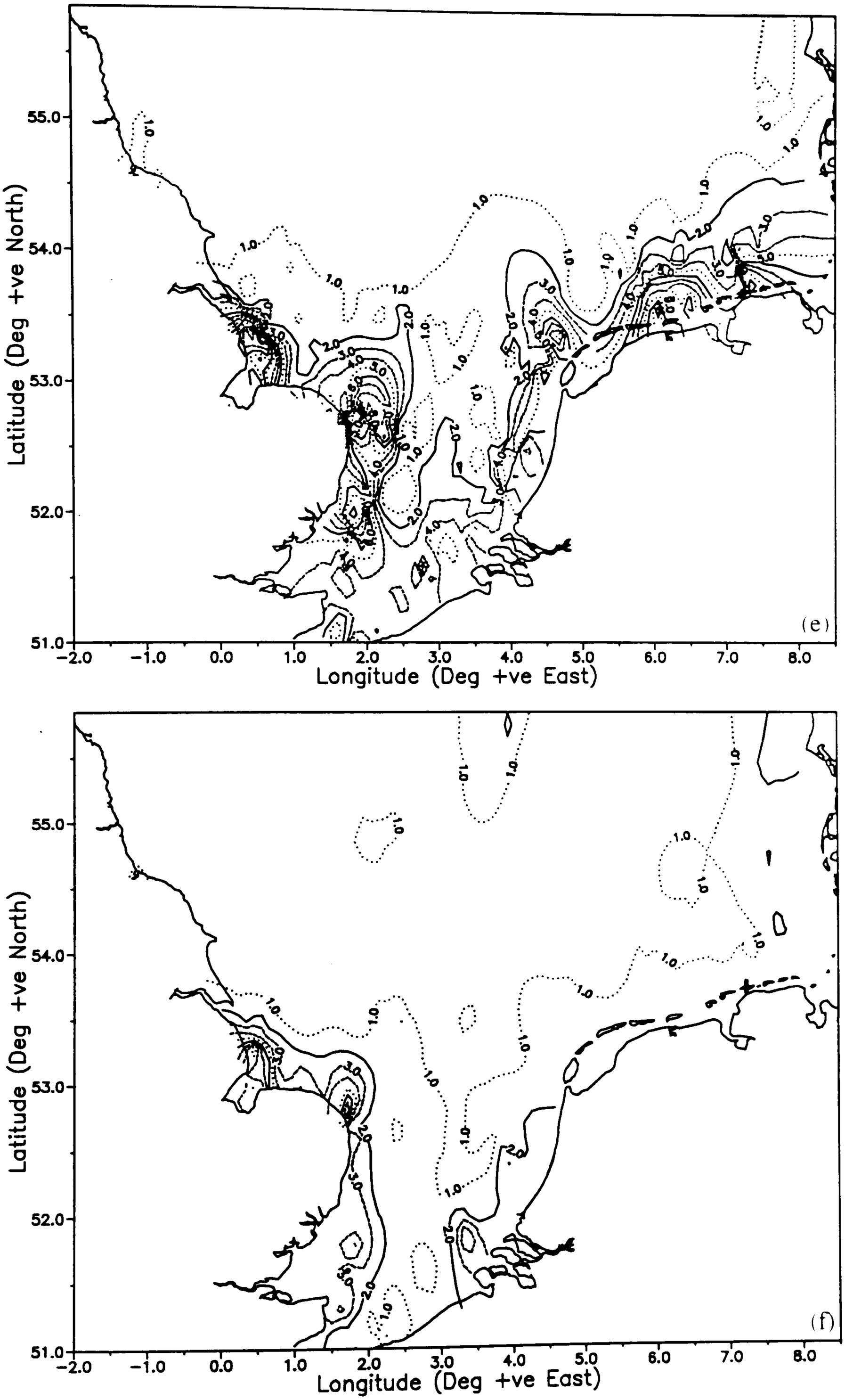

Figure 3.3 (cont/d): Distribution of TSM (mg l^{-1}) in the surface waters of the southern North Sea for (e) April, 1989 and (f) June-July, 1989. (Derived from surface transmissometer data only).

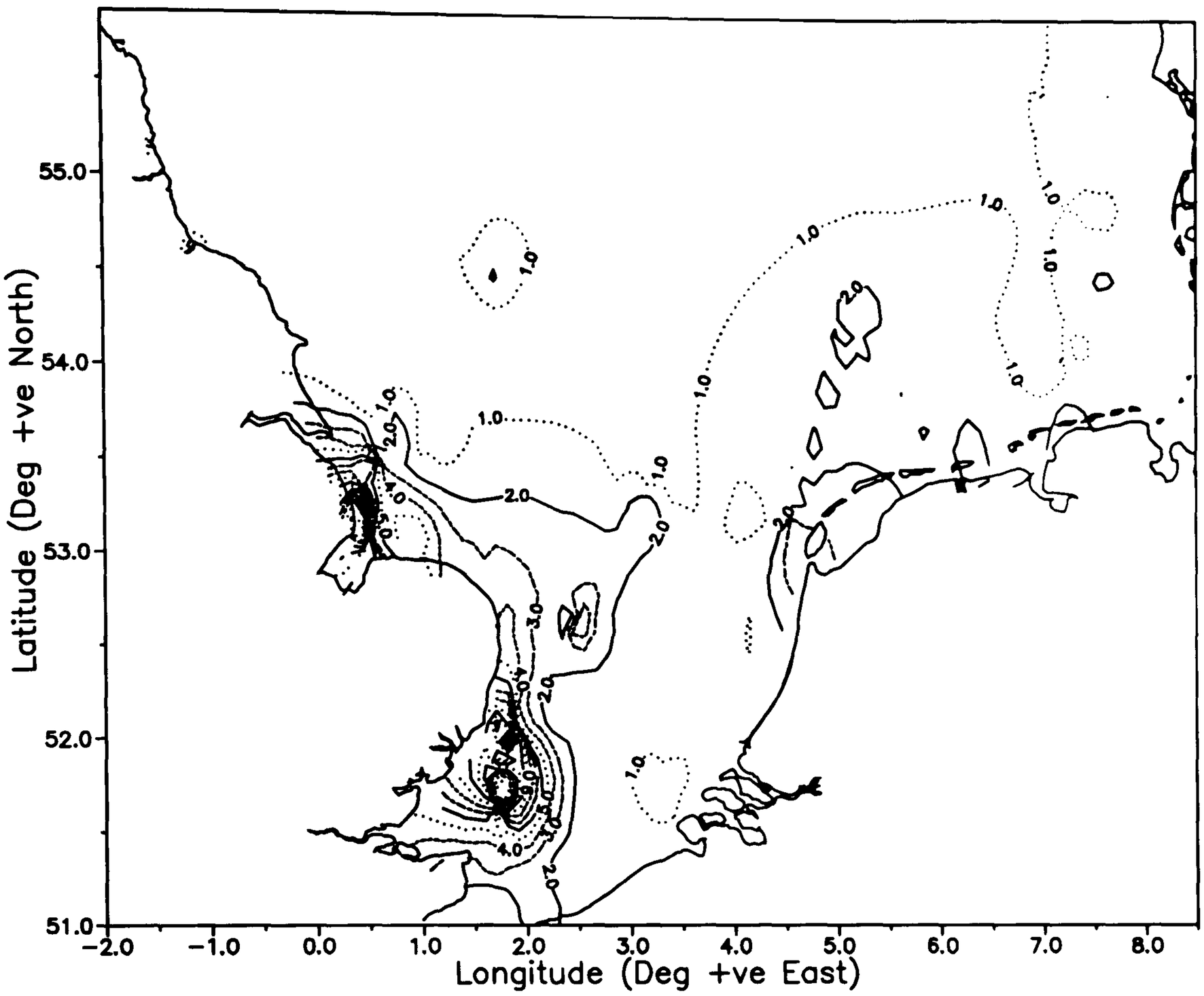

Figure 3.3g: Distribution of TSM (mg l^{-1}) in the surface waters of the southern North Sea for September-October, 1989. (Derived from surface transmissometer data only).

3.3 Horizontal Distributions - Seasonally Averaged Data

As described in §2.3, seasonally averaged TSM data were derived for typical winter, spring and summer conditions. The seasonal contour plots of TSM in the surface waters of the southern North Sea are presented in Figure 3.4. Similar plots for the bottom waters of the southern North Sea showed no significant differences from the surface water plots and so they have not been reproduced here.

The seasonally averaged plots of TSM reproduce the general patterns and features observed for the monthly cruise TSM distributions described in §3.1 and §3.2. For winter conditions [Figure 3.4a], the TSM distribution is characterised by a high turbidity zone off East Anglia and an associated plume of high concentration stretching across the top of the Southern Bight to the German Bight. The plume is flanked to the north by an extensive zone of lower concentrations. The TSM distribution for spring conditions [Figure 3.4b] is very similar to the pattern for winter conditions, although concentrations along the length of the continental European coastline are relatively higher by some 2-3 mg l^{-1}. By sharp contrast to the other two seasons, the TSM distribution for summer conditions [Figure 3.4c] is characterised by generally low concentrations of no more than 1-2 mg l^{-1}. Along the East Anglian coast, however, the high turbidity zone is still evident with concentrations of about 5 mg l^{-1} at the mouths of the Thames and Humber/Wash estuaries.

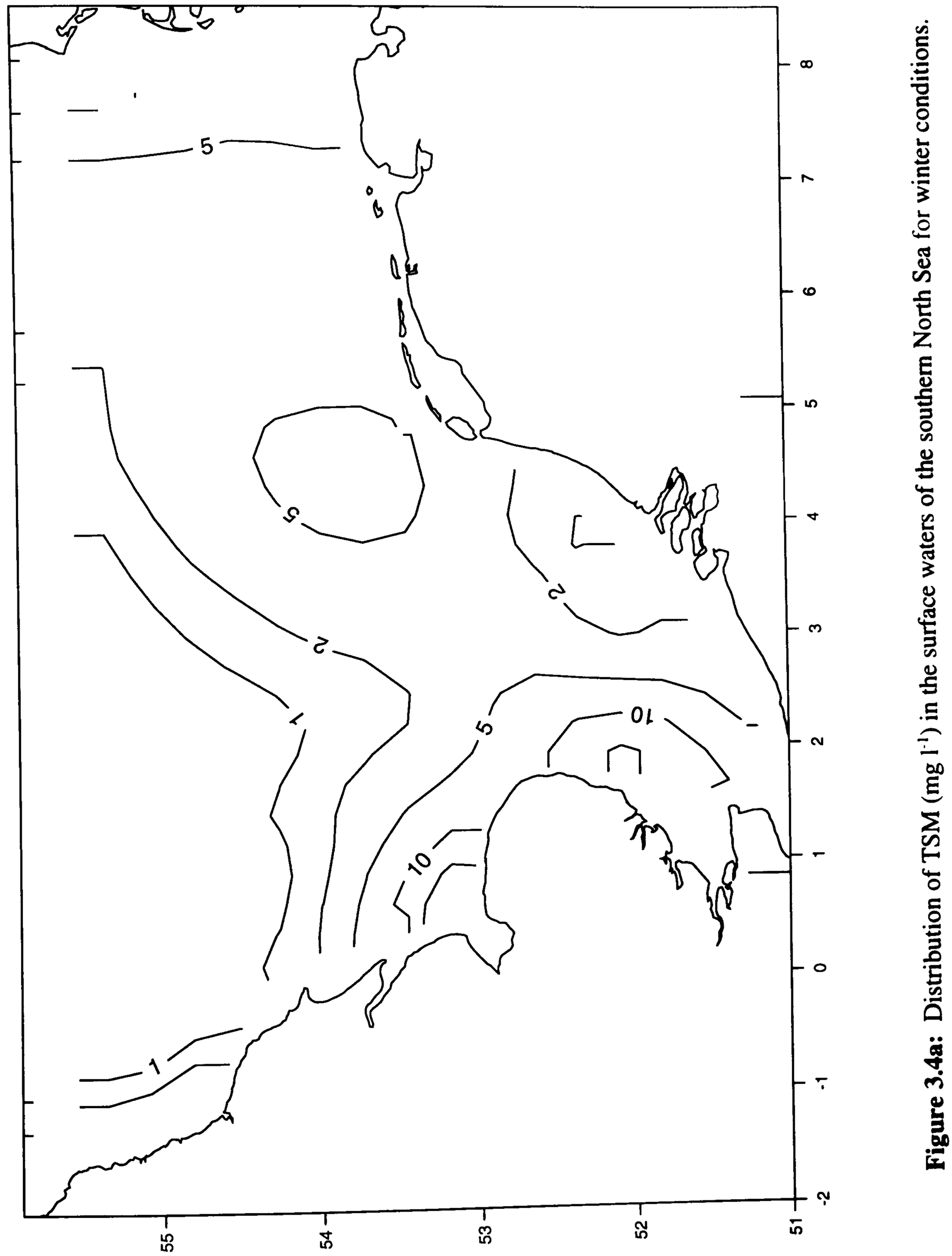

Figure 3.4a: Distribution of TSM (mg l^{-1}) in the surface waters of the southern North Sea for winter conditions.

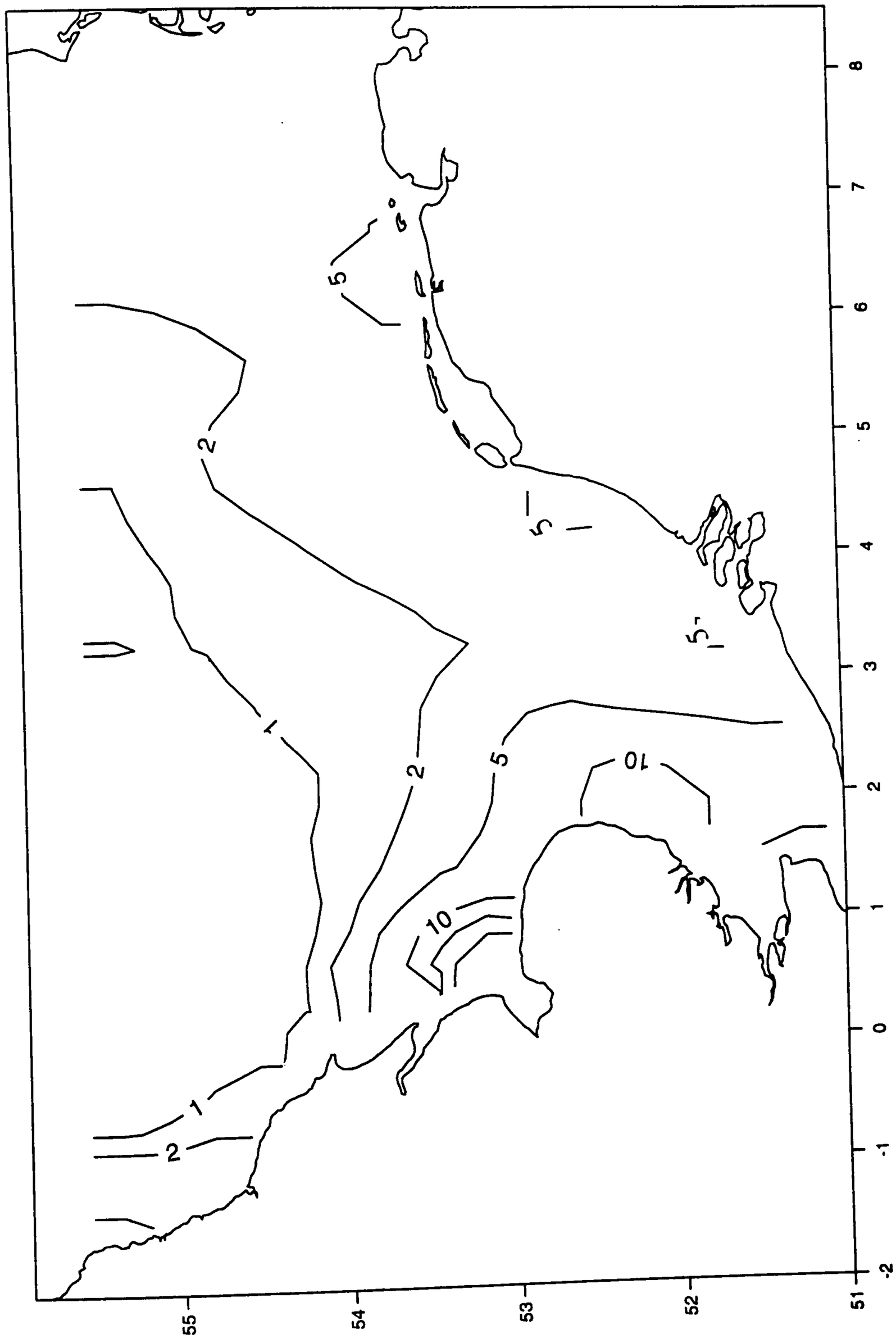

Figure 3.4b: Distribution of TSM (mg l^{-1}) in the surface waters of the southern North Sea for spring conditions.

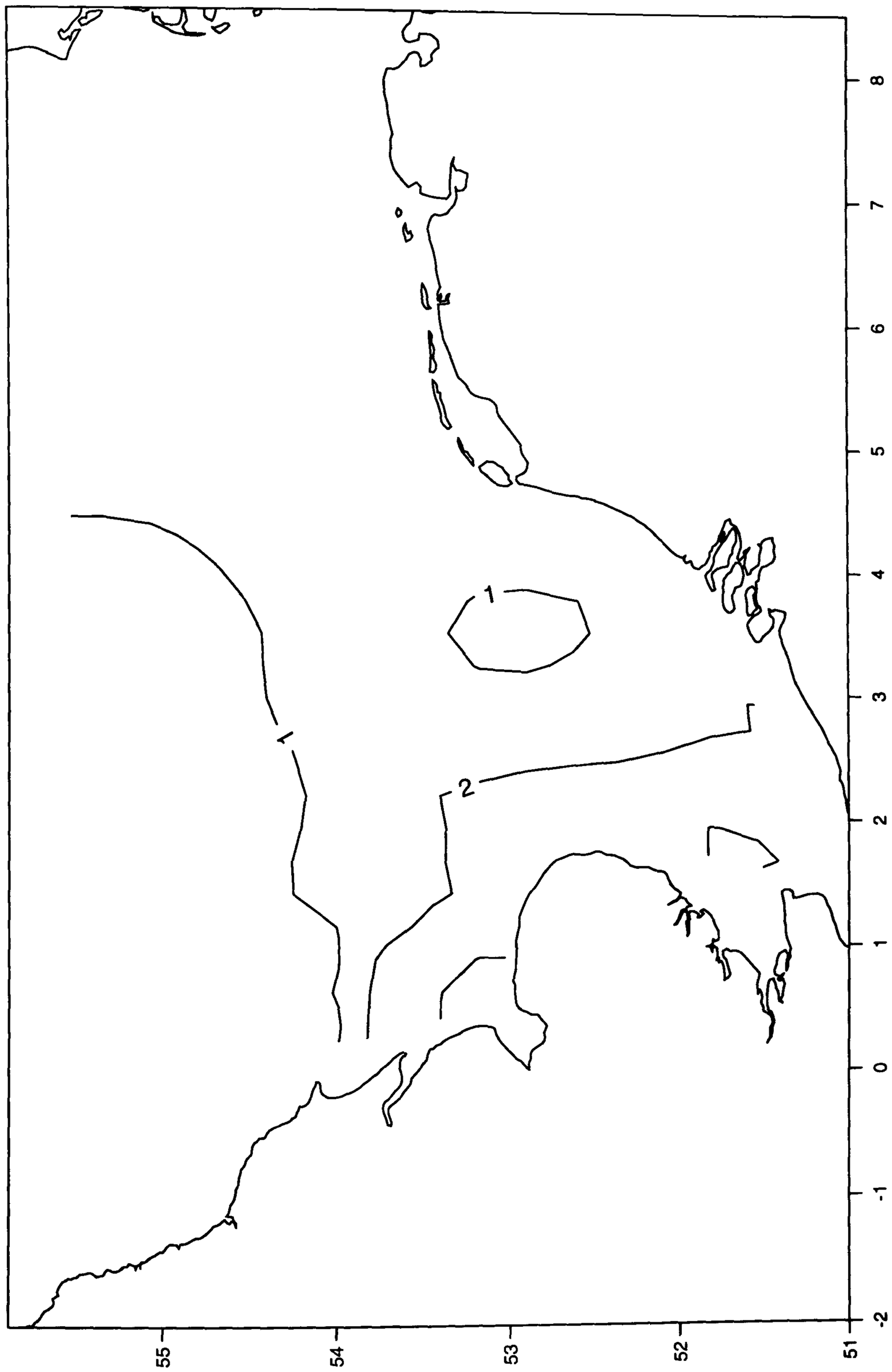

Figure 3.4c: Distribution of TSM (mg l^{-1}) in the surface waters of the southern North Sea for summer conditions.

3.4: Vertical Distributions

A number of section plots using seasonally averaged TSM data were chosen to illustrate the vertical distribution of TSM in the southern North Sea during winter, spring and summer conditions. The positions of these sections together with the survey stations involved are given in Figure 3.5.

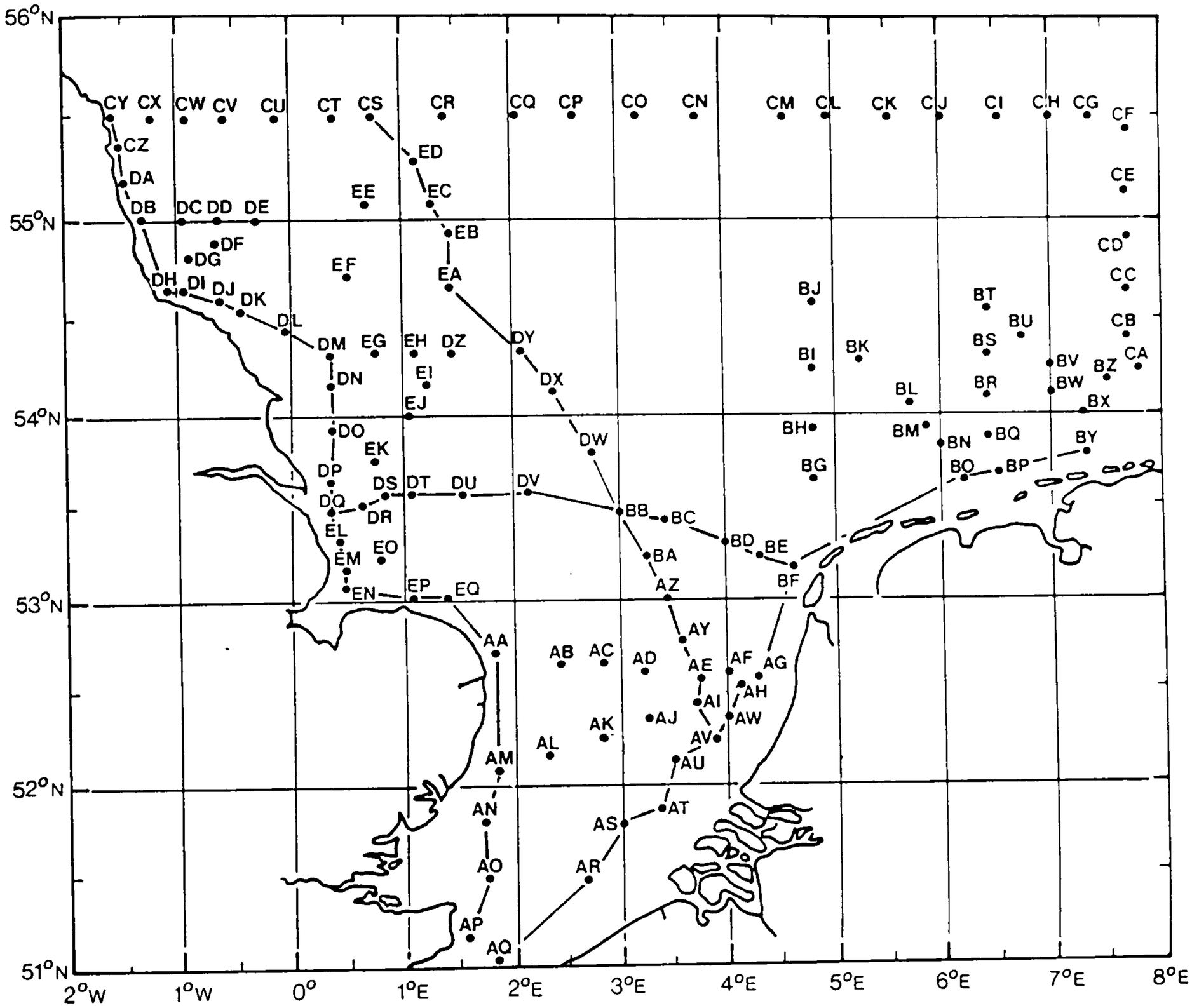

Figure 3.5: Positions of the vertical section plots.

The plots are essentially aligned to firstly, illustrate the features associated with the different turbidity regimes described in §3.1, especially across the zone of plume development, and secondly, to show any evidence for the existence of offshore and longshore gradients of TSM.

SECTIONS CS TO AV

The sections presented in Figure 3.6 are aligned in a general north-west to south-east orientation so that they transect the low turbidity region, the high-low turbidity boundary zone and the region of plume development.

For winter conditions [Figure 3.6a], the section plot is characterized by a zone of high concentration of TSM (> 2-3 mg l^{-1}) some 90-100 km wide between stations DW and AY. This high concentration zone corresponds with the area of plume development observed in the horizontal distributions [*cf.* Figures 3.1f and 3.2f, and Figures 3.1h and 3.2h]. To the north, concentrations decline as the deep depression of the Outer Silver Pit is reached (at station DX), suggesting that the northern boundary of the plume along this section may be bathymetrically confined. Concentrations within the Outer Silver Pit tend to increase with depth, implying that this may be an area of active deposition of sediment although it is not obvious in the other section plots. Further to the north and along the western margin of the Dogger Bank (between stations EC and EA) concentrations are generally less than 1 mg l^{-1}, corresponding to the zone of low turbidity observed in the horizontal distributions.

For spring conditions [Figure 3.6b], the zone of high concentration is still evident between stations DW and AY. Concentrations of TSM along the continental European coastline have also increased (out to about station AE) which are probably related to the onset of the period of spring phytoplankton blooms and to the increase supply of river-borne sediments from especially the Rhine. To the north, a localized surface TSM maximum is evident, centred about station EC over the Dogger Bank. This corresponds to the localized high concentration zone evident in the horizontal distribution for March 1989 [Figure 3.1h]. As suggested previously in §3.2 this localized high concentration zone may be associated with a *Coccolithophore sp.* bloom.

For summer conditions [Figure 3.6c], the vertical distribution of TSM along the section is not particularly engrossing since concentrations are very low, generally less than 1 mg l^{-1}.

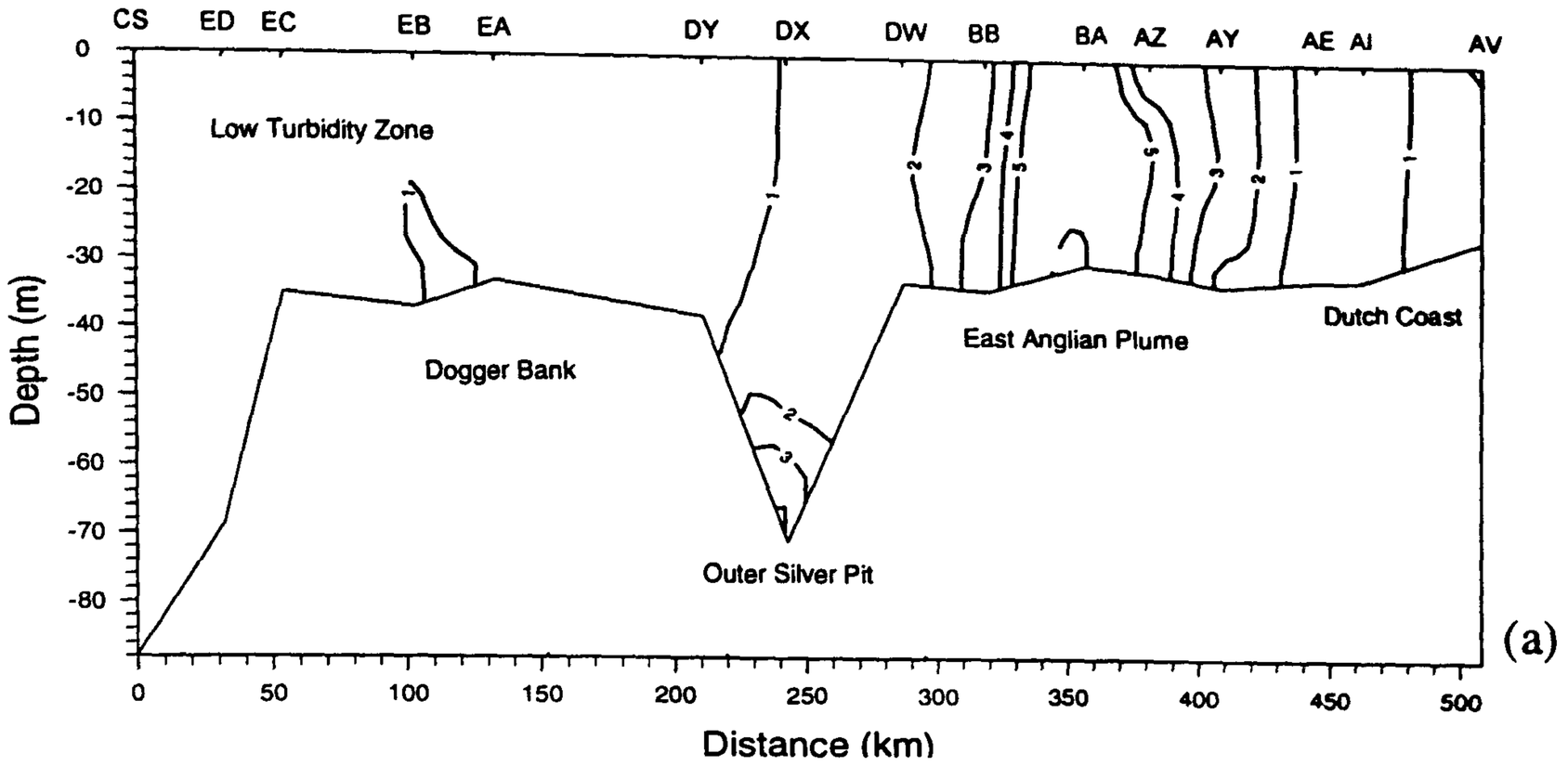

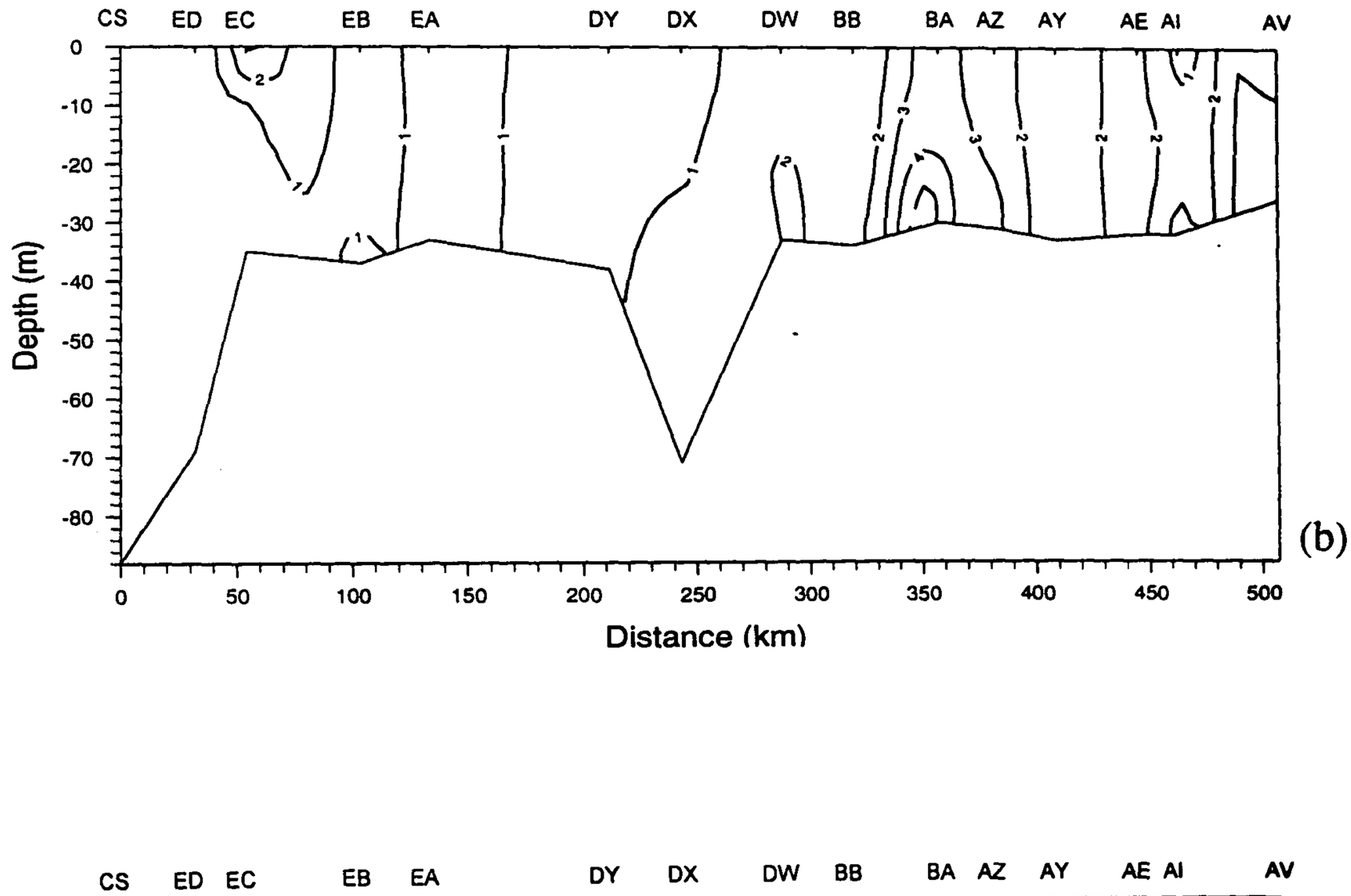

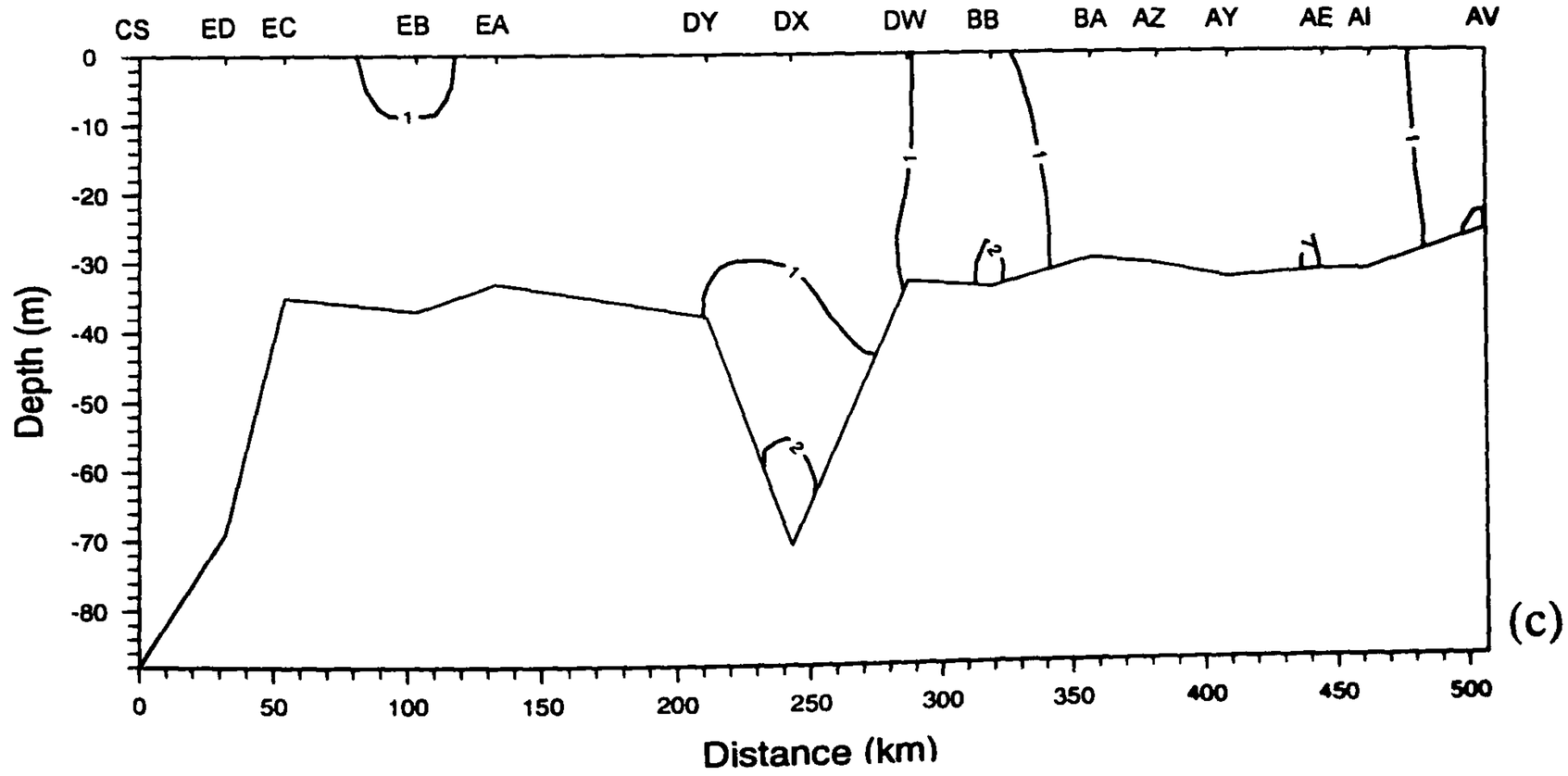

Figure 3.6: Vertical Distribution of TSM (mg l^{-1}) between survey stations CS to AV for (a) winter, (b) spring and (c) summer conditions.

SECTIONS DQ TO BF

The sections presented in Figure 3.7 are aligned in a general west to east orientation so that they are approximately perpendicular to the previous section CS to AV, and traverse the southern North Sea from the English coast to the Dutch coast.

For winter conditions [Figure 3.7a], the area off the English coast is characterized by a sharp gradient of TSM with concentrations decreasing from about 10 mg l^{-1} at station DQ to about 1 mg l^{-1} at station DS. The area also appears to be bathymetrically confined within the Silver Pit, the deep depression centred about station DR. The high concentrations associated within this area are primarily related to the supply of sediment from the Humber estuary and plume, and from the coastal erosion of the Holderness Cliffs to the north. Further to the east, across another deep depression centred about station DT, the Sole Pit, concentrations remain relatively low (1-2 mg l^{-1}) until a second area of high concentrations, some 70-80 km wide and situated between stations BB and BE. This latter area corresponds to the plume evident in the horizontal distributions [*e.g.* Figure 3.1d and 3.2d].

For spring conditions [Figure 3.7b], the concentrations within the TSM gradient off the English coast are generally much higher (between 5-10 mg l^{-1}) throughout the water column, which is consistent with an increase in river discharge and river-borne sediment from the Humber estuary. At the eastern margin of the section, the Dutch coast is characterised by a zone of high TSM between stations BD and BF. This general pattern is complicated by the presence of a TSM minimum at station BE. Similar concentration minima have been observed in other parts of the Dutch coastal waters [Lee and Folkard, 1969; Postma, 1981; Visser, 1993; Visser *et al.*, 1991]. It seems that these features are related to the formation of steep salinity gradients parallel to the coast which result from the high discharge from the Rhine, especially during the winter and early spring. These gradients in turn give rise to a density driven circulation that is directed offshore in the surface layer and onshore in the bottom layer, and the depletion of suspended sediment occurs at the seaward end of this circulation as particles sink into the bottom layer [Visser *et al.*, 1991].

As with the previous section, the distribution of TSM along the section for summer conditions is fairly uniform with concentrations generally much lower than for winter and spring conditions.

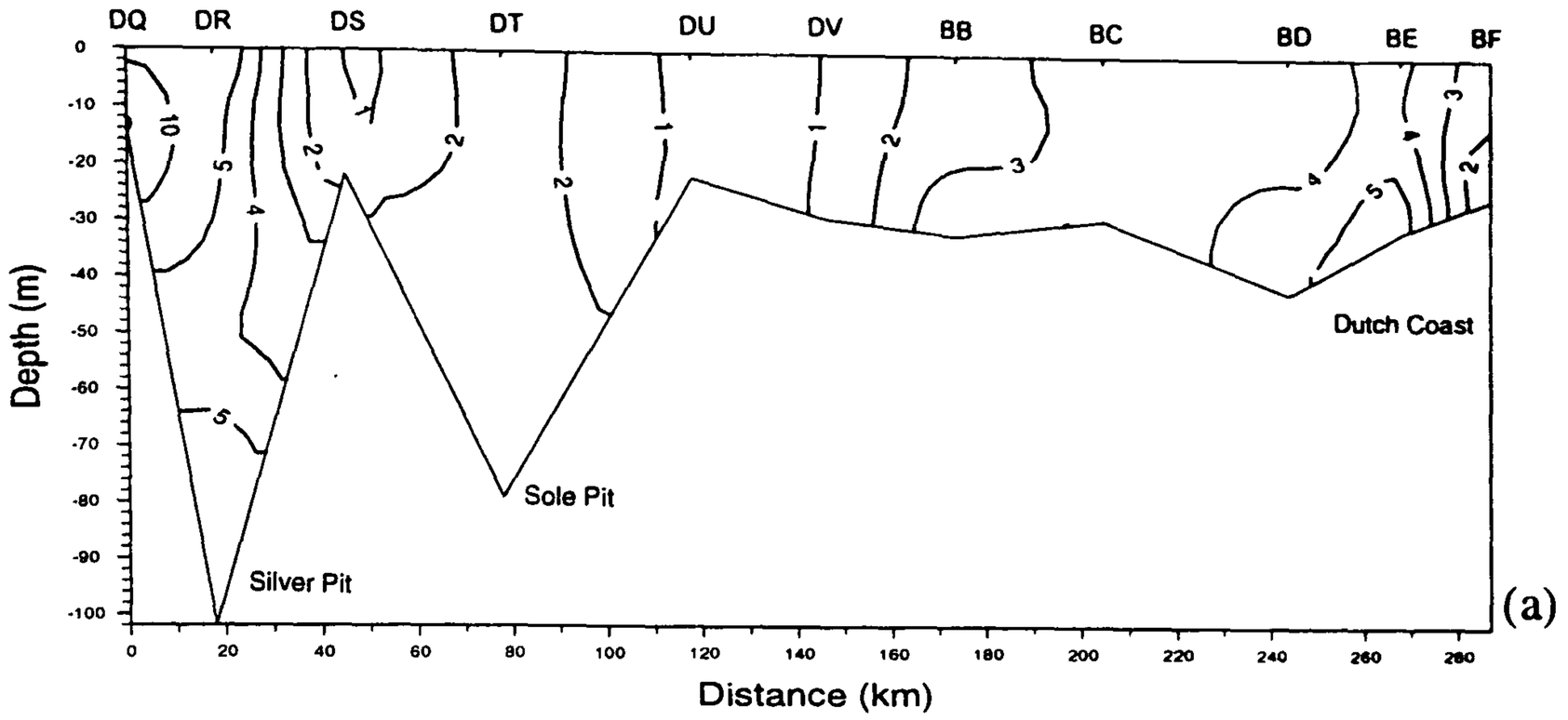

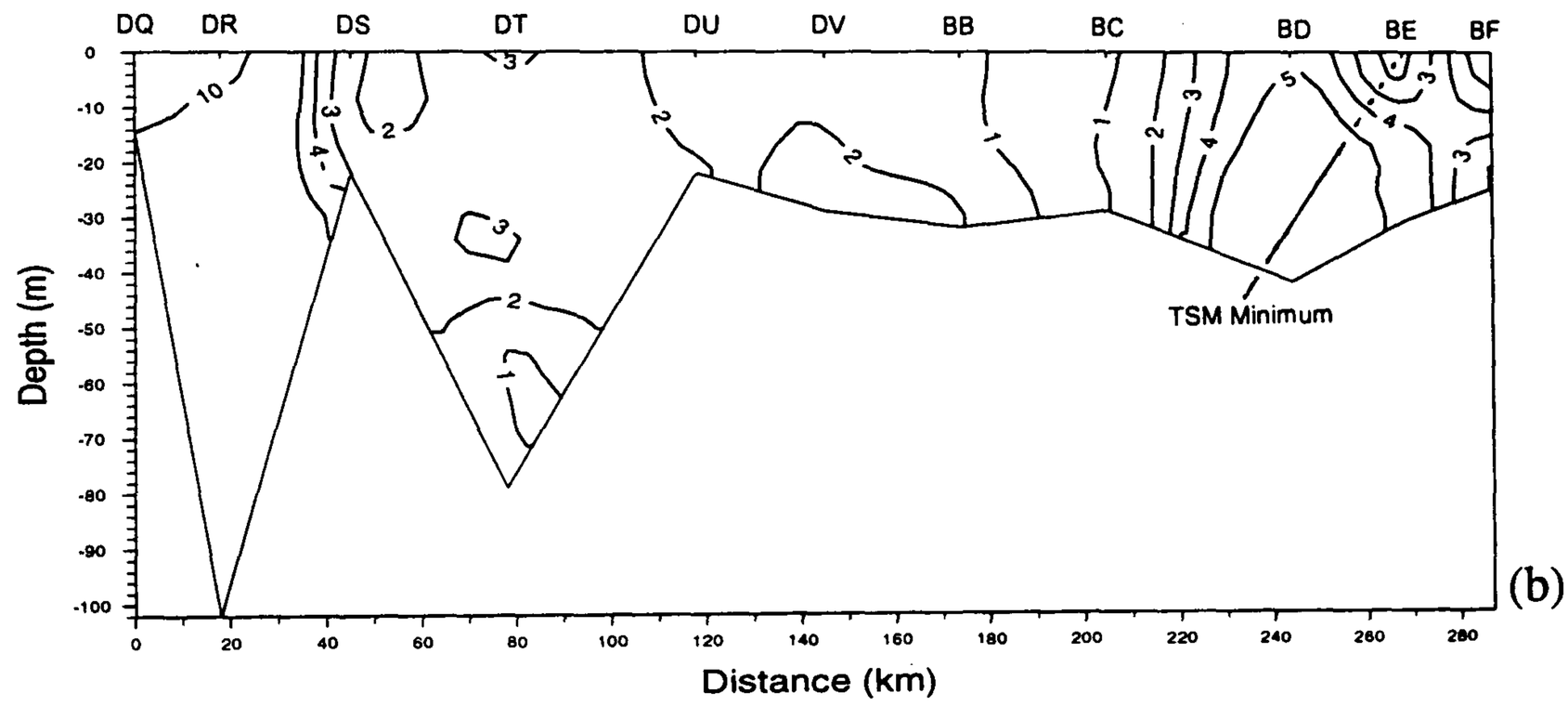

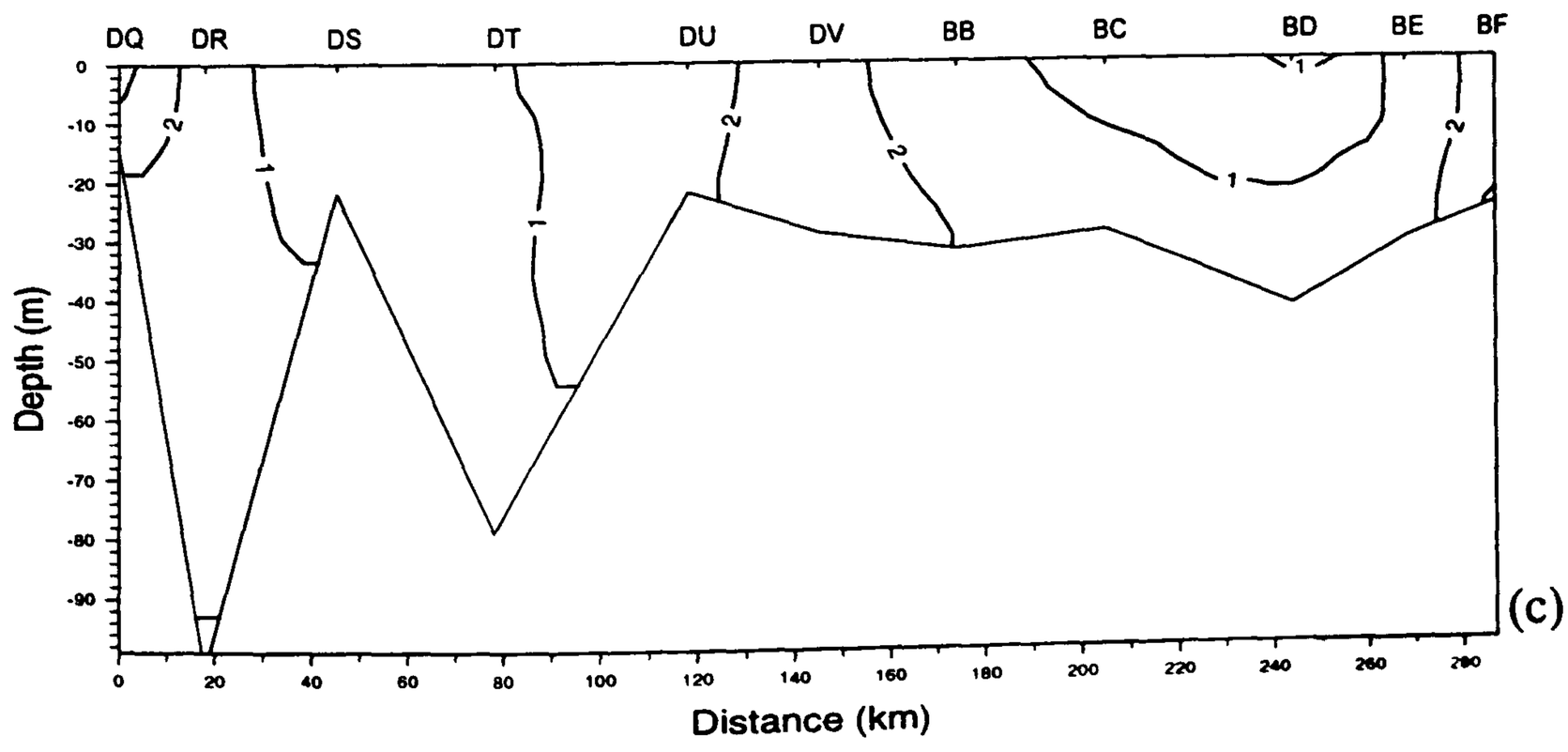

Figure 3.7: Vertical Distribution of TSM (mg l^{-1}) between survey stations DQ to BF for (a) winter, (b) spring and (c) summer conditions.

ENGLISH COASTAL WATERS

The sections presented in Figure 3.8 show the alongshore vertical distributions of TSM off the English coast from stations CY in the north to AP in the south. All three seasons are characterized by generally high concentrations along the length of the English coast except for the deeper waters to the north of station DP where the stations DJ to DO form part of the persistent low turbidity zone described for the horizontal distributions in §3.1. Some alongshore gradients and fronts are well-defined, reflecting in part the proximity to major fluvial and coastal erosion sources of suspended sediment. For example, to the north of station DP, the low turbidity zone is separated by a sharp gradient from a higher turbidity zone further to the north in which the stations are much closer to the Yorkshire coast. This high turbidity zone corresponds to a localized supply of suspended sediment from primarily the Tees and Tyne rivers

In the shallower water to the south of station DP, the sections are characterized by a well-defined zone of high TSM, some 80 km wide, centred about stations EM and EN with concentrations declining steeply to the north and south. This zone is related to both the significant discharge of suspended sediment from the Humber estuary and plume, and the entrapment and deposition of suspended sediment within the Wash basin. In this zone concentrations of TSM remain high for all three seasons implying that this part of the English coast includes an important source and a site of deposition of suspended sediment throughout the whole year.

Further along the section, to the south of station EP, there is another but much broader zone of high TSM, some 150-200 km wide, which corresponds to the persistent high turbidity zone off the coast of East Anglia resulting from primarily coastal run-off and cliff erosion. Concentrations of TSM typically rang from > 5 mg l^{-1} during the summer to > 20 mg l^{-1} during the winter seasons [Figures 3.8c and 3.8a respectively]. At stations AM and AN, the generally high concentrations, particularly in winter and spring, suggest that there may be some significant supply and/or interchange of suspended sediment associated with the discharge from and the coastal margins of the Thames estuary. Relatively high concentrations of TSM also continue as far south as station AP at the Dover Straits, further suggesting that some suspended sediment is being supplied through the Straits along the nearshore margins of the Kent coast and at fairly high concentrations.

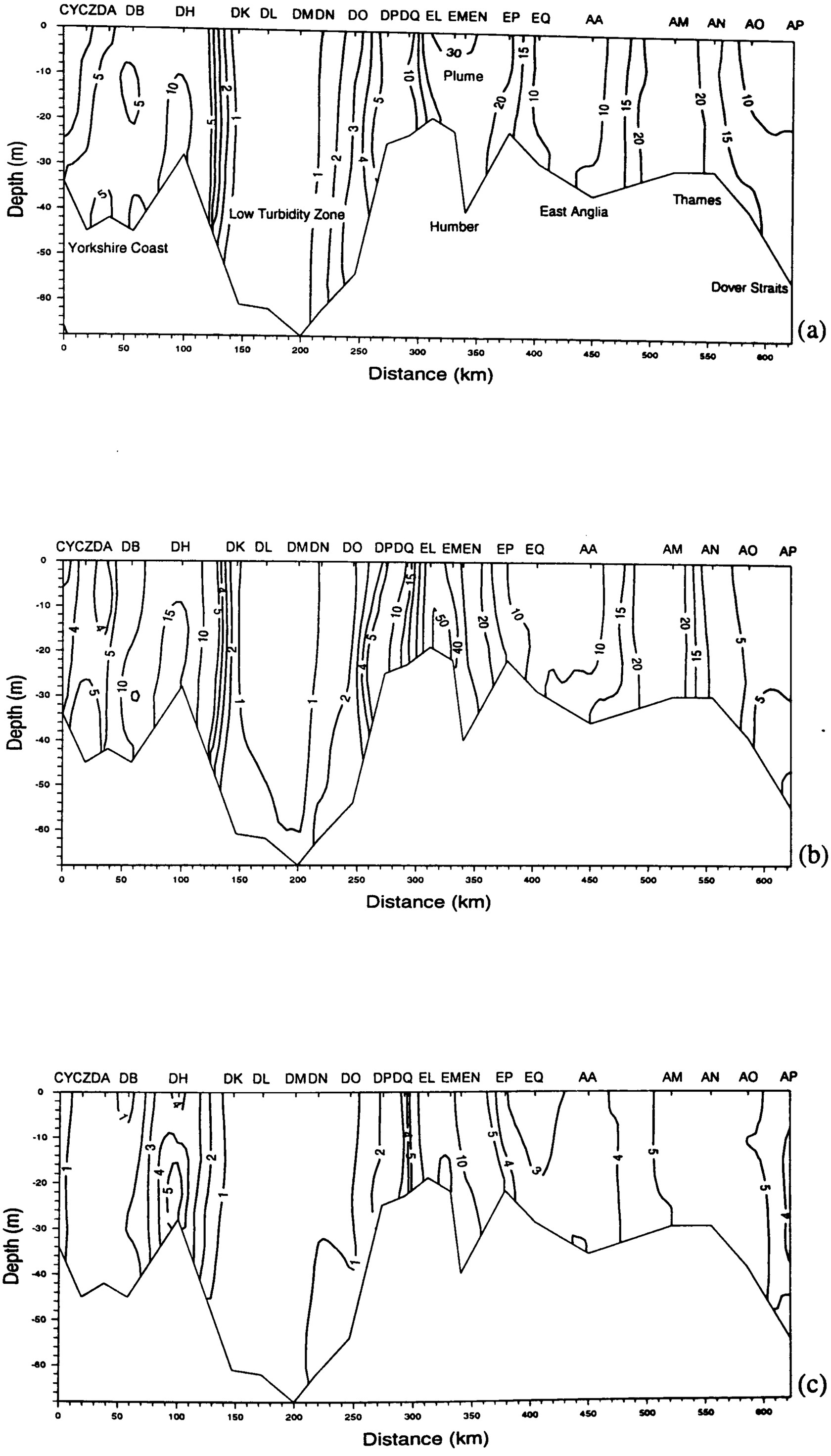

Figure 3.8: Vertical Distribution of TSM (mg l^{-1}) off the English coast between survey stations CY and AP for (a) winter, (b) spring and (c) summer conditions.

CONTINENTAL COASTAL WATERS

The sections presented in Figure 3.9 show the alongshore vertical distributions of TSM off the Continental European coast between stations BY to the north and AQ to the south.

For winter conditions [Figure 3.9a], the vertical distribution of TSM is fairly uniform along the section except for generally higher concentrations of about 3-5 mg l^{-1} along the northern part of the section between stations BY and BO, in the German Bight, and BO and BF off the Dutch coast. These high concentrations are likely to be related to primarily a large input of suspended sediment by the German rivers of the Elbe, the Weser and the Ems, and also to the development of the East Anglian plume which appears to be transporting suspended sediment across the top of the Southern Bight into this region [Figures 3.1f and 3.2f].

During the spring conditions [Figure 3.9b], concentrations within the relatively high turbidity zone in the German Bight increase to levels in excess of 10 mg l^{-1}. Similarly, elsewhere along the section, concentrations of TSM are the highest of all the three seasons. This largely corresponds with the presence of large quantities of organic suspended sediment associated with spring phytoplankton blooms that are known to develop along the coast. The fluctuations in the concentrations particularly in the near-surface waters along the section may therefore reflect to some degree a patchiness in the distribution of the blooms. Between stations AH and AV, there is a well defined zone of relatively higher TSM concentrations declining to the north and south. This corresponds well with the fluvial supply of suspended sediment from the Rhine which reaches a peak in Spring [§5].

For summer conditions [Figure 3.9c], TSM is generally well distributed along the section with concentrations at relatively low levels (*e.g.* < 2-3 mg l^{-1}), contrasting sharply with the other seasons.

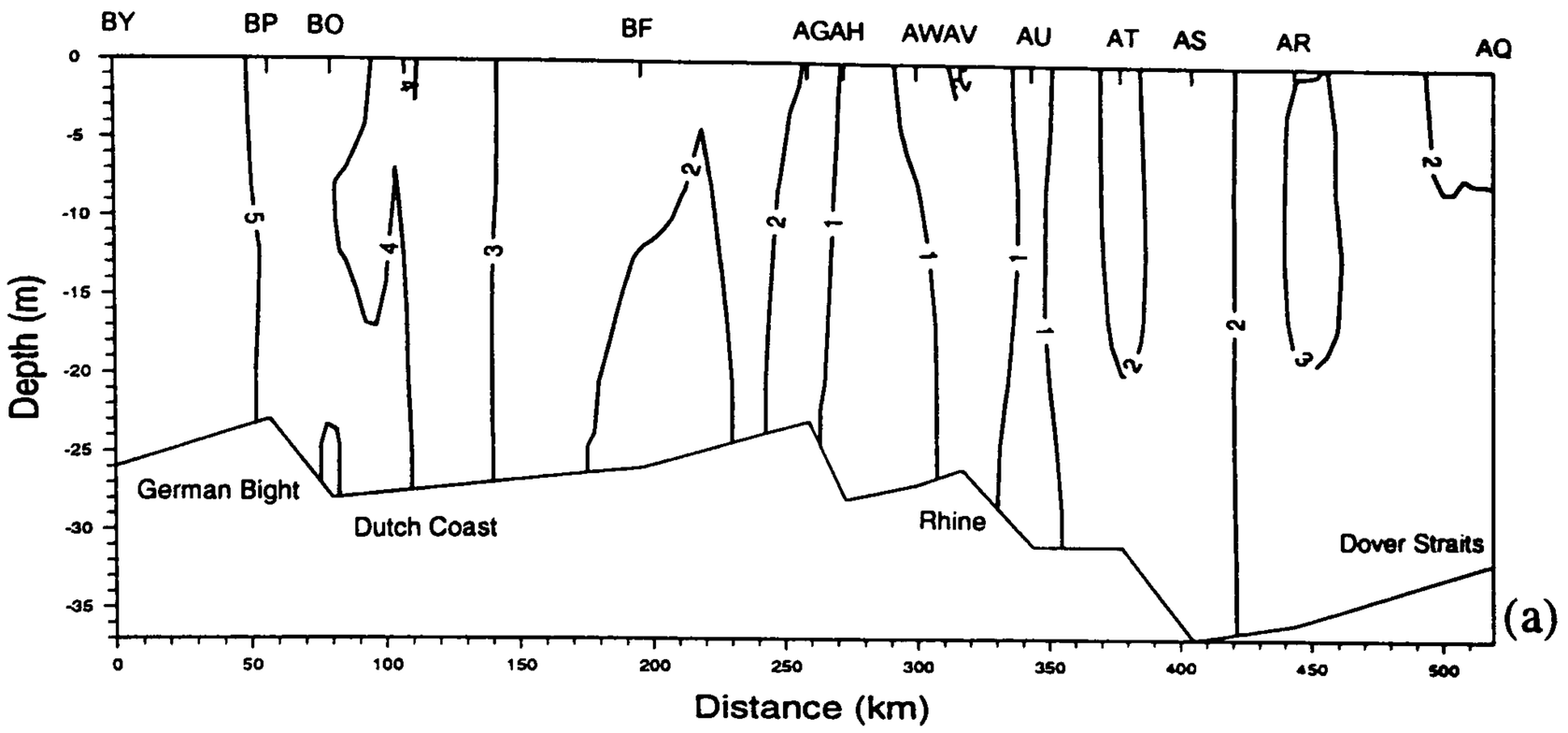

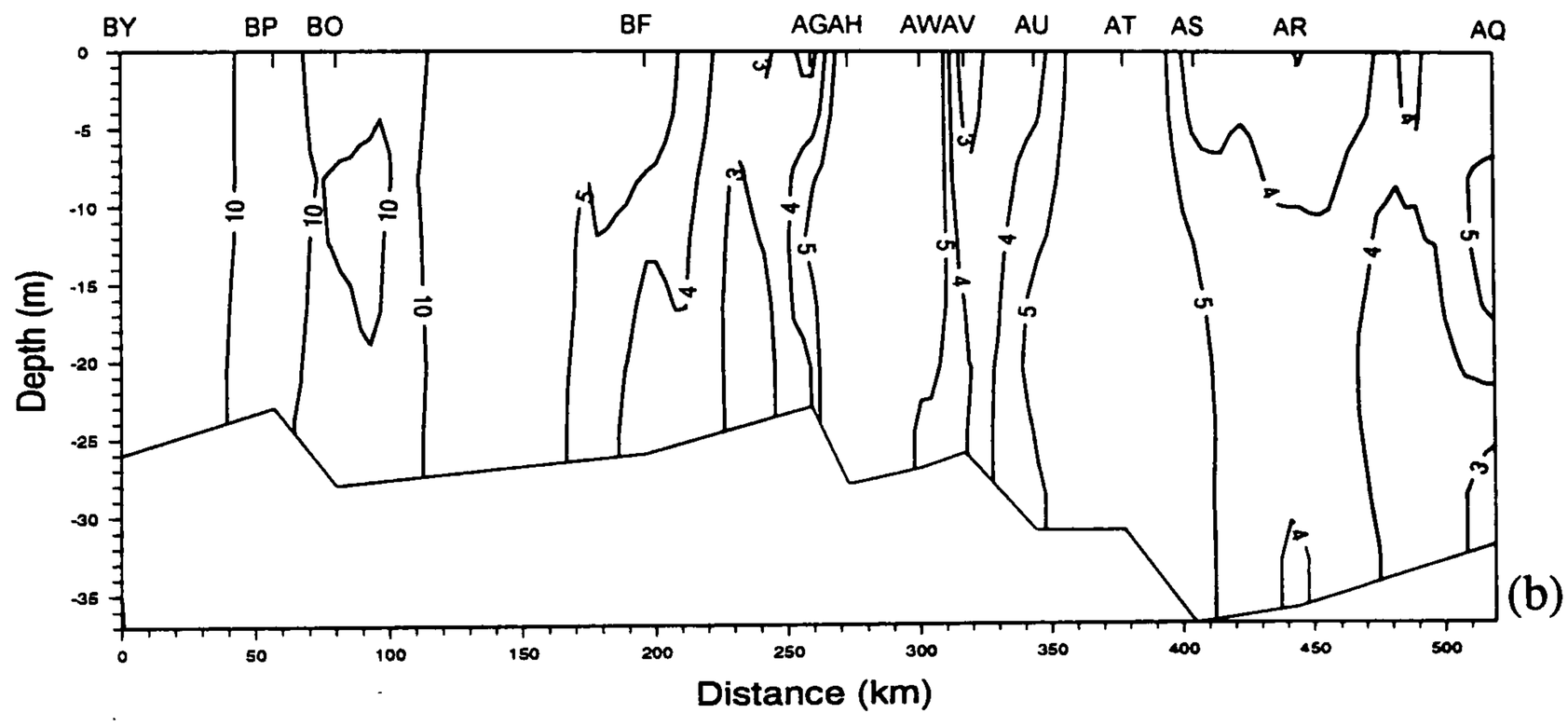

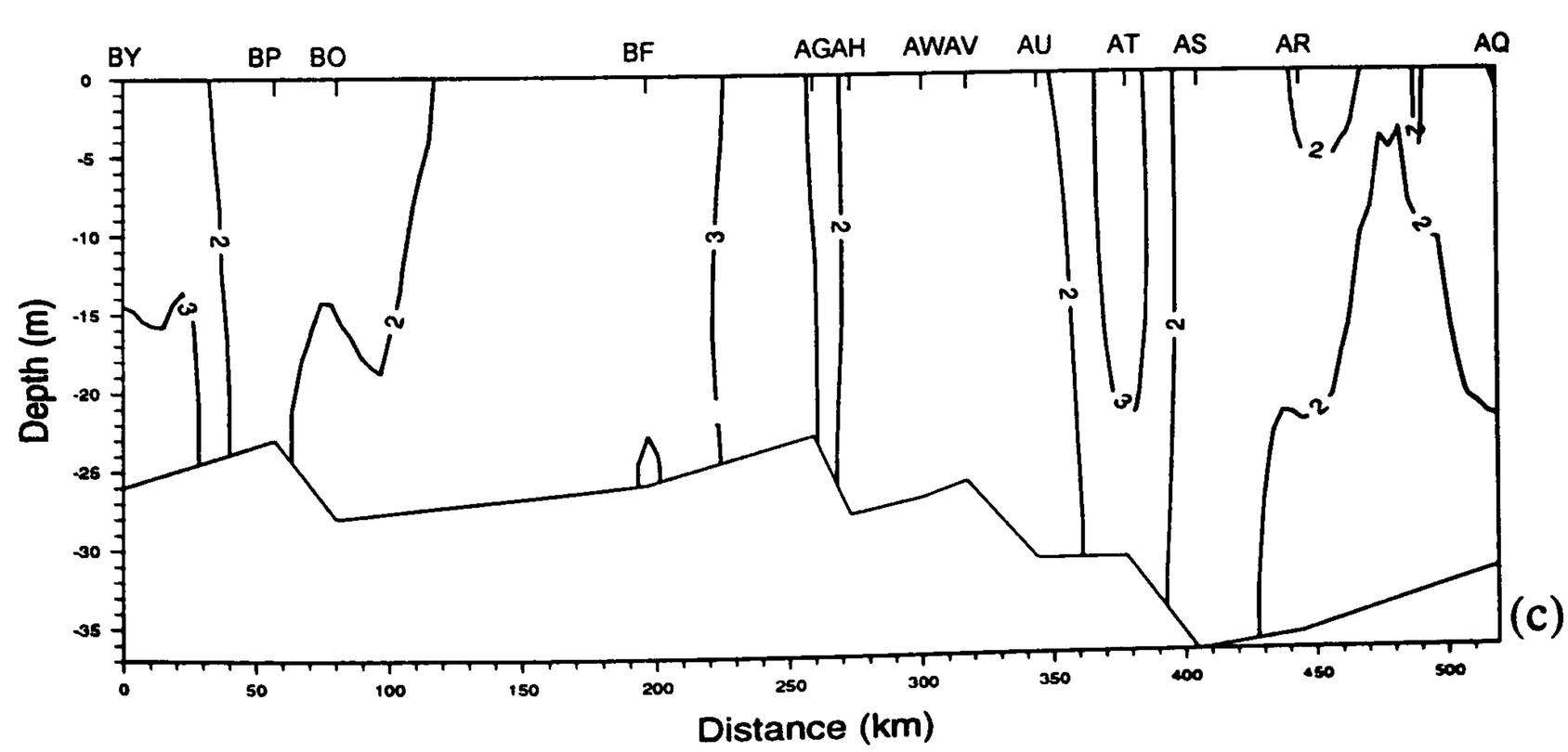

Figure 3.9: Vertical Distribution of TSM (mg l^{-1}) off the Continental European coast between survey stations BYand AQ for (a) winter, (b) spring and (c) summer conditions.

3.5: Summary

The chapter has presented plots showing the distributions of TSM in the southern North Sea for the period of the Survey Programme and has described in some detail the horizontal and vertical variations in both space and time. Some prominent features have been identified such as the persistent high turbidity zone off East Anglia and the development of an associated plume; and also some more ephemeral features have been identified such as the development of TSM minima off the Dutch coast. Possible explanations and suggestions for the observed features and their seasonal variations have been proposed. Physical parameters such as salinity/water masses, river discharge and meteorological conditions are certain to influence the supply and distribution of TSM over the annual cycle as will biological factors such as the development of phytoplankton blooms. Currents too, are certain to dominate the transport of suspended sediment. The influence and interactions of these parameters on the distribution and transport of suspended sediments are considered in §5 and §6. The next chapter describes the organic matter and content distributions.

ORGANIC SUSPENDED MATTER DISTRIBUTIONS

The previous chapter described the distributions of the total suspended matter (TSM) in the southern North Sea; this chapter describes the distributions of the organic/inorganic components of the TSM. The organic suspended matter (OSM) measurements and analyses were undertaken primarily to investigate the importance of primary production and sediment pick-up, and the spatial and temporal differences between them, in determining the components of the TSM distributions. The results of the organic suspended matter (OSM) analyses are presented using firstly, horizontal distributions of organic matter concentration (in mg l^{-1}) and secondly, horizontal distributions of the percentage organic content of the TSM. Although only a 11-month series of distribution data is available for the reasons given in §2.2, the data presented here are one of the most comprehensive surveys to date. As with the TSM distributions [§3.3], seasonally averaged distributions of OSM were also produced. However, since they repeat the general patterns shown by the monthly cruise distributions and thereby contribute little to the discussion on the distributions of OSM, they have not been reproduced here.

4.1. Organic Suspended Matter Distributions

The monthly distributions of OSM in the surface waters of the southern North Sea for the period of December, 1988 to October, 1989 are presented in Figure 4.1. The most striking feature of these distributions is that concentrations are comparatively low (typically $\leq$ 1 mg l^{-1}) over the central and northern parts, because the TSM concentrations are less than about 2 mg l^{-1} [*q.v.* Figure 3.1]. Concentrations were the highest (*e.g.* > 1-2 mg l^{-1}) in the western coastal waters of the Southern Bight and periodically off the Dutch and Belgian coasts and in the German Bight. The broad pattern of OSM distributions, therefore, was similar to that of the TSM distributions.

The high turbidity area off the East Anglian coast was characterized by relatively high concentrations of OSM, although they were typically an order of magnitude less than the TSM concentrations. The OSM distributions were also well correlated with the development of the high turbidity area; they remained well developed from December, 1988 until the late spring of 1989 [Figures 4.1a to 4.1f] with peak concentrations of > 5 mg l^{-1} observed in April, 1989 off the Wash and Lincolnshire coast [Figure 4.1e]. During the summer months, concentrations diminished to < 1 mg l^{-1} [Figures 4.1g to 4.1i] until the late summer and early autumn when concentrations began to increase again [Figures 4.1j and 4.1k].

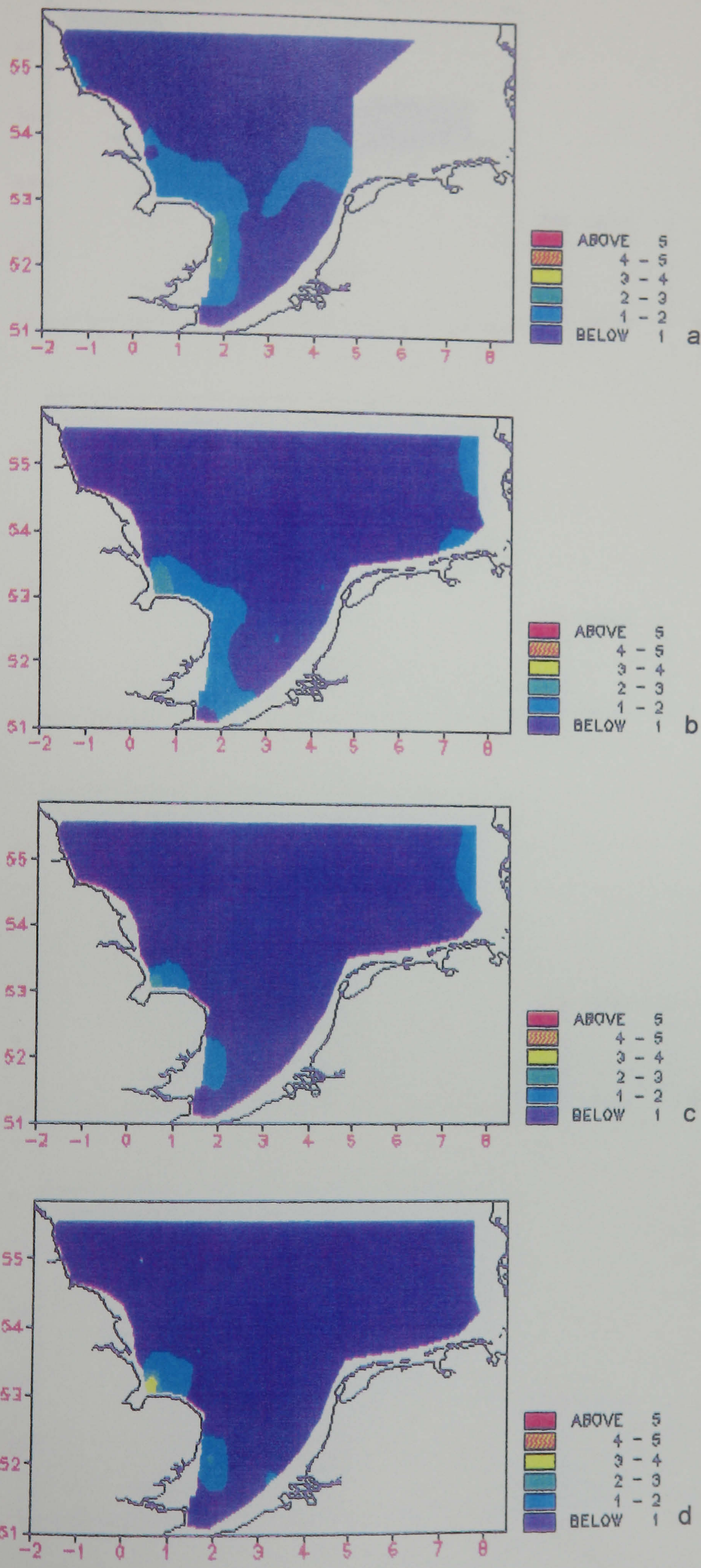

Figure 4.1: Distribution of OSM (mg l^{-1}) in the surface waters of the southern North Sea for (a) December 1988, (b) January 1989, (c) February 1989 and (d) March 1989.

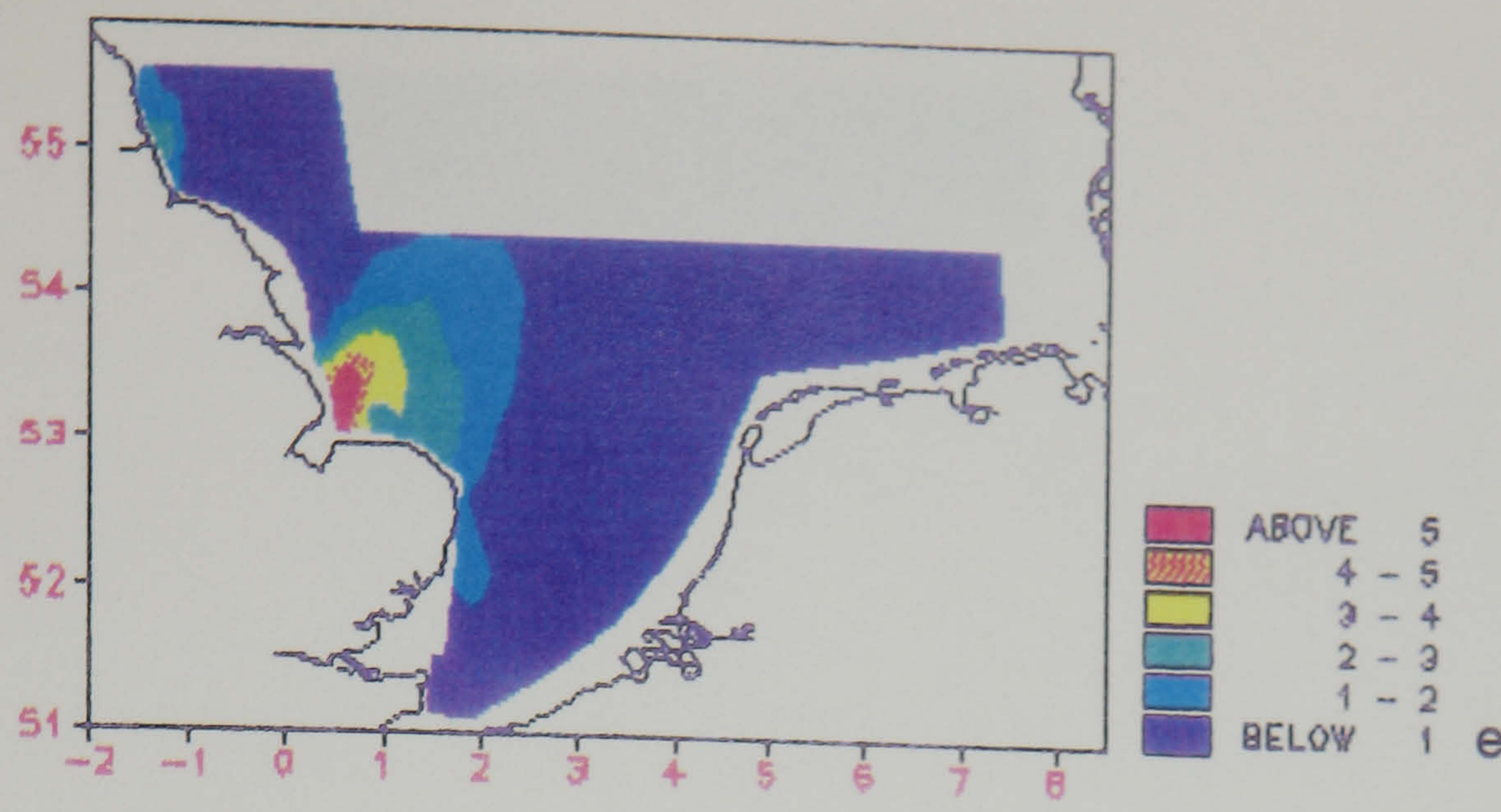

Figure 4.1 (cont/d): Distribution of OSM (mg l^{-1}) in the surface waters of the southern North Sea for (e) April 1989, (f) April-May 1989, (g) May-June 1989 and (h) June-July 1989.

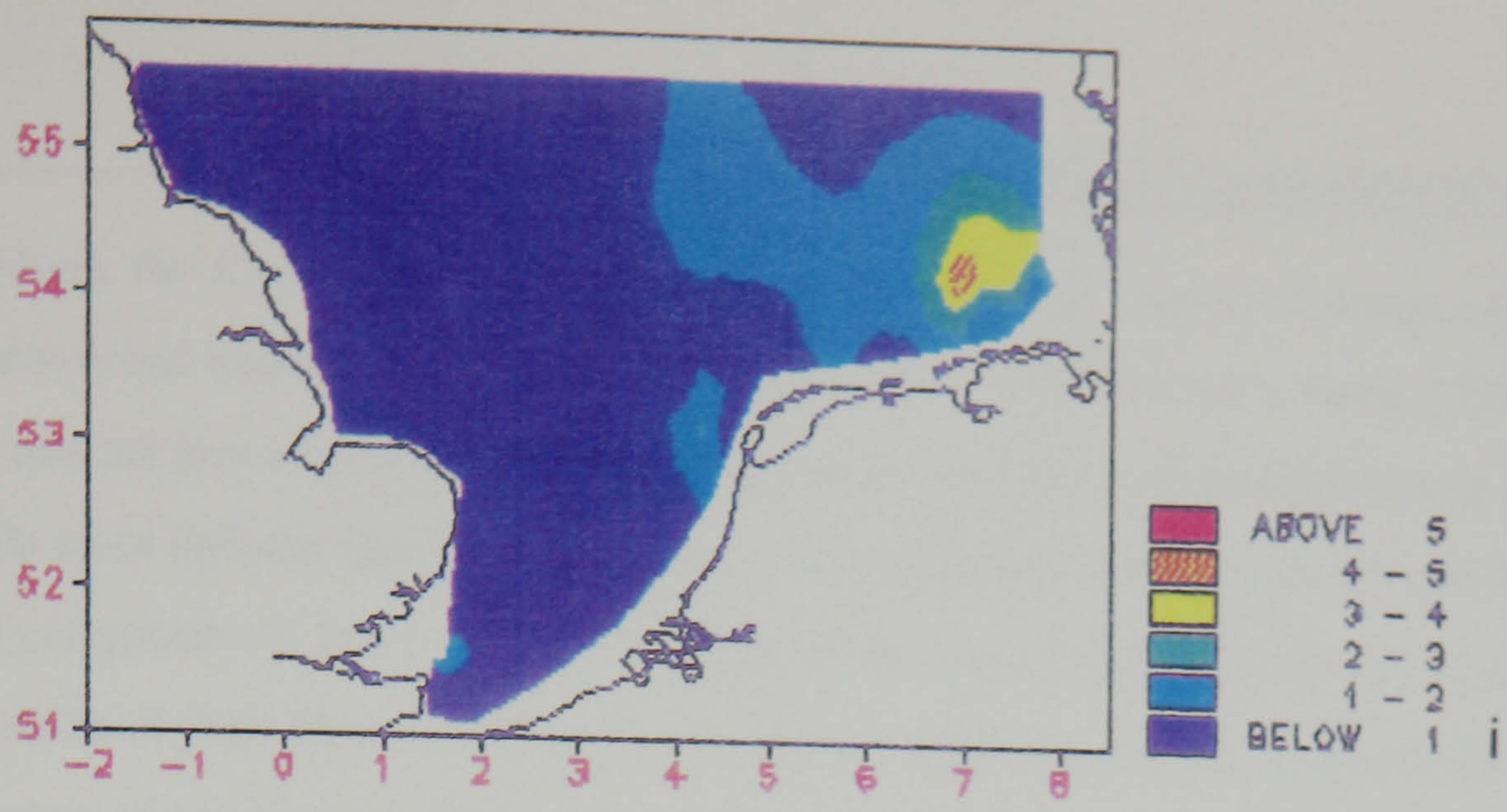

Figure 4.1 (cont/d): Distribution of OSM (mg l^{-1}) in the surface waters of the southern North Sea for (i) July-August 1989, (j) August-September 1989 and (k) September-October 1989.

Along the Continental European coastline, the limited spatial coverage and the limited sampling due to bad weather, for example during December, 1988 and early April, 1989 [Figure 4.1a and 4.1e], may not give a fair representation of the spatial and temporal distributions in these regions, particularly close inshore. Qualified in this way, concentrations along the Dutch and Belgian coasts remained comparatively low (< 1 mg l^{-1}) for the whole survey period except during the spring and summer months of 1989 [Figures 4.1f to 4.1i] when concentrations increased marginally to 1-2 mg l^{-1}. In some areas of the German Bight, however, concentrations were relatively higher in the winter months [*e.g.* Figures 4.1b and 4.1c]. These were sustained during the spring and summer months [Figures 4.1f and 4.1g] with a significant increase in concentrations to > 3-4 mg l^{-1} during July/August, 1989 [Figure 4.1i]. During the late summer and early autumn, concentrations in both regions diminished [Figures 4.1j and 4.1k].

The monthly distributions of OSM in the bottom waters of the southern North Sea for the period of December, 1988 to October, 1989 are presented in Figure 4.2. The general features observed in the surface waters are repeated, with relatively higher concentrations in the coastal waters of the Southern Bight and in the German Bight. Along the English coastline, bottom OSM concentrations tended to be marginally higher than the surface ones, most noticeably in the winter months of 1988-1989 off the Wash and East Anglia [*e.g.* Figures 4.2a and 4.2b] and during the early spring of 1989 [Figure 4.2e] particularly off the North Yorkshire coast. Bottom concentrations were comparable with surface concentrations off the Dutch and Belgian coasts except for the late spring and early summer of 1989 [Figures 4.2g and 4.2h] when concentrations were generally higher in the surface waters. In the German Bight, bottom concentrations were also comparable with surface ones, although there was much more variability and patchiness from month to month, especially during the summer months of 1989 [Figures 4.2g to 4.2i]. During July-August, 1989, the peak concentrations of > 3-4 mg l^{-1} observed in the surface waters of the German Bight were not evident in the bottom waters, although concentrations at the bottom were still relatively high.

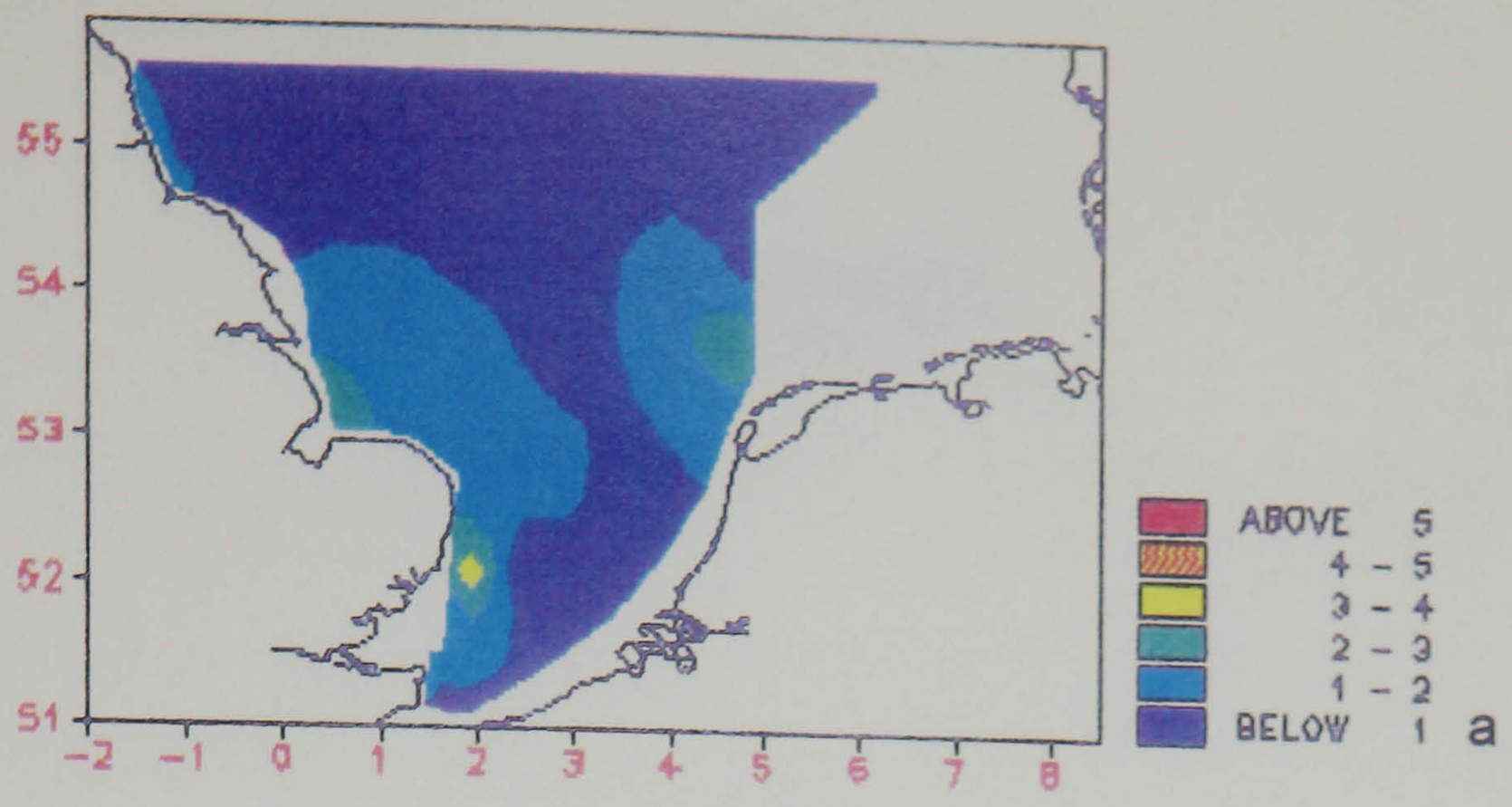

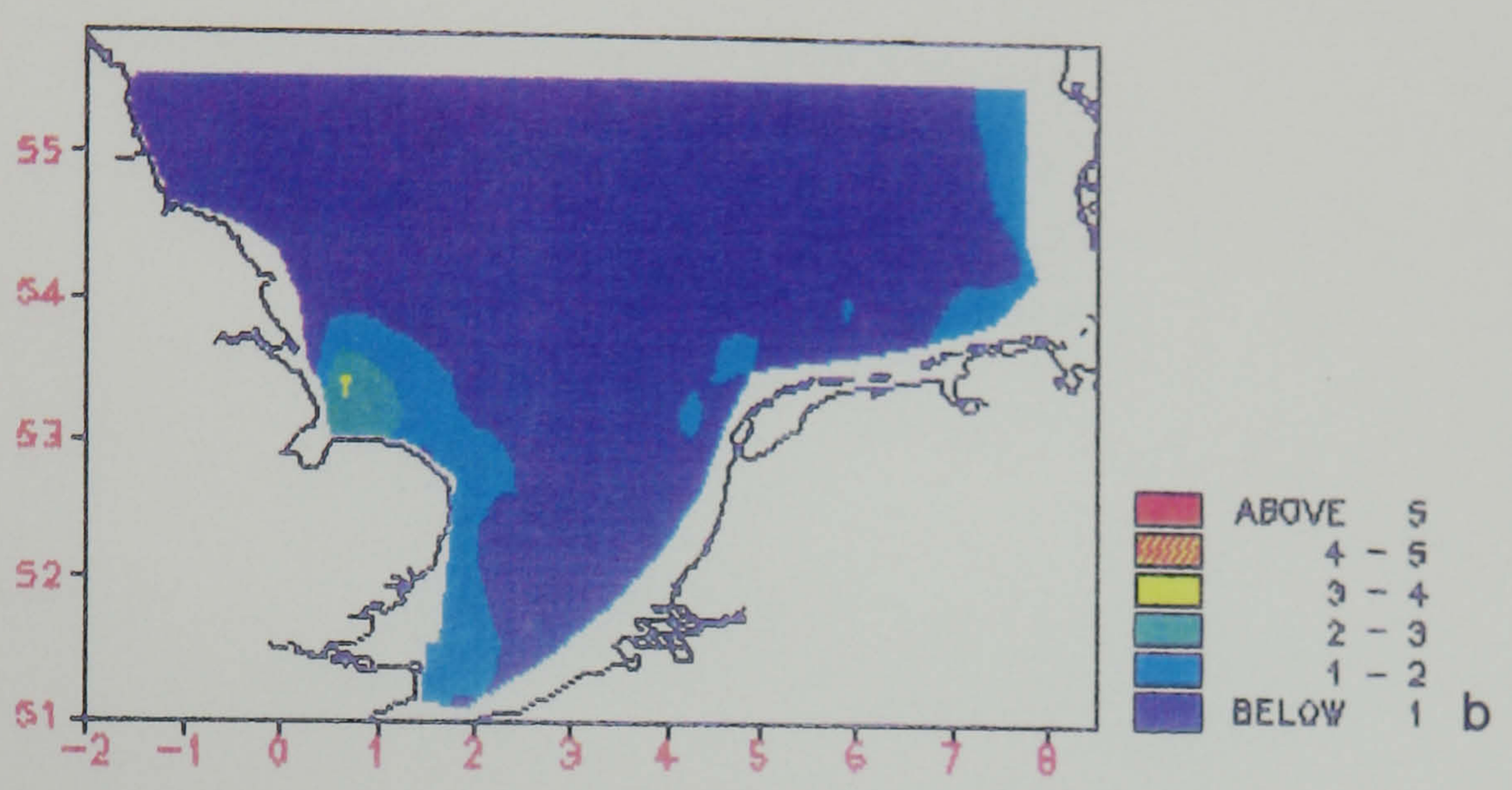

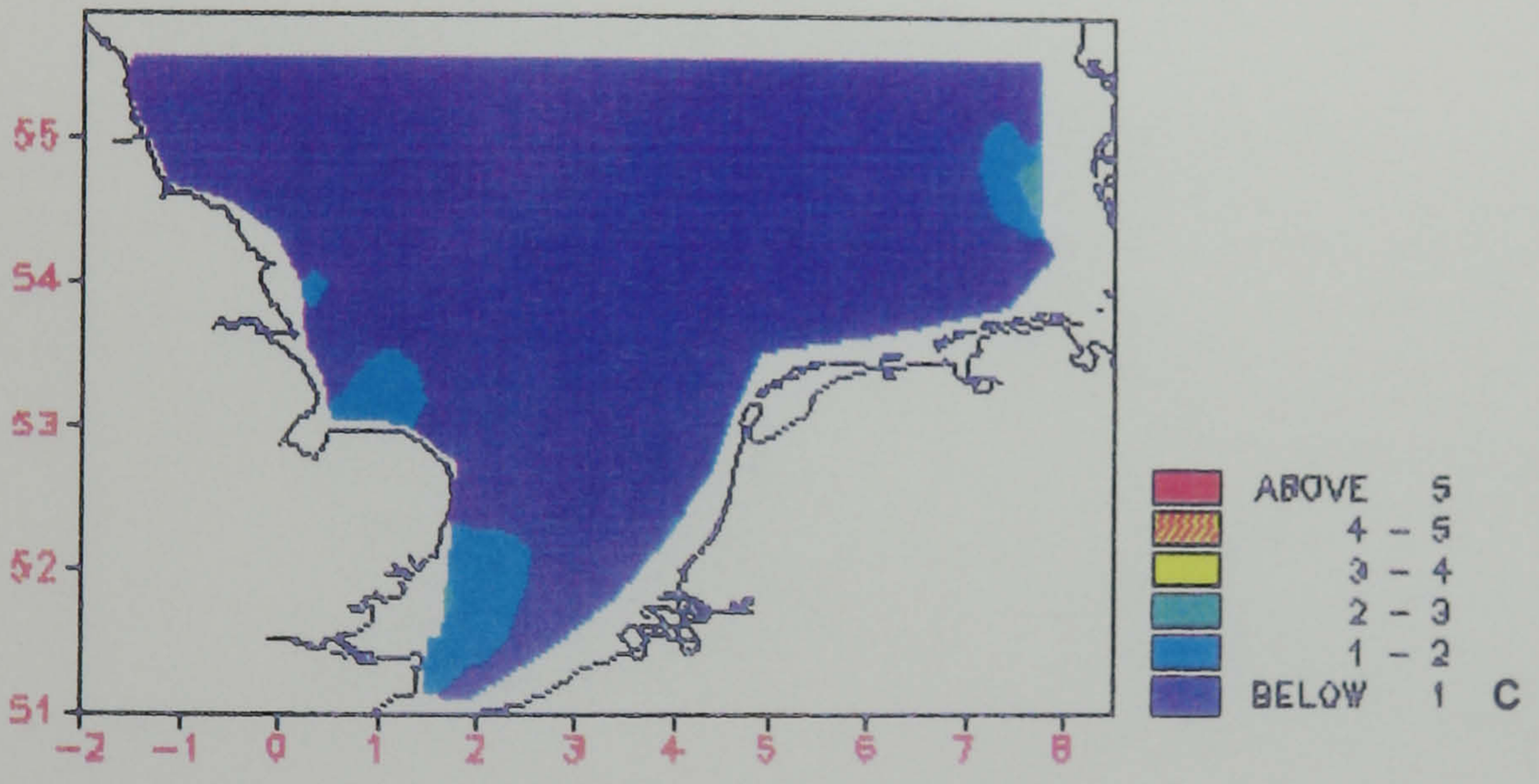

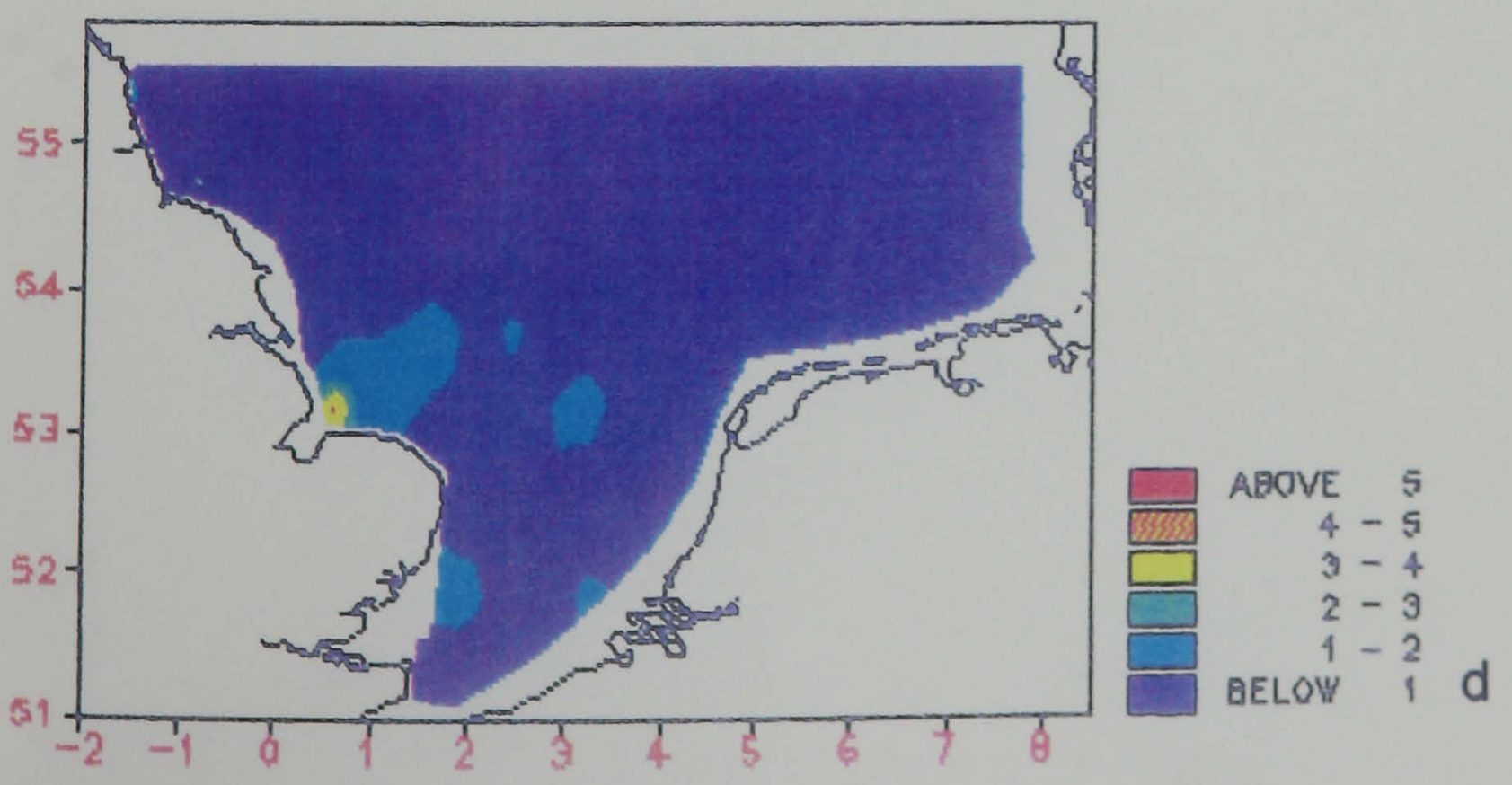

Figure 4.2: Distribution of OSM (mg l^{-1}) in the bottom waters of the southern North Sea for (a) December 1988, (b) January 1989, (c) February 1989 and (d) March 1989.

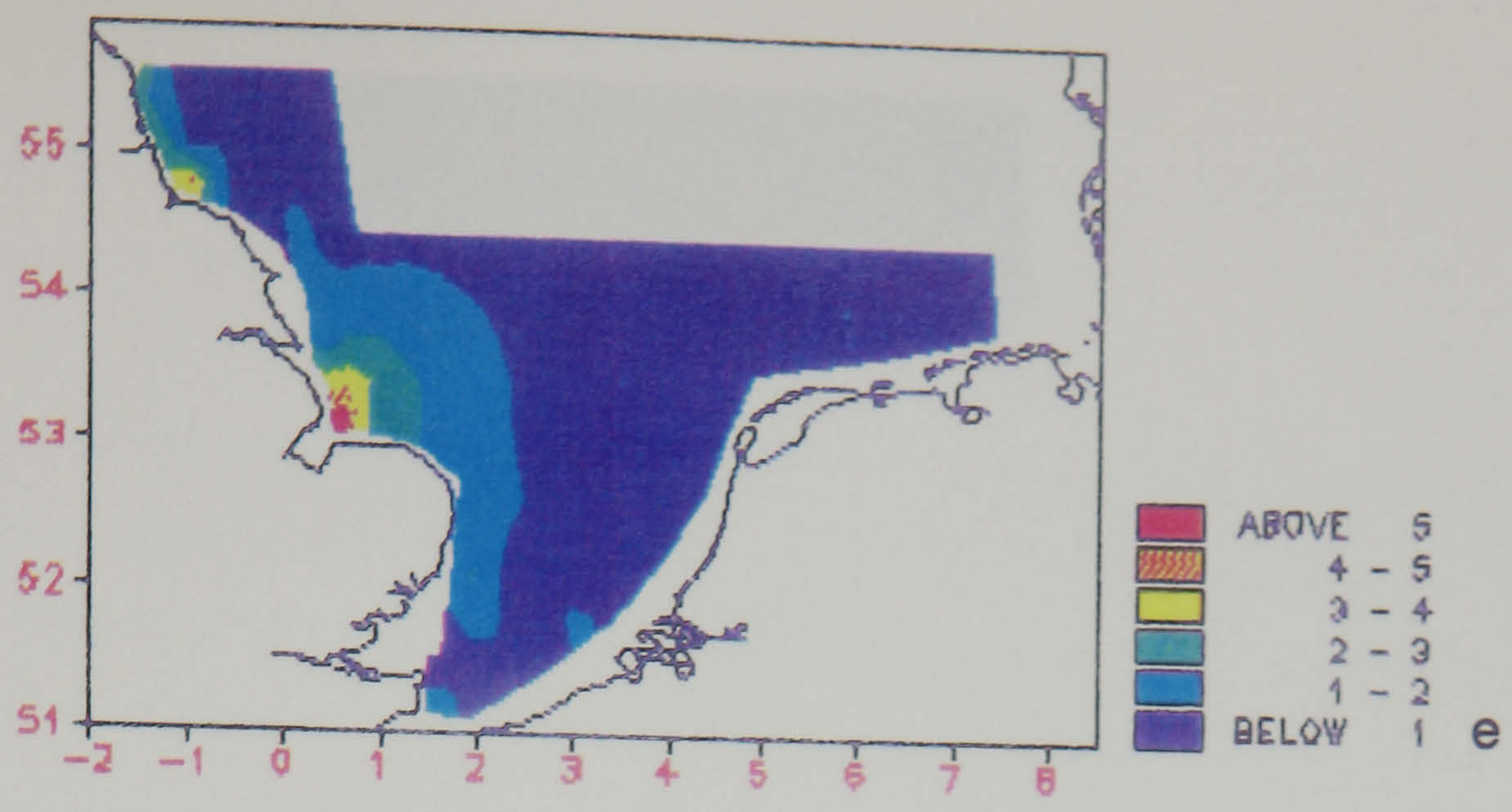

Figure 4.2 (cont/d): Distribution of OSM (mg l^{-1}) in the bottom waters of the southern North Sea for (e) April 1989, (f) April-May 1989, (g) May-June 1989 and (h) June-July 1989.

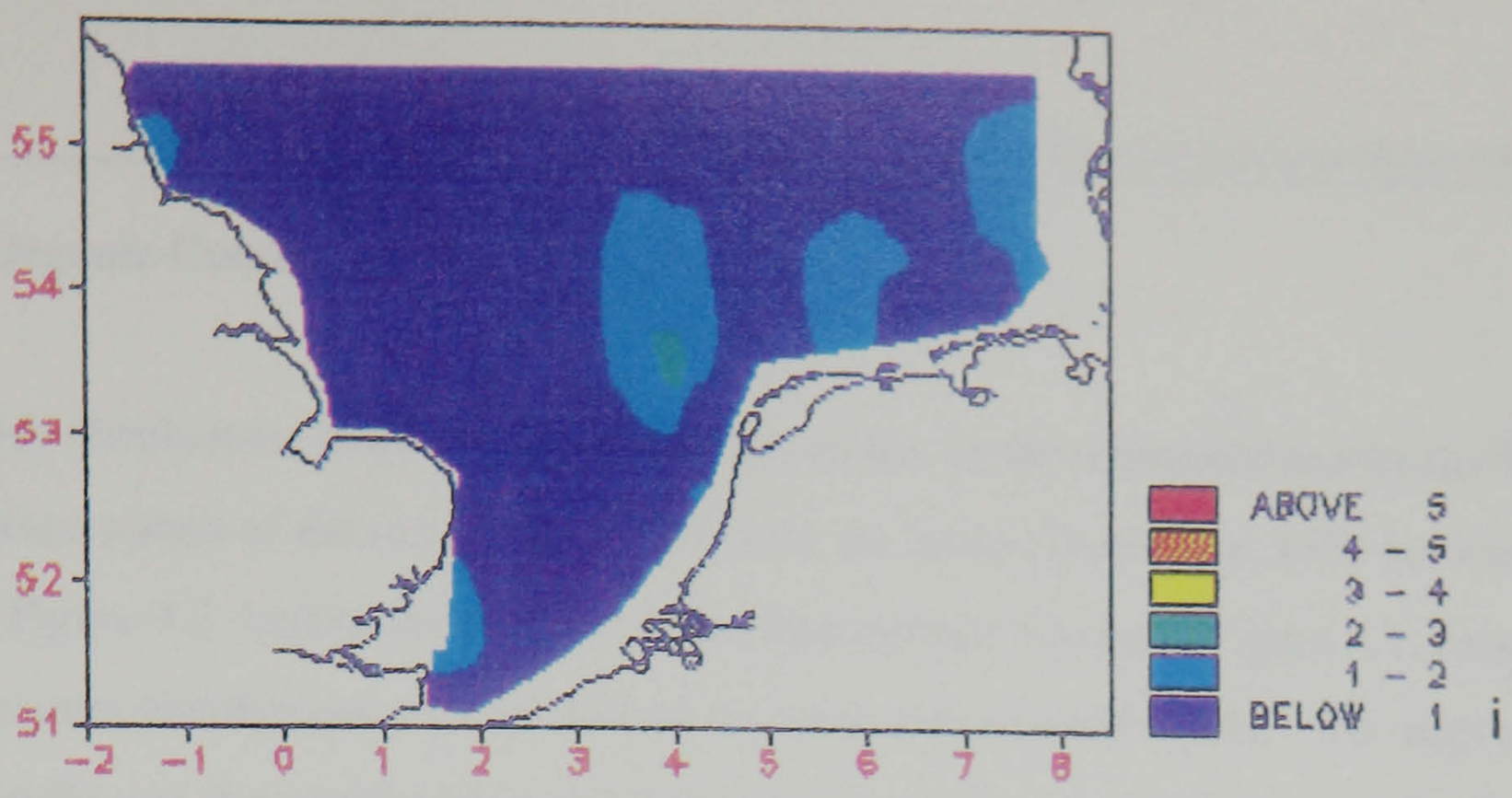

Figure 4.2 (cont/d): Distribution of OSM (mg l^{-1}) in the bottom waters of the southern North Sea for (i) July-August 1989, (j) August-September 1989 and (k) September-October 1989.

4.2 Organic Content Distributions

The monthly distributions of the content of organic matter in the suspended matter (in % of the TSM) in the surface waters of the southern North Sea for the period December, 1988 to October, 1989 are shown in Figure 4.3. Unlike the organic matter distributions shown in Figure 4.1, the corresponding organic content distributions exhibit distinct regional and seasonal trends. The high turbidity region off East Anglia was characterized by consistently low organic contents of less than 20-30% throughout the 11-month period. Although absolute organic matter concentrations in this region were comparatively higher than other parts of the southern North Sea, the organic contents were low. During the winter months, in the area of plume development [Figures 4.3a to 4.3d], organic contents were also low. This implies that the major part of the suspended matter off East Anglia, and that which is transported eastwards in the plume, is inorganic in origin, corresponding to the dominant indigenous sources of sediment from coastal erosion and river discharge. By contrast, in the northern and central parts of the southern North Sea organic contents are consistently high (> 40-50%) throughout the 11-month period. Of particular significance were the winter months from December, 1988 to March, 1989 [Figures 4.3a to 4.3d] when organic contents were relatively much higher than those observed in the coastal waters of the Southern and German Bights. Comparing these winter organic content distributions with the equivalent organic matter distributions [*cf.* Figures 4.1a to 4.1d], a distinct reverse trend was evident: organic matter concentrations were highest in the coastal waters of the Southern Bight and decreased towards the north, whereas organic contents were lowest in the coastal waters of the Southern Bight and increased towards the north. Such a winter-time trend has been observed before by Eisma and Kalf [1987b].

Following the winter period, organic contents increased dramatically throughout the region except for the coastal waters off East Anglia and Lincolnshire during the spring of 1989. The persistently high organic contents in the central and northern parts of the southern North were matched by increasing organic contents (of > 50-60%) along the continental European coastline in March and early April, 1989 [Figure 4.3e]. By April and early May, 1989, both regions had merged so that nearly the whole of the southern North Sea including the German Bight was dominated by high organic contents [Figure 4.3f]. Although during this period, the organic contents off East Anglia and Lincolnshire remained relatively low, elsewhere along the English coast to the north, off the North Yorkshire coast, organic contents increased during the spring [Figure 4.3f] as the northern region of high organic content encroached closer inshore. Along this stretch of the English coastline organic contents remained high right through to the late autumn of 1989 [Figure 4.3g to 4.3k].

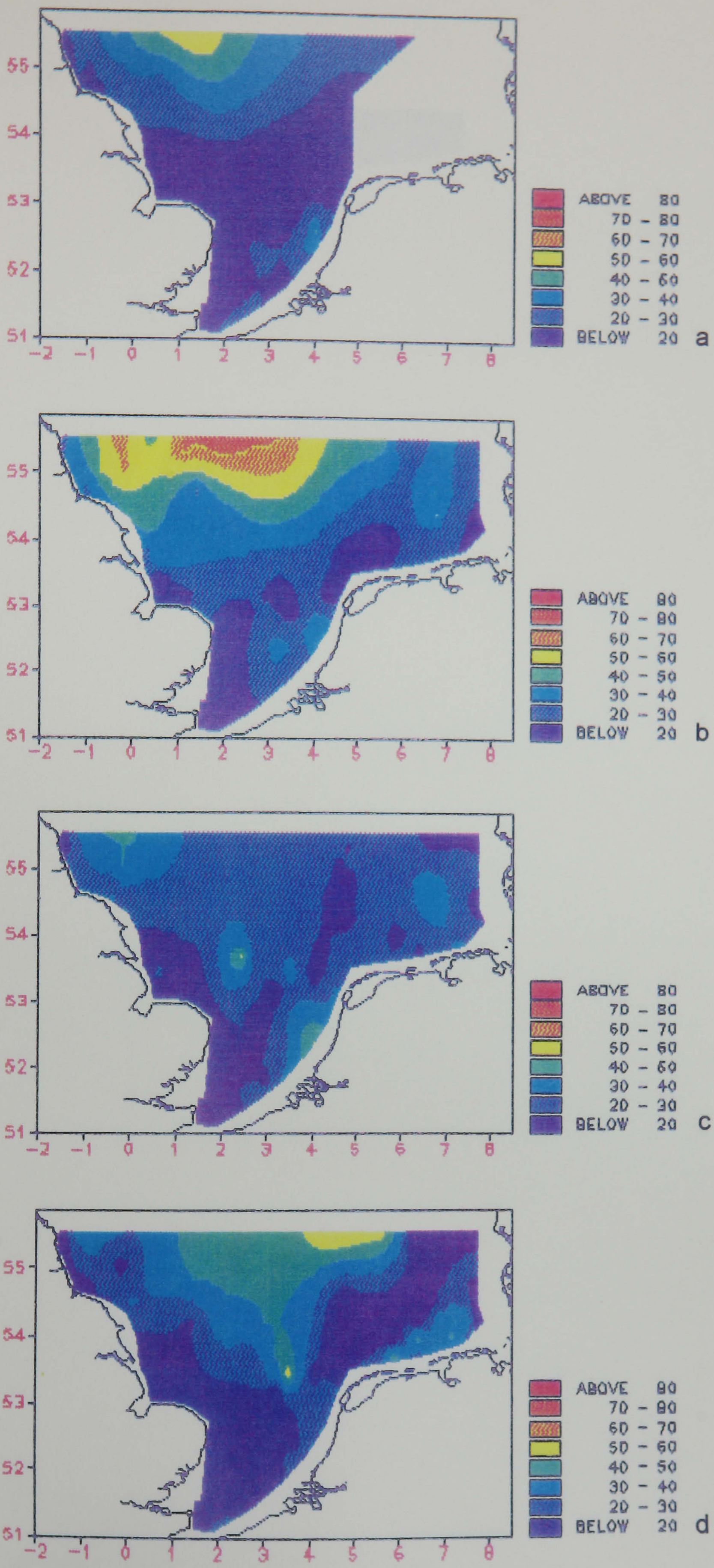

Figure 4.3: Distribution of Organic Content (% of TSM) in the surface waters of the southern North Sea for (a) December 1988, (b) January 1989, (c) February 1989 and (d) March 1989.

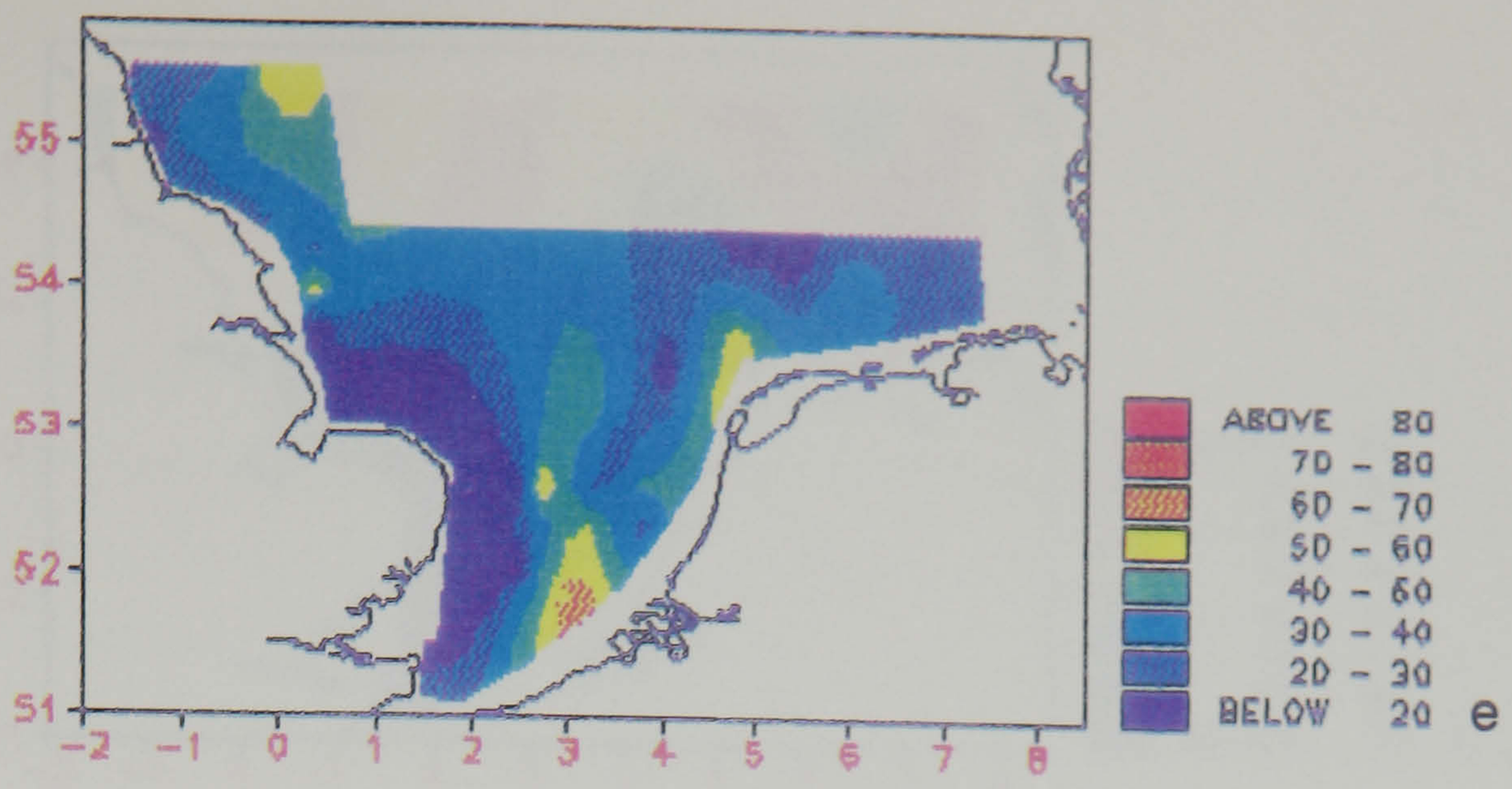

Figure 4.3 (cont/d): Distribution of Organic Content (% of TSM) in the surface waters of the southern North Sea for (e) April 1989, (f) April-May 1989, (g) May-June 1989 and (h) June-July 1989.

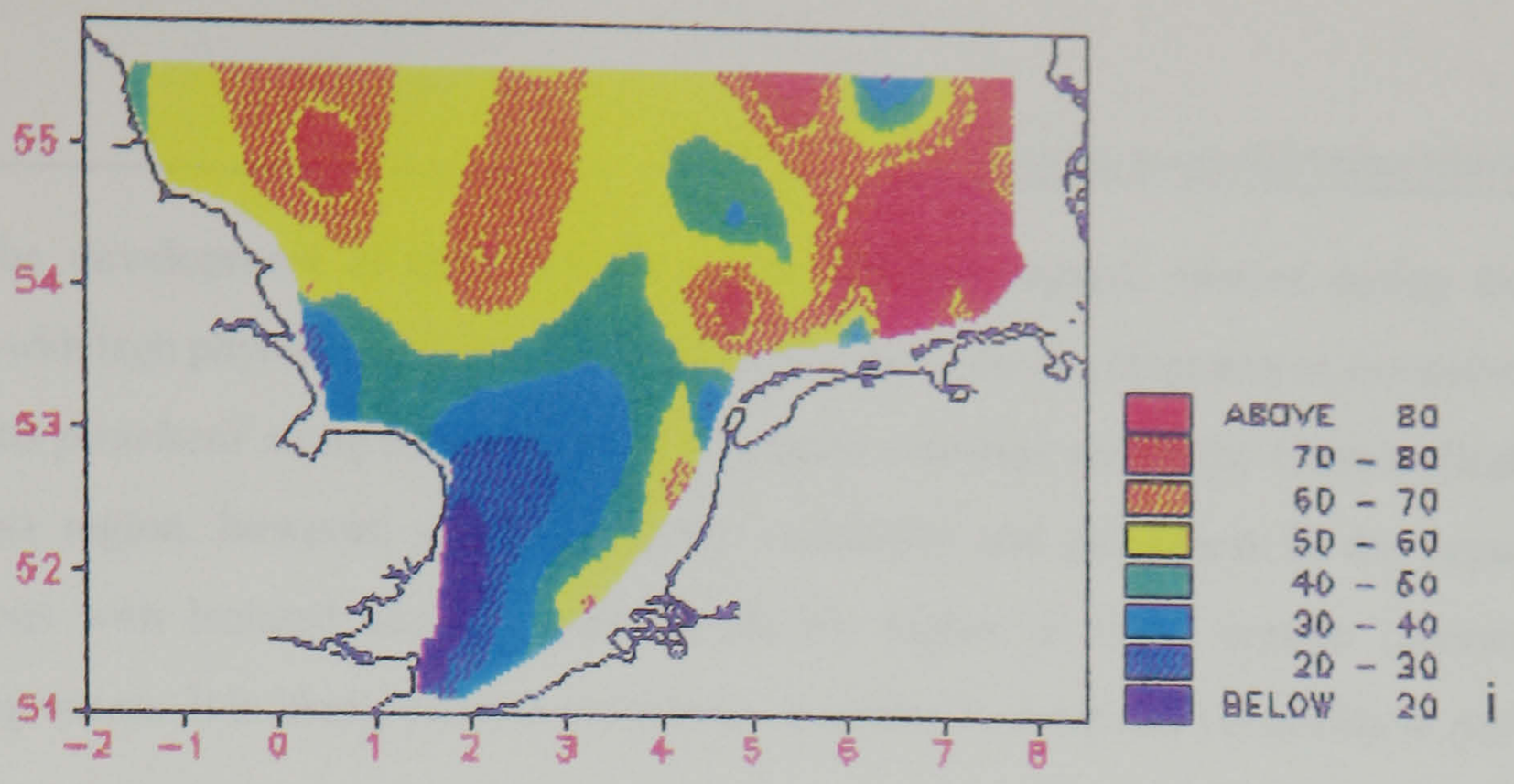

Figure 4.3 (cont/d): Distribution of Organic Content (% of TSM) in the surface waters of the southern North Sea for (i) July-August 1989, (j) August-September 1989 and (k) September-October 1989.

The development of the extensive region of high organic content during the spring is associated with high phytoplankton productivity, particularly the development of extensive blooms of *Phaeocystis pouchetii* along the continental European coastline and in the German Bight [see §5]. Within this region, however, there was some variability and patchiness in the organic content distributions with isolated areas of either relatively higher or lower organic contents than the surrounding waters. It is likely that this patchiness is related to localized variability in phytoplankton biomass.

The monthly distributions of the content of organic matter in the suspended matter (in % of the TSM) in the bottom waters of the southern North Sea for the period December, 1988 to October, 1989 are shown in Figure 4.4. Many of the features and trends noted for the surface organic content distributions are repeated, although there are some significant differences.

With respect to the similarities between the two sets of distributions, the bottom waters of the high turbidity zone off East Anglia were again characterized by relatively low organic contents (< 20-30%) throughout the 11-month period. Likewise, there was a persistent area of high organic content in the central and northern parts of the southern North Sea, conspicuous particularly during the winter months [*e.g.* Figures 4.4a and 4.4b]. During the spring of 1989, an extensive area of relatively high organic content developed, generally comparable in extent to the one observed in the surface waters. Organic contents in the region close to the Rhine outflow showed little variation between the surface and bottom waters [*cf.* Figures 4.3g and 4.3h and Figures 4.4g and 4.4h] but elsewhere, particularly in the region of the German Bight, there were significant differences. In the German Bight during the spring and summer months bottom organic contents were typically lower by as much as 40-50% [*cf.* Figures 4.3h and 4.4h]. Similarly, in the coastal waters off North Yorkshire and Northumberland, the high organic contents observed in the surface waters were not evident in the bottom waters [*cf.* Figures 4.3f and 4.4f].

The reasons for the temporal and spatial differences between surface and bottom organic contents noted above may in part be related to different water stratification conditions [see §5]. Typically, surface to bottom organic content differences are higher in regions of stratification. For example, in the northern part of the southern North Sea, there is either a permanent or summer temperature stratification (thermocline) as far south as about 54°N, except in the vicinity of the Dogger

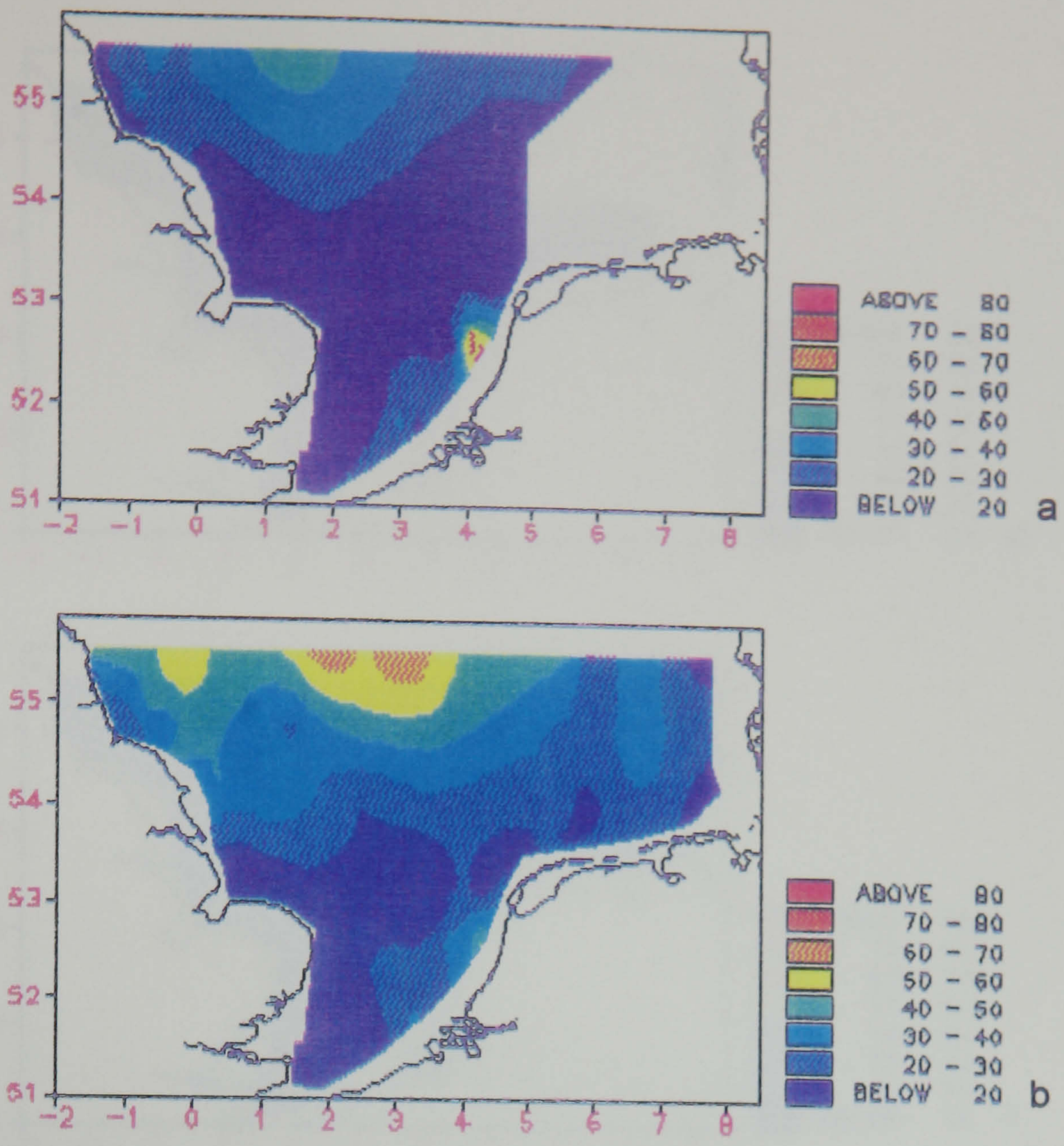

Figure 4.4: Distribution of Organic Content (% of TSM) in the bottom waters of the southern North Sea for (a) December 1988, (b) January 1989, (c) February 1989 and (d) March 1989.

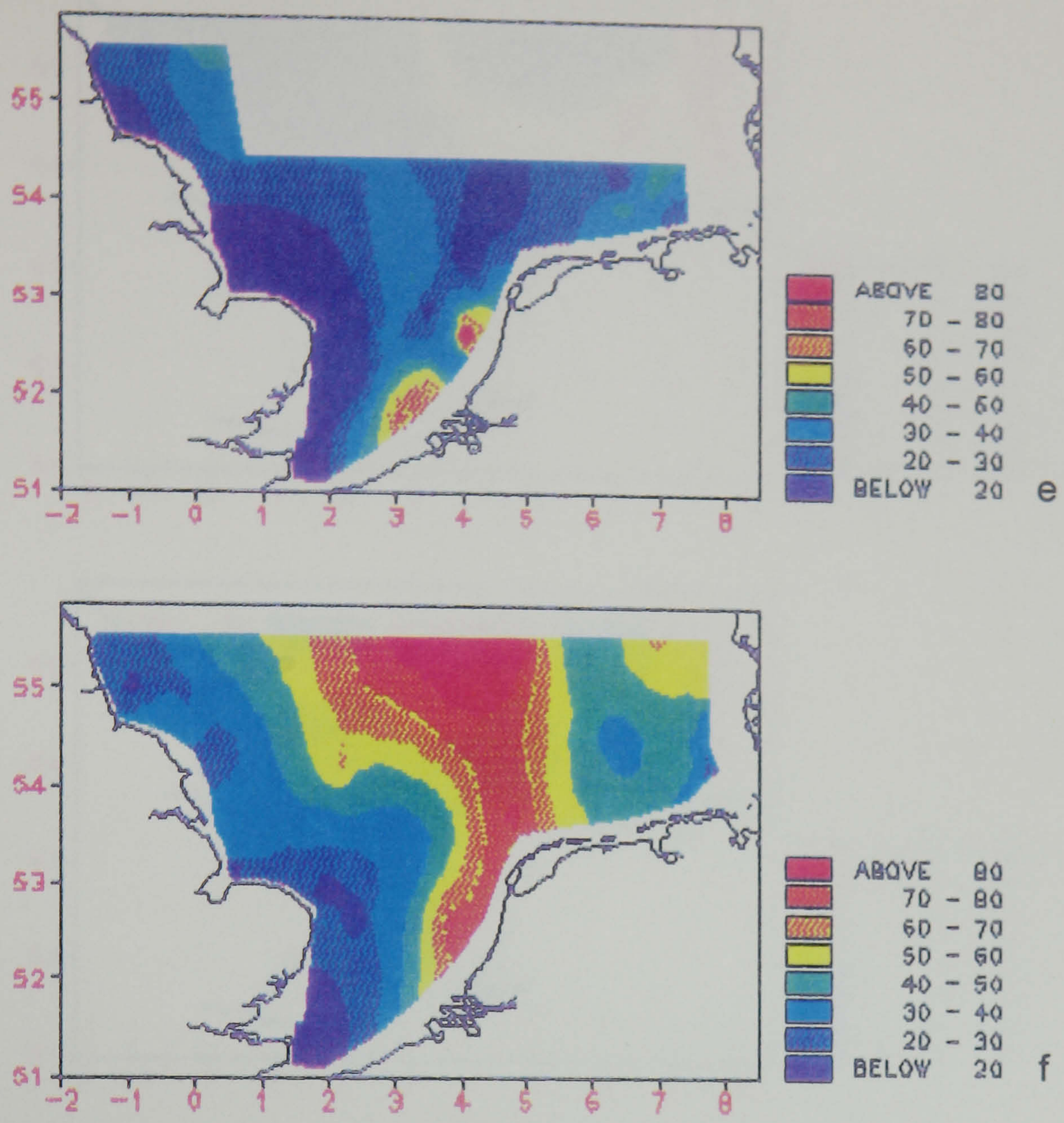

Figure 4.4 (cont/d): Distribution of Organic Content (% of TSM) in the bottom waters of the southern North Sea for (e) April 1989, (f) April-May 1989, (g) May-June 1989 and (h) June-July 1989.

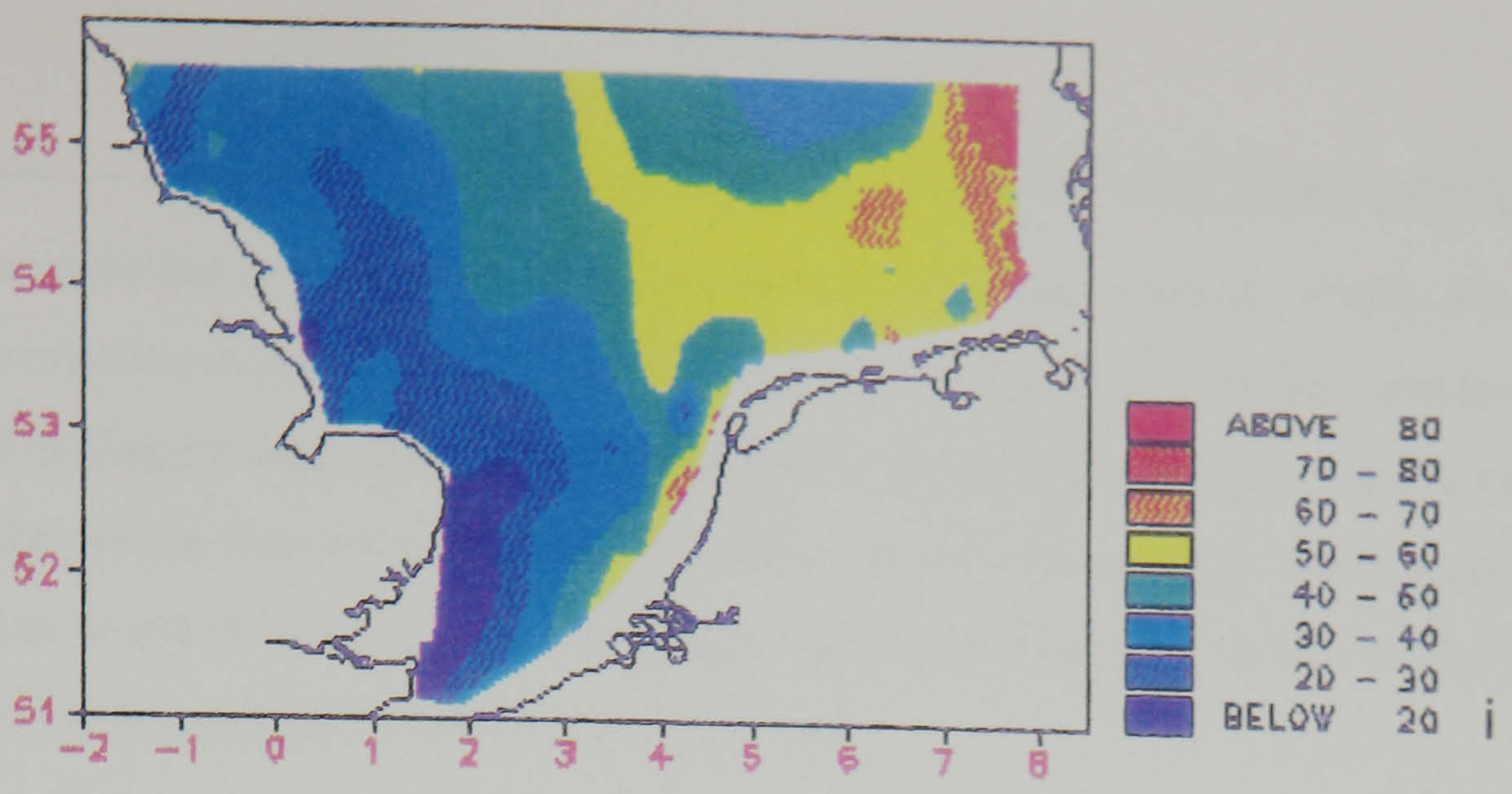

Figure 4.4 (cont/d): Distribution of Organic Content (% of TSM) in the bottom waters of the southern North Sea for (i) July-August 1989, (j) August-September 1989 and (k) September-October 1989.

Bank where water depths are shallow enough to prevent stratification [Eisma, 1987b; Howarth et al., 1993]. The organic contents in the Dogger Bank region were similar at the surface and the bottom. To the west of the Dogger Bank, where thermal stratification occurs in the summer, organic contents were higher at the surface than near the bottom. Similarly, in the German Bight where extensive salinity stratification occurs due to high river discharges, organic contents at the surface tended to be higher than at the bottom especially between April and June.

4.3 Summary

This chapter has presented distribution plots of organic matter concentration and organic content in the southern North Sea for a 11-month period and has described in some detail the horizontal and surface to bottom variations in both space and time. Organic matter concentrations tended to be highest in the coastal waters of the Southern Bight and in the German Bight, and lowest in the northern and central parts of the region. The organic content distributions exhibited the reverse trend during the winter. Levels of organic content exhibited a distinct seasonal trend, increasing dramatically during the spring as phytoplankton production increased. The existence of a region of high organic content in the central and northern parts of the southern North Sea in the vicinity of the Dogger Bank during the winter months also suggested that phytoplankton activity first started to increase in this region, rather than along the continental European coastline. The high turbidity area off East Anglia was characterized by persistently low organic contents, but along the north-east English coastal organic contents increased during the spring.

The distributions of organic matter and organic content, just like the TSM distributions, will be strongly influenced by the interactions of a number of parameters such as phytoplankton production and stratification. For example, different stratification conditions may provide a coarse explanation for some of the vertical variations in organic content. The next chapter uses some of the other data that were collected or derived during the survey period to establish more closely the relationships between the observed distributions and some of these parameters.

FACTORS AFFECTING THE SUSPENDED MATTER DISTRIBUTIONS

The preceding two chapters presented the main results of the research by describing the seasonal cycles of the TSM [§3] and OSM [§4] distributions during the 15 month survey period. These distributions are strongly influenced by a number of physical and biological variables, including water mass interactions, haline and thermal stratification, primary production, meteorological conditions and current patterns. The following chapter considers the inter-relationships between the suspended sediment distributions and water masses, salinity, river discharge, stratification and primary production. The influence of meteorological conditions and current patterns are discussed in the next chapter [§6] in relation to the transport of sediment within the plume.

5.1: Water Masses and Salinity Distribution

The distribution of TSM will depend to some extent on the water masses present within the southern North Sea. Different water masses can be discerned from an initial consideration of the salinity distribution within the southern North Sea. The mean depth-averaged salinity (in Practical salinity Units, PSU) derived from field measurements during the survey period is presented in Figure 5.1a. There is a pronounced spatial variation in the salinity distribution: the lowest salinities occurring along the English coast (typically less than 34.5 PSU) and along the Continental European coast (*eg.* less than 32 PSU in the German Bight), and the highest salinities (greater than 34.75 PSU) occurring in the central Southern Bight between East Anglia and the Netherlands, and in the northern part of the southern North Sea. This pronounced spatial variation is related to the main sources for salinity which occur at the lateral boundaries of the southern North Sea (exchanges with the oceans and run-off down rivers) in addition to evaporation/precipitation at the surface [Howarth *et al.*, 1993]. The saline sources result from the influx of Atlantic water through the Straits of Dover and into the northern North Sea. The fresh water sources result from coastal run-off and discharge by major rivers from the English and Continental coasts; the latter coast having much the larger run-off [Table 5.1 and Figure 5.2]. Over the seasonal cycle, the broad features of the salinity distributions changed little, except in the nearshore coastal regions, particularly off the Dutch coast and the German Bight, where the amplitude of the seasonal cycle was largest, in the range 0.25-1 PSU [Figure 5.1b]. Four specific coastal regions could be identified which were associated with rivers (Humber, Rhine, German Bight and Elbe) and where the salinity cycle was related to river discharge [Howarth *et al.*, 1993]. An offshore region could also be identified where it was related to the precipitation/evaporation cycle [hatched area of Figure 5.1b].

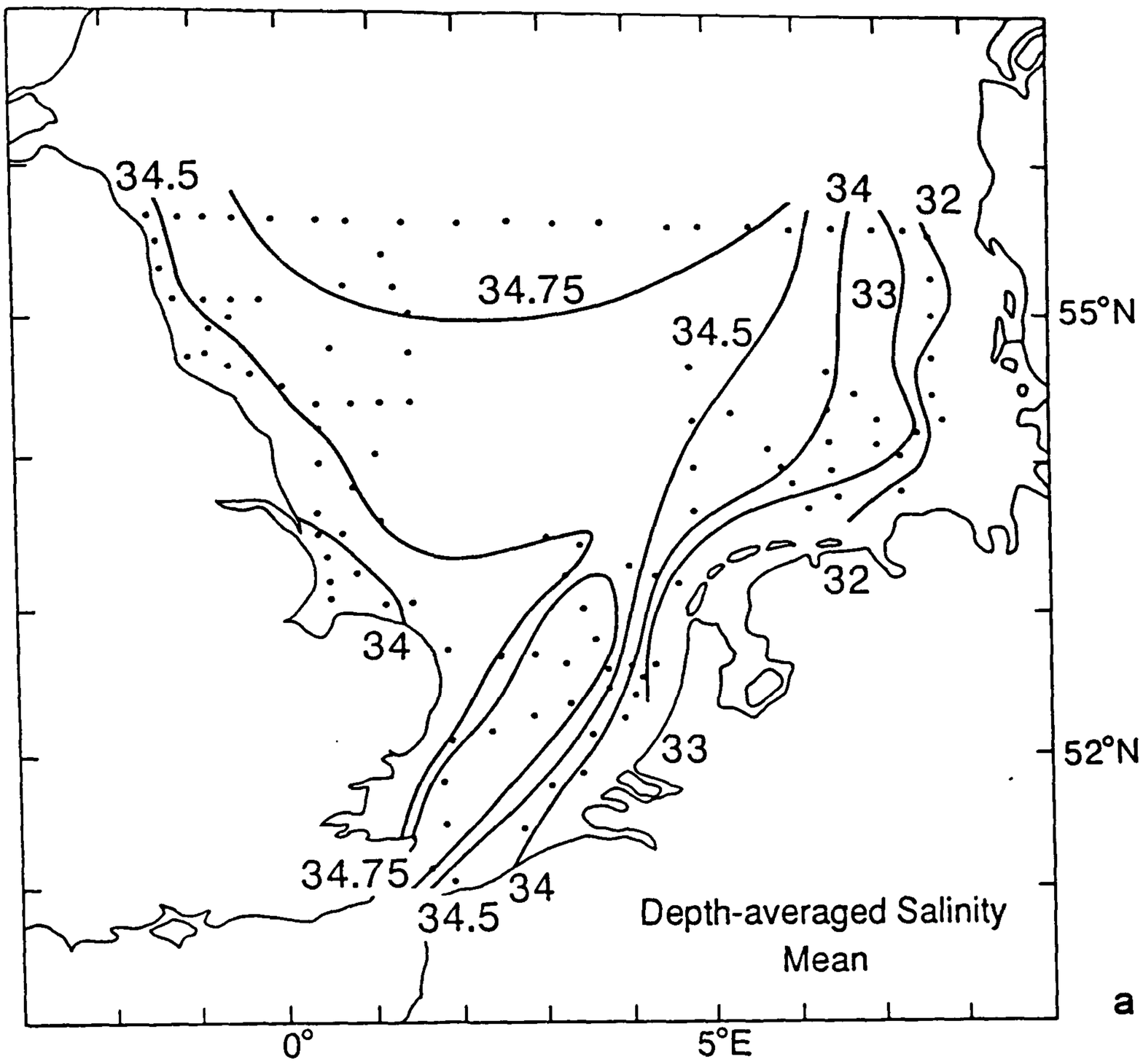

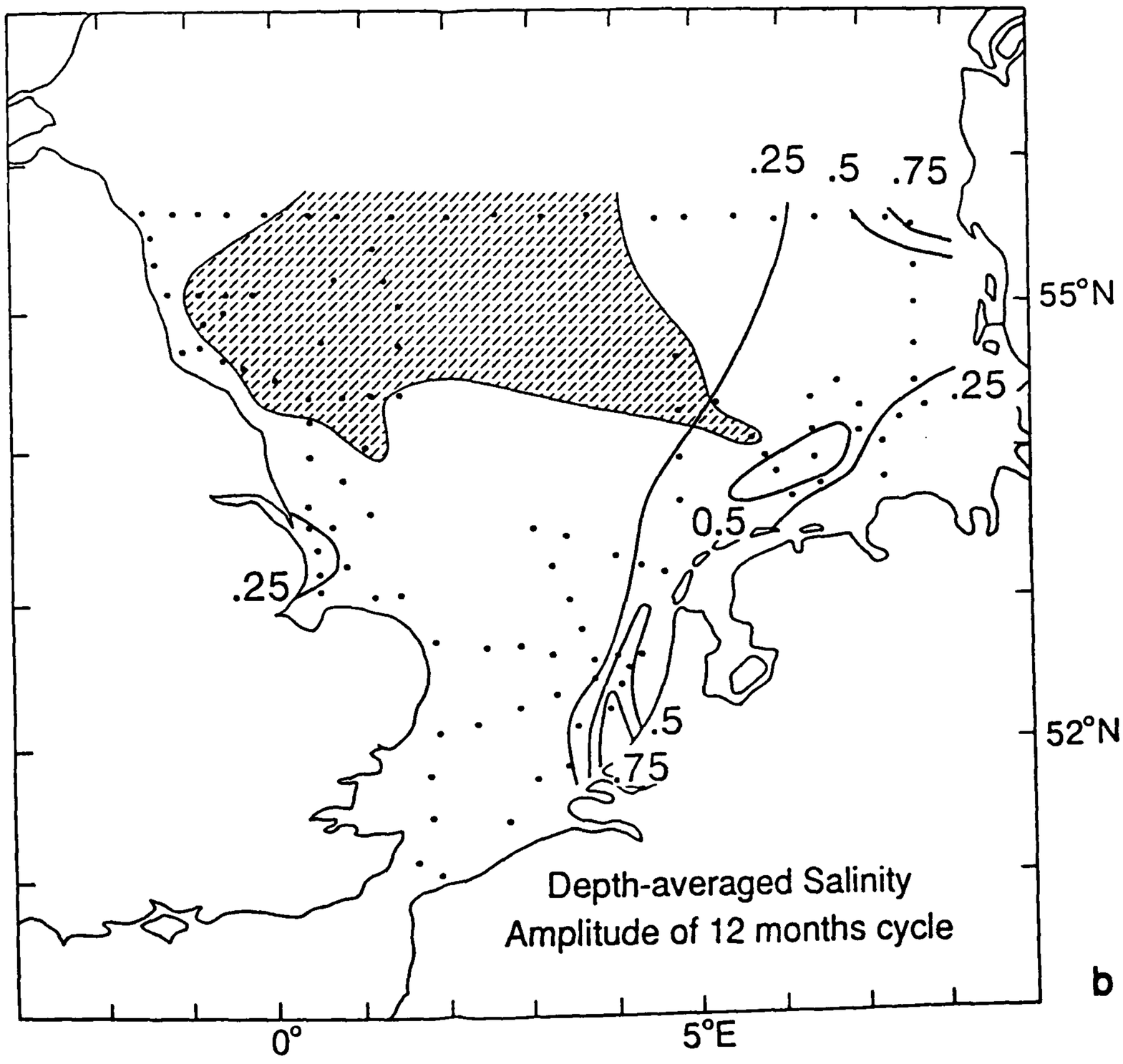

Figure 5.1: Depth-averaged salinity: (a) Mean; and (b) Amplitude of annual cycle [after Howarth *et al.*, 1993].

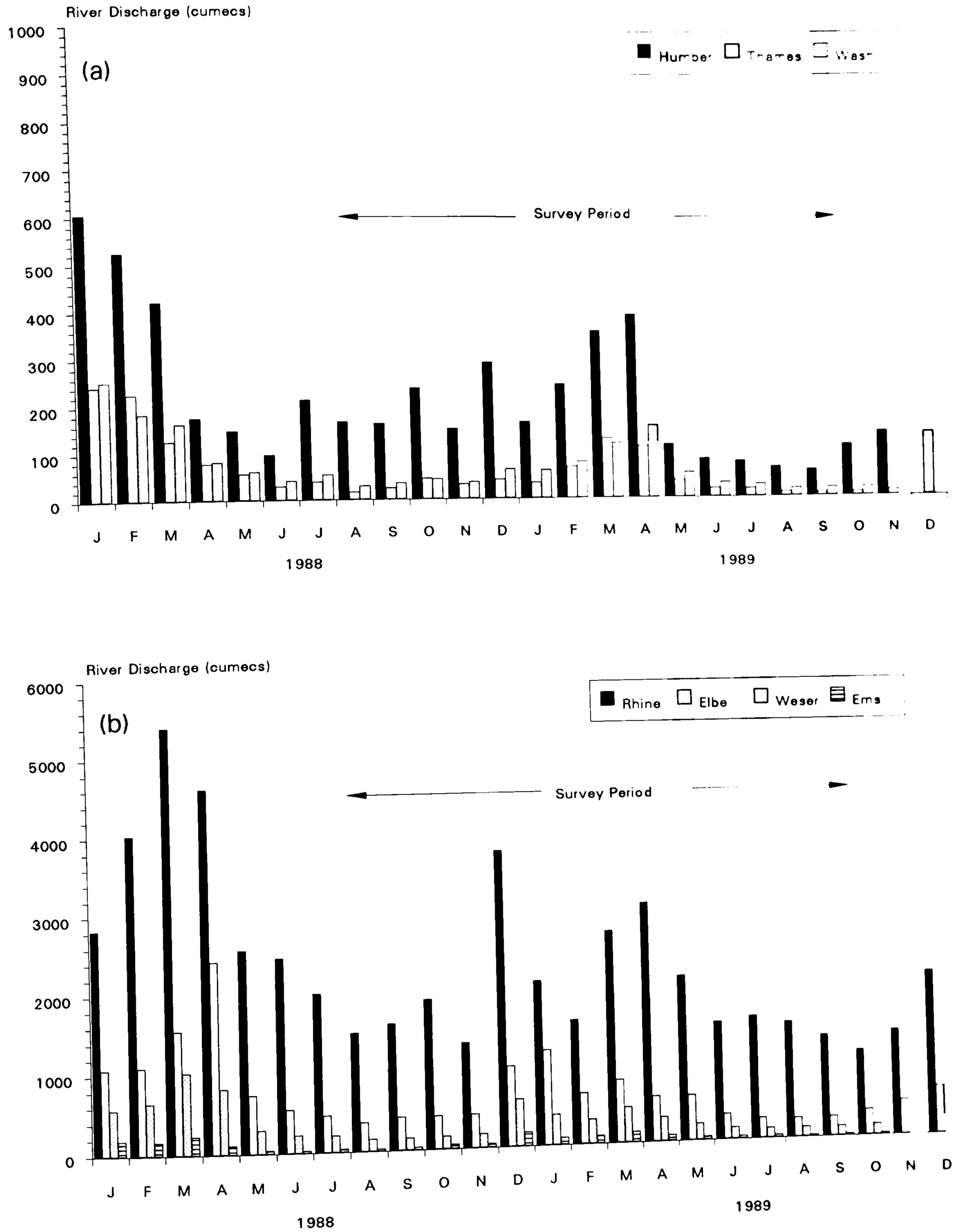

Figure 5.2: Bar Charts of Monthly Mean Fresh Water Discharge from (a) 3 UK rivers/estuaries and (b) 4 European river/estuaries bordering the southern North Sea for 1988 and 1989. (There are no data available for the Wash, Weser and Ems in November and December 1989, and no data for the Humber in December 1989).

Table 5.1: Average river discharges (in cumecs) for August 1988 to October 1989.

River	Discharge (m^3 s^{-1})	River	Discharge (m^3 s^{-1})
Humber	178	Rhine	1897
Wash	52	Ems	63
Thames	40	Weser	238
		Elbe	521

The salinity distribution is very similar to the general distributions of TSM described in §3 with the coastal waters being more turbid and less saline than the water of Atlantic origin further offshore. For example, in the Southern Bight, the East Anglian high turbidity area and associated plume corresponds to a tongue of relatively low salinity emanating from the coast in the same general north-easterly direction as the turbidity plume. The low turbidity zone to the south and east of the East Anglian turbid area and plume, and the one found in the northern and central parts of southern North Sea also correspond to areas of relatively high salinity associated with the influx of Atlantic Water.

The distribution of different water masses as described by the salinity distribution explains at a fairly basic level the broad features of the TSM distributions. However, other variables will modify these basic TSM/salinity patterns [see also §6]. For example, Lee and Folkard (1969) have reported that the zones of TSM and salinity maxima and minima found in the Southern Bight do not correspond exactly: the turbidity minimum is displaced towards the coast of the Netherlands and is some 30 km to the east of the salinity maximum. Likewise the turbidity maximum is displaced eastwards of the salinity minimum. These differences are attributed to the influence of other variables such as the patterns of tidal currents and the distribution of seabed sediments.

The possible spatial and temporal influence of other factors can also be demonstrated by seasonal scatter plots of mean salinity versus mean TSM [Figure 5.3] for hydrographic stations located within four specific regions of the southern North Sea based on the ICES subdivision [Figure 5.4]. ICES Boxes 3' and 3" have been combined to form a single English coastal region (ICES Box 3). ICES Boxes 7' and 7" have been combined to form a single central and northern region (ICES Box 7). ICES Box 4 corresponds to the Dutch/Belgian coastal waters, and ICES Box 5 corresponds to the coastal waters of the German Bight.

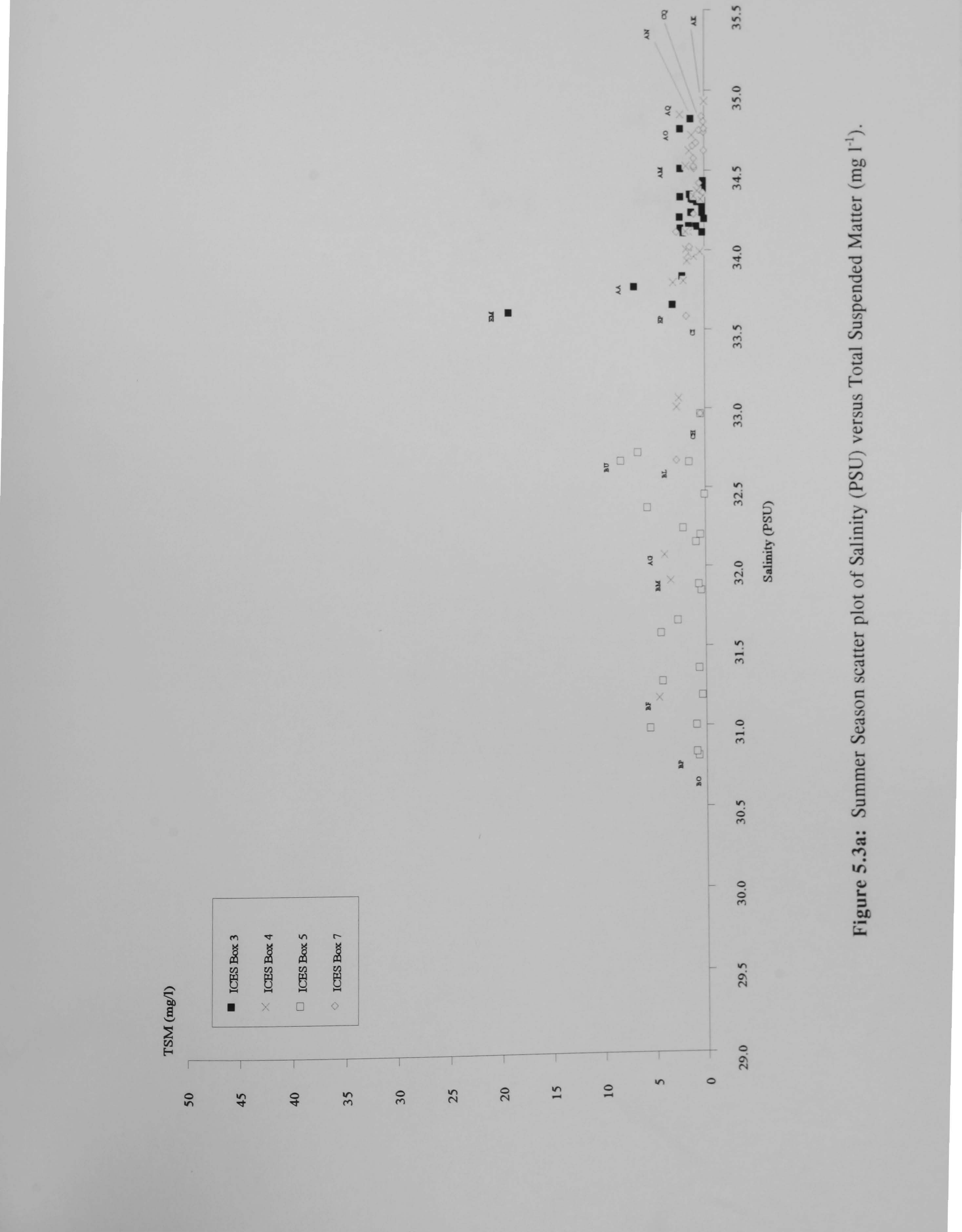

Figure 5.3a: Summer Season scatter plot of Salinity (PSU) versus Total Suspended Matter (mg l^{-1}).

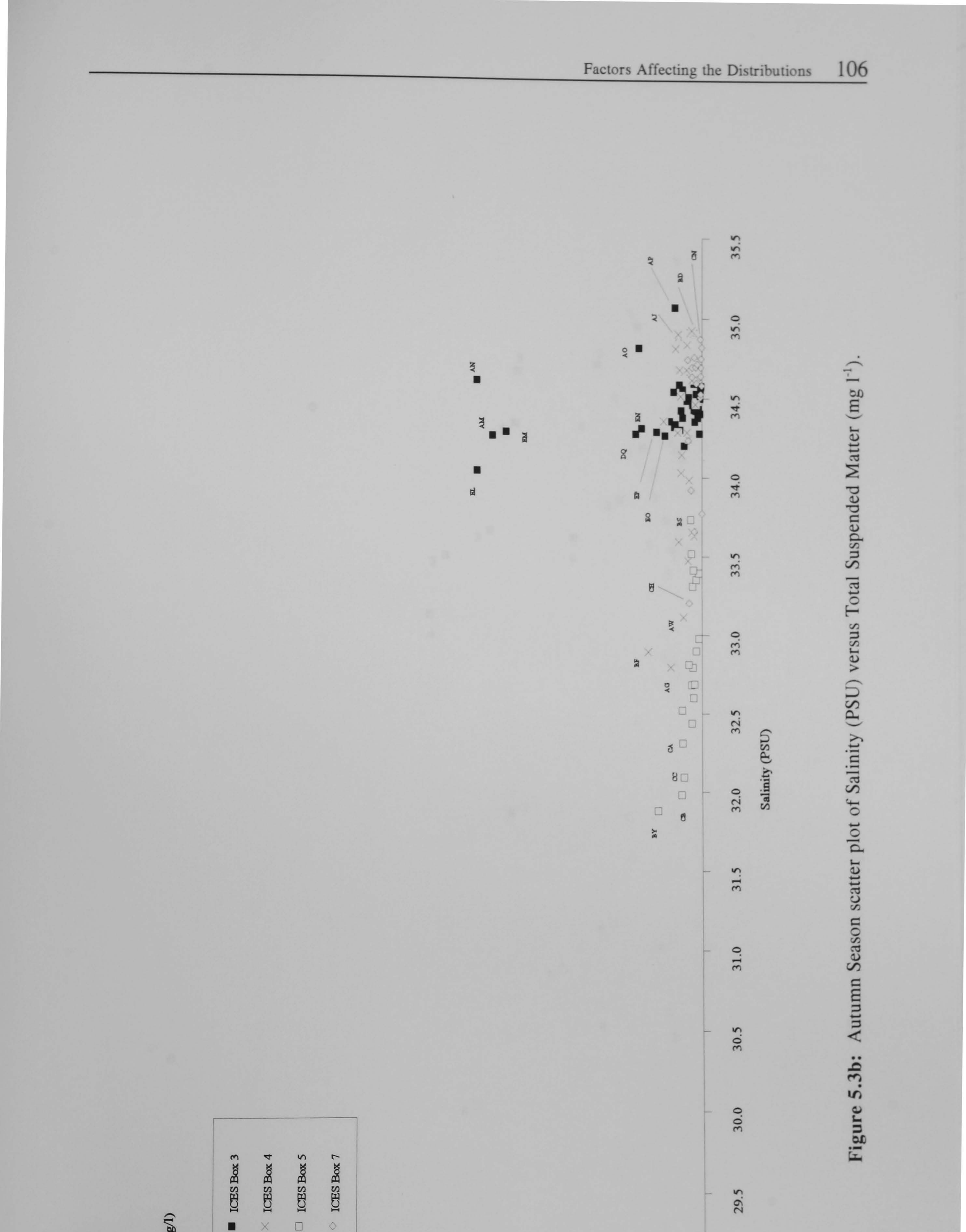

Figure 5.3b: Autumn Season scatter plot of Salinity (PSU) versus Total Suspended Matter (mg l^{-1}).

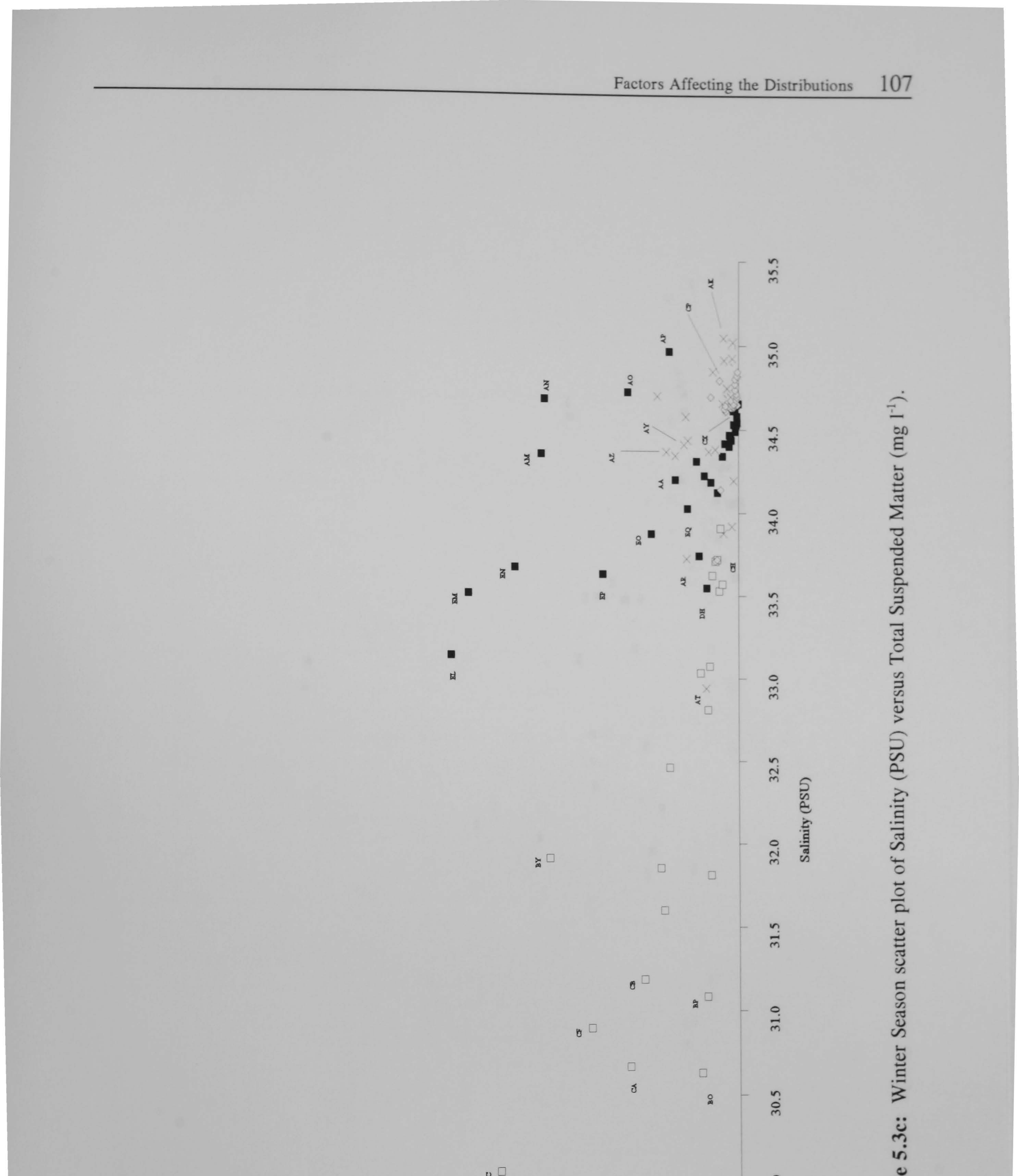

Figure 5.3c: Winter Season scatter plot of Salinity (PSU) versus Total Suspended Matter (mg l^{-1}).

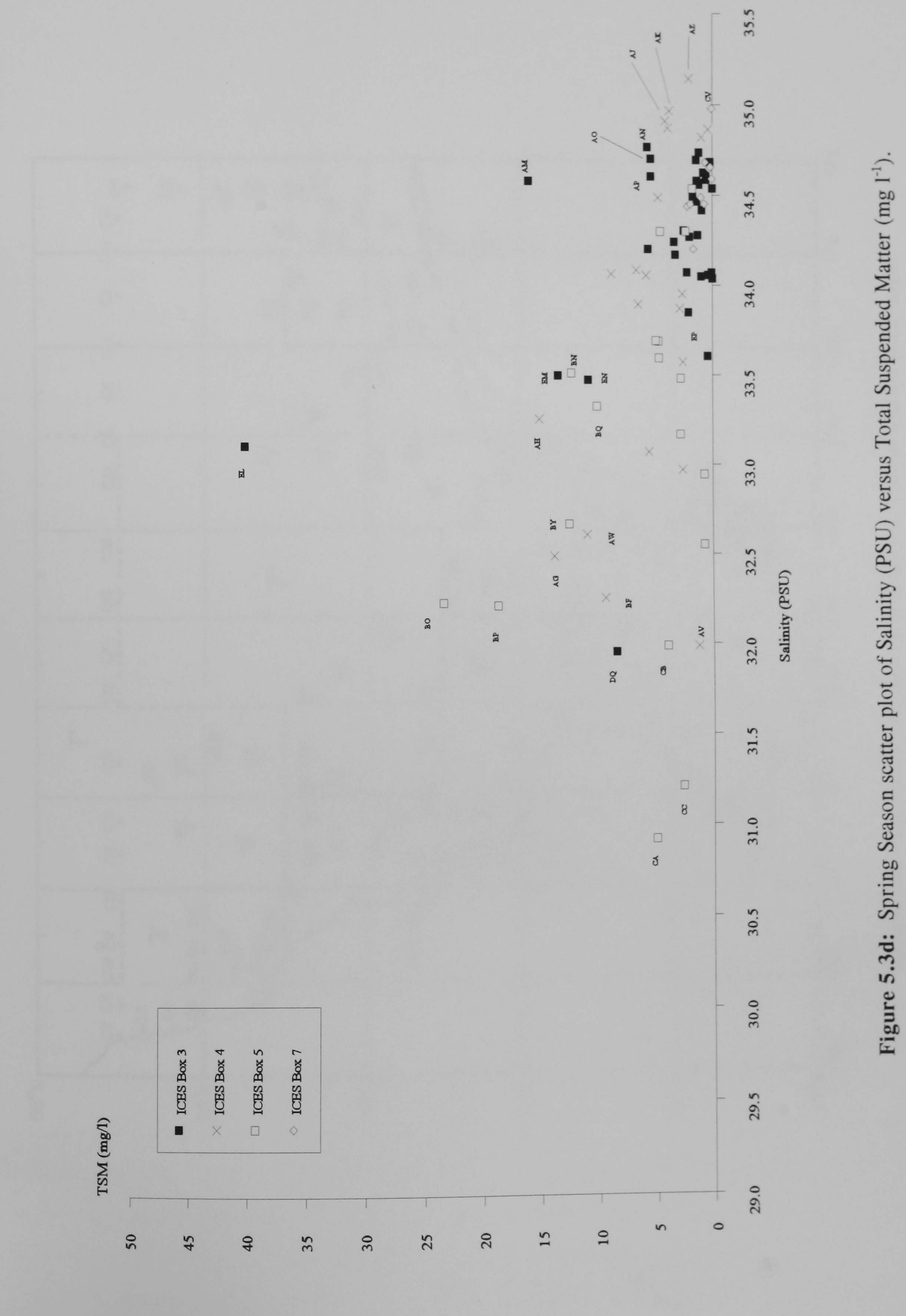

Figure 5.3d: Spring Season scatter plot of Salinity (PSU) versus Total Suspended Matter (mg l^{-1}).

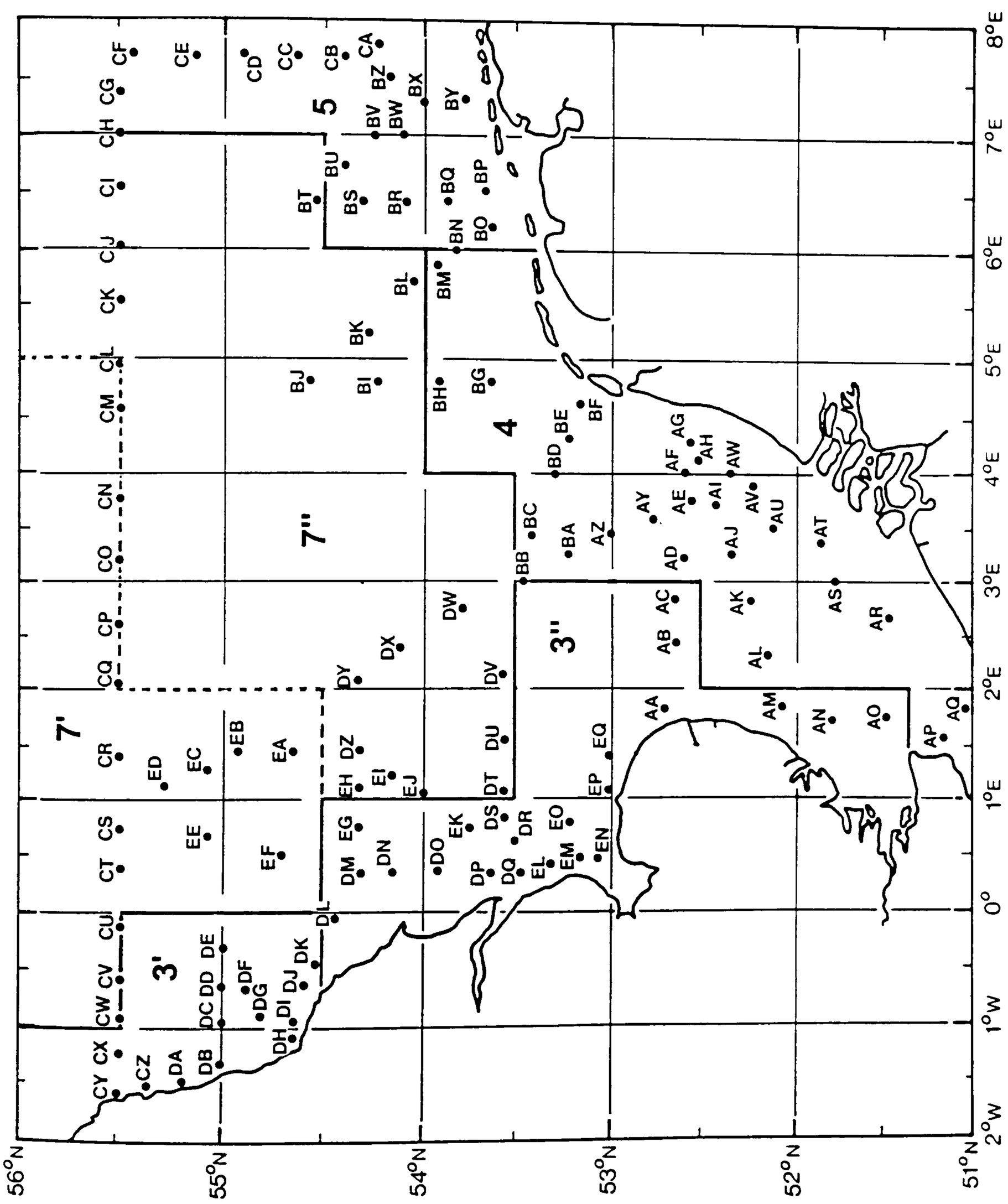

Figure 5.4: Map showing the Survey hydrographic stations and the ICES boxes.

The four regions display quite distinct regional characteristics in terms of salinity throughout the four seasons, similar to the basic patterns that have already been described; the stations that constitute the ICES Boxes 4 and 5 have a broad range of salinities and the stations of the ICES Boxes 3 and 7 have a relatively narrow range of salinities. With respect to intra-regional relationships between salinity and TSM, the situation is less clear and distinct.

For the two regions that have the broadest range of salinities, it might be expected that TSM concentrations would typically increase with decreasing salinity. For example, in the ICES Box 4 many of the nearshore stations will be strongly influenced by the fresh and more turbid water discharges from rivers such as the Rhine (*eg.* AG and AV), whilst other stations, further offshore will be strongly influenced by the influx of more saline and less turbid Atlantic water (*eg.* AJ and AK) through the Dover Straits. For this region, the basic relationship only holds true for the summer and spring seasons [Figures 5.3a and 5.3d]. In the spring, there was considerably more scatter in the distribution with some anomalously low TSM concentrations and low salinities at stations AV and BE. These stations are associated with development of near-surface TSM minima [see later]. Some of the scatter will also be caused by primary production which reaches its peak in the spring [see §5.2]. During the winter, maximum TSM concentrations tended to occur at the mid-range values of salinity [Figure 5.3c] corresponding to the development of the East Anglian plume which increased concentrations at stations AZ and AY, for example, as it extended in prominence. With respect to the ICES Box 5, this region is strongly influenced by the fresh water discharges from rivers such as the Elbe, Weser and Ems. During the autumn and winter seasons when the river discharges were large or increasing, and primary production was low [Figure 5.2], TSM concentrations tended to increase with decreasing salinity [Figures 5.3b and 5.3d]. However during the summer and spring, the relationship between salinity and TSM was considerably more variable [Figures 5.3a and 5.3d] indicating perhaps that primary production has a more significant influence during these seasons.

With respect to the regions characterized by a relatively narrow range of salinities, the stations that constitute the ICES Box 7 are also confined to a narrow band of relatively low TSM concentrations (typically more than 1 mg l^{-1}) characteristic of the water of Atlantic origin entering the region across its northern boundary. Stations located towards the lateral boundaries of the region adjoining the other regions tended to have marginally higher concentrations and lower salinities (*eg.* BL, CH, and CI) as a result of the proximity to and inter-mixing with more turbid and less saline coastal waters. The relationship between salinity and TSM for the ICES Box 3 is quite variable. The most prominent feature in this region is the distinct regional division between the stations contiguous to the Humber and the Wash (EL, EM and EN) and the stations at the outer margins of the Thames Estuary (AM, AN and AO). Generally, there was a tendency for the TSM concentrations to be higher and salinities to be lower off the Humber/Wash than off the Thames, particularly in winter and spring [Figures 5.3c and 5.3d]. During these seasons, river discharges were largest, but the Humber discharge was between 3-4

times greater than the discharge of the Thames [Figure 5.2]. Therefore the greater supply of fresh water and sediment from the Humber/Wash (together with the supply of sediment from cliff erosion and the proximity of the stations to the sources) compared with the Thames would to a large extent account for the regional differences. Furthermore, the stations of the Thames Estuary are closer to the source of Atlantic Water entering through the Dover Straits which will tend to keep the salinities of the stations higher than those off the Humber.

5.2 River Discharge and Waves

In addition to playing a significant role in the seasonal and spatial relationships between suspended sediment concentrations and water mass interactions [§5.1], the freshwater discharge from rivers will supply suspended sediment directly into the coastal zone. In §3 it was surmised that the river discharge from major rivers were contributing significantly to adjacent and quite localized areas of high TSM concentrations; the magnitudes of which varied according to fluctuations in the discharge. In order to test the hypothesis, a few stations near the outflows of the Humber/Wash, the Thames and the Rhine estuaries were selected to investigate whether the associated monthly station-averaged TSM concentrations closely reflected the corresponding monthly mean river charge, or the effects of wave action which were estimated from monthly mean 10m wind speeds derived from the Meteorological Office Model.

Figure 5.5 shows two time trends of the surface, bottom and depth-averaged TSM concentrations plotted against the monthly river discharge from the Humber/Wash and the monthly mean wind speed. With respect to Figure 5.5a, there is very good agreement between the peaks and troughs of the river discharge and the suspended sediment concentrations. The largest peaks coincided in April 1989 and were then followed by a sharp decline in both discharge and concentration during the months of May and June 1989. With respect to Figure 5.5b, the wind data are disjointed, but nevertheless there appears to be no clear-cut association between the sediment concentrations and the wind speed, with major discrepancies occurring in September 1988 and July 1989.

For the Thames Estuary, a contrasting picture emerges [Figure 5.6]. Unlike the Humber, the peak and troughs in the TSM concentrations show a very close correlation with the wind speed, particularly in the winter months between October 1988 and February 1989 [Figure 3.6b]. There is, however, a large anomaly between May and June 1989, which may be just an artefact created by short-term storm events biasing the monthly mean wind data. With respect to the river discharge [Figure 3.6a], the peak river discharge that occurred in March and April 1989 does not coincide with the peak suspended sediment concentrations. Since the survey stations used in the plots [stations AM, AN and AO; Figure 5.4], are situated at the margins of the Outer Thames Estuary, it is likely that they will not be influenced by the river discharge, unlike the stations off the Humber which are much closer to the

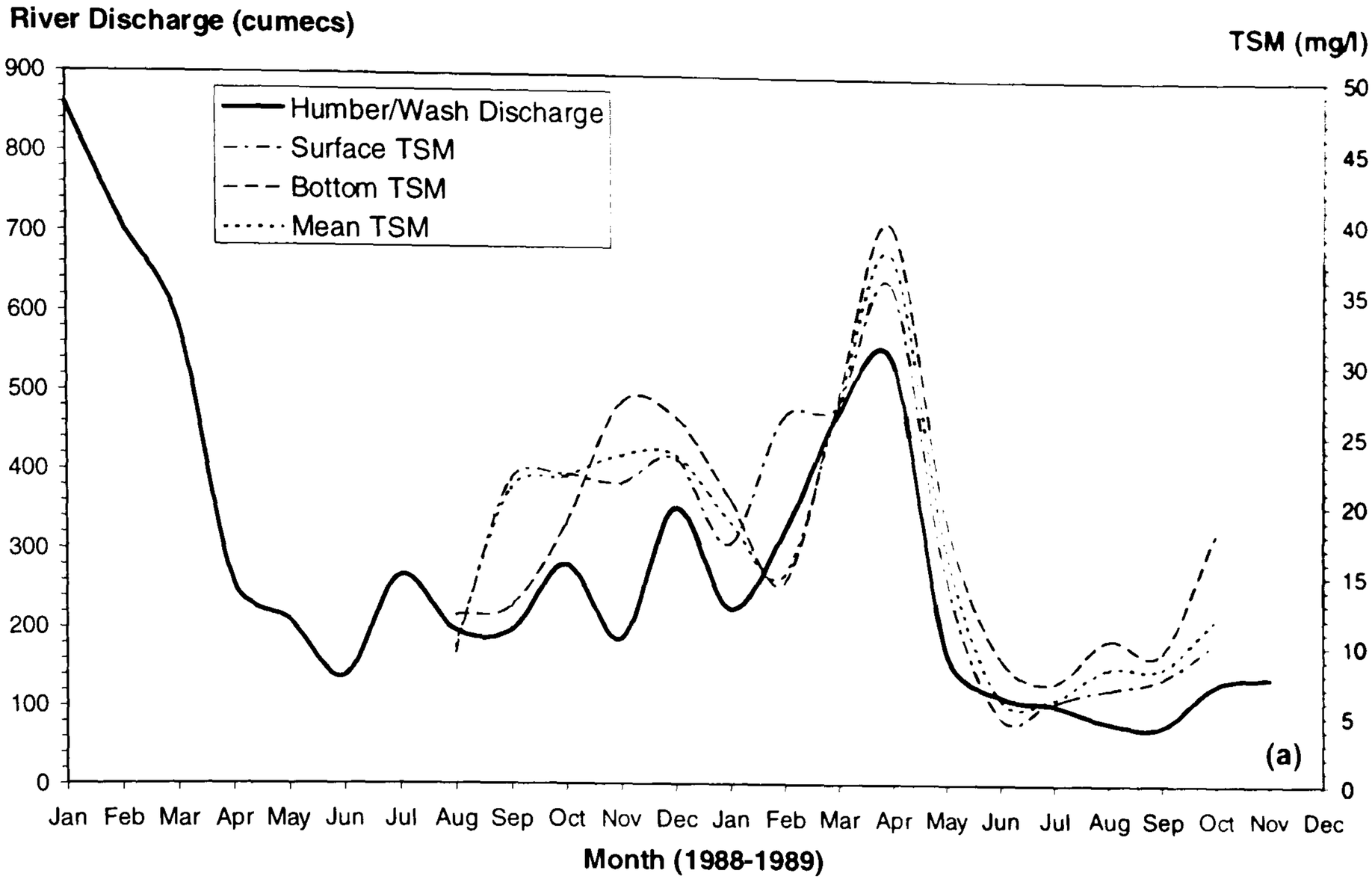

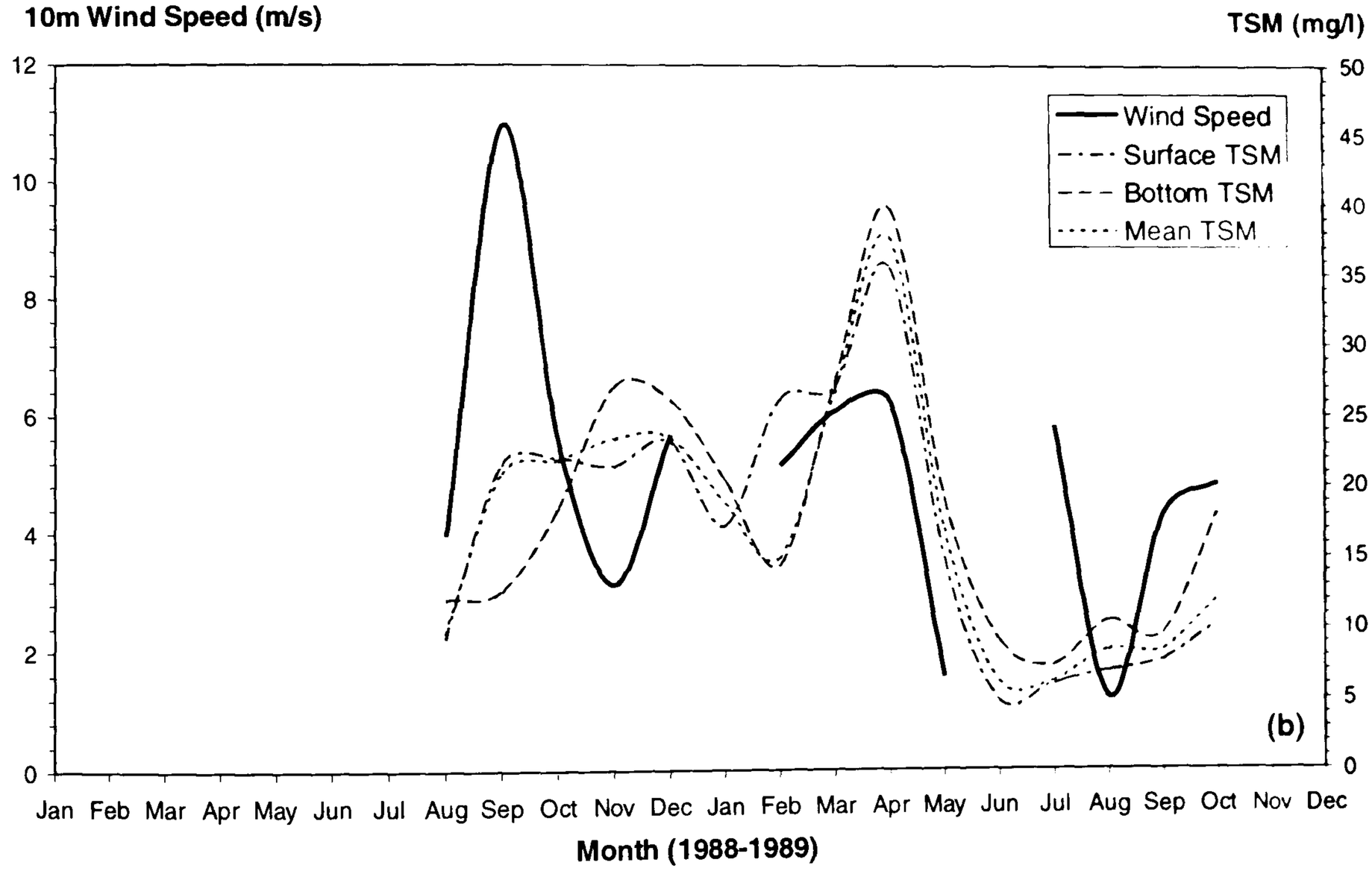

Figure 5.5: Time-trend plots for survey stations adjacent to the Humber/Wash Estuaries showing the relationship between the station-averaged TSM concentrations (mg l^{-1}) and (a) the monthly-averaged river discharge (cumecs) and (b) the monthly averaged predicted wind speed (m s^{-1}).

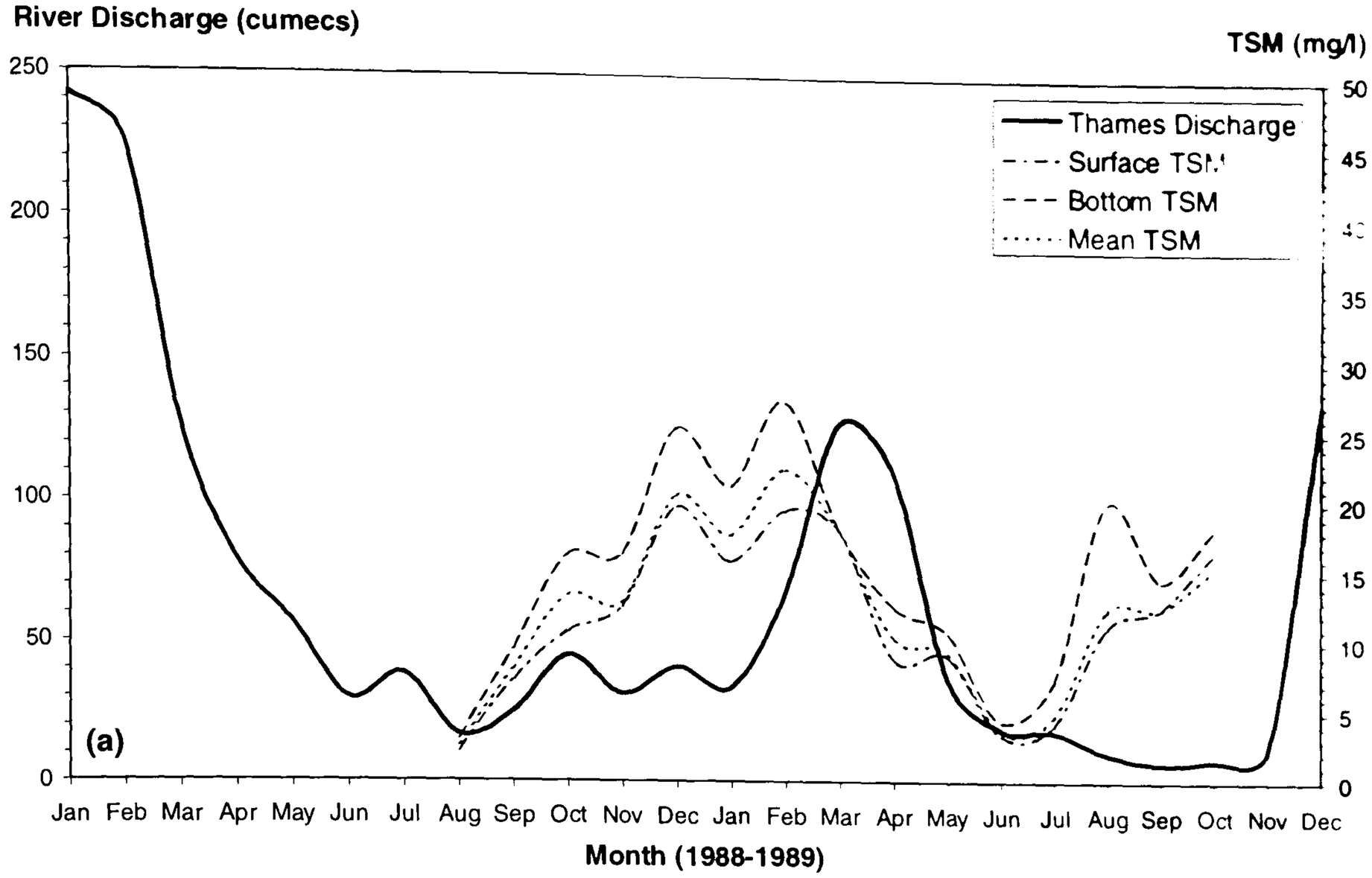

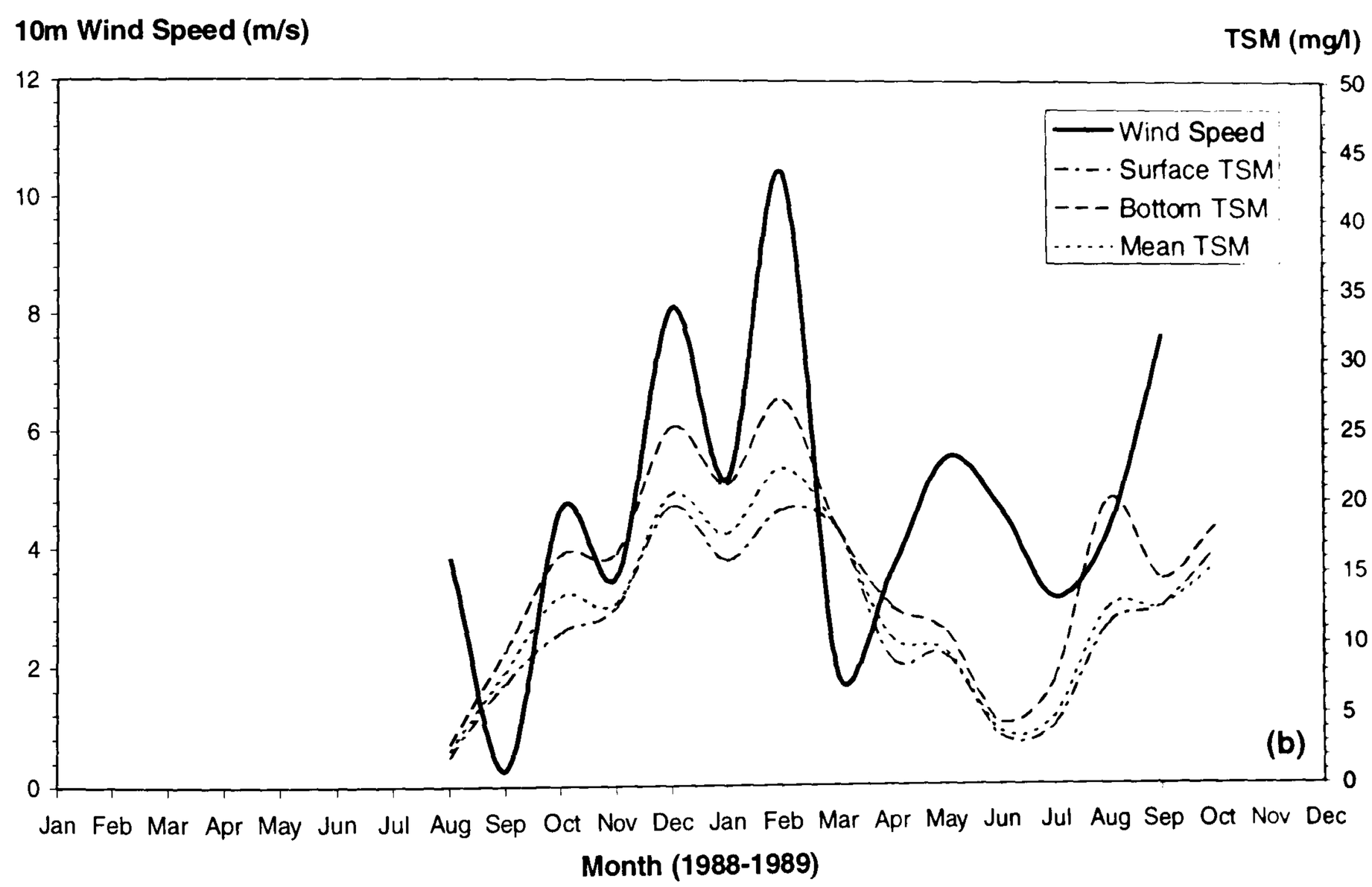

Figure 5.6: Time-trend plots for survey stations adjacent to the Thames Estuary showing the relationship between the station-averaged TSM concentrations (mg l^{-1}) and (a) the monthly-averaged river discharge (cumecs) and (b) the monthly averaged predicted wind speed (m s^{-1}).

outflow from the Humber (*e.g.* stations DQ, EL, EM and EN). By the same token, the stations off the Thames are subject more to the effects of the wind and wave action, leading to high TSM concentrations through resuspension on extensive banks and tidal flats.

With respect to the Rhine [Figure 3.7], the peaks and troughs in the suspended sediment concentrations correspond well with both the river discharge and the wind speed (*e.g.* in December 1988 and March 1989). However, during May 1989, the very large peak in the suspended sediment concentrations is not matched by either a high river discharge or wind speed. This major anomaly is attributable to the increase in primary production that occurs in this general area during the spring months [§5.4]. Clearly, the relatively high river discharge from the Rhine preceding this period may have some influence by supplying nutrients and organic matter to the coastal zone [see §5.5].

In summary, it is clear that proximity to the river outflows is a key factor in determining the contribution of river discharge to the suspended sediment concentrations. For survey stations close to the rivers, as in the case of the Humber, the river discharge has a dominant influence; whereas for stations further offshore, as in the case of the Thames, the suspended sediment concentrations appear to be more closely controlled by storm events and wave-induced resuspension. For other regions, such as off the Rhine, suspended sediment concentrations are controlled by both waves and river discharge, although a more dominant influence occurs in spring through primary production activity.

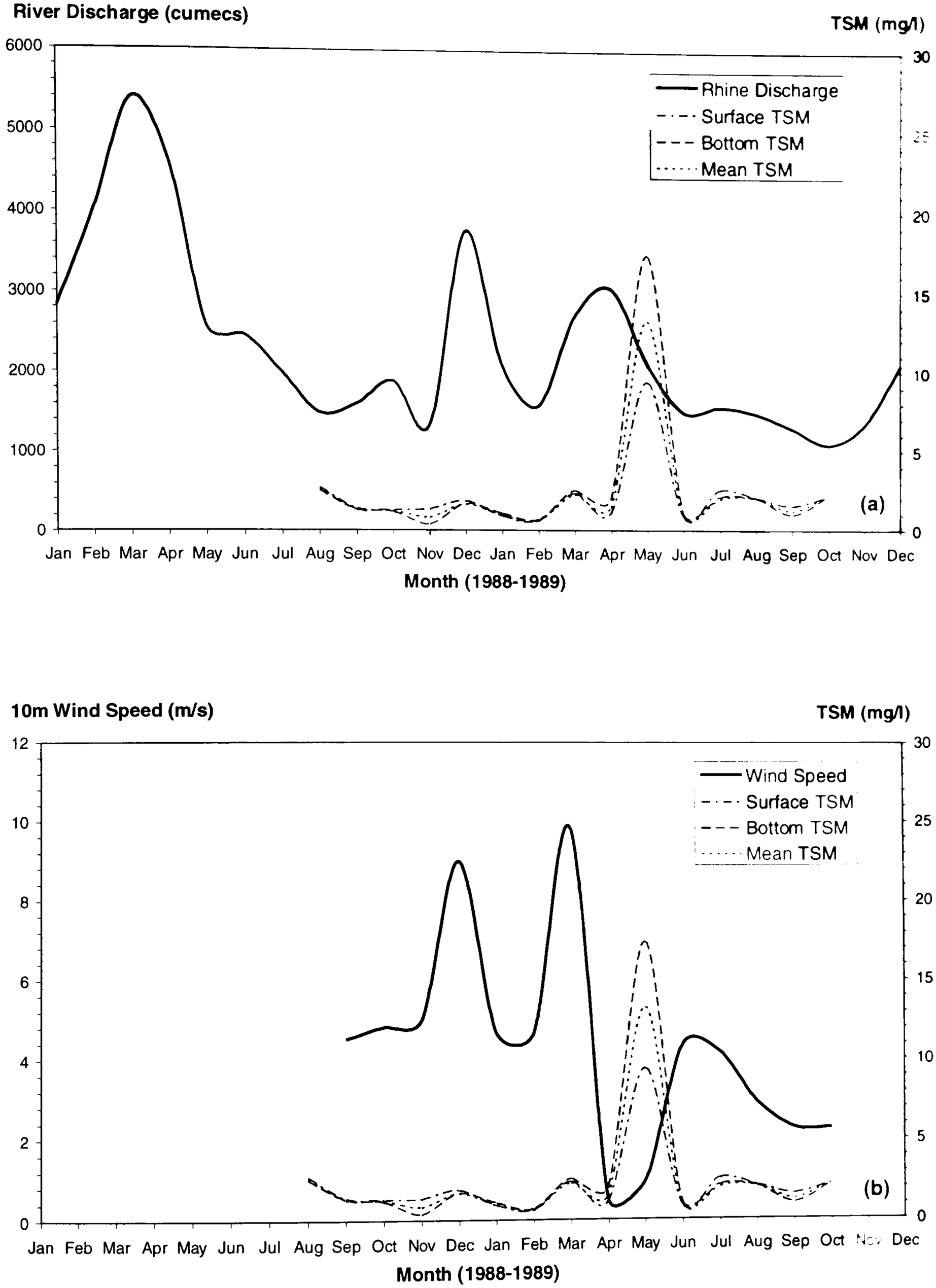

Figure 5.7: Time-trend plots for survey stations adjacent to the Rhine Estuary showing the relationship between the station-averaged TSM concentrations (mg l^{-1}) and (a) the monthly-averaged river discharge (cumecs) and (b) the monthly averaged predicted wind speed (m s^{-1}).

5.3: Water Density and Stratification

Stratification in the southern North Sea can be thermal and/or haline. The development of stratification is largely governed by mixing (generated by tides or storm waves) which may or may not be vigorous enough to overturn vertical water density differences. Thermal stratification (predicted in summer by the parameter h / u^3, where h is the water depth and u is the tidal current velocity) does not generally occur south of approximately 54°N because water depths are shallow and tidal currents strong enough to prevent the formation of a thermocline [Howarth *et al.*, 1993]. However to the north, to the east and west of the Dogger Bank stratification was observed during the survey period [Figure 5.8]. Thermal stratification started towards the end of April and reached its maximum spatial extent in June/July 1989. In the autumn, thermal stratification was broken down by cooling of the sea surface and by enhanced mixing by storms, earlier in the shallower eastern region than in the western.

Haline stratification in the southern North Sea occurs in coastal waters where water density differences are caused by the interaction of fresh water run-off from rivers and more saline waters of Atlantic origin, especially during the winter and spring peak discharge conditions. However, these areas are characterized by relatively shallow water which ensures that mixing is also large. Consequently, the pattern of haline stratification observed during the survey period [Figure 5.9] was patchy in both space and time, and less coherent than that for thermal stratification [Howarth *et al.*, 1993]. Haline stratification reached its maximum extent in spring when river discharges were greatest [Figure 5.2], with quite extensive stratification in the German Bight which helped to encourage thermal stratification in the area to the east of the Dogger Bank [Howarth *et al.*, 1993]. Elsewhere, stratification was limited, with localized regions resulting directly from the discharges from rivers, most notably the Rhine.

The development of stratification and water density differences affect the spatial and temporal distribution of suspended sediment in a number of ways. Stratification encourages phytoplankton production particularly in the surface mixed layer [see also §5.3]. As described in §4, during the spring and summer months, organic contents in the surface waters of some regions of the southern North Sea, (*eg.* the German Bight, to the west of the Dogger Bank and off the North Yorkshire and Northumberland coasts) were much higher than the organic contents in the bottom waters. It was surmised that stratification could in part explain these vertical variations. Figures 5.8 and 5.9 confirm this hypothesis. For example, in the German Bight, the maximum surface to bottom organic content differences of up to 40-50% are associated with extensive haline stratification. However, in other regions where haline stratification was particularly patchy, such as the Rhine, there were no significant differences between surface and organic contents, which probably reflects variations in tidal mixing between the Rhine and the German Bight (*ie.* stronger in the former).

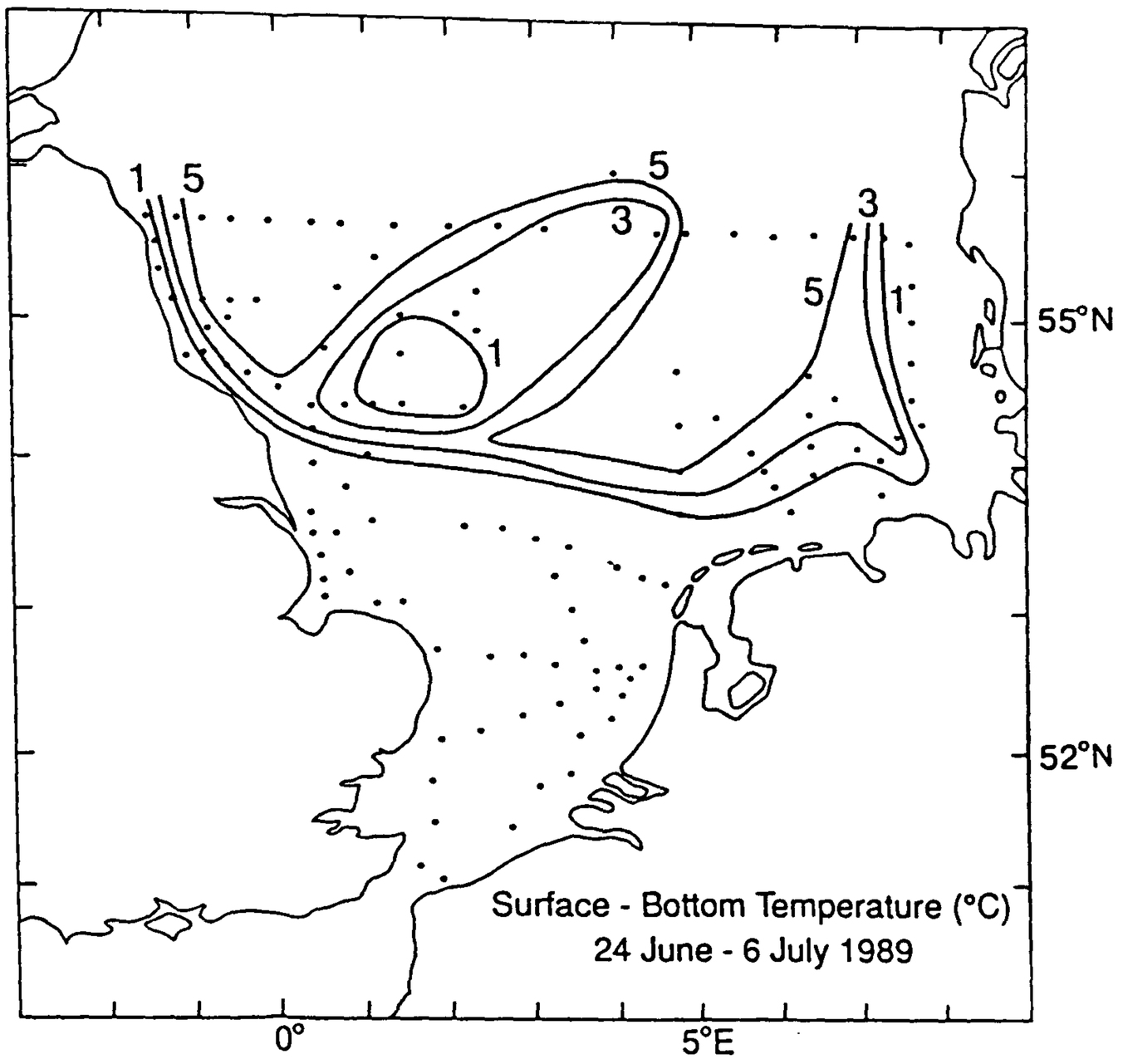

Figure 5.8: Surface to bottom temperature difference in °C for June/July 1989 [from Howarth *et al.*, 1993].

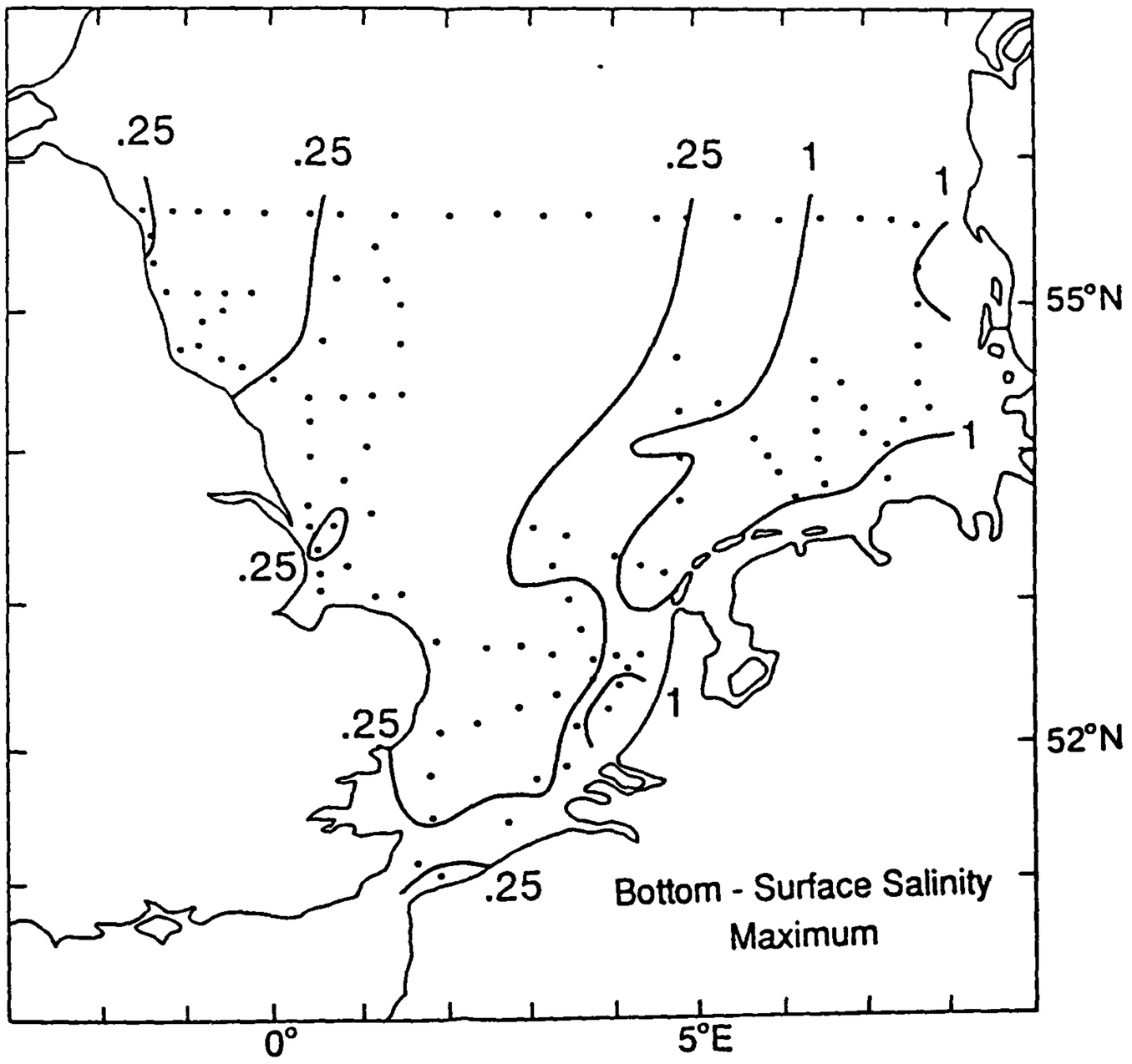

Figure 5.9: Maximum surface to bottom salinity difference in PSU [from Howarth *et al.*, 1993].

In the coastal waters of the southern North Sea, the differences in water density between the nearshore and offshore waters result in secondary circulations whereby the nearshore water moves away from the coast along the surface and offshore water moves landward along the bottom. These circulations have the dual effect of concentrating suspended sediment in the coastal zone, whose sources are mostly located nearshore, and inhibiting the dispersal of suspended sediment from the nearshore sources away from the coast. However, off the East Anglian coast these sediment trapping processes are broken down by the development of the turbidity plume which indicates the importance of advective transport of suspended sediment by currents away from the coast [see §6].

Another feature of the density differences and secondary circulations in the coastal waters of the southern North Sea is the development of near-surface TSM minima in the Dutch coastal zone during spring. As described in §3, a TSM minimum was observed at station BE [Figure 3.7b], and the development of minima seemed to be related to the formation of steep salinity gradients parallel to the coast resulting from the high discharge from the Rhine. Figure 5.9 confirms that there is significant haline stratification associated with the Rhine and its plume which extends north-eastwards parallel to the Dutch Coast.

5.4 Primary Production and Chlorophyll Distributions

Primary production produces living organic and non-living organic matter or detritus that forms part of the suspended sediment in the North Sea during the spring to autumn months. Measurements of chlorophyll and primary production were made during the survey period, thereby presenting a unique opportunity to compare the seasonal cycle of the suspended matter with the seasonal cycle of primary productivity in the southern North Sea.

The distributions of chlorophyll concentration (in mg m^{-3}) in the surface waters of the southern North Sea for a selected number of survey cruises, starting in August 1988, are shown in Figure 5.10. These maps show the seasonal changes in chlorophyll concentration which have been described fully by Joint and Pomroy [1992]. The changes in chlorophyll are not unlike the patterns of change that were observed for the surface organic content distributions [*cf.* Figure 4.3].

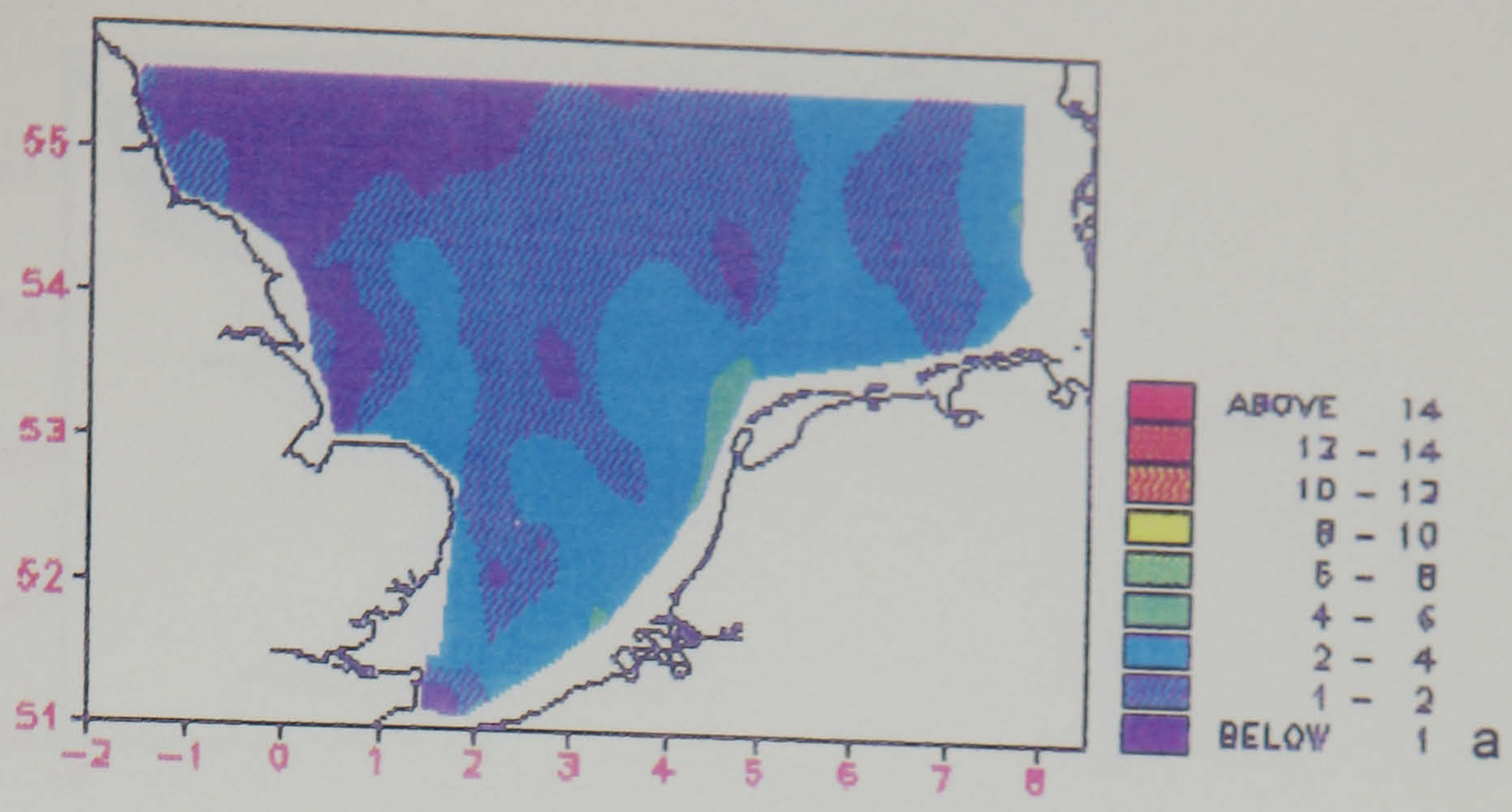

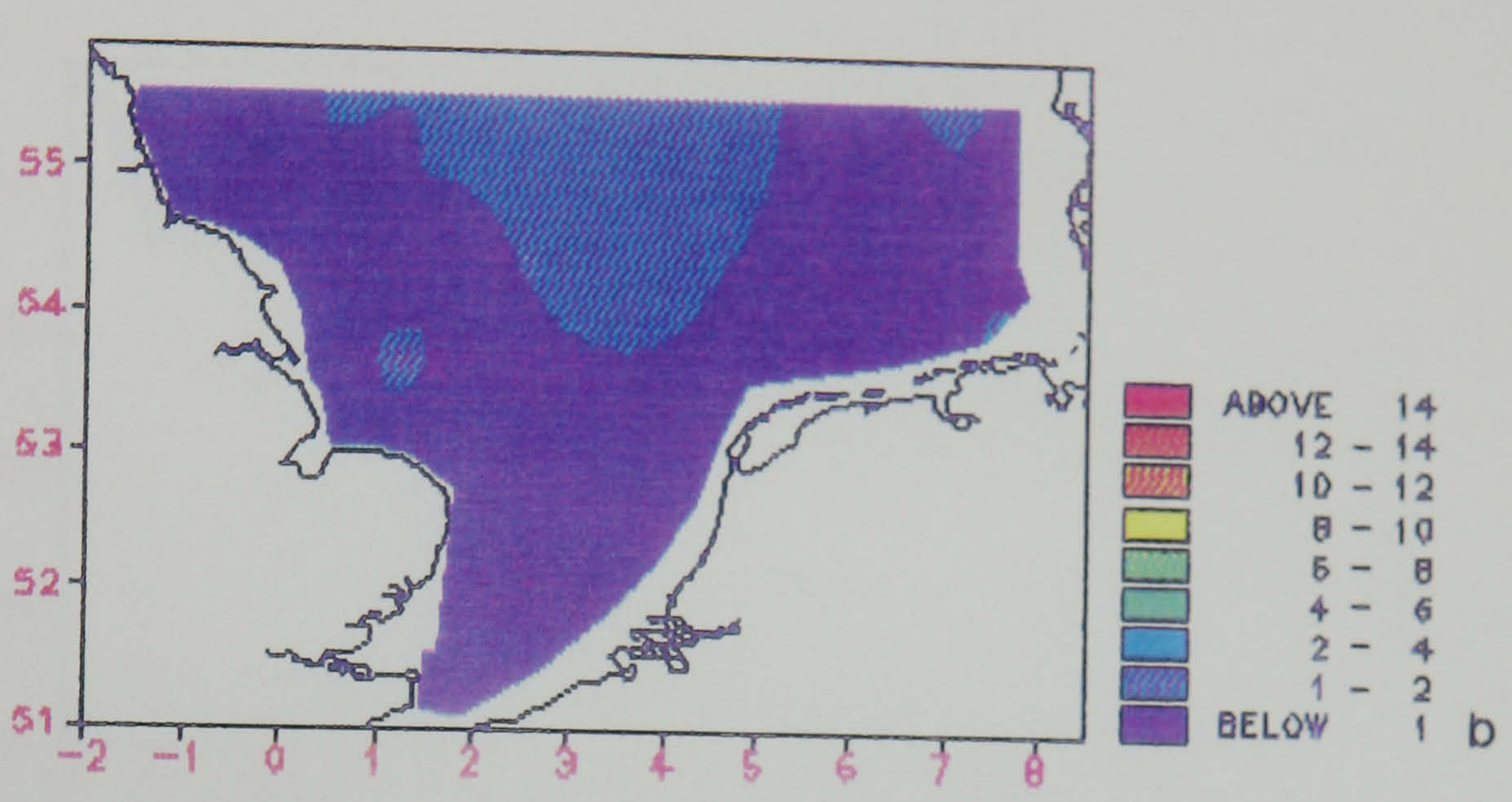

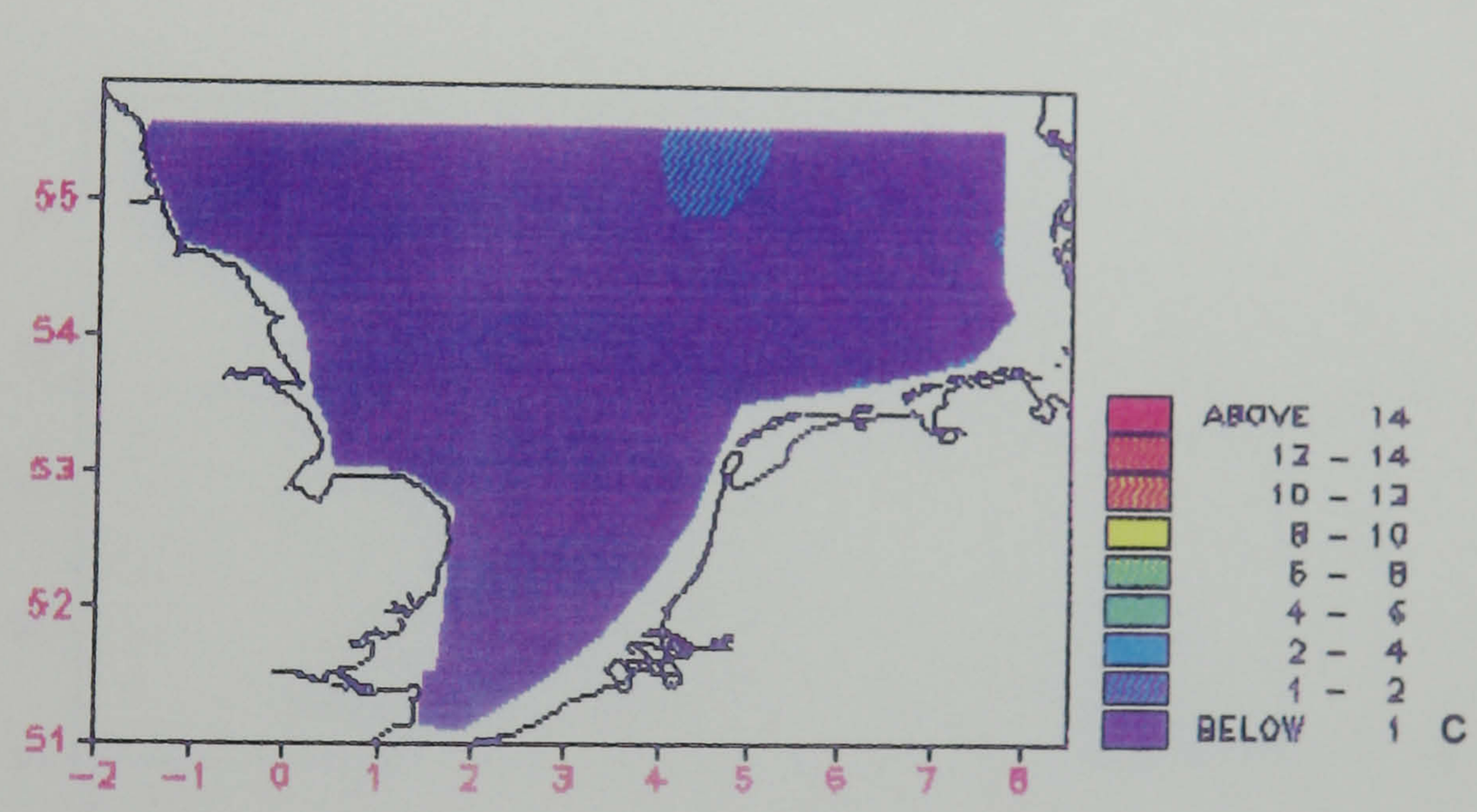

Figure 5.10: Distribution of Chlorophyll (mg m^{-3}) in the surface waters of the southern North Sea for (a) August 1988, (b) November 1988, (c) January 1989 and (d) March 1989.

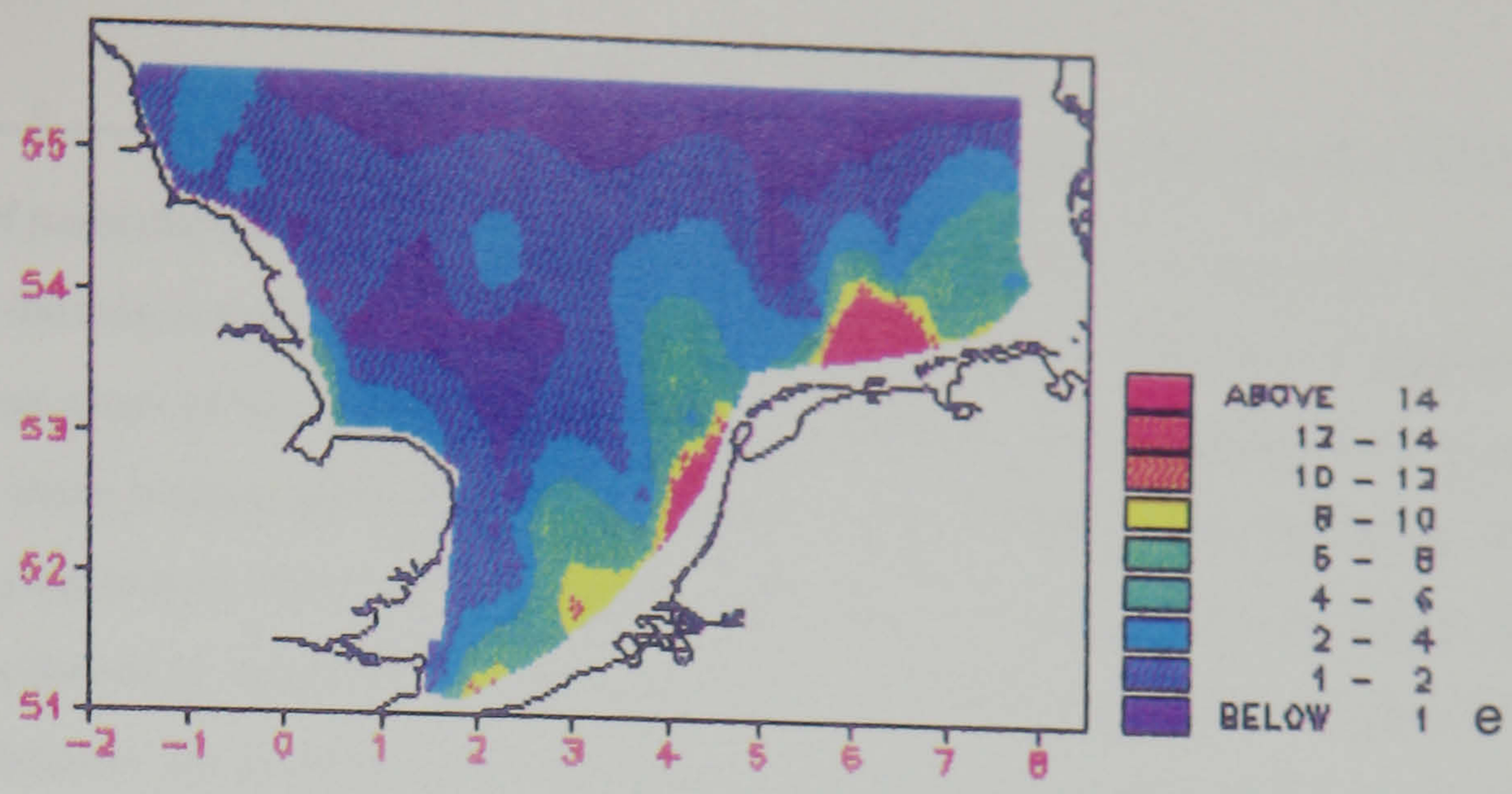

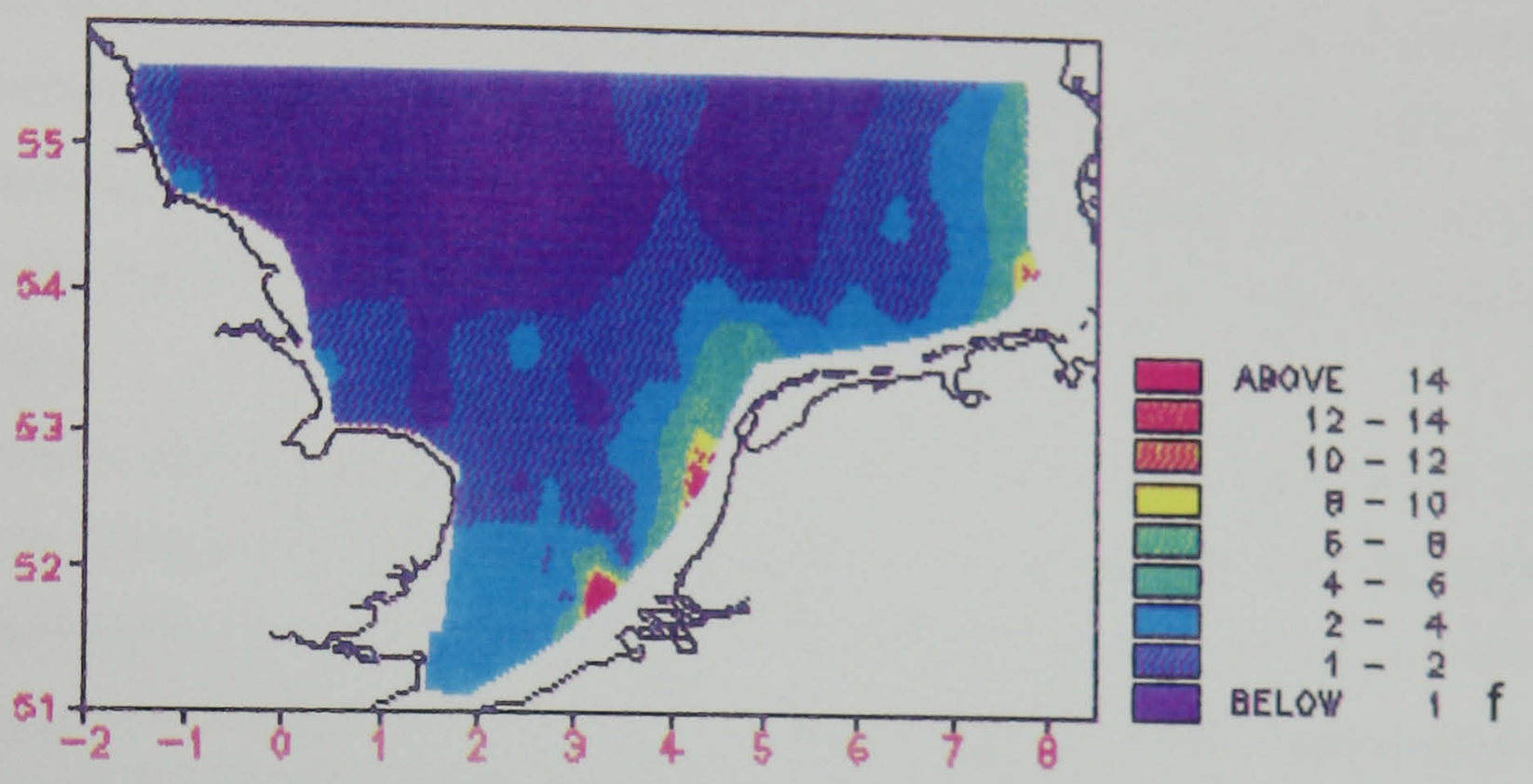

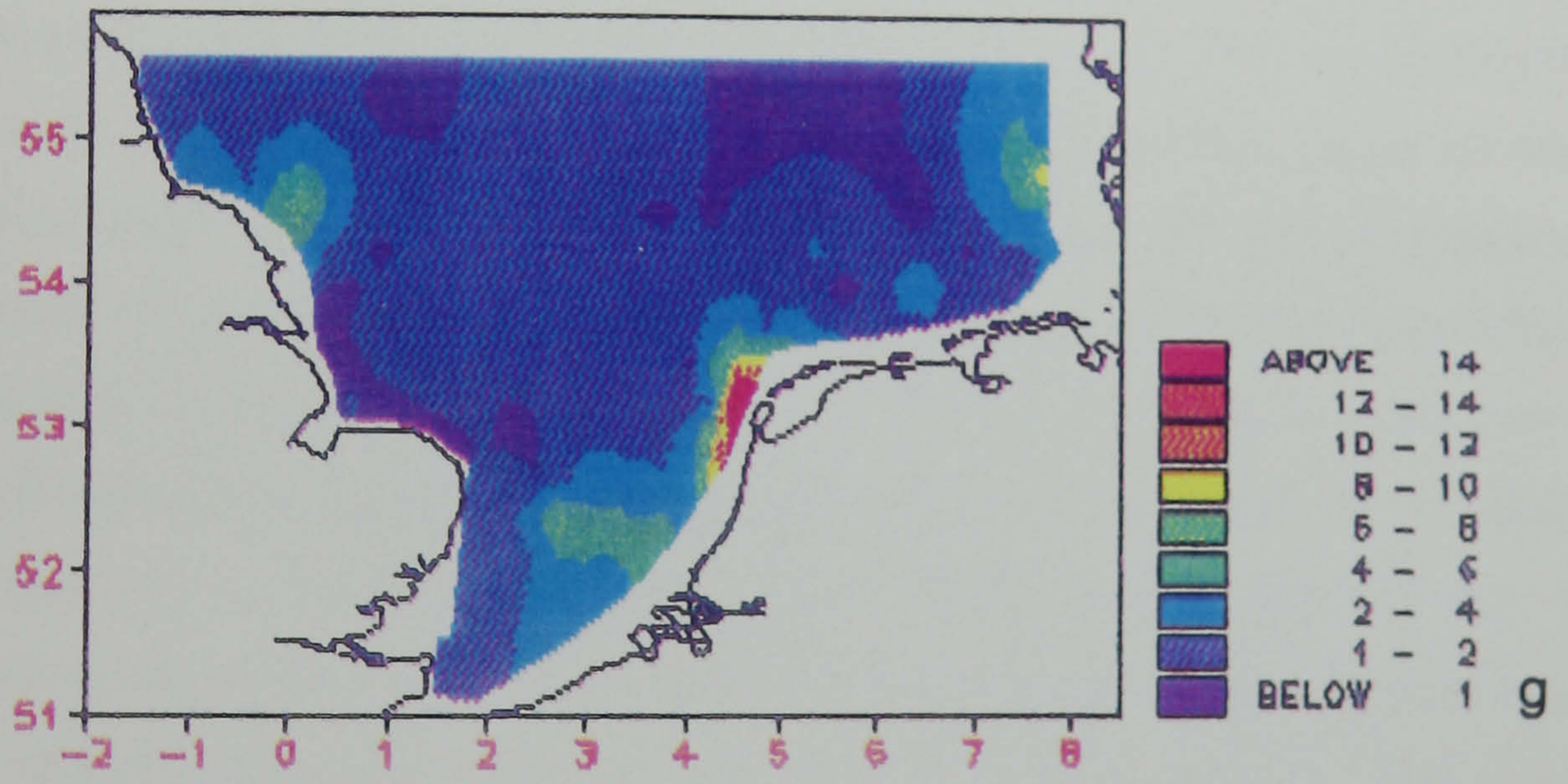

Figure 5.10 (cont/d): Distribution of Chlorophyll (mg m^{-3}) in the surface waters of the southern North Sea for (e) April-May 1989, (f) June-July 1989 and (g) September-October 1989.

Of particular interest is the high phytoplankton biomass that develops in the spring and early summer in the continental Europe coastal waters. During the winter of 1988/89 [*e.g.* Figures 5.10b and 5.10c], large areas of the survey region were characterized by concentrations of less than 1 mg m^{-3} except for some isolated and elevated concentrations in the central regions. By March 1989 [Figure 5.10d] phytoplankton biomass was increasing with some of the highest concentrations measured at 55.5°N. By the end of April [Figure 5.10e], very high phytoplankton biomass was found in the coastal waters of Belgium, the Netherlands and into the German Bight; concentrations were more than 6-8 mg m^{-3} over most of the eastern half of the southern North Sea. The high chlorophyll concentrations were associated with extensive blooms of *Phaeocystis pouchetii.* Over the same period and by contrast, the phytoplankton biomass in the English coastal region remained comparatively low except for some increases in chlorophyll concentration in the vicinity of the Humber, particularly in April-May, 1989 [Figure 5.10e].

Primary production rates also exhibited patterns similar to those of the chlorophyll concentrations. During the winter months, phytoplankton activity was very low in the southern areas of the survey region (typically less than 100 mgC $m^{-2}d^{-1}$) and the highest rates occurred in the central, northern region (*ca.* 500 mgC $m^{-2}d^{-1}$). By March, carbon fixation rates in the central region were more than 1 gC $m^{-2}d^{-1}$. In April and May, primary production increased along the continental European coast as the result of bloom formation; the highest rates of greater than 2.4 gC $m^{-2}d^{-1}$ occurred in the German Bight. As with the chlorophyll concentrations, the lowest rates were along the English coast.

The chlorophyll concentration measurements and estimates of carbon fixation rates indicate that the levels of primary production do have significant seasonal and regional effects on the composition of the suspended sediment in the southern North Sea. For example, during winter, organic contents were relatively low in all areas except for the central and northern parts where organic contents were high (greater than 40-50%). These high organic contents corresponded with relatively higher chlorophyll concentrations and production rates. Similarly, organic contents increased to levels well in excess of 50-60% in spring along the continental European coastline where the *Phaeocystis* blooms occurred. It is also significant that phytoplankton growth first increases in the central region of the North Sea, rather than in the southern regions where the *Phaeocystis* blooms occur. Along the English coast, organic contents were generally less than 30%. These were in accord with the low rates of production. However, organic matter concentrations and contents were frequently higher in the vicinity of the Humber and the North Yorkshire coast, and these corresponded to increases in chlorophyll concentration and primary production, particularly during the spring and summer months.

The spatial and temporal relationship between suspended sediment and primary production can also be demonstrated by seasonal scatter plots of mean chlorophyll versus mean TSM [Figure 5.11] for hydrographic stations located within the same ICES-based regions described in §5.1. The scatter plots display some basic relationships that have already been described. In particular they illustrate the underlying differences between the seasonal primary production and suspended sediment regimes of the western and eastern parts of the southern North Sea.

For the English coastal water stations of ICES Box 3, there were no correlations between chlorophyll and TSM for any of the seasons (best $r^2 = 0.37$). Although TSM concentrations attained high levels (20-30 mg l^{-1}), chlorophyll concentrations were typically less than 5 mg m^{-3}, except for isolated stations in the vicinity of the Humber (DQ during spring; Figure 5.11d) and the North Yorkshire coast (DG and DL during autumn; Figure 5.11b). The suspended sediment of this region of the southern North Sea is dominated by an inorganic component, as evident from the generally low organic contents, chlorophyll concentrations and primary production rates.

For the continental European waters of ICES Boxes 4 and 5, there were very good positive correlations ($r^2 = 0.86$ for each region) between chlorophyll and TSM in spring [Figure 5.11d]. Stations that were closer to the coastline (*e.g.* BO, BP, AG and AH) tended to have higher chlorophyll concentrations (in excess of 30 mg m^{-3}) and TSM concentrations (*ca.* 20 mg l^{-1}) than those stations further offshore. The suspended sediment of this region of the southern North Sea is dominated by a spring organic component as evident from the high organic contents, chlorophyll concentrations and primary production rates. The organic component also dominates throughout the summer to early autumn because of persistently high phytoplankton activity [as suggested by Figures 5.10a, 5.10f and 5.10g]. However in winter [Figure 5.11c], there was no correlation between chlorophyll and TSM owing to the seasonal decline of primary production during which time the suspended sediment becomes dominated by an inorganic component.

The reasons for the regional and seasonal differences in the composition of the suspended sediment between the English coastal and continental European waters are related to the different levels of primary production in each region. According to estimates of the annual primary productivity in the southern North Sea [Joint and Pomroy, 1992; Howarth *et al.*, 1993], continental European waters are about 2-3 times more productive than English coastal waters. The higher production off the continental European coast is related to a variety of factors, including higher chlorophyll and nutrient concentrations, more favourable stratification (especially haline) and tidal mixing conditions, and more favourable optical conditions than in English waters [Tett *et al.*, 1993].

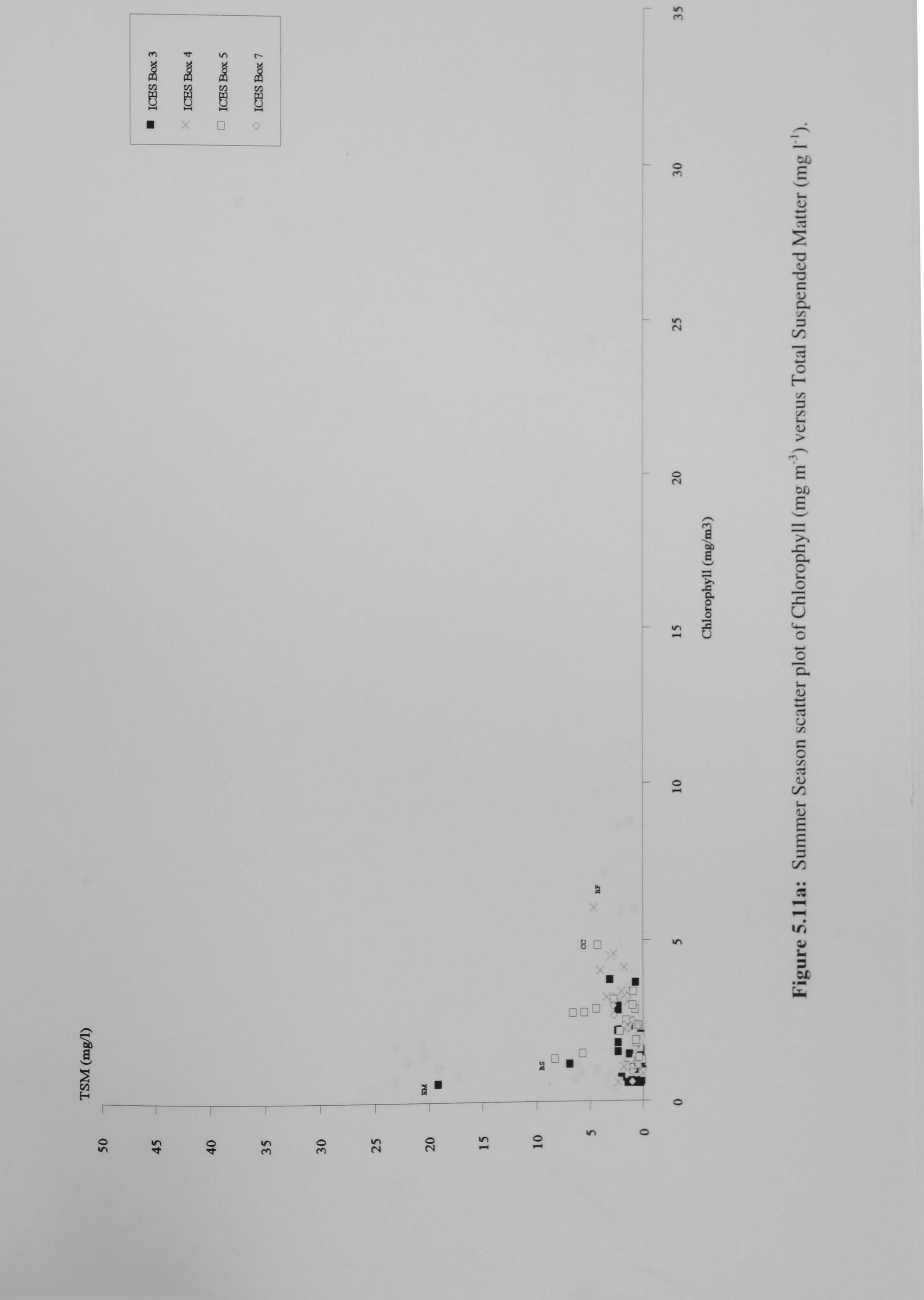

Figure 5.11a: Summer Season scatter plot of Chlorophyll

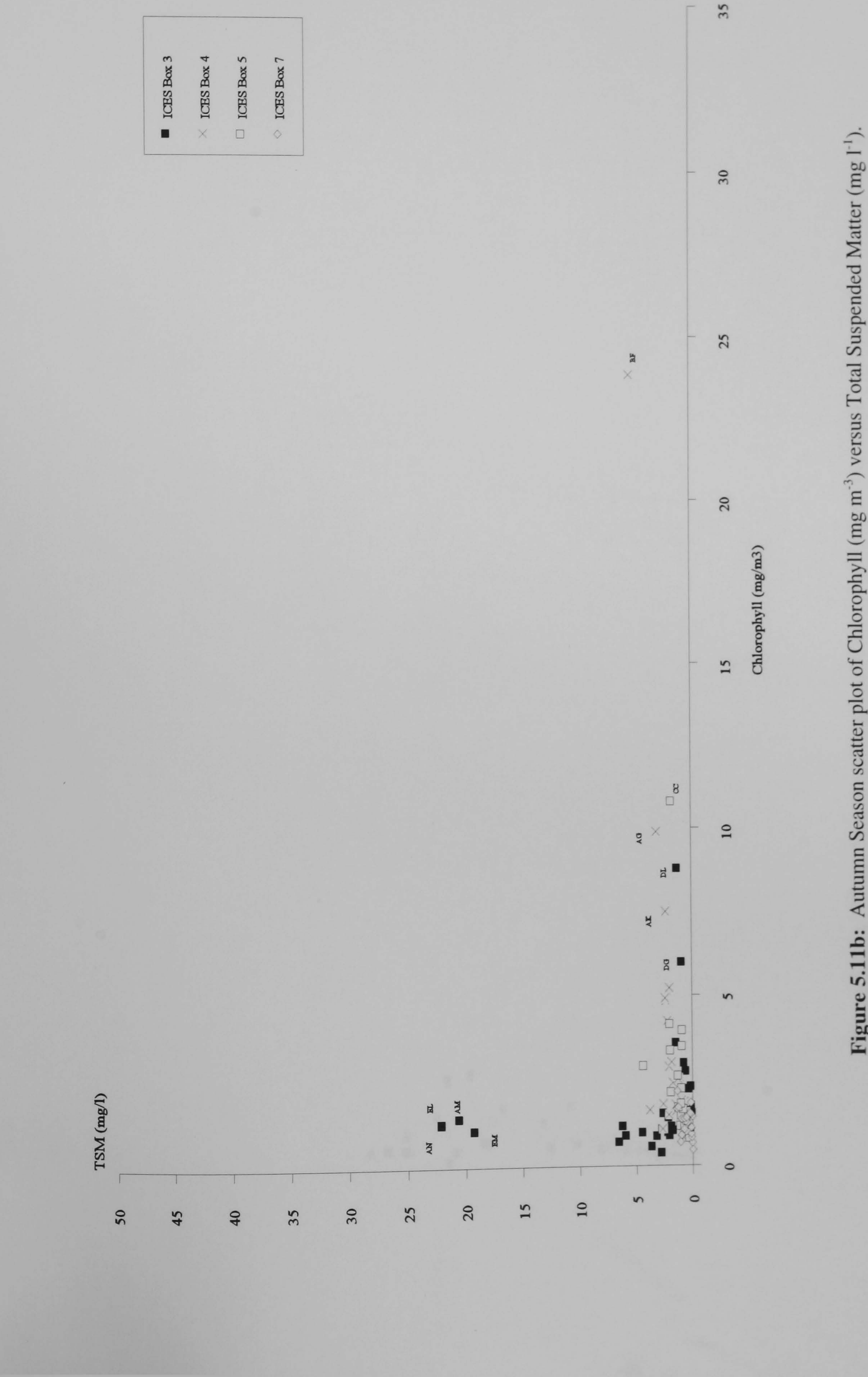

Figure 5.11b: Autumn Season scatter plot of Chlorophyll (mg m^{-3}) versus Total Suspended Matter (mg l^{-1}).

Figure 5.11c: Winter Season scatter plot of Chlorophyll (mg m^{-3}) versus Total Suspended Matter (mg l^{-1}).

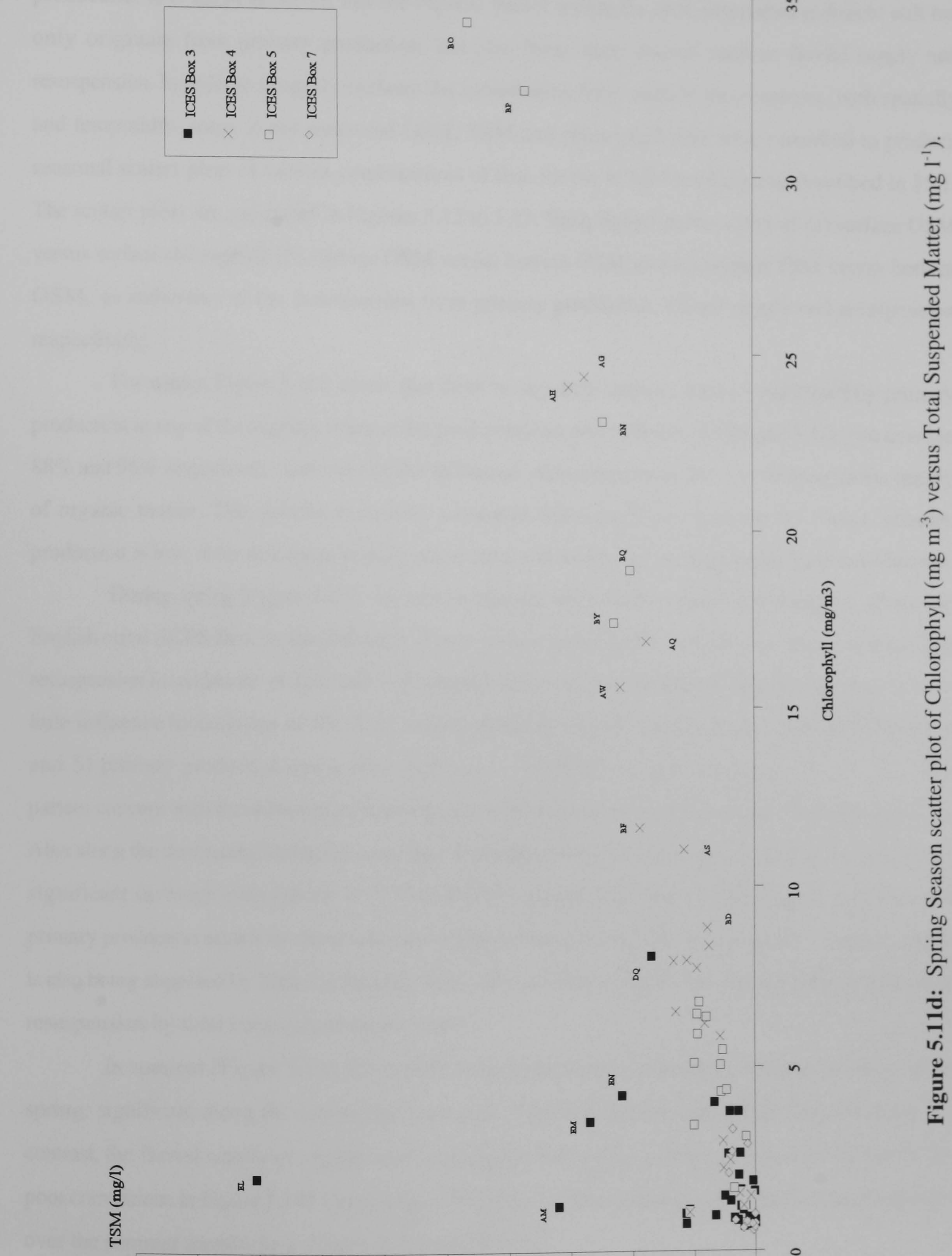

Figure 5.11d: Spring Season scatter plot of Chlorophyll (mg m^{-3}) versus Total Suspended Matter (mg l^{-1}).

5.5 Primary Production, Fluvial Supply and Resuspension

Section 5.4 describes the basic relationships between the suspended sediment distributions and primary production. It is likely however, that the organic matter within the total suspended sediment will not only originate from primary production, but also from other sources such as fluvial supply and resuspension. In order to properly evaluate the contribution from each of these sources, both spatially and temporally, some of the measured OSM, TSM and chlorophyll data were reworked to produce seasonal scatter plots of various combinations of data for the ICES-based regions described in §5.1. The scatter plots are presented in Figures 5.12 to 5.15. Each figure shows a plot of (a) surface OSM versus surface chlorophyll, (b) surface OSM versus bottom OSM and (c) bottom TSM versus bottom OSM; as indicative of the contributions from primary production, fluvial supply and resuspension respectively.

For winter, Figure 5.12a shows that there is very little organic matter contributed by primary production in any of the regions, whereas the good correlations in Figures 5.12b and 5.12c (on average 88% and 96% respectively) indicate that fluvial sources and resuspension are contributing to the supply of organic matter. This pattern is entirely consistent with conditions expected for winter: primary production is low, river discharge is high and storms and waves are stirring up the bottom sediments.

During spring [Figure 5.13], the pattern changes with distinct regional differences. Along the English coast (ICES Box 3), the dominant organic matter contribution comes from fluvial sources and resuspension (correlations of 88% and 91% respectively) whereas primary production appears to have little influence (correlation of 4%) By contrast, along the continental European coast (ICES Boxes 4 and 5) primary production has a more significant contribution (63% correlation on average). This pattern concurs with the different production rates between the two coastal regions described in §5.4. Also along the continental European coast the contribution from fluvial supply and resuspension is also significant (average correlations of 77% and 82% respectively). This would suggest that although primary production attains its maximum rates along this coast during the spring months, organic matter is also being supplied by high discharging rivers like the Rhine, the Weser and the Elbe, and through resuspension by tidal currents and storm events.

In summer [Figure 5.14], the contribution from primary production is much the same as for spring: significant along the continental European coast and insignificant off the English coast. By contrast, the fluvial supply of organic matter along the European coast has declined, as shown by the poor correlations in Figure 5.14b (on average 13%). This is consistent with a decline in river discharges over the summer months [*e.g.* Figure 5.7 for the Rhine].

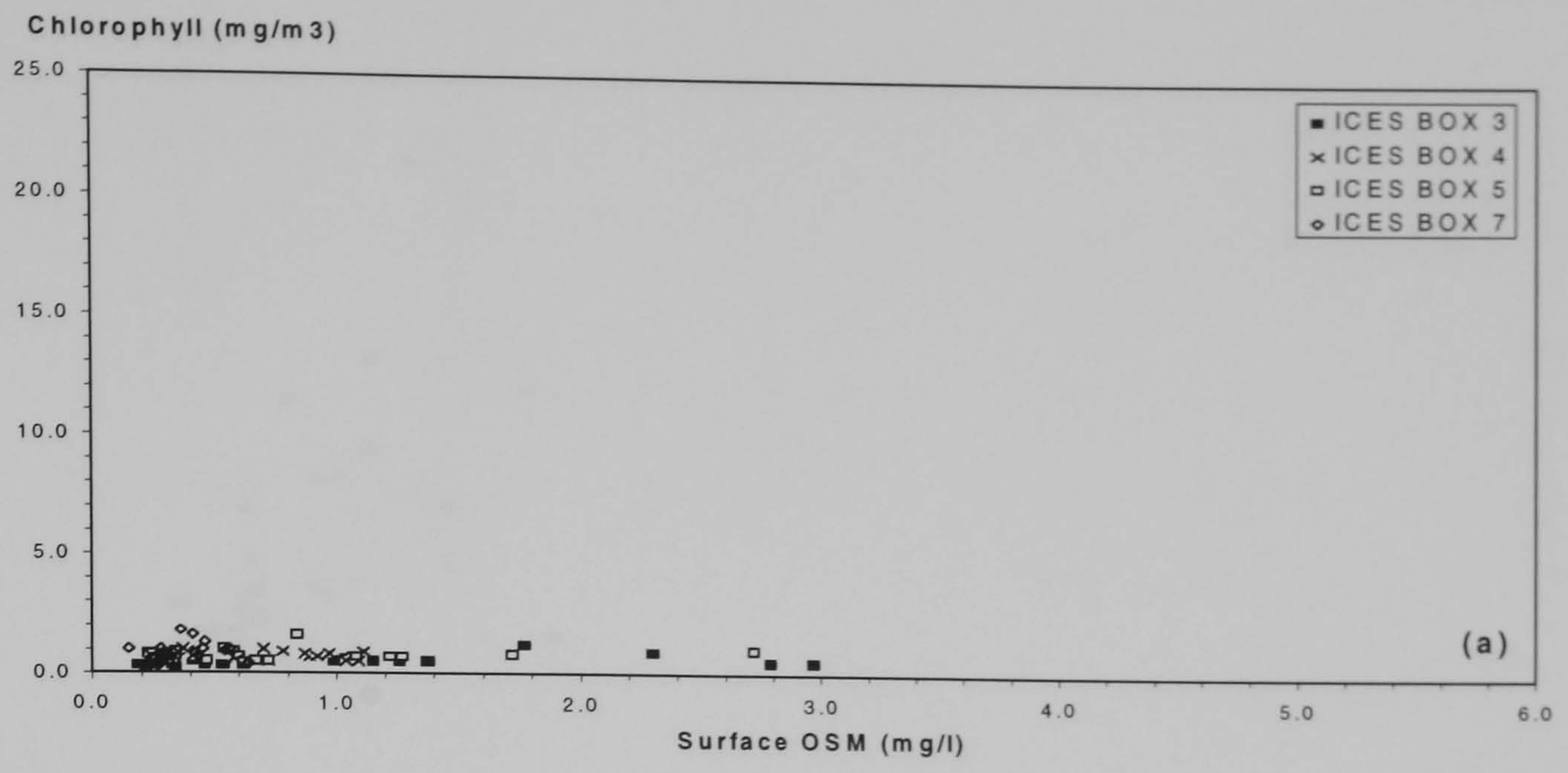

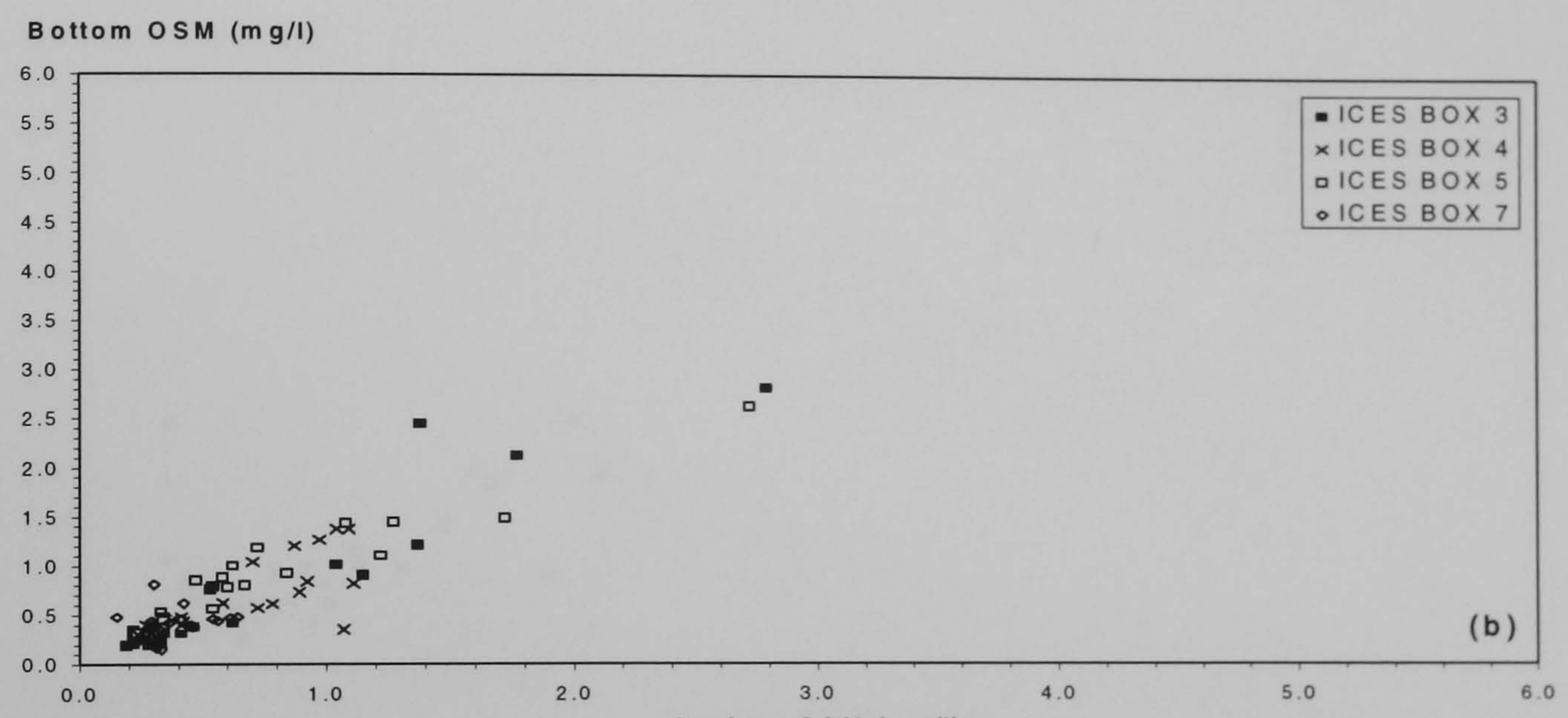

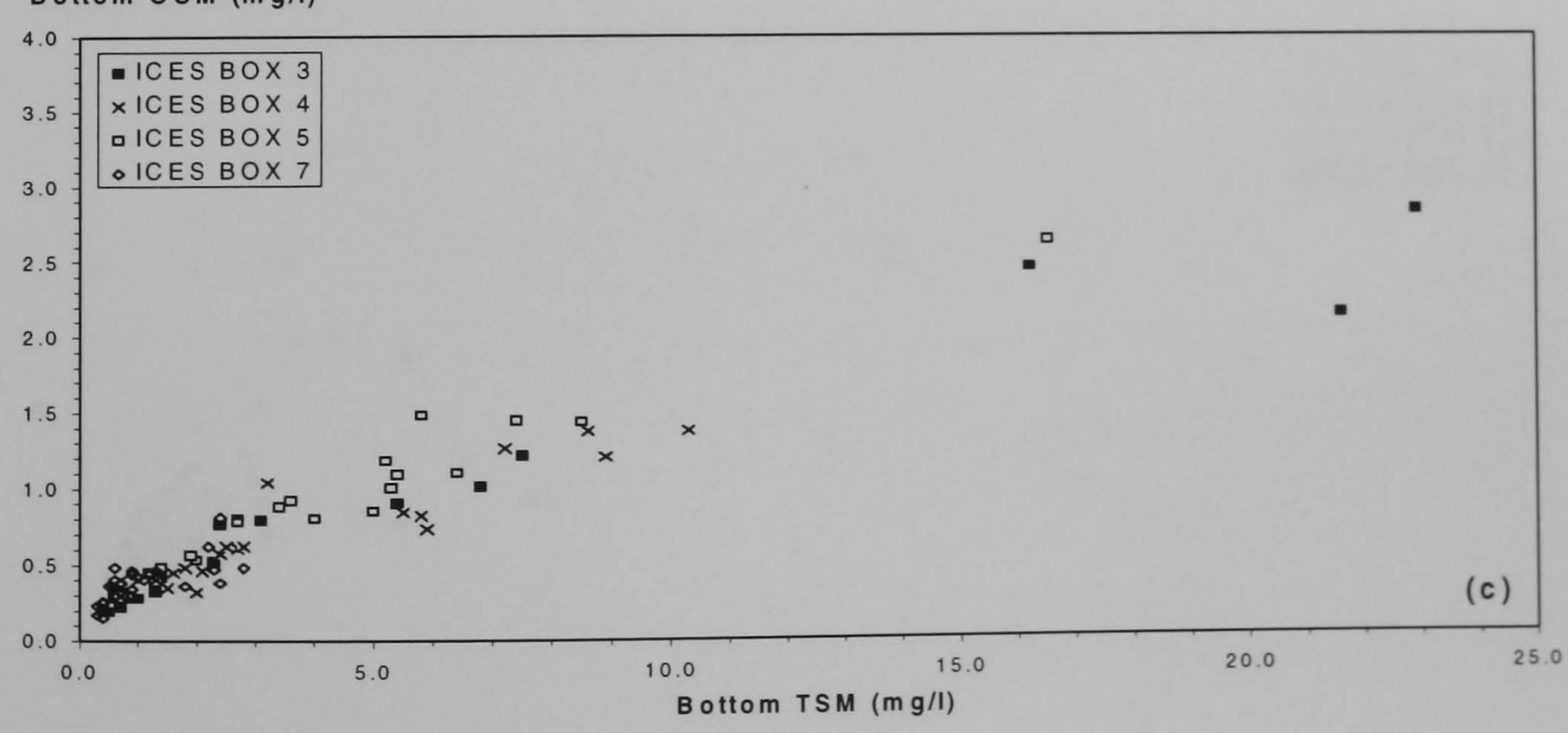

Figure 5.12: Winter season scatter plots of (a) surface organic matter (mg l^{-1}) versus chlorophyll (mg m^3), (b) surface organic matter versus bottom organic matter (in mg l^{-1}) and (c) bottom total suspended matter versus bottom organic matter (in mg l^{-1}).

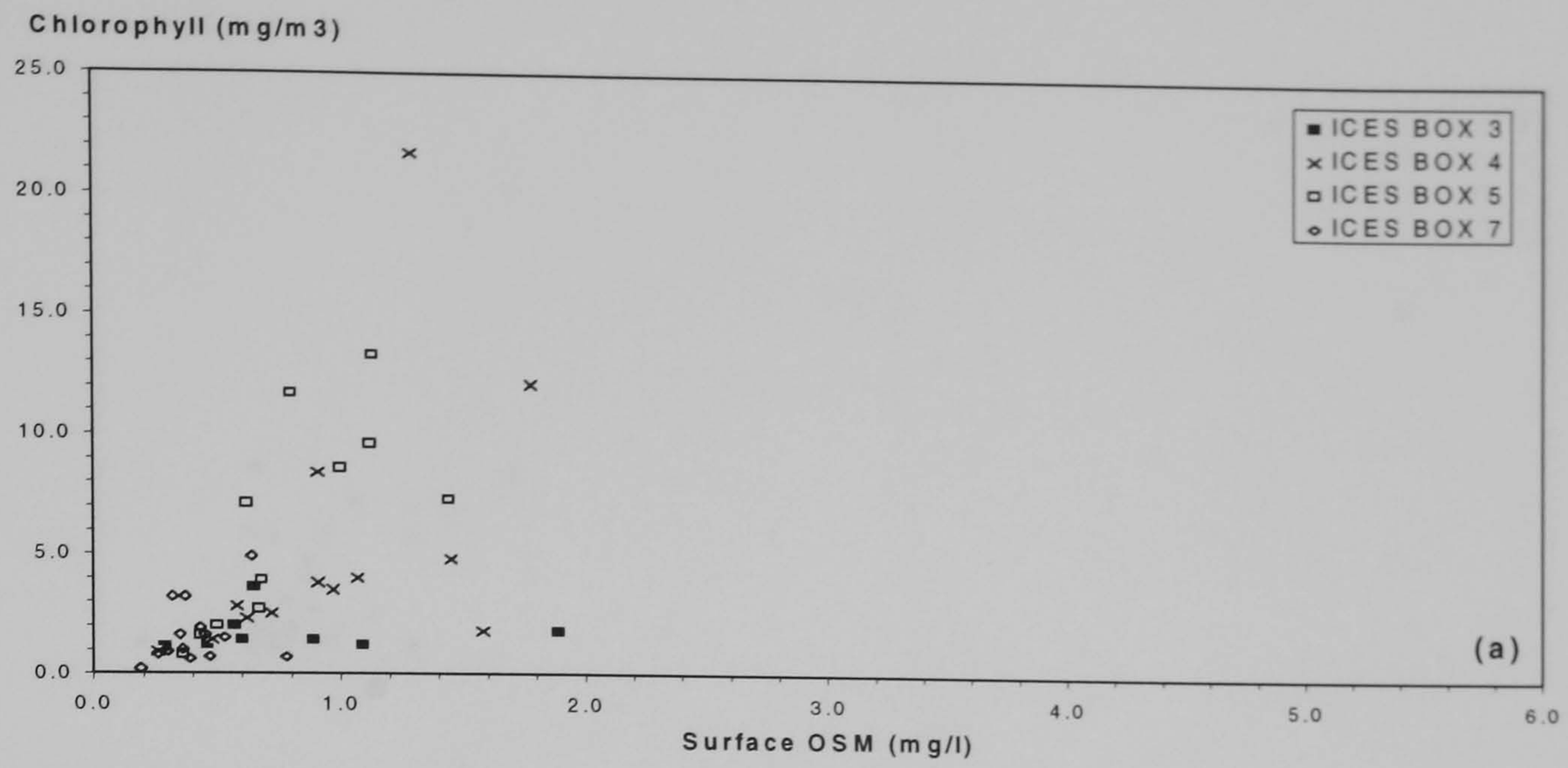

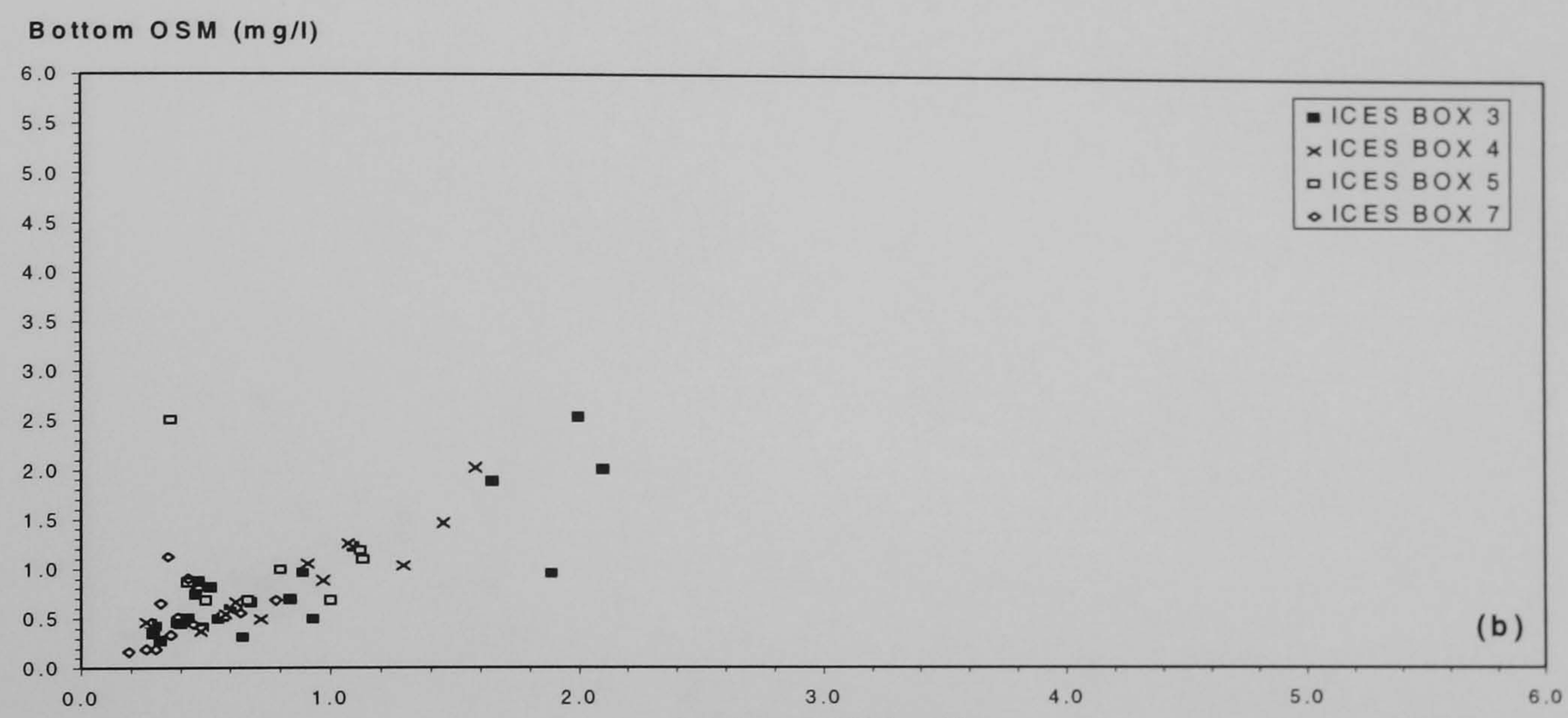

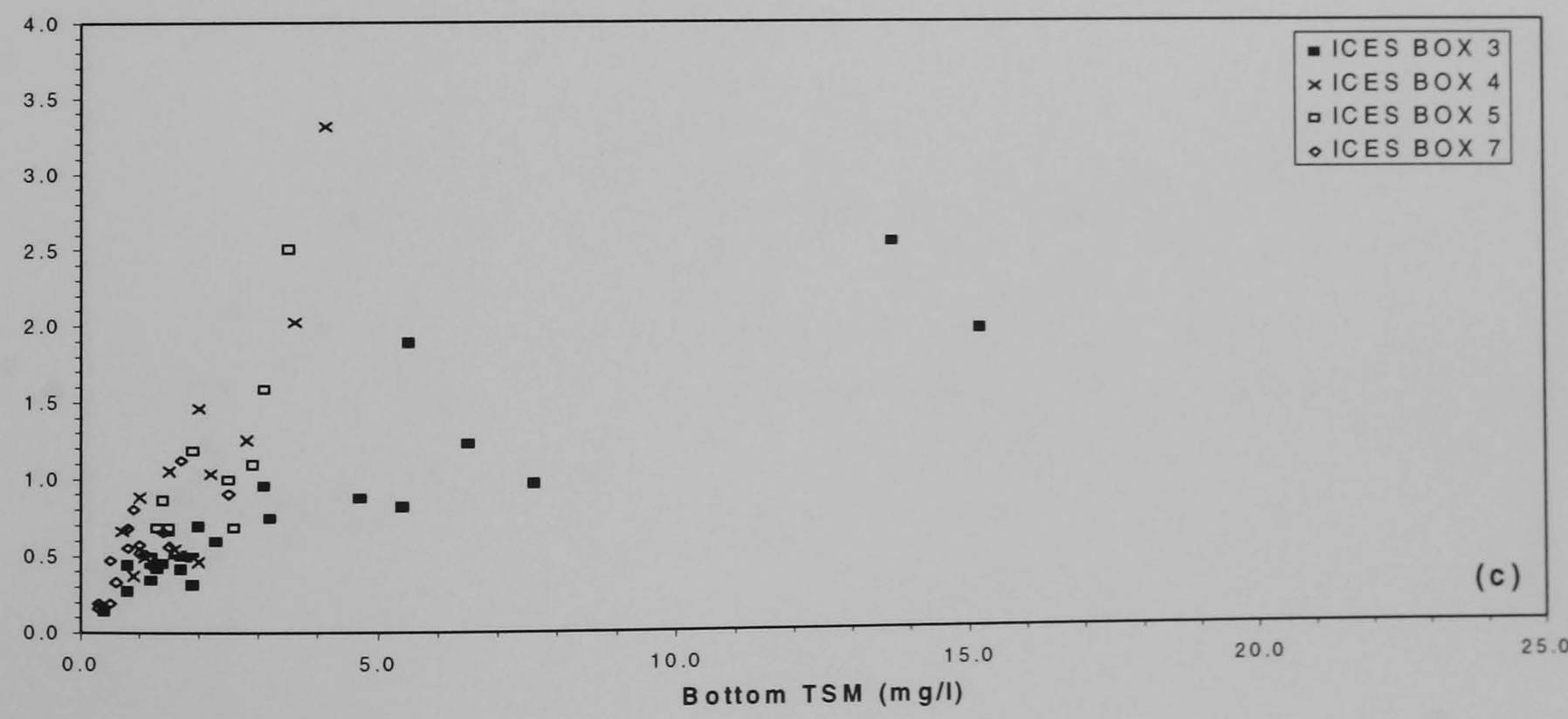

Figure 5.13: Spring season scatter plots of (a) surface organic matter (mg l^{-1}) versus chlorophyll (mg m^3), (b) surface organic matter versus bottom organic matter (in mg l^{-1}) and (c) bottom total suspended matter versus bottom organic matter (in mg l^{-1}).

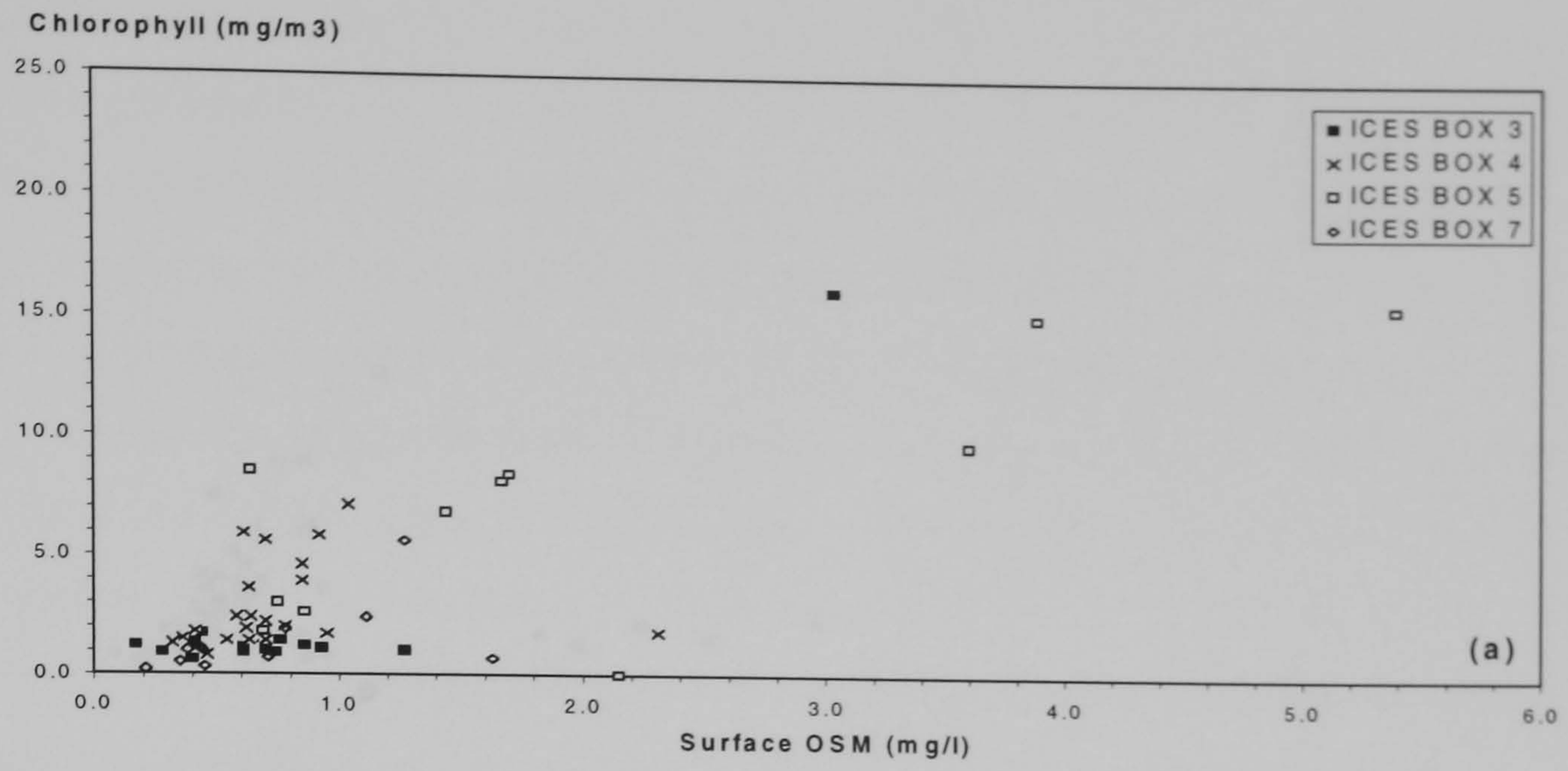

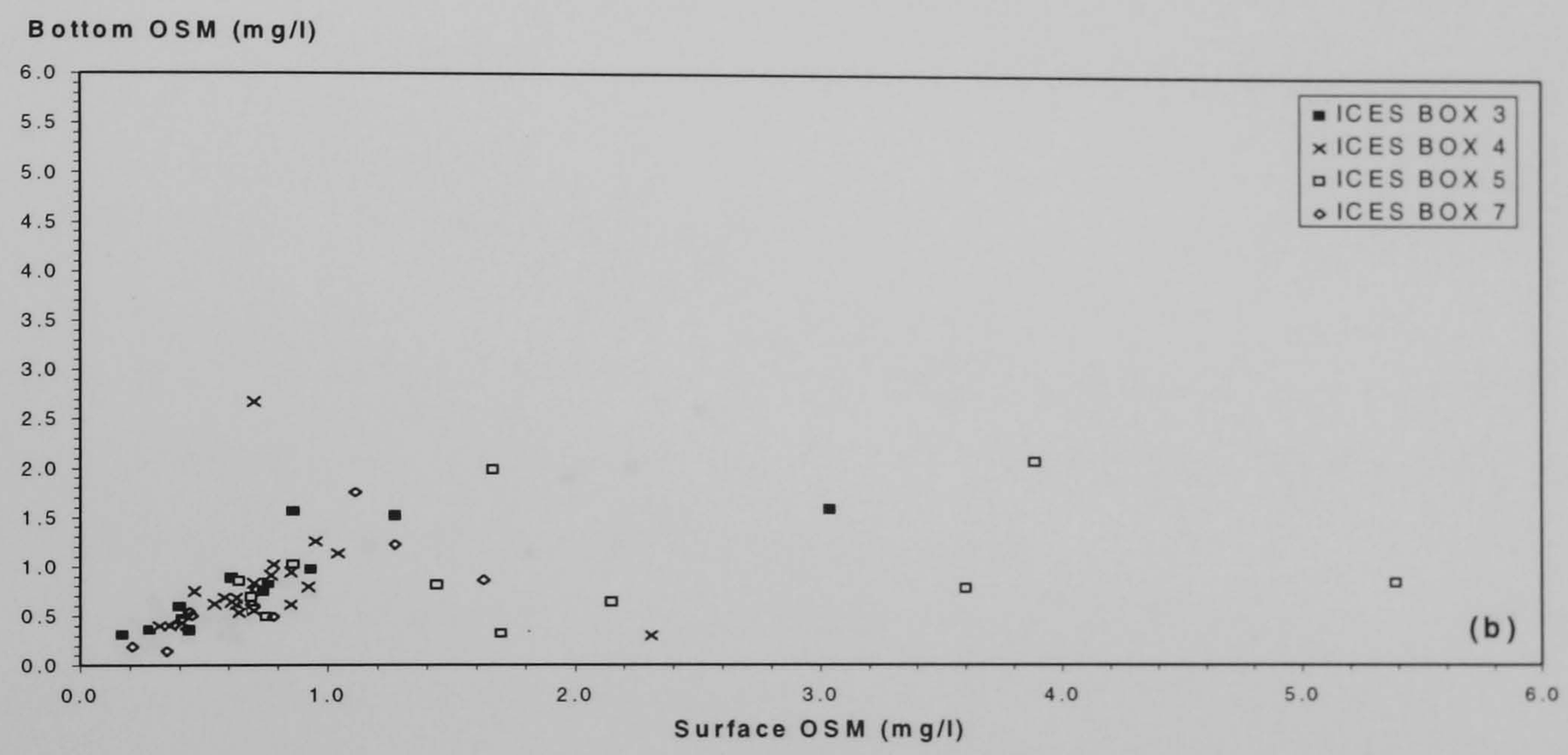

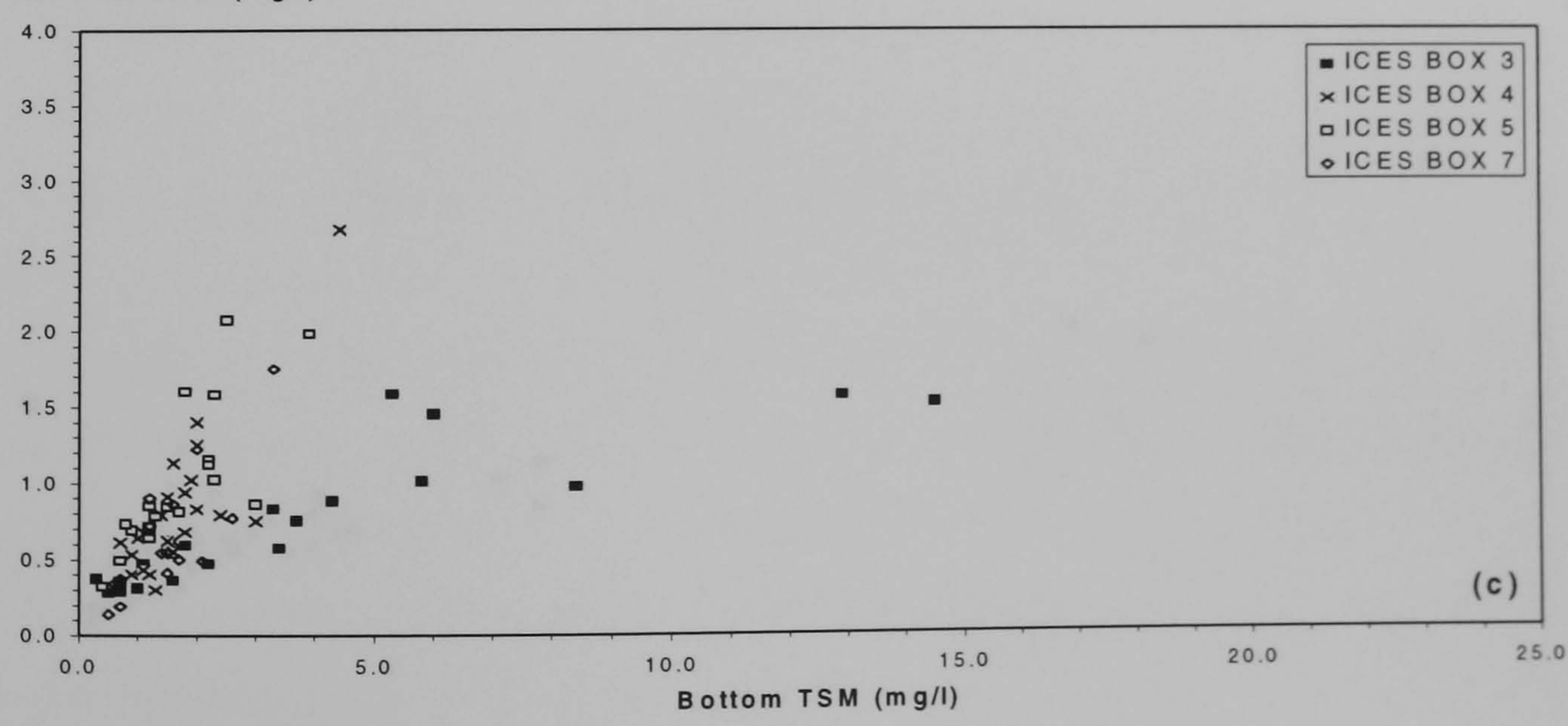

Figure 5.14: Summer season scatter plots of (a) surface organic matter (mg l^{-1}) versus chlorophyll (mg m^3), (b) surface organic matter versus bottom organic matter (in mg l^{-1}) and (c) bottom total suspended matter versus bottom organic matter (in mg l^{-1}).

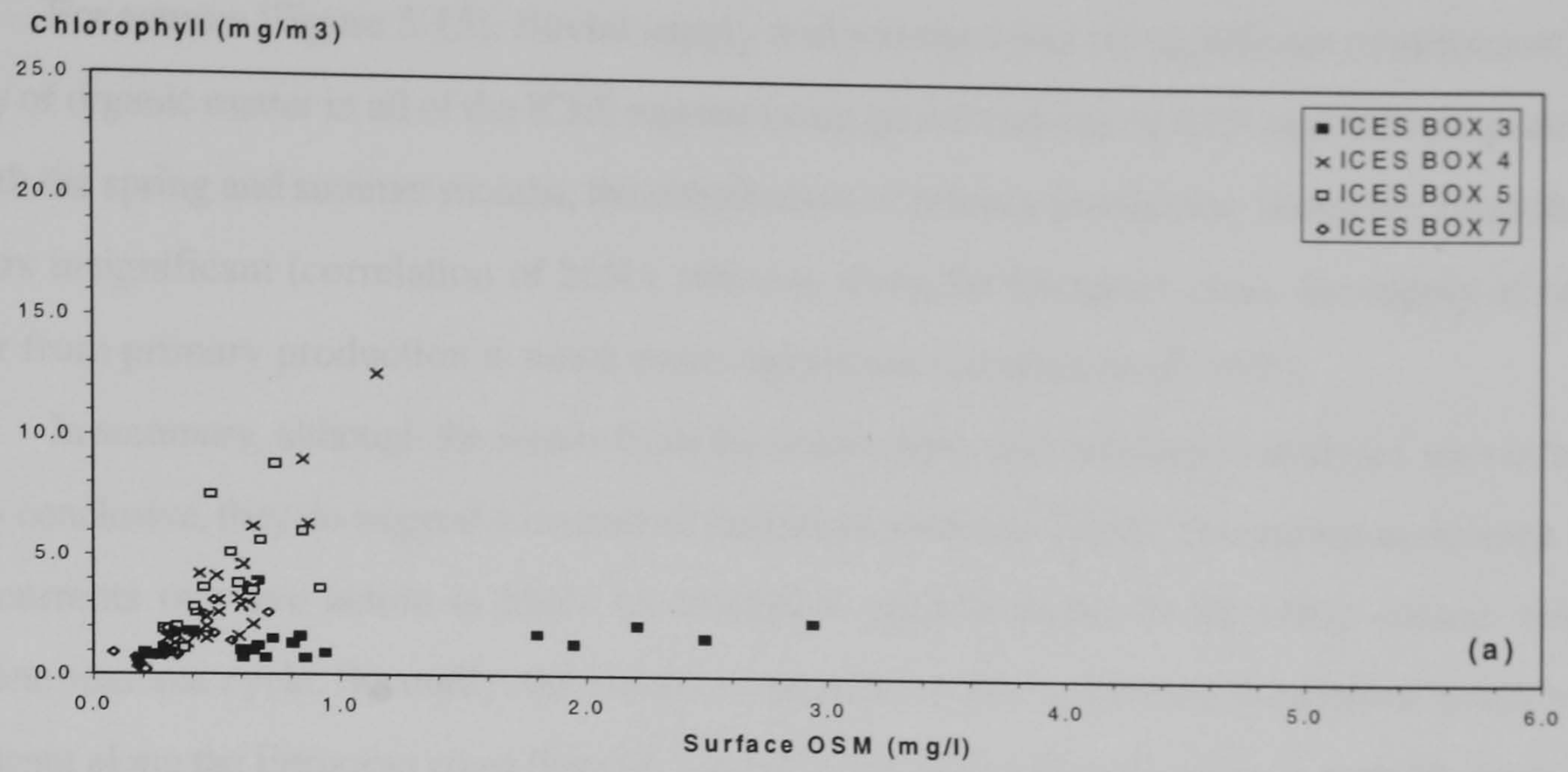

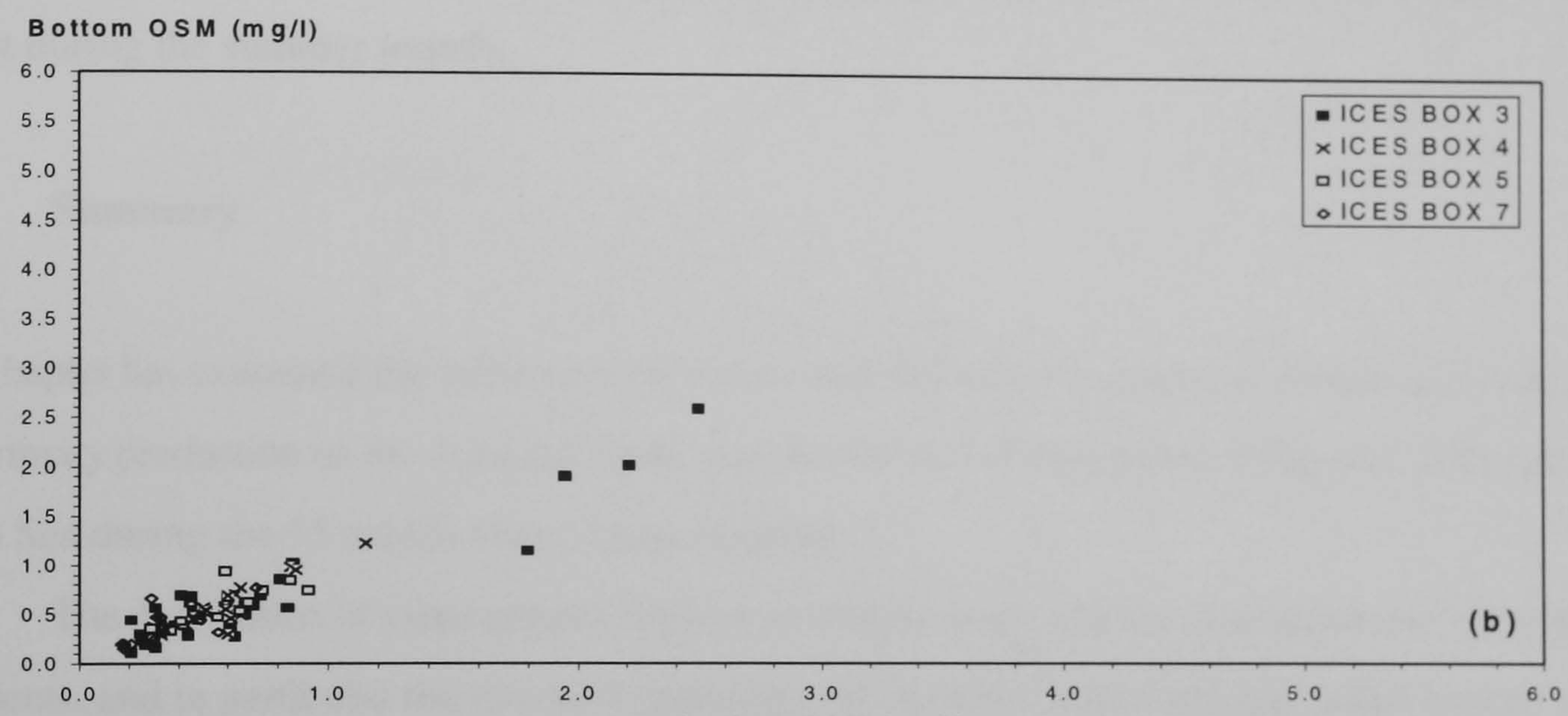

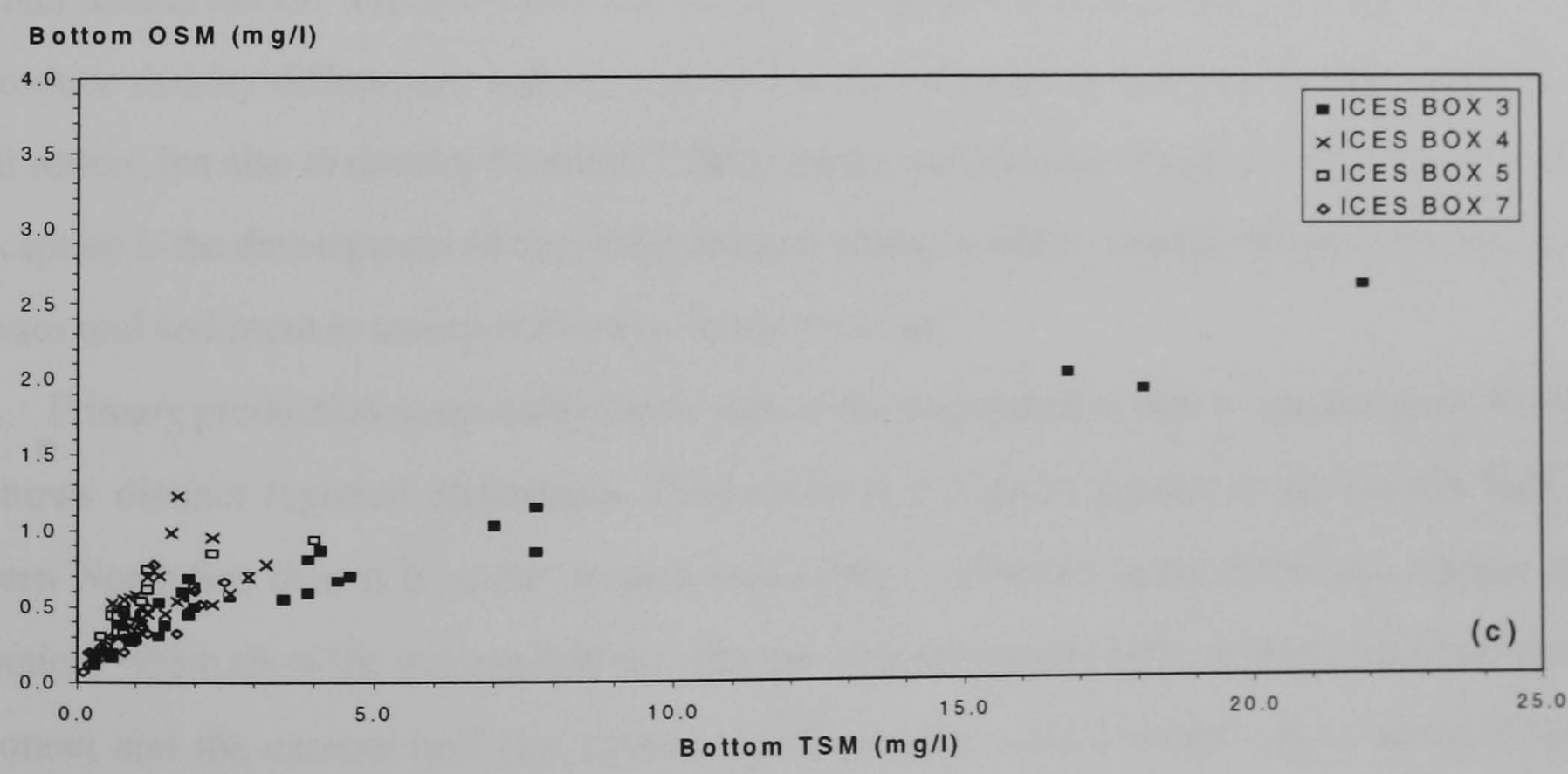

Figure 5.15: Autumn season scatter plots of (a) surface organic matter (mg l^{-1}) versus chlorophyll (mg m^3), (b) surface organic matter versus bottom organic matter (in mg l^{-1}) and (c) bottom total suspended matter versus bottom organic matter (in mg l^{-1}).

For autumn [Figure 5.15], fluvial supply and resuspension are significant contributors to the supply of organic matter in all of the ICES regions (average correlations of 85% and 80% respectively). As with the spring and summer months, the contribution of primary production along the English coast appears insignificant (correlation of 26%), whereas along the European coast, the supply of organic matter from primary production is much more significant (correlation of 75%).

In summary, although the results from the scatter plots and correlation analyses are not by any means conclusive, they do suggest a number of important patterns. Firstly, resuspension through either tidal currents or wave action is likely to contribute organic matter to the water column over the complete seasonal cycle. Secondly, the supply of organic matter by primary production is much more significant along the European coast than the English coast, where fluvial supply is a major source over the seasonal cycle. Along the European coast fluvial supply is an important source of organic matter except during the summer months.

5.6 Summary

This chapter has examined the influences of water mass interactions, haline and thermal stratification and primary production on the seasonal cycle and distribution of suspended sediments in the southern North Sea during the 15 month observational period.

The distribution of water masses explains at a basic level, the broad distribution of suspended sediments, and in particular the general partitioning of the more turbid and less saline coastal waters from the waters of Atlantic origin further offshore. Interactions between the fresh water sources from rivers and coastal run-off with the saline sources through the Dover Straits and from the northern North Sea produce density differences and associated circulation patterns that tend to trap sediment in the coastal waters, but also to develop localised TSM minima, particularly at times of high river discharge. An exception is the development of the plume because strong residual currents break down the trapping processes and sediment is transported away from the coast.

Primary production temporarily forms part of the suspended matter in the southern North Sea, and shows distinct regional differences. Production is 2-3 times greater in the eastern half of the southern North Sea than it is in the western half. This is reflected in the TSM and organic content distributions which show the western half (*i.e.* English coastal waters) to be dominated by an inorganic component and the eastern half (*i.e.* continental European coastal waters) by a spring-to-autumn organic component. Organic matter is supplied not only from primary production but also from fluvial supply and resuspension. Stratification also encourages primary production, creating higher organic contents in the surface waters than in the bottom waters, except in locations where strong currents stir the water column.

FLUXES OF SUSPENDED MATTER
The East Anglian Plume

Chapter 3 described the seasonal cycle of the TSM distributions during the 15 month survey period These distributions showed a persistent high turbidity zone off East Anglia, together with the seasonal development of an associated plume eastwards from East Anglia (herein called the East Anglian plume) which was most prominent during the winter. The following chapter examines firstly, the plume in relation to modelled residual current patterns and wind stress vectors for the survey period; secondly, it presents estimates of suspended sediment fluxes within the plume; and thirdly, it compares the fluxes with published sediment budgets for eastern England.

6.1: Residual Circulation

The East Anglian plume appears to be a significant transport path for suspended sediment across the Southern Bight towards the German Bight. This transport path would seem to fit well into the general pattern of suspended sediment transport which is driven by the residual circulation of the North Sea in a general anticlockwise gyre [§1.3].

The residual circulation is affected by the wind direction and speed, and it has been revealed by, for example, drifter measurements [Ramster, 1965; Lee and Ramster, 1968] and numerous mathematical modelling studies. Davies [1983b] applied a 3-dimensional model with tidal and meteorological forcing. The surface currents in the winter were considerably stronger in the summer, due to the seasonal variation in winds, and were of the order 6 cm s^{-1}. The tidal mean currents in the absence of wind were essentially the same as in the southern North Sea, and in the plume area the tidal residual was of the order of 4 cm s^{-1}. Backhaus and Maier-Reimer [1983] also compared baroclinic and barotropic models of the North Sea. They found that in the unstratified Southern Bight there was very little difference between the calculated residual circulations, and that strong eastward residuals occurred in the region of the plume. They tested their models with mean August and March winds, both of which gave strong eastward flow in the plume position. The response of the wind was also tested by Dolata *et al.* [1983]. They found that westerly and north-westerly winds distributed over the whole North Sea produced an anti-clockwise residual circulation. However, a north-westerly wind confined to the eastern North Sea created a clockwise circulation.

From these numerous studies it is apparent that the residual circulation is responsive to the wind field, and it is likely that the transport of suspended sediment will vary in intensity seasonally as well as over shorter time-scales. With respect to the regional wind field conditions during the survey

period, wind stress vectors at 3 hourly intervals derived from the Meteorological Office atmospheric model covering the north-west European shelf were weekly-averaged for the study area [J.E. Jones, *pers. comm.*].These showed three basic situations to have been present:

- variable winds, but with periods of moderate south-westerly winds, typically the autumn and spring periods (*i.e.* September/October 1988 and April/May 1989);
- strong south-westerly winds present over the winter (*i.e.* December 1988-March 1989);
- weak and variable winds during the summer (*i.e.* June/July 1989).

The residual circulation of the North Sea was derived from the model of Flather *et al.* [1991]. This is a depth-averaged 2-D barotropic model covering the north-west European shelf with a resolution of ~ 35km. The model is driven by tidal forcing along its open boundaries and by spatially varying winds and atmospheric pressures at hourly intervals obtained from the Meteorological Office fine grid weather prediction model. The output comprises tidal and surge currents which were averaged over twenty five hours to give daily means [Proctor and Smith, 1991]. These daily means were then averaged to give monthly-mean distributions of the residual circulation for the fifteen months of the survey period.

Comparisons between the modelled data and the results from three current meter sites [namely A, C and F; Figure 6.1] showed good agreement between the data in the winter months, with some discrepancies in the summer, particularly in the northern stratified region (site A), where density differences influenced the vertical current structure. Computed correlation coefficients were high in the winter months (*e.g.* 0.79-0.89 for the easterly components and 0.87-0.93 for the northerly components at site F) and lower in the summer months; although the differences were less in the well mixed southern North Sea (*e.g.* 0.36-0.99 for the easterly components and 0.59-0.93 for the northerly components at site F). Therefore, the modelled mean currents are a good representation of the observed residual currents.

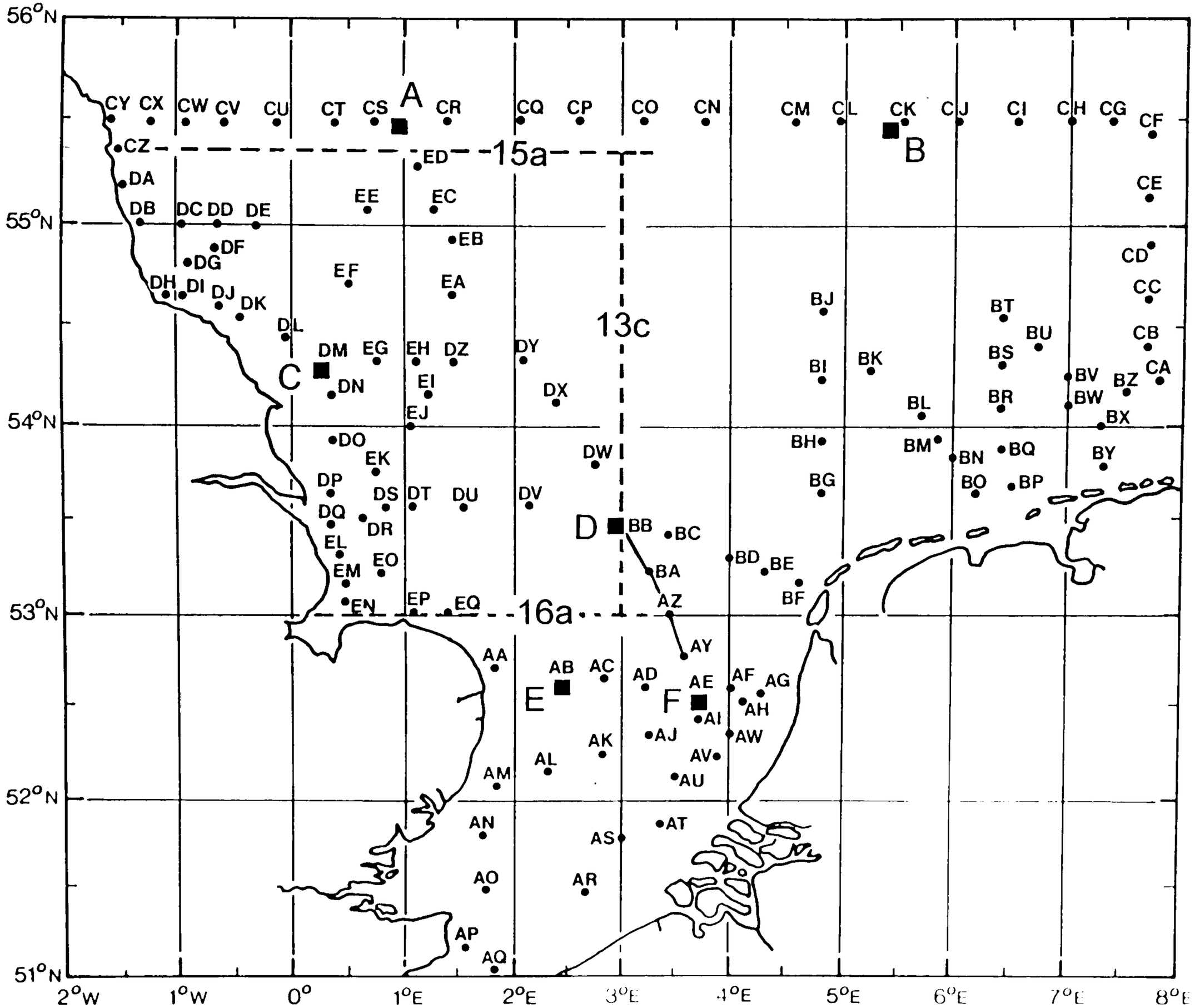

Figure 6.1: Map showing the hydrographic stations (circles), the sites of the current meter moorings (squares), the flux sections of Proctor and Smith [1991] (dashed lines), and the cross-sectional transect AY to BB (solid line).

The residual circulation for September 1988 is shown in Figure 6.2a and this is typical of a period with moderate south-westerly winds. There is a strong anti-clockwise circulation in the central area of the southern North Sea. A strong eastwards flow across the central part creates a northward coastal current flowing along the Dutch, German and Danish coasts. This flow is assisted by a northward flow through the Dover Straits and the Southern Bight.

For the winter period of strong south-westerly winds, typified by December 1988 in Figure 6.2b, a more complex residual flow field exists, with several gyres in the central area of the southern North Sea, a weaker northward current along the continental coast, and gyres developing in the German and Southern Bights. However, a significant feature of this circulation situation is a continued strong eastward residual current from East Anglia to the northern Dutch coast.

For the summer period of light winds, typified by June 1989 in Figure 6.2c, a complex circulation exists in the northern part of the southern North Sea. There is a strong southward flow down the Danish coast and along the German coast. Additionally there is a clockwise gyre off the Dutch coast, and anti-clockwise gyres off the English coast. The summer situation is likely to be affected by the presence of thermal stratification and a front which develops across the southern North Sea in the region of 54°N.

In addition to the daily means of residual currents, Proctor and Smith [1991] show the daily mean and monthly mean volumetric fluxes for the surge, or non-tidal component across various cross-sections in the North Sea. Those sections relevant to the southern North Sea (sections 13c, 15a and 16a) are shown in Figure 6.1, and are of interest, since they define a box against the English coast, with section 13c crossing the plume. The calculated monthly mean volume fluxes across the sections are shown in Figure 6.3. The fluctuations correspond with the seasonal wind patterns. It is apparent also that there is a good correlation between the southward flow across the northerly section (section 15a) and the eastward flow across the North Sea through section 13c.

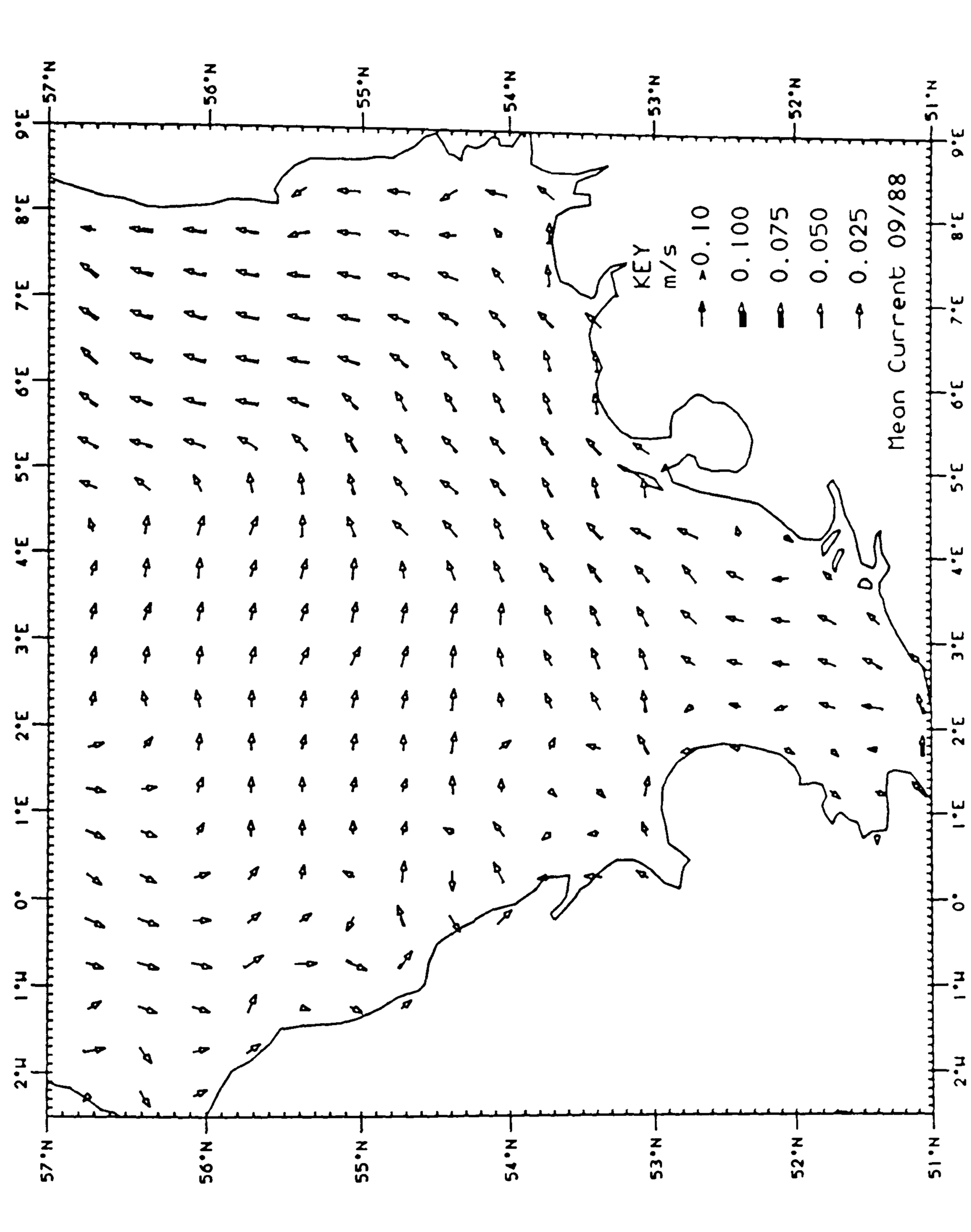

Figure 6.2a: Plot showing the calculated residual flows (m s^{-1}) of the southern North Sea for September 1988

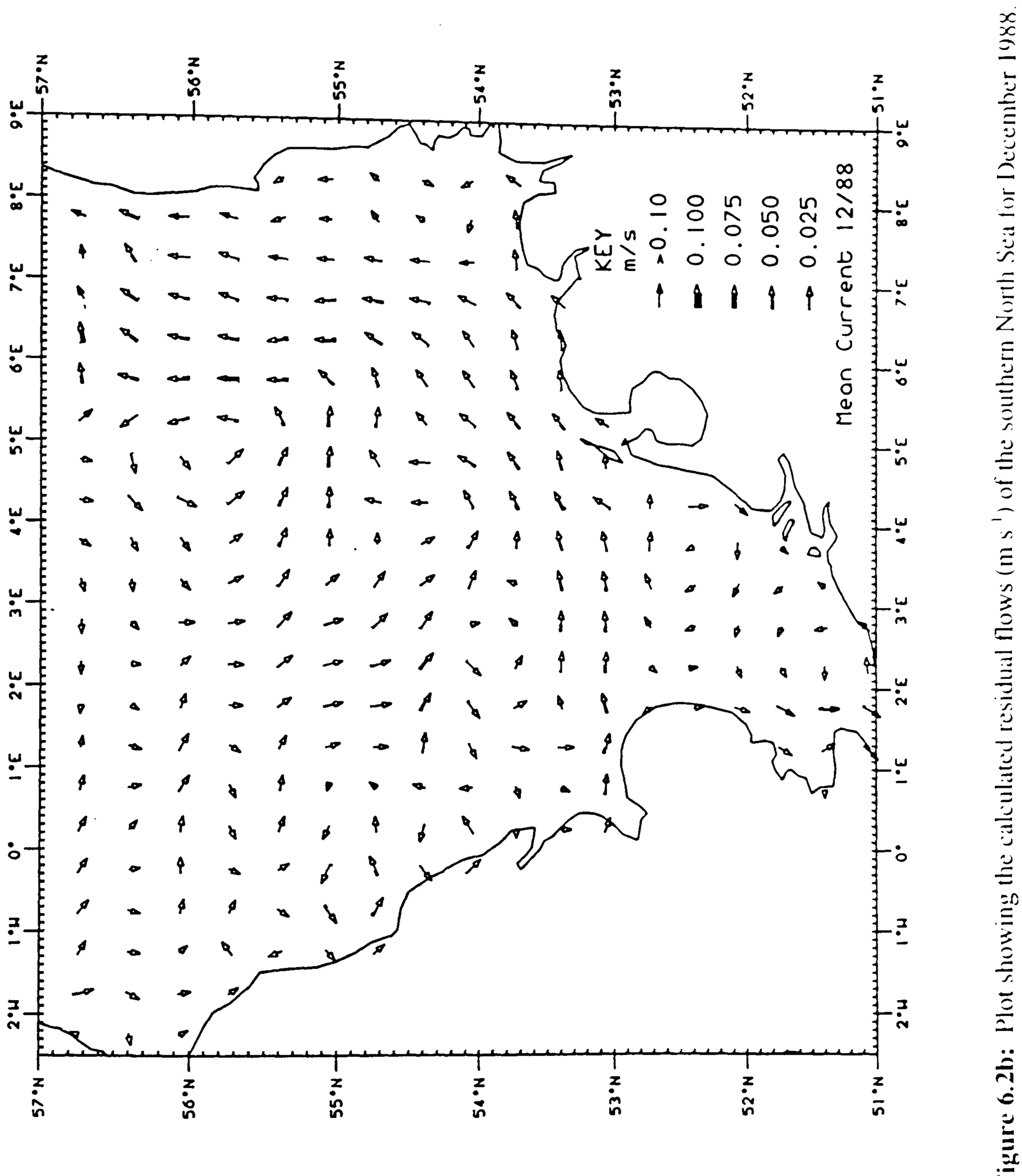

Figure 6.2b: Plot showing the calculated residual flows ($m\,s^{-1}$) of the southern North Sea for December 1988

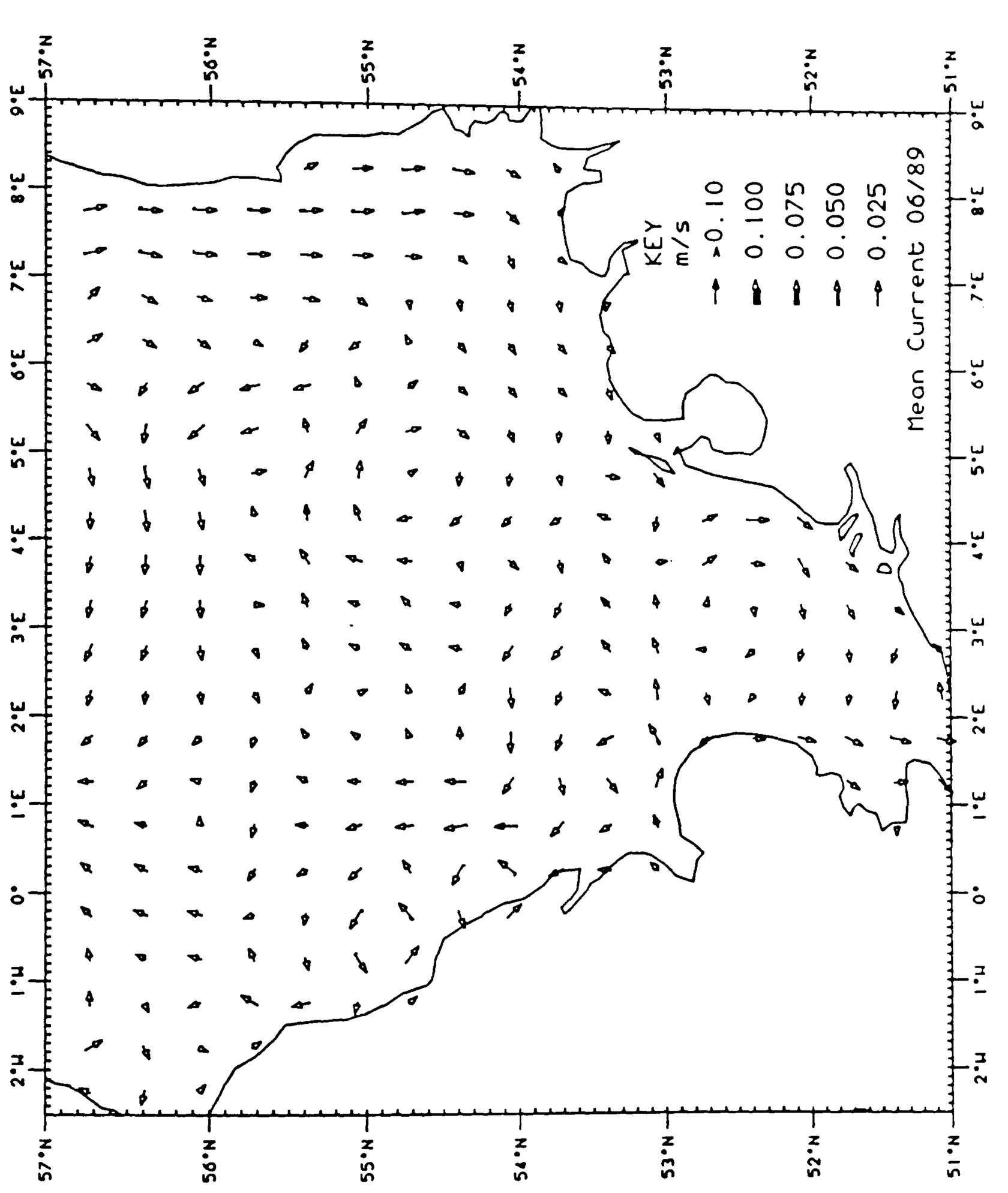

Figure 6.2c: Plot showing the calculated residual flows ($m\ s^{-1}$) of the southern North Sea for June 1989.

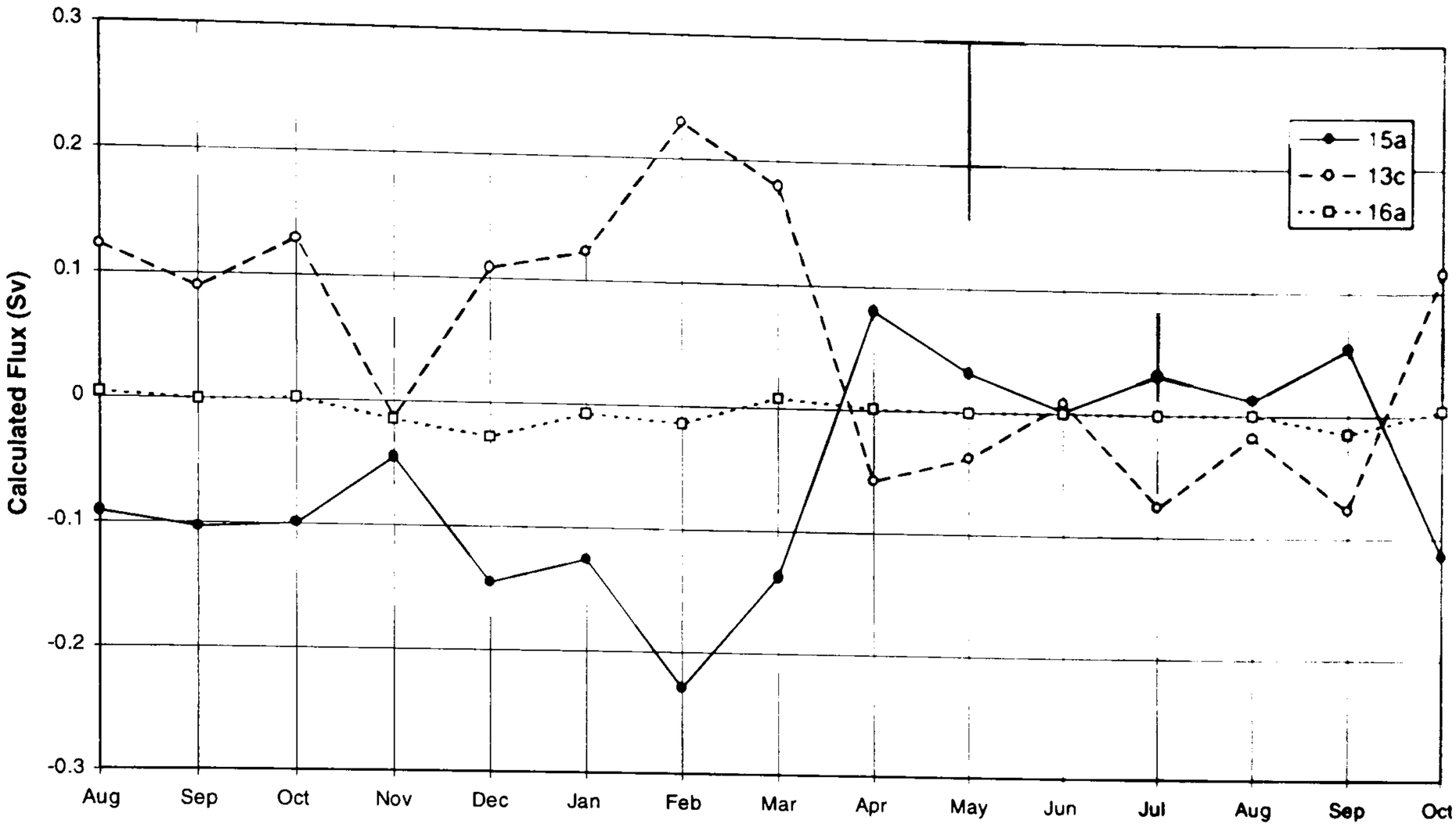

Figure 6.3: Plot showing the monthly mean volumetric fluxes (due to the surge component) across sections 15a, 16a and 13c, in Sverdrups (10^6 m^3 s^{-1}). Positive flow is either northward (sections 15a and 16a) or eastward (section 13c) [after Proctor and Smith, 1991].

To the surge component values must be added the tidal residual components which have been calculated by Proctor and Smith [1991] and later revised [R. Proctor, *pers. comm.*]. These vary seasonally, with maximum values at the equinoxes (April and September) as well as on a lunar time-scale with spring and neap tides.. The equinoxial monthly mean tidal fluxes for sections 13c, 15a and 16a are presented in Table 6.1, together with the minimum and maximum daily mean fluxes occurring in the month (for sections 13c and 16a only). The smallest monthly values were about 10% less than those shown.

Table 6.1: Equinoxial monthly mean fluxes (due to the tidal residual) across sections 15a, 16a and 13c, in Sverdrups (10^6 m^3 s^{-1}) [after Proctor and Smith, 1991; revised by R. Proctor, *pers. comm.*]. Positive flow is either northward (sections 15a and 16a) or eastward (section 13c).

Section Number	Tidal Flux (Sv)	Daily Mean Min. (Sv)	Daily Mean Max. (Sv)
15a	-0.0269		
13c	0.0705	0.0193	0.1317
16a	0.0184	-0.0224	0.0331

6.2: TSM Fluxes

There are a number of hydrographic stations within the zone covered by the plume, namely stations AY, AZ, BA and BB, which lie on a cross-section approximately normal to the major axis of the plume [Figure 6.1]. In order to calculate the TSM fluxes, suspended sediment concentrations and either measured or modelled current velocities are required. The four stations were sampled on every survey cruise [see Figure 2.3] so that each has a complete series of suspended sediment measurements.

With respect to current velocities, long-term current measurements were obtained at 6 sites within the survey area [reported by Knight *et al.*, 1990a; 1990b; 1990c; Knight *et al.*, 1991a; 1991b; 1991c]. Their positions are shown in Figure 6.1. Site D is located within the plume and comprised an acoustic doppler current profiler (ADCP). However, the data for this site were unsuitable for the flux calculations because firstly, the data coverage from this site was incomplete (59% over the fifteen months) and secondly, the results may not be applicable over the entire plume width. As a consequence modelled residual velocities were used.

At the nearest model grid point to each of the four stations the modelled residual depth-mean velocities were averaged over the duration of each survey cruise. The residual velocities calculated at station BA are shown in Figure 6.4 and include both the tidal and non-tidal components. There is a good correspondence with the transport across section 13c.

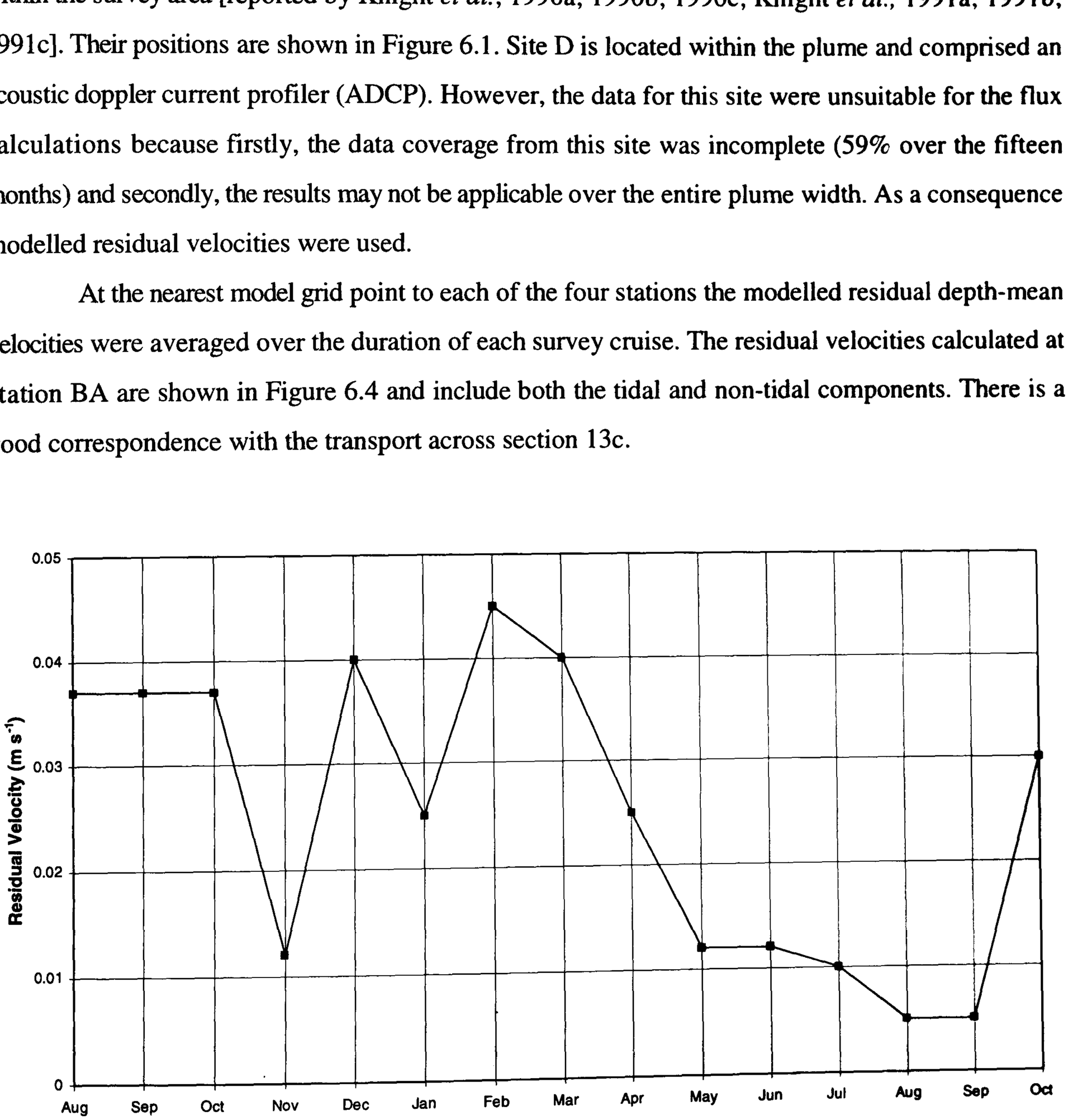

Figure 6.4: Monthly mean residual velocities at station BA ($m\ s^{-1}$)

The eastward components of the velocities were multiplied by the measured depth-mean TSM concentrations and the water depth to obtain an estimate of the TSM flux per metre. The calculated monthly fluxes for each station are shown in Figure 6.5. Maximum fluxes occurred at station BA where, in December 1988, the flux reached 24.7 g m^{-1} s^{-1}, and in March 1989, reached 10.5 g m^{-1} s^{-1}.

In order to calculate the total flux within the plume an integration needs to be made of the fluxes across the width of the plume. The fluxes at the four stations, when plotted at their relative spatial separation, showed that the plume could be represented by an exponential distribution centred on the flux given by station BA [Figure 6.6]. This distribution was used to integrate across a plume width of 80 km. The integrated fluxes are shown in Figure 6.7. The maximum flux of 3.3 Mt $month^{-1}$ occurred in December 1988, with a further peak of 1.4 Mt $month^{-1}$ in March 1989. The total flux over the 15 month observational period was 7.19 Mt, of which 71% occurred in two months when the winds were particularly strong from the south-west. This is equivalent to a flux of 6.6 Mt a^{-1}. Assuming an average organic content of 25% gives a flux of 5 Mt of inorganic material per year.

There are necessarily questions regarding the reliability and representativeness of the estimates made above. The flux estimates have been gained by the multiplication of relatively small TSM concentrations with large water transports. It is important therefore to determine some measure of the probable errors involved, despite the difficulty of doing this owing to the nature of the data acquisition and the averaging required for the calculations.

Variations in the TSM concentration can occur because of tidal currents, waves and inherent patchiness in the advective TSM field. The TSM values can vary tidally by about ± 50%, and significant enhancement can occur under wave action [Jago *et al.*, 1994]. However, the suspended load appears to be constrained by a finite supply of material, and elevated concentrations persist for several days. Jago [*pers. comm.*] reported that at Site B (54° 35′N, 04° 50′E), one of the study sites chosen to conduct resuspension process studies [summarised by Jago *et al.*, 1994], significant waves prior to observations in January 1989 produced concentrations of 5 mg l^{-1} compared with normal concentrations of 2 mg l^{-1}. Individual measurements also reached 20 mg l^{-1} because of patchiness in the advective field. Since a single TSM profile was taken as a measure of the monthly mean, errors of plus or minus a factor 2 are probable.

With respect to errors in the residual velocities, Table 6.1 gives the minimum and maximum daily mean fluxes for section 13c (0.0193 and 0.1317 Sverdrups respectively) around the maximum monthly mean of 0.0705. This occurs at the same time as a mean surge induced residual flux of -0.05 Sverdrups [*i.e.* flux for April in Figure 6.3]. Therefore, it is possible that errors in the velocities are ± 50%.

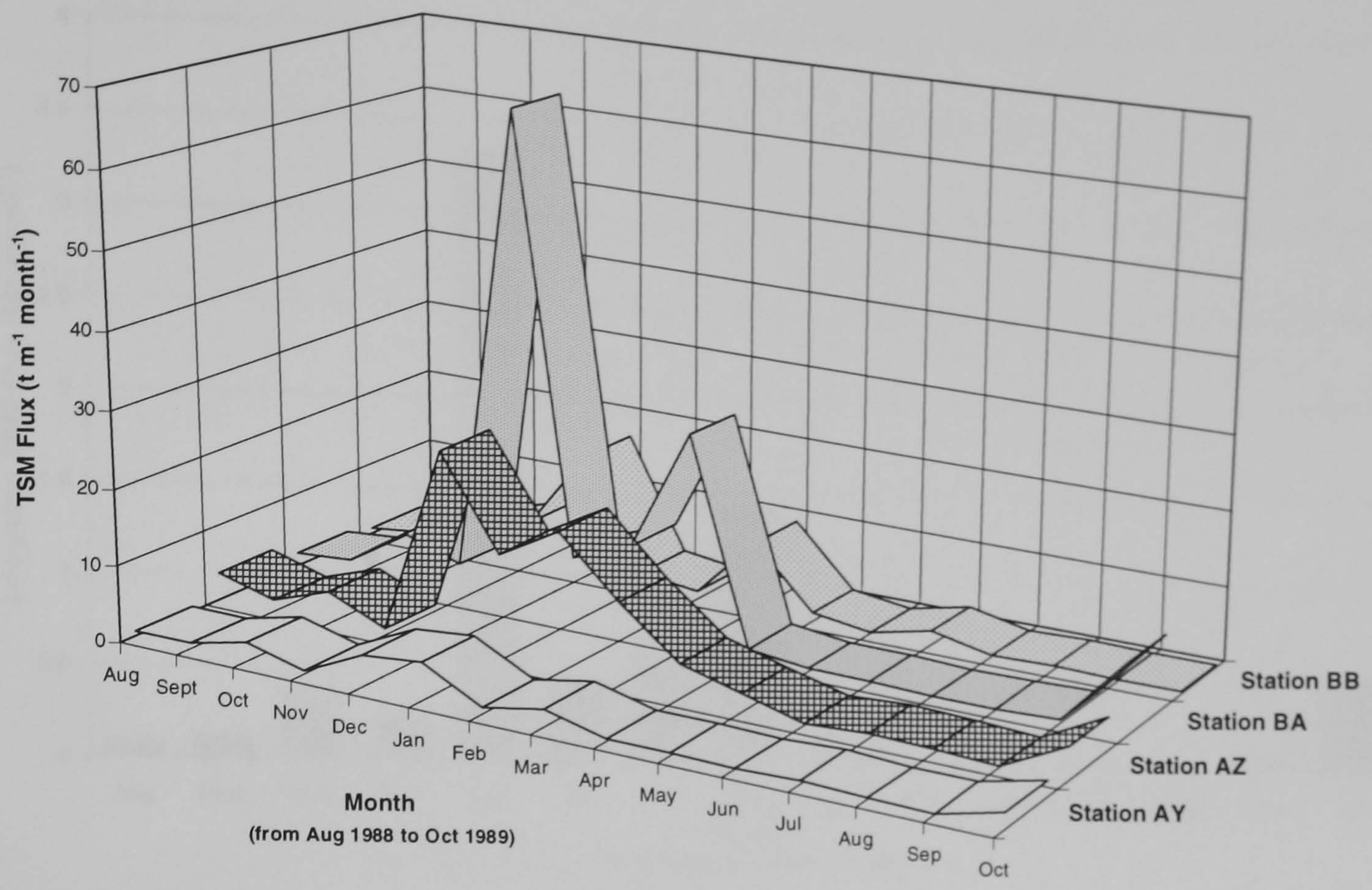

Figure 6.5: TSM fluxes for stations AY to BB, across the plume (t m^{-1} $month^{-1}$)

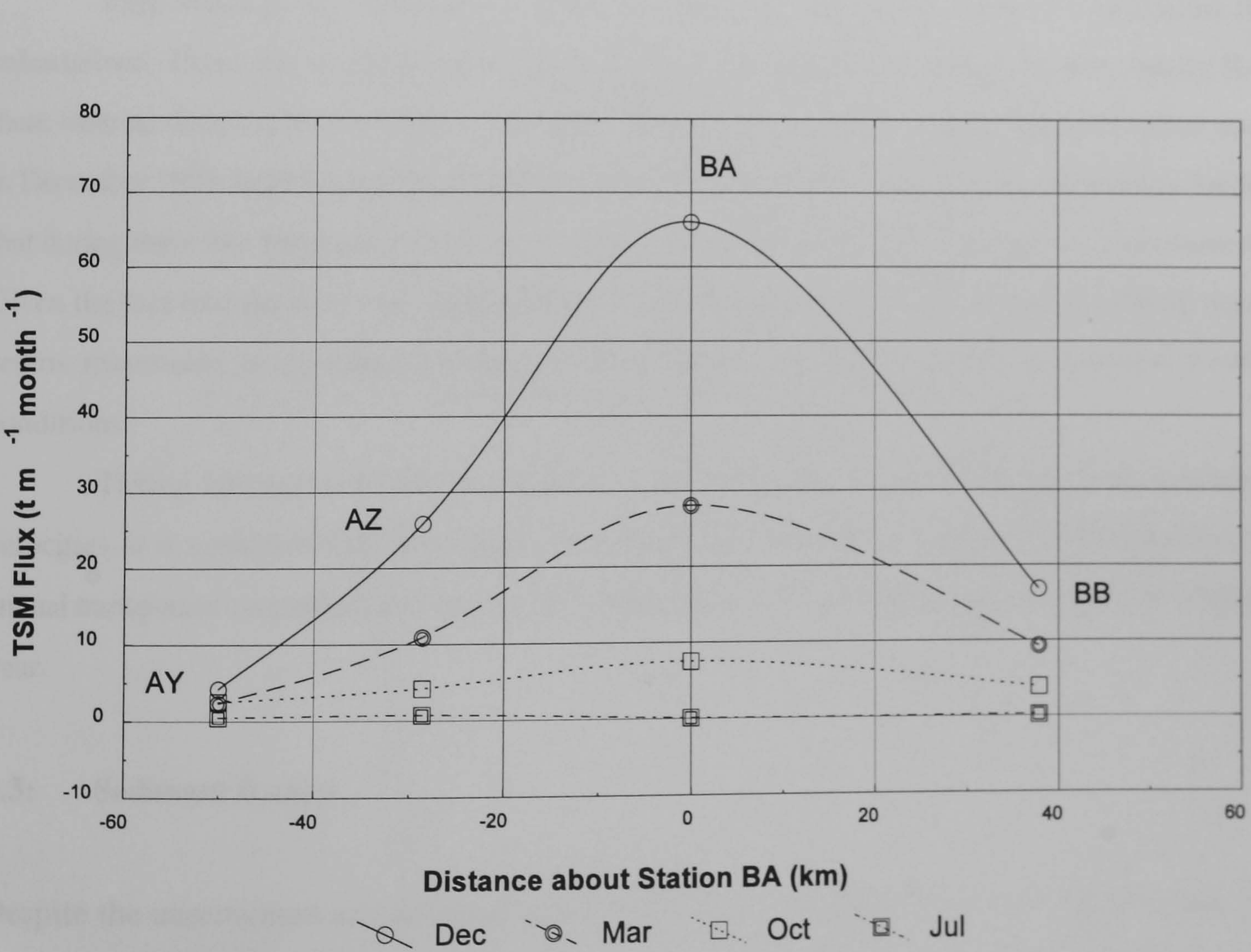

Figure 6.6: Example plots of TSM fluxes for stations AY to BB (t m^{-1} $month^{-1}$), spatially centred about station BA.

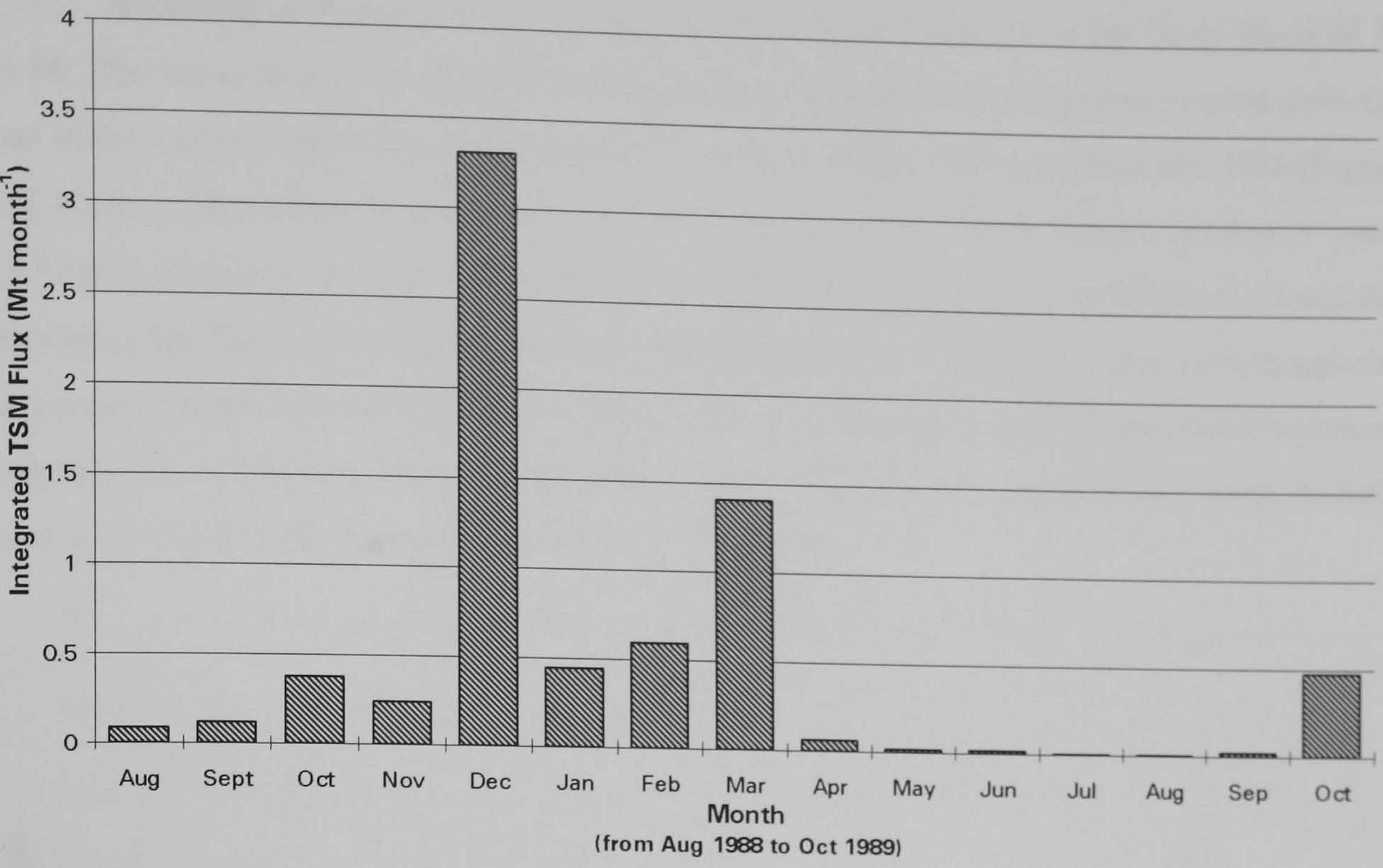

Figure 6.7: Integrated total suspended matter fluxes for the plume for the 15 months of measurement (Mt month^{-1}).

Tidal biases in the TSM concentrations at station BA can also be sources of error in the flux calculations. However, as discussed in §2.3 and shown in Figure 2.14 (which includes station BA), there were no discernable tidal biases in the data. The highest suspended matter fluxes shown to occur in December 1988 and March 1989 [Figure 6.7] are not related to any tidal biasing but more to the fact that during these two months the worst storm conditions of the whole survey period were encountered. Given the fact that the winter of 1988/89 was less windy than normal [Howarth *et al.*, 1993], then it seems reasonable to conclude that the calculated fluxes are typical of normal tidal and weather conditions.

Taking into account both the variation in the TSM concentrations and the modelled current velocities, it is estimated that the overall errors in the flux estimates are about ± 50%.Therefore, the annual transport of suspended sediment in the plume probably lies in the range of about 3 to 9 Mt per year.

6.3: Sediment Budget

Despite the uncertainties and probable errors in the flux calculations, the East Anglian Plume still represents a major pathway for suspended sediment transport across the southern North Sea. The question now arises regarding the sources for the material in the plume.

According to Eisma [1990], the total load of suspended material in the North Sea is 46.5-51 Mt. The integration of the suspended sediment concentrations during the survey period gives the load in the southern North Sea as about 100 Mt, rising to almost 400Mt in December 1988 [Figure 6.8]. Eisma [1990] defines the major suspended matter sources as the North Atlantic (10.4 Mt a^{-1}) and the English Channel (*ca.* 17 Mt a^{-1}) [see Table 1.5]. Much of this material is recirculated out into the Norwegian Sea. The magnitude of the load arises because the water volumes are large even though the suspended matter concentrations are low. These inflows contribute to a regional suspended sediment concentration of less than 1 mg l^{-1} in the northern North Sea. Some of the circulating North Atlantic water is involved in the fluxes calculated within the plume.

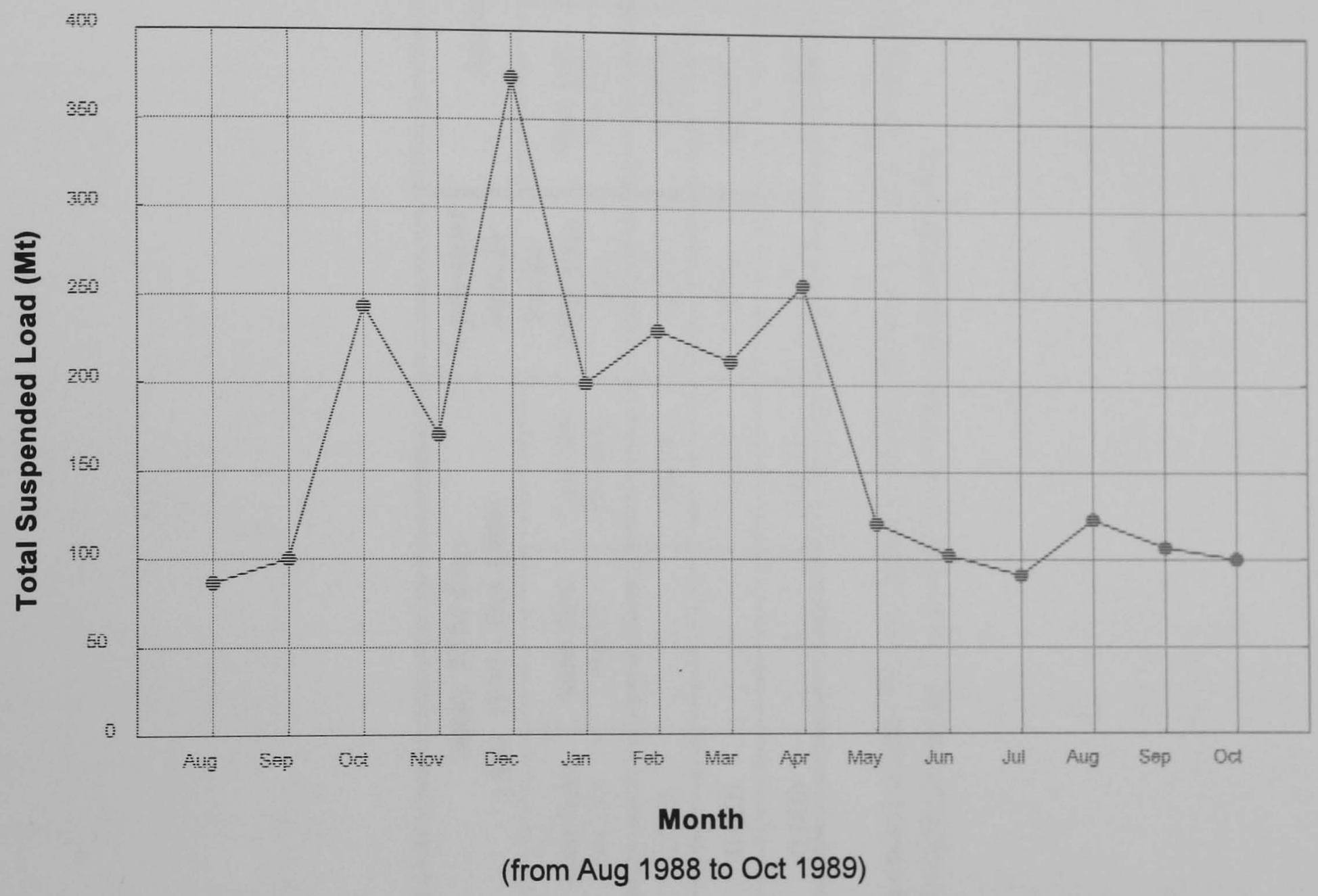

Figure 6.8: Total suspended load in the southern North Sea (Mt).

The contribution of the northern North Sea water circulation can be estimated by considering the transport across the cross-sections between the English coast at 55° 22′N eastward to 3°E (*i.e.* section 15a out to 3°E) and at 53°N eastward to 3°E (*i.e.* section 16a out to 3°E), and the cross-section connecting these two (*i.e.* section 13c) [Figure 6.1]. These form a box through which there should be volume continuity. The transports of water shown in Figure 6.3 are for slightly longer cross-sections, but the transport through the shorter sections should only be proportionately smaller. The fluxes of suspended matter across the sections were estimated using the water transports and TSM concentrations given in Table 6.2. The TSM flux due to the surge component also comprised two partial estimates because the monthly mean fluxes exhibited two distinct phases (August 1988-March 1989, and April-October 1989) [Figure 6.3]. These partial estimates were transformed into an equivalent total annual flux.

Section	Surge TSM Flux (Aug 1988 - Mar 1989)			Surge TSM Flux (Apr 1989 - Oct 1989)			Equivalent Annual Surge TSM Flux (Mt)	Annual Tidal TSM Flux			Annual TSM Flux (surge + tidal) (Mt)
	Mean Surge Flux (Sv)	Mean TSM (mg l^{-1})	Total TSM Flux (Mt)	Mean Surge Flux (Sv)	Mean TSM (mg l^{-1})	Total TSM Flux (Mt)		Mean Tidal Flux (Sv)	Mean TSM (mg l^{-1})	Annual TSM Flux (Mt)	
15a (to 3°E)	-0.123	2	-5.16	0.013	2	0.49	-3.73	-0.0520	2	-3.28	**7.01**
13c	0.121	5	12.69	-0.020	3	-1.14	9.25	0.0705	4	8.89	**18.14**
16a (to 3°E)	-0.007	10	-1.39	-0.002	5	-0.16	-1.24	0.0184	7.5	4.35	**3.11**

Table 6.2: Estimated suspended matter fluxes across sections 15a (out to 3 E), 13c and 16a (out to 3°E). Positive flux is either northward (sections 15a and 16a) or eastward (section 13c).

The calculations suggest that there are large inputs of suspended matter into the box southward across section 15a and northward across section 16a, totalling about 10 Mt a^{-1}. They also indicate a substantial export of suspended matter of about 18 Mt a^{-1} out of the box eastwards across section 13c (of which some 30-40% is transported in the plume). Although the quantities resulting from the calculations are prone to the same scale of errors described in §6.2, it is likely that the relative proportions will not change significantly. The input and export figures do not balance, suggesting that the export surplus of about 8 Mt a^{-1} (*i.e.* about 80% of the input) is produced by sources from within the box.

Although the enhanced suspended sediment concentrations observed within the English coastal waters and within the plume are produced by resuspension by waves, during storm events, the long term presence of the plume means that the transport of TSM is a sequential process of erosion, transport and deposition, since an individual sediment particle would only travel about 5 km day^{-1}. Therefore the remaining flux of suspended matter eastward from the English coastal waters and within the plume must result from river inputs, coastal erosion and near-coast sea bed erosion.

A sediment budget for the east coast of England has been formulated by McCave [1987] and this is shown in Table 6.3. The largest fine sediment supply is from the Holderness area, between the Humber and Flamborough Head. This provides an input of 1,400 kt a^{-1}. The other major source is coast erosion around Cromer in Norfolk which contributes 665 kt a^{-1}. By comparison, the Wash rivers and the Humber contribute about 200 kt a^{-1} between them. The east coast also encompasses some major sites of deposition, of which the Wash is the largest. This area has extensive mud areas and sand banks and is accreting rapidly at a rate between 1,600 and 790 kt a^{-1}, depending on the rate at which progradation is assumed to be taking place. Major deposition also occurs on the North Norfolk marshes, and the mudflats and marshes of the Lincolnshire and Humber area.

Thus, according to McCave [1987], taking the maximum deposition rate in the Wash leaves only about 0.5 Mt a^{-1} for transport in the plume. The most obvious poorly quantified source is the erosion of the nearshore sea bed. However, McCave [1987] estimates this as only accounting for an additional supply of the order of 160 kt a^{-1}. Therefore there does not appear to be sufficient material available to support the measured plume transport.

Further budgetary calculations have been carried out by Hydraulics Research Ltd. [1992] using data from Anglian Water [1988] and the results are shown in Table 6.3. Only erosion estimates have been made and the amounts have been adjusted assuming, as was done by McCave [1987], that mud constituted only 67% of the eroded material in Holderness, and 44% elsewhere. The figures are considerably higher than those estimated by McCave [1987]; and assuming that his deposition values are correct, they would provide sufficient material to supply the estimated transport within the plume.

The Hydraulics Research Ltd. [1992] budget sits well with the plume flux estimates, and assuming that a major proportion of the supply contributes to the plume transport (as suggested by the residual circulation and suspended sediment distributions), then the plume exports the majority of the fine sediment eroded from the coasts of eastern England. The main sites of deposition of this material are likely to be the Oyster Grounds [Zuo *et al*, 1989], the German Bight and the Norwegian Trench [Eisma and Kalf, 1987a].

There are undoubtedly uncertainties regarding the representativeness of both the suspended matter flux and budgetary estimates. For example, the budgetary figures are averages over several years, whereas the flux measurements are for a single year. Clearly there will be considerable short term variations in both sets of estimates. From the various meteorological information that was gathered for the survey period, the winter of 1988/9 was less windy than normal [Howarth *et al.*, 1993], with only two major storms rather than the average six. Nevertheless, some averaging of the coast erosion input is likely to occur by temporary accumulation of sediment along the transport path during calmer periods. Therefore, the material eroded will move along the plume transport path by a step-wise process of resuspension and sedimentation depending on the sequence of storm events.

The large differences in the budget figures presented in Table 6.3 illustrate the enduring problem of quantifying the critical information required for the budget calculations, such as the primary processes involved (*e.g.* rates of coastal and seafloor erosion, resuspension and deposition) and their spatial and temporal variability. The figures also illustrate the broader trend of previously published North Sea budgets [*e.g.* McCave, 1973; Eisma, 1981c; 1990; Eisma and Kalf; 1987a] in which estimates have increased by as much as 40-50%. However, what all these budgets have lacked are estimates of the transport of suspended sediments through the North Sea; budgets are too often just a balancing act between supply, deposition and outflow, and where imbalances are blamed on poorly quantified sources (commonly seafloor erosion), uncertainty and a lack of knowledge. The flux estimates within the plume, whilst improving substantially the knowledge of the transport of suspended sediment across the southern North Sea, have again highlighted the inadequacies and uncertainties in the budgets of eastern England. Clearly, more data are required before the results can be accepted unequivocally.

Table 6.3: Eastern England Sediment Budget (kt a^{-1}).

SUPPLY	McCave [1987]	Hydraulics Research [1992]
Fluvial:		
East Anglian Rivers	5.6	
Wash Rivers	≈ 100	
Humber	≈ 100	225
Thames		690
Cliffs:		
Norfolk Cliffs	665	2950
Suffolk	120	3320
Holderness	1400	2610
Total:	≈ 2500	9800
DEPOSITION		
Wash	790 - 1600	
Humber/North Lincolnshire	127	
North Norfolk Marshes	104	
East Anglia Estuaries	≈ 100	
Total:	≈ 1100 - 2000	
Lost from the system:	≈ 500 - 1400	

6.4: Summary

This chapter has built on the qualitative descriptions of the distribution and concentrations of suspended sediments in the southern North Sea of the previous chapters by quantifying the fluxes of suspended sediment within the plume, which is an important and major feature of the suspended sediment distributions. The modelled residual circulations confirmed that the zone of plume development coincided with strong eastward flowing residual currents, which developed in response to moderate or strong winds from the south west quarter during the autumn and winter months. During the summer months when winds were weak and more variable, residual flows were more complex and weak, and the plume lost its prominence.

Fluxes of suspended sediment were calculated for the plume across a cross-section of four survey stations. The total annual flux of TSM was estimated to be 6.6Mt ± 50%, of which 75% (≈ 5 Mt) was estimated to be inorganic material. The flux estimates were compared with two published sediment budgets for eastern England and only one of them, the Hydraulics Research [1992] budget was consistent with the flux estimates. Despite the uncertainties in the budgets, the comparison showed that the plume constitutes a major feature exporting sediment across the southern North Sea.

Nevertheless, there are still some important and interesting questions outstanding regarding the transport of suspended sediment in the southern North Sea (*e.g.* transport rates within the plume; the balance between advective transport and resuspension/sedimentation episodes; the extent and mechanisms of sediment loss from and retention within the coastal margin). Some of these issues together with a general discussion and areas of future work are discussed in the next and final chapter.

DISCUSSION AND CONCLUSIONS

This research has generated a comprehensive set of distributional data of suspended sediments (including total suspended matter and organic matter concentrations) for the southern North Sea. It represents a significant improvement in terms of data coverage compared to previous sampling efforts which were essentially random in both space and time. Such improvements are indicative of the innovative nature of the North Sea Project which adopted a systematic sampling strategy and enabled a whole series of coincident experiments and measurements to be carried out, some of which were relevant to the research.

7.1: Suspended Matter Distributions

For the first time suspended matter concentrations have been defined over a seasonal cycle. In addition to providing information on the horizontal distributions, the use of beam transmissometers also enabled detailed measurements of the vertical distributions of TSM at resolutions greater than could be practically realised using conventional water sampling techniques. The filtered water samples, which were used to calibrate the transmissometer measurements, provided information on organic matter concentrations and organic contents for a near-complete seasonal cycle which has not been achieved before.

The horizontal distributions of TSM [§3] display many of the features of the southern North Sea described by previous researchers, including the high turbidity region off the East Anglian coast, the low turbidity regions of the northern and central parts of the southern North Sea. More seasonally variable features are also evident such as the development of the East Anglian Plume during the winter, and the marked increase in TSM concentrations along the coastal waters of the eastern Southern Bight and the German Bight during the spring.

The vertical distributions of TSM [§3] constructed for two sections orientated across the southern North Sea and for two sections orientated alongshore of the English and continental European coasts exhibit some well defined gradient zones. These include offshore gradient zones with the higher concentrations inshore, and alongshore gradient zones off the English and continental European coasts with the higher concentrations corresponding to, for example, the East Anglian turbidity region and the sediment discharges from the Humber and Rhine rivers and associated plumes. The vertical distributions also provide further detail of major features such as the East Anglian Plume and relatively small scale features such as localized suspended matter minima.

The organic matter and organic content measurements [§4] allow the assessment of the different contributions of two major influences on the characteristics of suspended matter, that is primary production and sediment pick-up. As with the TSM distributions, organic matter concentrations tend to be highest in the coastal waters of the Southern and German Bights and lowest in the northern and central parts of the southern North Sea. The organic content distributions show distinct regional and seasonal trends, notably the high contents in spring along the continental European coastline which contrast sharply with the low contents off East Anglia; and the relatively high organic contents in the central and northern regions during winter.

7.2: Factors Affecting the Suspended Matter Distributions

The coincident measurements of salinity, temperature, chlorophyll and primary production that were made during the North Sea Project [§5] present a rare opportunity to examine the seasonal cycles of these parameters in relation to the seasonal cycle of suspended matter in the southern North Sea.

The distribution of water masses as described by the distributions of salinity explain at a general level the broad features of the suspended matter distributions, that is the partition between the more turbid and less saline coastal waters of the Southern Bight and the water of Atlantic origin further offshore. These spatial variations are related to both the sources for salinity and sediment which occur at the lateral boundaries of the southern North Sea, and the density differences caused by the interactions of the fresh water sources from rivers and coastal run-off with the influx of more saline waters through the Dover Straits and from the northern North Sea. Density differences in the coastal waters of the southern North Sea produce water circulations that tend to trap sediment in the coastal zone and inhibit the dispersal of suspended sediment away from the coast. However, in the case of the East Anglian plume, strong offshore residual currents break down these trapping processes.

Primary production temporarily forms part of the suspended matter as evident from blooms of *Phaeocystis pouchetii* along the continental European coast of the southern North Sea during the spring to autumn months when organic contents of the TSM are up to 50-60%. However, as well as seasonal differences, there are regional differences between the primary production and suspended matter regimes of the western (*i.e.* English coastal waters) and eastern (*i.e.* continental European waters) parts of the southern North Sea. The suspended matter of the western half is dominated by an inorganic component whereas the eastern half is dominated by a spring-to-autumn organic component. The reasons for this difference are related to the different levels of primary productivity between the two areas, with the eastern half being 2-3 times more productive than the western half.

7.3: Fluxes of Suspended Matter

The East Anglian plume is one of the major features described by the research and appears to be a major sediment transport path across the southern North Sea [§6]. Previous turbidity studies have also defined a zone of high turbidity off East Anglia with a continuation as a plume located over the Norfolk Banks and extending across the Southern Bight. However, the development and extent of the plume has not been well defined up until the present research.

The plume is a permanent feature directed east-north-eastwards from East Anglia, although it is more distinctive in the winter than in the summer when it becomes rather discontinuous. The plume also fits well into the general anti-clockwise circulation of residual currents which drives the transport of suspended sediment. The suspended sediment measurements, in combination with modelled currents, have allowed the estimation of the seasonal variation in the magnitude of the plume and the fluxes of suspended matter. The total flux within the plume is calculated to be 6.6 Mt a^{-1} of suspended matter, of which approximately 5 Mt is inorganic material. Estimating the errors in the flux estimates is difficult because of the nature of the data acquisition and the averaging required for the calculations. However, the probable errors in the flux calculations are estimated to be ± 50%.

A comparison with published sediment budgets for the North Sea and further flux calculations indicate that there is a substantial flux of suspended matter eastwards across the southern North Sea, part of which is contributed by the circulating Atlantic water. The remaining flux results from the sequential process of erosion, transport and deposition of sediments emanating from the east coast of England, mostly within the plume. When comparing the calculated plume transport with two sediment budgets for the east coast of England, only one of these budgets would provide sufficient material to supply the plume transport. This highlights the enduring problems associated with flux and budget calculations and the reliable quantification of the critical information required. Nonetheless the calculated plume transport provides a significant benchmark, which was previously unattainable, against which further calculations can be tested as more data become available.

7.4: Implications for Shelf Sea Suspended Sediments Research

Shelf sea suspended sediment research has focused on the fluxes of suspended sediment from rivers and estuaries, and from coastal run-off and erosion, as transport mechanisms for natural and anthropogenic materials and the dispersal of pollutants into the coastal zone and into the open sea. The research has confirmed the broad characterizations of the distribution of suspended sediment in shelf seas made by previous researchers [§1], such as the seaward decrease in suspended sediment concentration and the existence of plumes of high concentration which are transporting suspended sediment from nearshore areas.

More importantly however, the research has highlighted the complexity of the interactions between the physical and biological factors that affect the distributions and transport of suspended sediments at both spatial and temporal scales. The consequences of these factors manifest themselves in the seasonal cycle which is the fundamental and predominant shelf sea process. Fluctuations in climatic/meteorological conditions for instance, control the concentration, distribution and composition of suspended sediments by influencing the supply from coastal and seafloor erosion, from riverine and estuarine inputs, and from primary production in both short-term (*e.g.* storm events) and medium-term (*e.g.* seasonal) time scales. Likewise, some of the same fluctuations contribute to the temporary transformation of the prevailing current circulation and the concomitant modification of suspended sediment transport paths. The seasonal cycle is not only reflected in terms of changing meteorological and circulation conditions but also in the temperature and salinity distributions and any resultant water density differences and stratification. All of these factors impact on the distribution of suspended sediments, their transport and the ultimate dispersal of associated contaminants. The research in the North Sea has increased the understanding of the relationship between suspended sediment distribution and transport and the seasonal cycle, and many of the processes and interactions described will apply to other shelf sea areas.

The research has also pointed out some remaining deficiencies and unresolved questions in the understanding of shelf sea processes, particularly in relation to the coastal zone. For instance, the flux calculations associated with the East Anglian plume suggest that the plume is a major feature exporting large quantities and the majority of fine sediment eroded from the coasts of eastern England. However the probable errors involved in the flux and sediment budget calculations are large, which illustrates the difficulty of estimating sediment budgets and large-scale sediment movements from limited data. Clearly, the need for the better definition of the sediment budget of eastern England is one of the major outcomes of the North Sea Project requiring further study. With respect to the East Anglian plume, there is uncertainty not only with the plume transport calculations but also with the nature and mechanisms of the sediment transport along the path of the plume. There is also uncertainty with respect to the coastal sources and sinks of the sediment (*e.g.* rivers, estuaries and banks), the degree to which the sediment is re-circulated within the coastal zone of eastern England and then deposited in nearshore or offshore sinks, and the mechanisms of sediment loss and retention within the coastal zone. The need to understand and quantify these aspects is important because of coastal protection issues and the dispersal of pollutants into the coastal zone.

7.5: Further Work

The data collected during the course of the research have been incorporated along with the results of the other experiments into the BODCs Database for the North Sea. This database is in the public domain and available through a variety of media including compact disk (CD-ROM), ensuring that further research and study using the database can continue. There is scope for investigating the three-dimensional nature of the suspended sediment distributions beyond the main surface and bottom horizontal distributions described by the present research (*e.g.* horizontal distributions at different depths). However, the main uses of the data set are in modelling and remote sensing applications.

The simulation of suspended sediment transport requires mathematical models which adequately describe the sediment dynamics, the interplay of atmospheric forcing, the hydrographical field, and the dispersal and deposition of sediment [Sündermann, 1994]. This can only be achieved using field measurements and experimentation. The North Sea suspended sediment data can be used to validate models of suspended sediment transport [*e.g.* Hydraulics Research, 1992]. Modelling also offers opportunities for multiple scenario investigations to determine, for instance, the fate of sediment from particular sources and sites of deposition, in ways that field measurements could not achieve in isolation. Increasingly suspended sediment modelling is being linked to water quality models. In the case of the North Sea, a model under development comprises a sophisticated model to represent the physics, and a series of sub-models of suspended sediments, microbiology and metal interactions for processes controlling, for example, nutrients, dissolved oxygen, phytoplankton, detritus and trace metals [Huthnance *et al.*, 1994]. Such modelling strategies are intended to help predict the fate of contaminants in shallow seas for environmental management and policy applications.

Remote sensing, especially from satellites, is being increasingly used to monitor trends in the optical properties of shelf seas. Images from the Coastal Zone Colour Scanner (CZCS) and sea surface temperature images from the Advanced Very High Resolution radiometer (AVHRR) have been used to show the seasonal complexity of surface phytoplankton, suspended sediment and temperature distributions in the North Sea [Holligan *et al.*, 1989]. Satellite or airborne sensors provide synoptic pictures of patterns in optical properties and structural detail that are superior in spatial and temporal resolution to that achievable by shipboard measurements (accepting that such advantages are only applicable to surface water properties). However, although many features are shown in the images, they are difficult to interpret in terms of specific optical properties. The two main reasons for this are firstly, the lack of sea truth measurements and secondly, the crude nature of the algorithms used for the quantitative determination of parameters such as chlorophyll and suspended sediment. The database of suspended sediment measurements along with coincident remote sensing images should provide a basis for improving the methods of interpretation for images. This is important for future research programmes [see later] and new instruments like the Compact Airborne Spectrographic Imager (CASI).

Further work is also required to more adequately quantify the fluxes of suspended sediment within plumes like the East Anglian plume and within the coastal zone. Recent developments in the use of acoustic doppler current profilers (ADCP) in the measurement of the flux of suspended materials seem to offer opportunities for providing long term estimates of shelf sediment fluxes [Simpson, 1994]. The intensity of the back-scattered signal from the ADCP provides a measure of the particle concentration in a particular size range. By combining the sediment signal with the current velocity measurements gives a measure of the instantaneous flux over a large part of the water column depth. With respect to the East Anglian plume, for example, the long-term deployment of arrays of acoustic doppler current meters and self-recording beam transmissometers across the long axis of the plume in combination with a programme of gravimetric calibration should provide the basis for more accurate estimates of the fluxes within the plume.

With respect to the further work required in the coastal zone, there are currently a number of inter-related international and European initiatives. The Land-Ocean Interactions in the Coastal Zone (LOICZ) Project aims to elucidate the role of coastal seas in the global climate system and the potential response of coastal systems to all sources of global change. LOICZ comes within the framework of the IGBP (International Geosphere-Biosphere Programme) Global Change Programme and will operate through both international research efforts such the European Land-Ocean Interaction Studies (ELOISE) and national research efforts such as NERCs Land-Ocean Interaction Study (LOIS). The research efforts will provide the scientific data necessary to manage coastal environments and resources in a sustainable manner [ELOISE Steering Committee, 1994].

LOIS is a 6 year research project aimed at quantifying the exchange, transformation and storage of material at the land-ocean boundary. It is an important follow-on research programme to the North Sea Project and it will address some of the deficiencies, like sediment budgets, identified during the North Sea research [Natural Environment Research Council, 1994]. A key component of LOIS is the Rivers, Atmosphere, Estuaries and Coasts Study (RACS) which aims to estimate and model the fluxes of materials (*e.g.* water, fine sediment, biogeochemically important elements and representative contaminants) into, through and out of the coastal zone, and also the physical, chemical and biological transformation processes that govern such fluxes.

The main geographical study area for RACS is the east coast of England from Great Yarmouth to Berwick-upon-Tweed. The East Coast study area was chosen for its soft coastline and susceptibility to coastal erosion/rising sea-level, as a focus on a major estuary, the Humber, and to provide a link with the North Sea Project. The fieldwork programme of RACS (Coasts and Estuaries) will include survey and experimental work within the estuaries and associated plume regions of the Humber, Tyne, Tees and Tweed. A major experiment is also planned off the Holderness Coast involving shipboard measurements, moorings, bottom-mounted rigs, and shore-based, airborne and satellite remote sensing. This experiment will investigate the impact of waves, tides and storms on particle transport processes

at a rapidly eroding coastal site. Since the East Coast study was implicated by the North Sea research as a major source of suspended sediments, supplying material to the East Anglian plume, then the sediment fluxes and dynamics aspects of RACS should help to more accurately define the suspended sediment supply rates and directions of transport and deposition within this area.

In addition to RACS, the Land-Ocean Perspective Study (LOEPS) aims to reconstruct the sea level/coastal changes of the east coast of England through the Holocene (*ca.* 10,000 year ago) to the present. LOEPS will also determine the regional history of sediment fluxes, sources and sinks within the East Coast study area, in particular the relative importance of fluvial, coastal and sea-bed sediment sources. LOEPS should provide important information regarding the supply and deposition of suspended sediments, including erosion and sedimentation rates, not only from the geological/historical past but also for the present, and for the future (*i.e.* the next 50-100 years) in response to predicted sea-level changes.

Another component of LOIS is the North Sea Modelling Study (NORMS), which is responsible for all the major simulation modelling objectives of LOIS and has strong links with RACS and LOEPS. NORMS will continue to develop the water quality model for the North Sea (mentioned above) by incorporating other models of water quality variables in the coastal zone resulting from riverine and coastal inputs (*e.g.* Humber and Wash) as well as extending the model to cover the north-west European Shelf. In this way a contiguous series of models will become available which will be capable of simulating the flux and transformation of materials from the land to the ocean basin.

REFERENCES

Abdel-Moati, A.R. (1990). Adsorption of dissolved organic carbon (DOC) on glass fibre filters during particulate organic carbon (POC) determination. *Water Res.* **24**, 763-764.

Anglian Water (1988). *Anglian Coastal Management Atlas*. Sir William Halcrow & Partners.

Backhaus, J.O. and Maier-Reimer, E. (1983). On seasonal circulation patterns in the North Sea. In: *North Sea Dynamics*. Sündermann, J. and Lenz, W. (eds.). Springer-Verlag, Berlin, pp. 63-84

Baker, E.T. and Lavelle, J.W. (1984). The effect of particle size on the light attenuation coefficient of natural suspensions. *J. Geophys. Res.* **89**, 8197-8203.

Balistrieri, L., Brewer, P.G. and Murray, J.W. (1981). Scavenging residence times of trace metals and surface chemistry of sinking particles in the deep ocean. *Deep Sea Res.* **28**, 101-121.

Bartz, R., Zaneveld, J.R.V. and Pak, H. (1978). A transmissometer for profiling and moored observations in water. *Proc. S.P.I.E.* **160**, *Ocean Optics V*, 102-108.

Bewers, J.M. and Yeats, P.A. (1977). Oceanic residence times of trace metals. *Nature* **268**, 595-598.

Biscaye, P.E. and Eittreim, S.L. (1974). Variations in Benthic Boundary Layer phenomena: nepheloid layer in the North American Basin. In: *Suspended Solids*. Gibbs, R.J. (ed.), Plenum Press, New York, pp. 227-260.

Bishop, J.K.B. (1986). The correction and suspended particulate matter calibration of Sea Tech transmissometer data. *Deep Sea Res.* **33**, 121-134.

Böhnecke, G. (1922). Salzgehalt und Strömungen der Nordsee. *Veröff. Inst. Meeresk. Univ. Berlin, Neue Folge, A: Geogr.-naturwiss., R.M.* **10**, 1-34.

British Oceanographic Data Centre (1989). *The BODC Generalised Screening System: A Program for the Iris Graphics Workstation*. Loch, S.G., Version 2.2., N.E.R.C., Bidston, 21 pp.

Brock, T.D. (1983). *Membrane Filtration: A User's Guide and Reference Manual*. Springer-Verlag, Berlin, 381 pp.

Burton, J.D. (1976). Basic properties and processes in estuarine chemistry. In: *Estuarine Chemistry*. Burton, J.D. and Liss, P.S. (eds.). Academic Press, London, pp. 1-36.

Carder, K.L., Betzer, P.R. and Eggimann, D.W. (1974). Physical, chemical, and optical measures of suspended-particle concentrations: their intercomparison and application to the West African Shelf. In: *Suspended Solids*. Gibbs, R.J. (ed.), Plenum Press, New York, pp. 173-193.

Caston, V.N.D. (1972). Linear sand banks in the Southern North Sea. *Sedimentology* **18**, 63-78.

Caston, V.N.D. (1979). The Quaternary sediments of the North Sea. In: *The North-West European Shelf Seas: the Sea Bed and the Sea in Motion, I, Geology and Sedimentology*. Banner, F.T., Collins, M.B. and Massie, K.S. (eds.). Elsevier, Amsterdam, pp. 195-270.

Cranston, R.E. and Buckley, D.E. (1972). The application and performance of microfilters in analyses of suspended particulate matter. *Unpublished Report*. BI-R-72-7. Bedford Inst. Oceanogr., Canada, 14 pp.

Daily Telegraph (1988). North Sea or Dead Sea ? *Telegraph Weekend Magazine, October 8th*. Daily Telegraph plc., London, pp. 16-26.

Danielsson, L.R. (1982). On the use of filters for distinguishing between dissolved and particulate fractions in natural waters. *Water Res.* **16**, 179-182.

Davies, A.M. (1983a). Comparison of computed and observed residual currents during JONSDAP '76. In: *Physical Oceanography of Coastal and Shelf Seas*. Johns, B. (ed.). Elsevier, Amsterdam, pp. 357-386.

Davies, A.M. (1983b). Application of a three-dimensional shelf model to the calculation of North Sea currents. In: *North Sea Dynamics*. Sündermann, J and Lenz, W (ed.). Springer-Verlag, Berlin, pp. 44-62.

Davies, A.M. (1987). A three dimensional numerical model of semi-diurnal tides on the European continental shelf. In: *Three Dimensional Models of Marine and Estuarine Dynamics*. Nihoul, J.C.J. and Jamart, B.M. (eds.). Elsevier, Amsterdam, pp. 221-244.

Dickson, R.R. and Reid, P.C. (1983). Local effects of wind speed and direction on the phytoplankton of the Southern Bight. *J. Plankton Res.* **5**, 441-455.

Dietrich, G. (1950). Die natürlichen Regionen von Nord und Ostsee auf hydrographischer Grundlage. *Kieler Meeresforsch.* **7**, 35-69.

Dolata, L.S., Roeckner, E. and Behr, H. (1983). Prognostic storm surge simulation with a combined meteorological/oceanographic model. In: *North Sea Dynamics*. Sündermann, J and Lenz, W (ed.). Springer-Verlag, Berlin, pp. 266-278.

Duinker, J.C. (1980). Suspended matter in estuaries: adsorption and desorption processes. In: *Chemistry and Biogeochemistry of Estuaries*. Olausson, E. and Cato, I. (eds.). Wiley, Chichester, pp. 121-151.

Dyer, K.R. and Moffat, T.J. (1992). Suspended Sediment Distributions in the North Sea. *Inst. Mar. Studies Rep.*, University of Plymouth, 42 pp.

Eisma, D. (1981a). Suspended matter as a carrier for pollutants in estuaries and the sea. In: *Marine Environmental Pollution, 2: Dumping and Mining*. Elsevier, Amsterdam, pp. 281-295.

Eisma, D. (1981b). Supply and deposition of suspended matter in the North Sea. In: *Holocene Marine Sedimentation in the North Sea Basin*. Nio, S.D., Shüttenhelm, R.T.E. and van Weering, Tj. C.E. (eds.). I.A.S. Spec. Publ. 5, Blackwell Sc. Publ., Oxford, pp. 451-459.

Eisma, D. (1981c). The mass-balance of suspended matter and associated pollutants in the North Sea. *Rapp. P.-v. Réun. Cons. int. Explor. Mer.* **181**, 7-14.

Eisma, D. (1987a). The North Sea: an overview. In: *The Status of the North Sea Environment: Reasons for Concern, Volume 2*. Peet, G. (ed.). Proc. 2nd Int. North Sea Seminar, Rotterdam. Werkgroep Noordzee, Amsterdam, pp. 11-28.

Eisma, D. (1987b). The North Sea: an overview. *Phil. Trans. R. Soc. Lond.* **B 316**, 461-485.

Eisma, D. (1990). Transport and deposition of suspended matter in the North Sea and the relation to coastal siltation, pollution, and bottom fauna distribution. *Reviews in Aquatic Sciences* **3**, 181-216.

Eisma, D., Jansen, J.H.F. and van Weering, Tj.C.E. (1979). Sea-floor morphology and recent sediment movement in the North Sea. In: The Quaternary History of the North Sea. Oele, E., Shüttenhelm, R.T.E. and Wiggers, A.J. (eds.). *Acta Univ. Ups. Symp. Univ. Ups. Ann. Quing. Celebr.* **2**, 217-231.

Eisma, D. and Kalf, J. (1979). Distribution and particle size of suspended matter in the Southern Bight of the North Sea and the Eastern Channel. *Neth. J. Sea Res.* **13**, 298-324.

Eisma, D. and Kalf, J. (1987a). Dispersal, concentration and deposition of suspended matter in the North Sea. *J. Geol. Soc. Lond.* **144**, 161-178.

Eisma, D. and Kalf, J. (1987b). Distribution, organic content and particle size of suspended matter in the North Sea. *Neth. J. Sea Res.* **21**, 265-285.

Eisma, D., Cadée, G.C. and Laane, R. (1982). Supply of suspended matter and particulate and dissolved organic carbon from the Rhine to the coastal North Sea. *Mitt. Geol.-Paläont. Inst. Univ. Hamburg* **52**, 483-505.

ELOISE Steering Committee (1994). *European Land-Ocean Interaction Studies: Science Plan.* Version 31 March 1994. 40 pp.

Flather, R.A., Proctor, R. and Wolf, J. (1991). Oceanographic Forecast Models. In: *Computer Modelling in the Environmental Sciences*. Farmer, D.G. and Rycroft, M.J. (eds.). Clarendon Press, Oxford, pp15-30.

Gardner, W.D., Biscaye, P.E., Zaneveld, J.R.V. and Richardson, M.J. (1985). Calibration and comparison of the LDGO nephelometer and the OSU transmissometer on the Nova Scotia Rise. *Mar. Geol.* **66**, 323-344.

Gibbs, R.J. (ed.) (1974). *Suspended Solids in Water*. Plenum Press, New York, 320 pp.

Goldberg, E.D. (ed.) (1973). *North Sea Science*. N.A.T.O. North Sea Science Conference 1971, M.I.T. Press, Cambridge, Mass., 500 pp.

Greenpeace (1987). *The Tide Must Turn*. Greenpeace Environmental Trust, London, 39 pp.

Hey, E. and Peet, G. (eds.) (1986). *The Status of the North Sea Environment: Reasons for Concern. Volume 1*. Proc. 2nd Int. North Sea Seminar, Rotterdam. Werkgroep Noordzee, Amsterdam, 54 pp.

Hill, H.W. (1973). Currents and water masses. In: *North Sea Science*. Goldberg, E.D. (ed.). N.A.T.O. North Sea Science Conference 1971, M.I.T. Press, Cambridge, Mass., pp. 17-42.

Hill, H.W. and Dickson, R.R. (1978). Long-term changes in North Sea hydrography. *Rapp. P.-v. Réun. Cons. int. Explor. Mer.* **172**, 310-334.

Hölemann, J. and Wirth, H. (1988). Concentration, major element ratios and scanning electron microscopy of suspended particulate matter from the North Sea. *Mitt. Geol.-Paläont. Inst. Univ. Hamburg* **65**, 183-206.

Holligan, P.M., Aarup, T. and Groom, S.B. (1989). The North Sea Satellite Colour Atlas. *Cont. Shelf Res.* **9**, 665-765.

Houbolt, J.J.H.C. (1968). Recent sediments in the Southern Bight of the North Sea. *Geologie en Mijnbouw* **47**, 245-273.

Howarth, M.J. (1983). Observations of tides over the continental shelf of North-West Europe. In: *Physical Oceanography of Coastal and Shelf Seas*. Johns, B. (ed.). Elsevier, Amsterdam. pp.135-188.

Howarth, M.J. (ed.) (1987). North Sea Project: Survey Plans. *Unpublished report*. Version 1, November 1987, Proudman Oceanographic Laboratory. Birkenhead, 52 pp.

Howarth, M.J. (1990). *Atlas of Tidal Elevations and Currents around the British Isles*. Offshore Technology Report, OTH-89-293., H.M.S.O., London. 43 pp.

Howarth, M.J., Dyer, K.R., Joint, A.R., Hydes, D.J., Purdie, D.A., Edmunds, H., Jones, J.E., Lowry, R.K., Moffat, T.J., Pomroy, A.J. and Proctor, R. (1993). Seasonal cycles and their spatial variability. *Phil. Trans. R. Soc. Lond.* A **343**, 383-403.

Huntley, D.A. (1979). Tides on the North-West European Continental Shelf. In: *The North-West European Shelf Seas: the Sea Bed and the Sea in Motion, II, Physical and Chemical Oceanography, and Physical Resources*. Banner, F.T., Collins, M.B. and Massie, K.S. (eds.). Elsevier, Amsterdam, pp. 301-351.

Huthnance, J.M., Allen, J.I., Davies, A.M., Hydes, D.J., James, I.D., Jones, J.E., Millward, G.E., Prandle, D., Proctor, R., Purdie, D.A., Statham, P.J., Tett, P.B., Thomson, S. and Wood, R.G. (1994). Towards water quality models. In: *Understanding the North Sea System.* Charnock, H., Dyer, K.R., Huthnance, J.M., Liss, P.S., Simpson, J.H. and Tett, P.B. (eds.). Chapman and Hall, London for the Roy. Soc., pp. 191-206.

Hydraulics Research Limited (1992). *Particulate Pollutants in the North Sea*. Report SR. 292. Hydraulics Research, Wallingford.

Irion, G., Wunderlich, F and Schwedhelm, E. (1987). Transport of clay minerals and anthropogenic compounds into the German Bight and the provenance of fine-grained sediments SE of Helgoland. *J. Geol. Soc. Lond.* **144**, 153-160.

Jago, C.F., Bale, A.J., Green, M.O., Howarth, M.J., Jones, S.E., McCave, I.N., Millward, G.E, Morris, A.W., Rowden, A.A. and Williams, J.J. (1994). Resuspension processes and seston dynamics, southern North Sea. In: *Understanding the North Sea System.* Charnock, H., Dyer, K.R., Huthnance, J.M., Liss, P.S., Simpson, J.H. and Tett, P.B. (eds.). Chapman and Hall, London for the Roy. Soc., pp. 97-113.

James, I.D. (1983). A three-dimensional model of shallow-sea fronts. In: *North Sea Dynamics*. Sündermann, J. and Lenz, W. (eds.). Springer-Verlag, Berlin. pp. 173-199.

Jerlov, N.G. (1976). *Marine Optics*. Elsevier, Amsterdam, 231 pp.

Jerlov, N.G. and Nielsen, E.S. (eds.) (1974). *Optical Aspects of Oceanography*. Academic Press. London, 494 pp.

Joint, I.R. and Pomroy, A.J. (1992). Phytoplankton Biomass and Production in the North Sea. *Plymouth Mar. Lab.*, 32pp.

Joseph, J. (1953). Die Trübungsverhältnisse in der südwestlichen Nordsee während der "Gauss"-Fahrt im Februar/März 1952. *Ber. d. Dtsch. wiss. Komm. f. Meeresforsch.* **13**, 93-103.

Joseph, J. (1955). Extinction measurements to indicate distribution and transport of watermasses. *Proc. U.N.E.S.C.O. Symp. on Physical Oceanogr., Tokyo*, 59-75.

Kautsky, H. (1973). The distribution of the radio nuclide Caesium 137 as an indicator for North Sea watermass transport. *Dtsch. Hydrogr. Zeit.* **26**, 241-246.

Kenyon, N.H., Belderson, R.H., Stride, A.H. and Johnson, M.A. (1981). Offshore tidal sand-banks as indicators of net sand transport and as potential deposits. In: *Holocene Marine Sedimentation in the North Sea Basin*. Nio, S.D., Shüttenhelm, R.T.E. and van Weering, Tj. C.E. (eds.). I.A.S. Spec. Publ. 5, Blackwell Sc. Publ., Oxford, pp. 257-268.

Knight, P.J., Falconer, J. and Howarth, M.J. (1990a). *Current Meter Records: Site B 55 °30 N 05 °31 E. August 1988 - September 1989. North Sea Project.* Proudman Oceanogr. Lab. Rep. No. 13, 205pp.

Knight, P.J., Falconer, J. and Howarth, M.J. (1990b). *Current Meter Records: Site E 52 °43 N 02 °251 E. August 1988 - September 1989. North Sea Project.* Proudman Oceanogr. Lab. Rep. No. 12, 205pp.

Knight, P.J., Falconer, J. and Howarth, M.J. (1990c). *Current Meter Records: Site F 52 °37 N 03 °46 E. August 1988 - September 1989. North Sea Project.* Proudman Oceanogr. Lab. Rep. No. 11, 158pp.

Knight, P.J., Howarth, M.J. and Flatt, D. (1991a). *Acoustic Doppler Current Profiler Records: Site A 55 °30 N 00 °54 E. August 1988 - September 1989. North Sea Project.* Proudman Oceanogr. Lab. Rep. No. 15, 147pp.

Knight, P.J., Howarth, M.J. and Flatt, D. (1991b). *Acoustic Doppler Current Profiler Records: Site C 54 °20 N 00 °24 E. August 1988 - September 1989. North Sea Project.* Proudman Oceanogr. Lab. Rep. No. 16, 163pp.

Knight, P.J., Howarth, M.J. and Flatt, D. (1991c). *Acoustic Doppler Current Profiler Records: Site D 53 °30 N 03 °00 E. August 1988 - September 1989. North Sea Project.* Proudman Oceanogr. Lab. Rep. No.17, 166pp.

Kullenberg, G. (1974). The distribution of particulate matter in a Northwest African coastal upwelling area. In: *Suspended Solids*. Gibbs, R.J. (ed.), Plenum Press, New York, pp. 195-210.

Laevestu, T. (1963). *Surface water types of the North Sea and their characteristics.* Serial Atlas of the Marine Environment, Folio 4. Amer. Geogr. Soc., New York. 1pp. (2 charts).

Lancelot, C. (1990). *Phaeocystis* blooms in the continental coastal area of the Channel and the North Sea. In: *Eutrophication and Algal Blooms in the North Sea Coastal Zones, the Baltic and Adjacent Areas: Prediction and Assessment of Preventive Actions*. Lancelot, C., Billen, G. and Barth, H. (eds.). Water Pollution Research Report No. 12, Environmental Research and Development Programme, Commission of the European Communities, Brussels, pp.27-54.

Lancelot, C., Billen, G. and Barth, H. (eds.) (1990). *Eutrophication and Algal Blooms in the North Sea Coastal Zones, the Baltic and Adjacent Areas: Prediction and Assessment of Preventive Actions*. Water Pollution Research Report No. 12, Environmental Research and Development Programme, Commission of the European Communities, Brussels, 281 pp.

Lee, A.J. (1970). The currents and water masses of the North Sea. *Oceanogr. Mar. Biol. Ann. Rev.* **8**. 33-71.

Lee, A.J. (1980). North Sea: physical oceanography. In: *The North-West European Shelf Seas: the Sea Bed and the Sea in Motion, II, Physical and Chemical Oceanography, and Physical Resources*. Banner, F.T., Collins, M.B. and Massie, K.S. (eds.). Elsevier, Amsterdam, pp. 467-493.

Lee, A.J. and Folkard, A.R. (1969). Factors affecting turbidity in the Southern North Sea. *J. Cons. int. Explor. Mer.* **32**, 292-302.

Lee, A.J. and Ramster, J. (1968). The hydrography of the North Sea: a review of our knowledge in relation to pollution problems. *Helgol. wiss. Meeresunters.* **17**, 44-63.

Ling, S.C. and Pao, H.P. (1988). Study of micro-bubbles in the North Sea. In: *Sea Surface Sound*. Kerman, B.R. (ed.). Kluwer Academic Publ., Dordrecht, pp. 197-210.

Mackenzie, F.T. and Garrels, R.M. (1966). Chemical mass balance between rivers and oceans. *Amer. J. Sci.* **264**, 507-525.

Maier-Reimer, E. (1977). Residual circulation in the North Sea due to the M_2-tide and mean annual wind stress. *Dtsch. Hydrogr. Zeit.* **30**, 69-80.

Manheim, F.T., Meade, R.H. and Bond, G.C. (1970). Suspended matter in the surface waters of the Atlantic Continental Margin from Cape Cod to the Florida Keys. *Science* **167**, 371-376.

Marine Forum (1990). *North Sea Report*. The Marine Forum for Environmental Issues, 164 pp.

McCave, I.N. (1971). Sand waves in the North Sea off the coast of Holland. *Mar. Geol.* **10**, 199-225.

McCave, I.N. (1972). Transport and escape of fine-grained sediment from shelf areas. In: *Shelf Sediment Transport: Process and Pattern*. Swift, D.J.P., Duane, D.B. and Pilkey, O.H. (eds.). Dowden, Hutchinson and Ross, Stroudsburg , Pa., pp. 225-248.

McCave, I.N. (1973). Mud in the North Sea. In: *North Sea Science*. Goldberg, E.D. (ed.). N.A.T.O. North Sea Science Conference 1971, M.I.T. Press, Cambridge, Mass., pp. 75-100.

McCave, I.N. (1979). Suspended sediment. In: *Estuarine Hydrography and Sedimentation*. Dyer, K.R. (ed.). Cambridge Univ. Press, Cambridge, pp. 131-185.

McCave, I.N. (1981). Location of coastal accumulations of fine sediments around the Southern North Sea. *Rapp. P.-v. Réun. Cons. int. Explor. Mer.* **181**, 15-27.

McCave, I.N. (1983). Particulate size spectra, behaviour and origin of nepheloid layers over the Nova Scotian Continental Rise. *J. Geophys. Res.* **88**, 7647-7666.

McCave, I.N. (1987). Fine sediment sources and sinks around the East Anglian Coast (UK). *J. Geol. Soc. Lond.* **144**, 149-152.

McCave, I.N., Caston, V.N.D. and Fannin, N.G.T. (1977). The Quaternary of the North Sea. In: *British Quaternary Studies: Recent Advances*. Shotton, F.W. (ed.). Oxford Univ. Press, London, pp. 187-204.

Ministerial Declaration (1987). Second International Conference on the Protection of the North Sea. Department of Environment (G.B.), London.

Moody, J.A., Butman, B. and Bothner, M.H. (1987). Near-bottom suspended matter concentration on the continental shelf during storms: estimates based on in situ observations of light transmission and a particle size dependent transmissometer calibration. *Cont. Shelf Res.* **7**, 609-628.

Natural Environment Research Council (1994). *Land-Ocean Interaction Study (LOIS): Implementation Plan for a Community Research Project*. N.E.R.C., Swindon, 61 pp.

Newman, P.J. and Agg, A.R. (eds.) (1988). *Environmental Protection of the North Sea*. Heinemann Profess. Publ., Oxford, 886 pp.

Nolting, R.F. and Eisma, D. (1988). Elementary composition of suspended particulate matter in the North Sea. *Neth. J. Sea Res.* **22**, 219-236.

North Sea Forum (1987). *Report of the North Sea Forum*. 198 pp.

Oceanography Sub-Group (1987). *Report of the Oceanography Sub-Group*. Scientific and Technical Working Group, Second International Conference on the Protection of the North Sea. Department of Environment (G.B.), London, 68 pp.

Odum, W.E., Woodwell, G.M. and Wurster, C.F. (1969). DDT residues absorbed from organic detritus by fiddler crabs. *Science* **164**, 576-577.

Otto, L. (1966) Light attenuation in the North Sea and the Dutch Wadden Sea in relation to secchi disc visibility and suspended matter. *Neth. J. Sea Res.* **3**, 28-51.

Otto, L. (1967). Investigations on optical properties and water masses of the Southern North Sea. *Neth. J. Sea Res.* **3**, 532-551.

Pak, H. (1974). Distribution of suspended particles in the Equatorial Pacific Ocean. In: *Suspended Solids*. Gibbs, R.J. (ed.), Plenum Press, New York, pp. 261-270.

Pak, H. and Zaneveld, J.R.V. (1978). Intermediate nepheloid layers observed over the continental margins of Oregon. *Proc. S.P.I.E.* **160**, *Ocean Optics V*, 9-17.

Pak, H., Zaneveld, J.R.V. and Kitchen, J. (1980). Intermediate nepheloid layers observed off Oregon and Washington. *J. Geophys. Res.* **85**, 6697-6708.

Parker, M. and Tett, P. (eds.) (1987). Exceptional Plankton Blooms. A Special Meeting held in Copenhagen, 4-5 October, 1984. *Rapp. P.-v. Réun. Cons. int. Explor. Mer.* **187**, I.C.E.S., Copenhagen, 114 pp.

Peet, G. (ed.) (1987). *The Status of the North Sea Environment: Reasons for Concern, Volume 2*. Proc. 2nd Int. North Sea Seminar, Rotterdam. Werkgroep Noordzee, Amsterdam, 351 pp.

Pegrum, R.M., Rees, G. and Naylor, D. *Geology of the North-West European Continental Shelf. Volume 2: The North Sea*. Trotman Dudley, London, 225 pp.

Peterson, R.E. (1978). *A study of suspended particulate matter: Arctic Ocean and Northern Oregon Continental Shelf*. Ph.D Thesis, Oregon State Univ., Corvallis, Oregon, 122 pp.

Phillips, D.M. and Scholz, M.L. (1982). Measured distribution of water turbidity in Gulf St. Vincent. *Aust. J. Mar. Freshw. Res.* **33**, 723-727.

Pingree, R.D. and Griffiths, D.K. (1978). Tidal fronts on the shelf seas around the British Isles. *J. Geophys. Res.* **83**, 4615-4622.

Postma, H. (1961). Suspended matter and secchi disc visibility in coastal waters. *Neth. J. Sea Res.* **1**, 359-390.

Postma, H. (1981). Exchange of materials between the North Sea and the Wadden Sea. *Mar. Geol.* **40**, 199-213.

Prandle, D. (1984). A modelling study of the mixing of ^{137}Cs in the seas of the European Continental Shelf. *Phil. Trans. R. Soc. Lond.* **310**, 407-436.

Proctor, R. and Smith, J.A. (1991). *The Depth-Averaged Residual Circulation on the North West European Shelf: August 1988 - October 1989.* Proudman Oceanogr. Lab. Rep. No. 20, 255pp.

Qin, Y., Fan, L., Xu, S., Milliman, J. and Limeburner, R. (1988). Study on suspended matter in the Southern Yellow Sea. *Chin. J. Oceanol Limnol.* **6**, 201-215.

Ramster, J.W. (1965). Studies with the Woodhead Sea-bed Drifter in the southern North Sea. *Lab. Leafl. Fish. Lab. Lowestoft* **6**, 1-4.

Ramster, J.W. (1977). Development of cooperative research in the North Sea. *Mar. Pol.* **1**, 318-325.

Reid, P.C., Taylor, A.H. and Stephens, J.A. (1988). The hydrography and hydrographic balances of the North Sea. In: *Pollution of the North Sea: An Assessment*. Salomons, W., Bayne, B.L., Duursma, E.K. and Förstner, U. (eds.). Springer-Verlag, Berlin, pp. 3-19.

Sackett, W.M. (1978). Suspended matter in sea-water. In: *Chemical Oceanography, Volume 7*. Riley, J.P. and Chester, R. (eds.). Academic Press, London, pp. 127-172.

Salomons, W., Bayne, B.L., Duursma, E.K. and Förstner, U. (eds.) (1988). *Pollution of the North Sea: An Assessment*. Springer-Verlag, Berlin, 687 pp.

Scientific and Technical Working Group (1987). *Quality Status of the North Sea*. Second International Conference on the Protection of the North Sea. Department of Environment (G.B.), London, 88 pp.

Sea Tech (1988). *25cm Transmissometer Operating Instructions*. Sea Tech Inc., Corvallis, Oregon, 19 pp.

Sheldon, R.W. (1972). Size separation of marine seston by membrane and glass-fibre filters. *Limnol. Oceanogr.* **17**, 494-498.

Sheldon, R.W. and Sutcliffe, W.H. (1969). Retention of marine particles by screens and filters. *Limnol. Oceanogr.* **14**, 441-444.

Simpson, J.H. (1994). The North Sea Project: an overview and the way forward. In: *Understanding the North Sea System*. Charnock, H., Dyer, K.R., Huthnance, J.M., Liss, P.S., Simpson, J.H. and Tett, P.B. (eds.). Chapman and Hall, London for the Roy. Soc., pp. 207-218.

Smith, R.C. and Baker, K.S. (1981). Optical properties of the clearest natural waters (200-800 nm). *Appl. Opt.* **20**, 177-184.

Spinrad, R.W. (1986a). An optical study of the water masses of the Gulf of Maine. *J. Geophys. Res.* **91**, 1007-1018.

Spinrad, R.W. (1986b). Characteristic variations of bio-optical properties in the Central North Pacific. *Proc. S.P.I.E.* **637**, *Ocean Optics VIII*, 314-320.

Spinrad, R.W., Zaneveld, J.R.V. and Kitchen, J.C. (1983). A study of the optical characteristics of the suspended particles in the benthic nepheloid layer of the Scotian Rise. *J. Geophys. Res.* **88**, 7641-7645.

Stride, A.H. (1973). Sediment transport by the North Sea. In: *North Sea Science*. Goldberg, E.D. (ed.). N.A.T.O. North Sea Science Conference 1971, M.I.T. Press, Cambridge, Mass., pp. 101-130.

Stride, A.H., Belderson, R.H., Kenyon, N.H. and Johnson, M.A. (1982). Offshore tidal deposits: sand sheet and sand bank facies. In: *Offshore Tidal Sands*. Stride, A.H. (ed.). Chapman and Hall, London, pp. 95-125.

Su, M.-Y., Ling, S.-C. and Cartmill, J. (1988). Optical micro-bubble measurements in the North Sea. In: *Sea Surface Sound*. Kerman, B.R. (ed.). Kluwer Academic Publ., Dordrecht, pp. 211-223.

Sunday Times (1988). The North Sea: a short, sharp, shallow, spiteful sea. *Sunday Times Magazine, June 12th*, Times Newspapers Ltd., London, pp. 24-47.

Sündermann, J. (1994). Suspended particulate matter in the North Sea: field observations and model simulations. In: *Understanding the North Sea System*. Charnock, H., Dyer, K.R., Huthnance, J.M., Liss, P.S., Simpson, J.H. and Tett, P.B. (eds.). Chapman and Hall, London for the Roy. Soc., pp. 45-52.

Sündermann, J. and Degens, E.T. (eds.) (1989). *The North Sea: Water Exchange and Pollution*. Brochure of the Z.I.S.C.H. and T.O.S.C.H. projects, University of Hamburg, 49 pp.

Terwindt, J.H.J. (1971). Sand waves in the Southern Bight of the North Sea. *Mar Geol.* **10**, 51-67.

Tett, P.B., Joint, I.R., Purdie, D.A., Baars, M., Oosterhuis, S., Daneri, G., Hannah, F., Mills, D.K., Plummer, D., Pomroy, A.J., Walne, A.W. and Witte, H.J. (1994). Biological consequences of tidal stirring gradients in the North Sea. In: *Understanding the North Sea System*. Charnock, H., Dyer, K.R., Huthnance, J.M., Liss, P.S., Simpson, J.H. and Tett, P.B. (eds.). Chapman and Hall, London for the Roy. Soc., pp. 115-130.

Turekian, K.K. (1977). The fate of metals in the oceans. *Geochim. Cosmochim. Acta* **41**, 1139-1144.

Turner, A. (1991). *Chemical Dynamics in North Sea Estuaries and Plumes*. Ph.D. Thesis, Polytechnic South West, Plymouth, 237 pp.

Tyler, J.E., Austin, R.W. and Petzold, T.J. (1974). Beam transmissometers for oceanographic measurements. In: *Suspended Solids*. Gibbs, R.J. (ed.). Plenum Press, New York, pp. 51-59.

Veenstra, H.J. (1971). Sediments of the Southern North Sea. In: *The Geology of the East Atlantic Continental Margin, 3, Europe (contd.)*. Delany, F.M. (ed.). Report 70/15, Instit. Geological Sciences, London, pp. 10-23.

Visser, M. (1993). *On the Transport of Fine Marine Sediment in the Netherlands Coastal Zone*. Ph.D Thesis, University of Utrecht, Netherlands, 176 pp.

Visser, M., de Ruijter, W.P.M. and Postma, L. (1991). The distribution of suspended matter in the Dutch coastal zone. *Neth. J. Sea Res.* **27**, 127-143.

Visser, M.P. (1970). The turbidity of the Southern North Sea. *Dtsch. Hydrogr. Zeit.* **23**, 97-117.

van Weering, Tj.C.E., Berger, G.W. and Kalf, J. (1987). Recent sediment accumulation in the Skagerrak, Northeastern North Sea. *Neth. J. Sea Res.* **21**, 177-189.

Whatman (1988). *Laboratory Filtration Product Guide*. Whatman Ltd., Maidstone, 37 pp.

Wirth, H. and Seifert, R. (1988). Mineralogy, geochemistry and SEM-observations of suspended particulate matter from the North Sea, Spring 1984. *Mitt. Geol.-Paläont. Inst. Hamburg* **65**, 163-181.

Zijlstra, J.J. (1988). The North Sea ecosystem. In: *Ecosystems of the World, 27, Continental Shelves*. Postma, H. and Zijlstra, J.J. (eds.). Elsevier, Amsterdam, pp. 231-277.

Zuo, Z., Eisma, D. and Berger, G.W. (1989). Recent sediment deposition rates in the Oyster Ground, North Sea. *Neth. J. Sea Res.* **23**, 263-269.